DEVELOPMENT AND EVALUATION OF AN ACTIVELY HEATED AND VENTILATED POULTRY TRANSPORT VEHICLE

A Thesis Submitted to

the College of Graduate Studies and Research

in Partial Fulfillment of the Requirements

for the Degree of Doctor of Philosophy

in the Department of Chemical and Biological Engineering

University of Saskatchewan

Saskatoon

By

KA PO CATHERINE HUI

PERMISSION TO USE AND DISCLAIMER

ABSTRACT

The harsh winter conditions on the Canadian prairies impose special challenges in providing acceptable environmental conditions for broiler chickens during transportation. A research program was developed aiming to improve the transport conditions for broilers. As part of the research program, a research project was developed to design and construct an experimental trailer equipped with active ventilation and heating, to characterize the performance of the experimental trailer in field tests under Canadian Prairie winter conditions, to develop, calibrate and validate CFD models used for simulating the environmental conditions found inside the experimental trailer, and to utilize one of the CFD models to predict the performance of the experimental trailer when subjected to different operational conditions.

This dissertation consists of six chapters. The first introductory chapter reviews economical, logistical and legislative aspects surrounding the poultry transport industry. This chapter also includes a discussion of important parameters for the design of an experimental transport system, a review of fundamental concepts of the Computational Fluid Dynamics (CFD) modeling method, and why CFD was chosen as a tool to complement the experimental work in this project. The second chapter reviews the designs of commercial poultry transport equipment and how they inspired the design of an actively heated and ventilated experimental vehicle. The setup of the experimental trailer was also discussed in detail.

The third chapter reviews the experimental protocol used to evaluate the performance of the experimental trailer. The performance of this experimental trailer was evaluated in a series of field tests conducted under commercial loading operations, in winter conditions on the Canadian Prairies. It was found that the average load temperature varied from 7.1 to 15.6°C in the nine sts of data. The system was able to maintain an environment above -1°C. As for the humidity level

inside the trailer, the majority of sensors had representative relative humidity (*RH**) values between 10 and 40%, with the rest having *RH** values below saturation.

The fourth chapter reviews the development, calibration and validation of the 3-D CFD models developed to simulate the environmental conditions inside the experimental trailer. A total of three CFD models were developed to simulate the three different ventilation regimes encountered in field tests. Sensitivity studies revealed that inlet velocities, heat and moisture production had a great impact on the results obtained from the CFD models. The levels of porosity investigated did not play a significant role. The standard error of estimate (σ_{est}) was selected as a statistical measure to evaluate the accuracy of the CFD models against experimental data. For temperature data, σ_{est} varied from 3.2 to 7.3°C. For humidity ratio, σ_{est} varied from 1.7 to 5.0 g of water vapour per kg of dry air. The CFD models were able to recreate the temperature trends as observed from experimental data. It was concluded that these CFD models have adequate accuracy to be used as a design tool for comparative studies.

The fifth chapter investigates the use of the 1-fan CFD model to study several scenarios. Three cases were investigated, based on conditions which may be encountered by the poultry transport industry. The first case examined the effects of vehicle travel speed and ambient temperature. The second case looked at the effects of bird size, loading density and ambient temperature. The last case studied the effects of side tarp insulation and ambient temperature. For the range of values examined, results from the simulations concluded that ambient temperature, bird sizes, loading density and side tarp insulation value were important factors to consider in the design of an actively ventilated poultry transport vehicle.

The last chapter of this dissertation summarizes the main findings in this research project, discussed future work and presented final conclusions. Overall, this research project answered two key questions in the poultry transport research program. Firstly, the experimental work proved that the concept of active ventilation and heating is a promising option to improve the transport conditions for broiler chickens during cold ambient conditions. Secondly, the CFD work demonstrated that CFD modeling is a valuable tool for designing the next generation of actively ventilated poultry transport vehicle.

RÉSUMÉ

Les conditions hivernales difficiles des Prairies Canadiennes imposent des défis spécifiques pour procurer les conditions environnementales acceptables au transport des poulets à griller (broiler chickens). Un programme de recherche fut développé dans le but d'améliorer les conditions de transport des poulets. Comme partie intégrante de ce programme de recherche, un projet de recherche fut développé pour concevoir et construire une remorque expérimentale équipée d'un système de ventilation et de chauffage actif, afin de caractériser la performance de la remorque expérimentale en conditions réelles. De plus, ce projet vise à développer, calibrer et valider de(s) modèle(s) CFD utilisé(s) pour simuler les conditions environnementales mesurées dans la remorque expérimentale, ainsi que pour utiliser un modèle de CFD pour prévoir la performance expérimentale de la remorque lorsque soumise à différentes conditions d'opération.

Cette thèse comporte six chapitres. Le premier chapitre d'introduction révise les aspects économique, logistique et législatif entourant l'industrie du transport du poulet. Ce chapitre comprend aussi une discussion des paramètres importants pour le conception d'un système de transport expérimental, une révision des concepts fondamentaux de la méthode de modélisation de CFD (Computational Fluid Dynamics) et la raison pour laquelle la méthode CFD fut choisie comme un outil complémentaire du travail expérimental de ce projet. Le deuxième chapitre est une revue des concepts d'équipements commerciaux de transport de poulets et de quelle façon ils inspirent le concept d'un véhicule expérimental avec un système actif de ventilation et de chauffage. La configuration de la remorque expérimentale fut aussi discutée en détails.

Le troisième chapitre est une revue du protocole expérimental pour évaluer la performance de la remorque expérimentale. La performance de la remorque expérimentale fut évaluée lors d'une série de tests en conditions réelles réalisés lors de chargements commerciaux

en conditions hivernales dans les Prairies Canadiennes. Il fut déterminé que la température d'un chargement moyen a varié de 7,1 à 15,6°C dans les neuf ensembles de données. Le système fut capable de maintenir un environnement bien au-dessus de -1°C. Dans le cas du niveau d'humidité à l'intérieur de la remorque, la majorité des senseurs ont mesuré une valeur d'humidité relative représentative (*RH**) entre 10 et 40%, tandis que les autres ont mesuré des valeurs en bas du niveau de saturation.

Le quatrième chapitre est une revue du développement, de la calibration et de la validation des modèles de CFD en trois dimensions qui furent développés pour simuler les conditions environnementales à l'intérieur de la remorque expérimentale. Un total de trois modèles de CFD furent développés pour simuler les trois différentes régimes de ventilation retrouvés dans les conditions réelles. Des analyses de sensibilité ont révélé que la vitesse d'air à l'entrée, la chaleur ainsi que la production d'humidité par les poulets ont eu un impact important sur les résultats obtenus avec les modèles de CFD. Les niveaux de porosité étudiés n'ont pas joué un rôle significatif. L'erreur standard d'estimation (σ_{est}) fut choisie comme mesure statistique pour évaluer le précision des modèles de CFD versus les données expérimentales. Pour ce qui est des données de température, σ_{est} a varié de 3,2 à 7,3°C. Pour le ratio d'humidité, σ_{est} a varié de 1,7 à 5.0 g d'eau évaporée par kg d'air sec. Les modèles de CFD furent capables de récréer les tendances de températures observées dans les données expérimentales. Il fut conclu que les modèles de CFD ont la précision adéquate pour être utilisés comme un outil de conception pour des études comparatives.

Le cinquième chapitre est une évaluation de l'utilisation d'un modèle CFD d'un ventilateur pour étudier quelques scenarios alternatifs. Trois cas furent analysés, basés sur des conditions qui peuvent être rencontrées dans l'industrie du transport de poulets. Le premier cas a examiné les effets de la vitesse du véhicule et de la température ambiante. Le second cas a analysé les effets de la grosseur des poulets, de la densité de chargement et de la température ambiante. Le dernier cas a étudié les effets des bâches latérales d'isolation et de la température ambiante. Pour les valeurs examinées, les résultats des simulations ont démontré que la température ambiante, les grosseurs des poulets, la densité de chargement et les bâches latérales d'isolation furent d'importants facteurs à considérer lors de la conception d'un véhicule de transport de poulets avec ventilation active.

Le dernier chapitre de cette thèse établit un sommaire des principales découvertes de ce projet de recherche, discute les travaux nécessaires pour l'avenir et présente des conclusions finales. En général, ce projet de recherche a répondu à deux questions primordiales du programme de recherche sur le transport de poulets. Premièrement, le travail expérimental a prouvé que le concept d'un système actif de chauffage et de ventilation est une option très prometteuse pour améliorer les conditions de transport des poulets durant les conditions ambiantes froides. Deuxièmement, les activités de CFD ont démontré que les modèles de CFD sont des outils utiles pour la conception de la nouvelle génération de véhicules pour le transport de poulets.

ACKNOWLEDGEMENTS

It started with a desire to understand and control an engineering system. It ended up as a great exploration in some uncharted territories. My sincere gratitude to my supervisor, Dr. Trever Crowe, for inviting me to the University of Saskatchewan to participate in this research project. Thank you for your guidance and patience. You showed me what it takes to be a good researcher and teacher. I'll miss our scientific discussion at our weekly meetings. Many thanks to my graduate committee members, Drs. Ernie Barber, Stéphane Lemay, Jim Bugg and Oon-Doo Baik for challenging my thoughts. Thank you Dr. Richard Gates for serving as my external examiner.

One of the joys in being part of this project was to work with people from different institutions. I'm thankful to Mr. Sunny Mak, Mr. Melvin Karakochuk and staff members from Lilydale Inc.; Mr. Peter Kettlewell from England; technical support staff from ANSYS Inc.; Dr. Hank Classen, Mr. Myles Bantle, Mr. Wayne Morley, Mr. Mike Miller, Mr. Louis Roth, Ms. Agnes Northeast, Ms. Tennille Knezacek, Ms. Karen Schwean-Lardner, Ms. Toni Schleicher, Ms. Natasha Burlinguette, staff of the Engineering Computer Center and other members at the University of Saskatchewan. The experimental research was facilitated with the help of Ms. Sherry Cochran in organizing and conducting the field tests. Thank you Mr. Randy Lorenz for your assistance in the field tests and keeping us safe on the road.

I'm grateful for the financial support provided by the Natural Sciences and Engineering Research Council of Canada, Agriculture and Agri-Food Canada, the Chicken Farmers of Saskatchewan, Le Fonds Québécois de la Recherche sur la Nature et les Technologies, Saskatchewan Chicken Industry Development Fund and the University of Saskatchewan in this project.

Finally, I want to thank my friends for cheering alongside on this journey, thank you, merci, 感謝. As to the readers, I hope you will enjoy reading this labour of love. Let your curiosity guide you.

To my family

TABLE OF CONTENTS

LIST OF FIGURES

Appendix B

Appendix C

Appendix E

Appendix F

LIST OF TABLES

List of Symbols

Chapter 2

ΔT = change in air temperature due to heating (°C)

Cp = specific heat of air (J/kg-K)

$\dot{m}$ = mass flow rate (kg/s)

Q = amount of heat produced by heater (W)

Chapter 3

$\Delta\overline{T}_{inlet}$ = temperature gain in ambient air at diffuser screen 1 (°C)

$\Delta\overline{T}_{inlet\ i}$ = time-averaged temperature gain in ambient air at diffuser screen 1, for thermocouple i (°C)

$\Delta\overline{T}_{j}$ = temperature gain in inlet air for data logger j (°C)

i = index of thermocouple

j = index of data logger

$\overline{T}_{ambient}$ = time-averaged temperature of ambient air measured outside the vehicle (°C)

$\overline{T}_{inlet\ i}$ = time-averaged temperature at diffuser screen 1 for thermocouple i (°C)

$\overline{\overline{T}}_{inlet}$ = overall averaged temperature at diffuser screen 1 from 15 thermocouples (°C)

$\overline{T}_{j}$ = time-averaged load temperature of data logger j (°C)

Chapter 4

α = inverse of viscous resistance coefficient (m^2)

ε = void fraction (in decimal)

γ = porosity of the porous medium (in decimal)

σ_{est} = standard error of estimate

ν = kinematic viscosity at T_{film} (m^2/s)

C_2 = inertial resistance coefficient (m^{-1})

D_p = mean particle diameter (m)

H = height of the rectangular box (m)

$\overline{h}$ = average convection heat transfer coefficient of the tarp surface (W/m^2-K)

k = thermal conductivity at T_{film} (W/m-K)

k_{eff} = effective thermal conductivity in the porous medium (W/m-K)

k_f = thermal conductivity of fluid including the turbulent contribution (W/m-K)

k_s = thermal conductivity of solid medium (W/m-K)

L = length of the rectangular box (m)

L_{tarp} = length of the tarp sidewall (m)

n = number of data points

$\overline{Nu}_L$ = average Nusselt number of the tarp sidewall

Pr = Prandtl number at T_{film}

r = equivalent spherical radius of a broiler chicken (m)

Re_L = Reynolds number based on the length of the tarp sidewall

T_{film} = film temperature (K)

Ts = surface temperature of the tarp sidewall based on the surface temperatures at the inlet and outlet (K)

T_{inf} = outdoor temperature (K)

U_{inf} = traveling velocity (m/s)

V_{solid} = total volume of all solid particles within one rectangular box (m^3)

V_{total} = total volume of one rectangular box (set of three drawers) (m^3)

W = width of the rectangular box (m)

Y_{exp} = result from field experiment

Y_{num} = result from numerical model

Appendix A

Φ_l = latent heat production (W)

Φ_s = sensible heat production (W)

$\Phi_{s(hpu)}$ = sensible heat production per hpu (W/hpu)

Φ_{tot} = total heat production (W)

$\Phi_{tot(hpu)}$ = total heat production per hpu (W/hpu)

$\Phi_{tot(mass)}$ = total heat production in the barn based on mass (W)

F = moisture dissipation (g/h)

F^* = modified moisture dissipation (kg/s)

h_{fg} = enthalpy of vaporization for saturated water as function of temperature (kJ/kg)

m = animal weight (kg)

r = 0.680 for water at 20ºC (W-h/g)

T = temperature (ºC)

Appendix D

ϕ = relative humidity (in decimal point)

C_8 = constant = -5.800 220 6 E+03

C_9 = constant = 1.391 499 3 E+00

C_{10} = constant = -4.864 023 9 E-02

C_{11} = constant = 4.176 476 8 E-05

C_{12} = constant = -1.445 209 3 E-08

C_{13} = constant = 6.545 967 3 E+00

p = total pressure of moist air (Pa)

p_w = partial pressure of water vapour in moist air (Pa)

p_{atm} = atmospheric pressure (Pa)

p_{ws} = pressure of saturated pure water (Pa)

RH^* = representative relative humidity (%)

t = index for time

T = absolute temperature (K)

T_t = temperature at time t (ºC)

$\overline{T}$ = time-averaged temperature (ºC)

W = humidity ratio (in decimal point)

W_t = humidity ratio at time t (in decimal point)

$\overline{W}$ = time-averaged humidity ratio (in decimal point)

x = number of temporal data

Z = altitude (m)

Appendix G

ϕ = relative humidity (in decimal point)

γ = specific humidity of moist air (decimal point)

C_8 = constant = -5.800 220 6 E+03

C_9 = constant = 1.391 499 3 E+00

C_{10} = constant = -4.864 023 9 E-02

C_{11} = constant = 4.176 476 8 E-05

C_{12} = constant = -1.445 209 3 E-0.8

C_{13} = constant = 6.545 967 3 E+00

p_{ws} = pressure of saturated pure water (Pa)

p = total pressure of moist air (Pa)

p_w = partial pressure of water vapour in moist air (Pa)

p_{ws} = pressure of saturated pure water (Pa)

T = absolute temperature (K)

W = humidity ratio

1 GENERAL INTRODUCTION

The transportation of broilers in Western Canada possesses unique challenges. This introductory section reviews economical, logistical and legislative aspects surrounding the industry. It summarizes important parameters for the design of an experimental transport system, including limits of environmental conditions suitable for housing chickens, their heat and moisture production rates, climatic conditions in Southern Saskatchewan and conditions found within commercial transport systems. This chapter also reviews some fundamental concepts of the Computational Fluid Dynamics (CFD) modeling method and why it was chosen as a tool to complement the experimental work in this project. Finally, the research objectives of this project are outlined at the end of this chapter.

1.1 OVERVIEW OF POULTRY TRANSPORT INDUSTRY

1.1.1 ECONOMICAL AND LOGISTICAL ASPECTS

The poultry industry occupies an important role in the Canadian agricultural economy. In 2010, the chicken meat industry generated over 1.96 billion dollars of farm cash receipts, representing 4.4% of the total cash receipts received by Canadian farming operations (CFC, 2011). In the same year, Canada ranked as the 14^{th} country producing the most chicken in the world which produced 1,022 million kilograms of chicken (eviscerated weight; CFC, 2011). Canada was ranked the 15^{th} highest country in chicken meat consumption per capita with each Canadian consuming 31.1 kg of chicken in 2010 (CFC, 2011). In the same year, the province of Ontario had the largest annual production, followed by Quebec and British Columbia (CFC, 2011).

The chicken production industry in Saskatchewan experienced a growth of 65.4% between 2000 and 2010 (CFC, 2011). Saskatchewan was the 6^{th} largest chicken producer in Canada in 2010, representing 3.9% of the total Canadian production (CFC, 2011). In 2010, Saskatchewan had 76 chicken producers who produced a total of 39.9 million kilograms (eviscerated weight) of chickens, bringing in 78.6 million dollars of farm cash receipts (CFC, 2011). There are two federally registered processing plants in the province, one located in Wynyard and the other in Saskatoon (AAFC, 2009).

Most of the chickens destined for meat production are broiler chickens. In 2009, approximately 620 million chickens were slaughtered in registered stations in Canada (AAFC, 2010). Similar to the U.S. and UK systems, Canada features centralized slaughter facilities. Most chickens are raised on farms geographically separated from processing plants, and all these animals must be transported from dispersed farms to the centralized facilities. On average, almost 1.7 million of chickens are being transported daily in Canada, under all sorts of weather conditions. The slaughtering process is highly mechanized, some plants can process up to 25,000 broiler chickens per hour (AAFC, 2008).

Transportation of animals is a crucial step in the production process. Vieira et al. (2010, 2011) suggested temperature, relative humidity, time of transport (time of the day and season), loading density in transport container, loading density in the transport system, duration of transport, transport distance, duration of lairage (period of time which animals are waiting in transport containers, usually prior to departure or unloading), and lairage environment are all factors which may cause mortality during transport. Warriss et al. (2005) observed there was a seasonal effect on mortality in their study. Vecerek et al. (2006) also observed the seasonal effect on mortality, along with an effect caused by transport distance. Chauvin et al. (2010) concluded mortality during transport may be related to several factors at the same time: health conditions of the flocks, physical injuries during catching and loading, and the climatic conditions experienced during transport. If animals are miss-handled or exposed to undesirable transport conditions, they may die in transit, resulting in financial losses and a waste of resources. Even if it does not result in mortality, previous researches have showed that the transportation process may cause reduction in marketable live weight, and/or affect meat quality (Bianchi et al., 2005; Dadgar et al., 2010; Yalçin and Güler 2012).

The logistics involved in the transportation process are intensive, many parties are involved. Every trip requires the collaboration of chicken producers, loading personnel, drivers, receiving personnel, and inspection officers. It is in the best interest of the entire poultry industry to ensure animals are being transported under suitable environmental conditions and are being handled in the best possible way.

1.1.2 Legislative Aspects

Aside from the economic incentive to reduce the numbers of chickens which are found "dead on arrival" (DOA), industry representatives and Canadian regulatory agencies have collaborated to develop codes of practice and regulations related to transportation of all animals - from the welfare point of view. According to the code of practice published by Agriculture Canada (1989), the welfare of all animals during transportation is the responsibility of the driver, and coverings should be adjusted to protect animals against various climatic conditions. In the code of practice published by the Canadian Agri-Food Research Council (CARC 2001), it includes a list of signs drivers should monitor to identify if animals are under heat or cold stress. The CARC code of practice recommends to keep animals dry during transport when exposed to cold weather, they should be protected from extreme climate and sufficient airflow needs to be provided throughout the transport system. In addition, the CARC (2001) recommended monitoring load conditions by routinely observing the animals or using sensors; ventilation be adjusted based on variations in temperature; and opening vents should be adjusted to protect animals from wind while still providing adequate ventilation. These codes of practice are to be followed on a voluntary basis. They were designed to recommend best practices and to educate those involved in the industry. On the other hand, the poultry industry is bound by the Health of Animals Regulations published by the Minister of Justice in Canada (2009). Part XII, section 143 of the regulations states that no animals should be transported under "undue exposure to the weather" or "inadequate ventilation" that is likely to cause injury or "undue suffering" to them. Therefore, from the legislative point of view, it is important to transport broilers under humane conditions.

1.2 CONSIDERATIONS IN DESIGNING A POULTRY TRANSPORT VEHICLE

1.2.1 LIMITS OF ENVIRONMENTAL CONDITIONS DURING TRANSPORTATION

When it comes to the design of a transport vehicle, it is necessary to define the "humane" conditions in a technical and scientific manner. Much of the research conducted by other groups has focused on the transportation of chickens under moderate to hot climatic conditions. Some research was conducted for cold climates, which dated back to the 1990s. Until recently, limited research has targeted the impact of Canadian winter conditions on broiler transportation.

Research conducted by Bayliss and Hinton (1990) suggested that thermal stress was one of many factors which contributed to the mortality of broilers during transport. Broiler chickens on transport vehicles have limited ability to control the exchange of heat and moisture with their environment. The two codes of practice (Agriculture Canada 1989 and CARC 2001) recommend a loading density of 63 kg/m^2 for cold weather. Broilers are loaded at high density inside confined containers with limited open space surrounding them. Their movements are restricted, hampering their ability to self-regulate their body temperature using conventional coping mechanisms. Despite the relative short transport times (as compared to time spent in barns), the thermal environment must be maintained within a narrow range to reduce the level of thermal stress which broilers are subjected to within transport vehicles.

Some research was conducted to determine the acceptable environmental conditions for broilers during transportation. Webster et al. (1993) suggested well-feathered broilers or laying hens would be comfortable at temperatures ranging between 15 and 26°C. Hens with fewer feathers would be comfortable at 28-32°C, with an air velocity of 0.5 m/s. Mitchell and Kettlewell (1998) measured the physiological response of broiler chickens in transport drawers under a range of temperature and humidity conditions. They discovered high levels of relative humidity (70-80%) in commercial transport vehicles and concluded that heat stress can be expected when temperatures reach 25°C.

Hunter et al. (1999) studied the physiological responses of dry and wetted broiler chickens exposed to cold ambient conditions. Groups of eight chickens were placed in crates inside a controlled climate chamber equipped with a wind tunnel. To simulate transport conditions encountered in the UK's commercial vehicles, birds were subjected to chamber temperatures ranging from -4 to 12°C, at an air velocity of 0.7 m/s. In some tests, birds were sprayed with a fine mist of water, whereas in others, birds were left in their dry state. Hunter et al. (1999) concluded that broiler chickens subjected to an air velocity of 0.7 m/s could be safely transported at crate temperatures as low as –4°C, if they are dry. However, with wetting, moderate hypothermia would occur at temperatures as high as 8°C. Thus, wet birds are more easily subject to hypothermia. In a study conducted by Classen et al. (2002) in Saskatchewan, it was discovered that drawer temperatures on broiler transport vehicles could routinely drop below –4°C during the winter season. The study by Hunter et al. (1999) did not examine temperatures lower than –4°C.

In the code of practice by Agriculture Canada (1989), it is recommended to maintain the air temperatures between 5 and 30°C around chickens during transportation. No recommendation was made about the acceptable levels of humidity. In the CARC code of practice (2001), no specific temperature values were recommended; it did not reaffirm values given in the 1989 code of practice. In the two codes of practice (Agriculture Canada 1989 and CARC 2001), they both recommended not to load birds when the ambient temperature is greater than 32°C unless the delivery occurs on the same day. It is difficult to ascertain the origins of the recommended range of 5 to 30°C in the code of practice by Agriculture Canada (1989), as no reference was listed. It also does not discuss how humidity levels may affect this "recommended" range of temperatures. One could assume, based on published scientific evidence (such as from Hunter et al. (1999)), that it would be reasonable to transport broilers at a lower temperature if they are kept dry. There is a need to review and update the previously published codes of practice.

1.2.2 HEAT AND MOISTURE PRODUCED BY BROILER CHICKENS

Broiler chickens produce significant amounts of heat and moisture during transportation. Both the heat and moisture must be removed from the loading area inside the vehicle to prevent overheating and wetting of birds. Heat and moisture production data exist for broilers kept inside commercial barns but few data exist for broilers exposed to transport environments.

In 2002, a report published by CIGR (2002) reviewed various models for estimating heat and moisture production rates for different types of animals. As discussed in the report, heat production is a function of the body weight, physiology of the animal, its level of activities as affected by feeding intake/routines and photoperiod, and the environmental conditions which surround the animal (CIGR, 2002). The environmental factors which can affect heat production are air temperature, radiation from surfaces, air velocity and bedding conditions (CIGR, 2002). The conditions of 20°C, "normal" production conditions over a period of 24 h were chosen by the authors as benchmark conditions (CIGR, 2002).

In the report, several equations were proposed for broiler chickens. These equations are summarized in Appendix A. The total heat loss can be sub-divided into sensible and latent heat losses. The sensible heat loss is driven by temperature difference between the animal's deep body temperature and the ambient conditions. The latent heat is the heat released during moisture evaporation (CIGR, 2002). Thus, the heat production rate originates solely from sensible heat loss, while the latent heat value is related to the moisture production rate. After calculating the total and sensible heat production from the equations, the latent heat value can be obtained by taking the difference between these two values. The resulting latent heat can then be divided by the enthalpy of vaporization to obtain the moisture production rate.

The equations in Appendix A are valid for temperatures ranging from 0 to 30°C and possibly higher (CIGR, 2002), but not for temperatures below 0°C. The two main equations for total and sensible heat production yield results in units of "W/hpu". The heat production unit (hpu) is defined as the quantity of animals producing 1000 W of total heat at 20°C (Pedersen and Thomsen, 2000). The CIGR report did not provide a clear explanation on how to convert these values to unit of "W" for temperatures other than 20°C, which imposed another limitation of using these equations. Nonetheless, these equations did take into account the mass of the broilers and established a relationship on how the heat and moisture production rates vary with ambient temperatures. An example of calculations is included at the end of Appendix A to demonstrate the detailed steps required in using these equations.

Knowing the relationship of heat and moisture production rates versus ambient temperature is important, as the temperature inside a transport vehicle is known to be non-uniform. Using a model (instead of discrete point data) can help to estimate the production rates at various temperatures. For example, assuming the air temperature inside a trailer varies from 0 to 30°C, and each broiler weighs 1.75 kg, Table 1.1 summarizes the calculated heat and moisture production rates for this range of temperature. As shown in Figure 1.1, the values of the total and sensible heat production rates decrease with increasing temperatures.

Table 1.1. Sensible and latent heat production rates for one broiler at 1.75 kg (refer to Appendix A for method of calculation).

Temperature T (°C)	Enthalpy of vaporization h_{fg} (kJ/kg)	Total heat Φ_{tot} (W)	Sensible heat Φ_s (W)	Latent heat Φ_l (W)
0	2 501.4	22.62	13.80	8.82
5	2 489.6	21.01	12.72	8.28
10	2 477.7	19.39	11.46	7.93
15	2 465.9	17.77	10.01	7.76
20	2 454.1	16.16	8.38	7.78
25	2 442.3	14.54	6.57	7.97
30	2 430.5	12.93	4.57	8.36

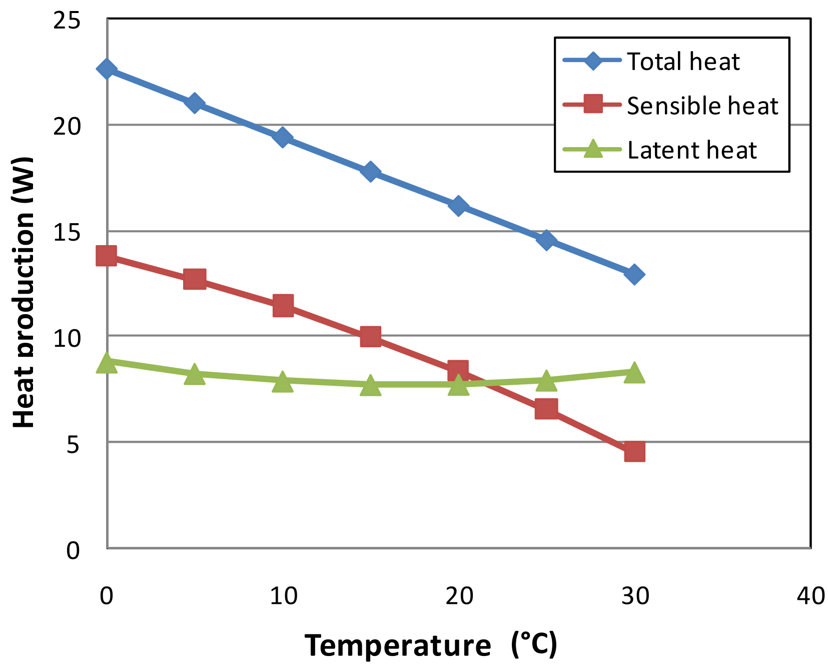

Figure 1.1. Total, sensible and latent heat production as a function of temperature for a broiler at 1.75 kg.

It is important to point out broilers are exposed to very different conditions in barns versus in transport vehicles. Prior to and during transport, broilers are deprived of feed and water. For example, feed may be withdrawn 2 to 4 hours prior to loading and water may be unavailable to the birds 1 hour before loading. Because litter is not used in transport trailers for broilers, wastewater has no opportunity to be absorbed in the litter. Therefore, the duration of feed and water withdrawal prior to transport will affect the amount of waste produced by birds during transport, which in turn will affect the amount of moisture produced. In addition, the movements of broilers are not restricted inside commercial barns. They are allowed to stand, sit, walk, extend/contract their feathers and body parts as they wish. During transportation, broilers are placed inside confined containers and their movements are very much restricted. Due to the small dimensions of the containers (height wise and others) and the high loading density, broilers have to assume a sitting position, keeping their wings and neck contracted during transportation.

Birds cannot self-regulate their body temperature by extending their body parts as they normally would when exposed to warm conditions in barns. Under cold conditions, broilers would huddle in transport containers to limit the amount of heat being released to the air, but their mobility is limited by the confined spacing. The air temperature which the broilers are subjected to, the level of radiation loss or gain from surfaces, and the level of air velocity which surrounds the animals are also very different during transportation.

All these differences suggest the heat and moisture production data obtained in commercial barns cannot be applied directly to broilers inside transport trailers. Changes in feed and water withdrawal practices, bedding, behaviour, physiology, and ambient conditions will affect the heat and moisture production rates. Data documenting heat and moisture production rates in cold environments, consistent with those found in transport trailers in western Canada, were not available in the literature at the time when this study was carried out.

At relatively warmer ambient conditions, Kettlewell et al. (2000) measured the heat and moisture production rates for broiler chickens on a truck and drawbar trailer equipped with a mechanical ventilation system in the UK In the six tests conducted, the broiler final live weight ranged from 1.66 to 1.81 kg. The inlet temperature ranged from 9.4 to 17.4^{o}C, the outlet temperature ranged from 14.8 to 25.4^{o}C, and the ventilation rate ranged from 2.65 to 5.34 m^3/s. Under these conditions, the total heat production of broilers varied from 4.6 W/kg to 13.3 W/kg (of live weight). The latent heat represented 40.6 and 35.5% of total heat production at each of these conditions, respectively.

Considering the scenario in which the birds produce heat at the highest published rate of 13.3 W/kg (Kettlewell et al., 2000), a fully-loaded 16.15-m trailer, carrying 8 892 broilers at 1.75 kg/bird, will generate 134 kW of sensible heat and produce moisture at a rate of approximately

108.8 kg/h (with an enthalpy of vaporization (h_{fg}) at 2 430.5 kJ/kg). Clearly, the combination of heat and moisture production during transport is a significant issue. To avoid the presence of localized hot spots and condensation within the load, the excess heat and moisture must be removed. It's important to note that the heat and moisture production rates developed by Kettlewell et al. (2000) were evaluated at relatively warm ambient conditions. The amounts of heat and moisture produced may differ in colder conditions presented by Canadian climates.

1.2.3 Climatic Conditions on the Canadian Prairies

The climatic conditions on the Canadian Prairies are unlike many regions around the world. Because much of the scientific information relevant to poultry transportation originated in the United Kingdom, it is important to compare the ambient conditions between the two locations. Table 1.2 lists temperatures for different cities on the Canadian Prairies and in the UK These temperatures are commonly used to design heating and ventilation systems and are based on long-term hourly observations of at least 12 years of data (ASHRAE, 2001). Based on these values, the summer climatic conditions in Saskatchewan were slightly hotter and drier than in the UK The winter data demonstrate significant differences between the two regions. The winter design temperatures in Western Canada were below -30˚C, which is considerably colder than the winter design temperatures in the UK

Table 1.2. Climatic conditions used for design of heating and cooling systems in Canada and United Kingdom (ASHRAE, 2001).

		SUMMER [1]		WINTER [2]
		Temperature (˚C)	Relative Humidity[3] (%)	Temperature (˚C)
Canada	Saskatoon, SK	30.6	28.11	-34.8
	Wynyard, SK	29.6	32.28	-34.1
	Winnipeg, MB	30.8	36.78	-32.8
	Calgary, AB	28.5	25.73	-30.0
	Edmonton, AB	27.6	35.82	-33.4
UK	London, Gatwick	26.4	46.45	-5.6
	London, Heathrow	27.4	43.59	-4.0

[1] On an annual basis, the summer temperatures (dry and wet-bulbs) is above this design value 0.4% of the time (35 hours in a year of 8760 hours).

[2] On an annual basis, the winter temperature is below this design value 0.4% of the time (35 hours in a year of 8760 hours).

[3] The relative humidity values were calculated based on the dry-bulb and mean coincident wet-bulb temperatures from ASHRAE (2001).

The extreme winter conditions on the Canadian Prairies result in a unique challenge for ventilation of spaces housing animals. Ambient air at lower temperatures is capable of absorbing less moisture than warmer air. Assuming a consistent rate of moisture production by animals, the excess moisture (not absorbed by the ventilated air) will condense and possibly freeze on the trailer infrastructure or animals in winter temperatures. Condensation is undesirable, as animals become wet and will become less tolerant to cold temperatures (Hunter et al., 1999). Thus, transport equipment designed in the UK and the associated practices and processes for comparatively warmer conditions are likely not directly applicable for winter conditions on the Canadian Prairies.

1.3 CONDITIONS INSIDE COMMERCIAL TRANSPORT SYSTEM

1.3.1 POULTRY TRANSPORT RESEARCH AROUND THE WORLD

Barbosa Filho et al. (2009) conducted a research project to monitor the microclimatic condition inside commercial trailers transporting broilers. Temperature and relative humidity data were collected from farm to slaughterhouse inside three shipments. The field tests were conducted under the Brazilian winter conditions, with an average ambient temperature of around 21 ˚C and a relative humidity of 63%. The traveling distance ranged from 15 to 30 km, corresponding to transport time of 15 to 40 minutes. The three tests were conducted in three different time of the day: morning, afternoon or evening. By placing 47 data loggers inside the transport containers, the average temperature and relative humidity in the load were found to be 22.4˚C and 67% in the morning trial; 25.2 ˚C and 89% in the afternoon trial; 22.8˚C and 78% in the evening trial. Barbosa Filho et al. (2009) concluded the morning is a better time to transport animals for processing.

Ritz et al. (2005) conducted a study in U.S. (Georgia) to evaluate the effect of hot weather conditions during the live haul process. Sensor globes were placed in the midst of broilers in barns prior to loading and later transferred into transport containers during loading. The sensors were used to monitor the temperatures which broilers were subjected to during the entire live haul process (precatch to live-hang). Data was collected on 24 commercial trailers. Ritz et al. (2005) observed temperatures during catch, lairage prior to transport, and lairage prior to unloading were higher. These segments of the transportation process could potentially induce heat stress to the animals.

1.3.2 POULTRY TRANSPORT RESEARCH IN CANADIAN PRAIRIES

A poultry transport research program was established in 1999 at the University of Saskatchewan (U of S), in response to the need expressed by a local poultry processing company. In phase one of the program, the main objective was to characterize the conditions to which broiler chickens were exposed during transportation on the Canadian Prairies. Initially, four preliminary tests were conducted to monitor load conditions from farms to the processing company under winter conditions. The transport conditions found inside the commercial 53-ft semi-trailers were reported in Knezacek et al. (2010). The temperature inside the transport modules was heterogeneous, ranging from 10.9 to 30.7, -0.7 to 16.5, 8.9 to 28.1, and 2.5 to 26.1˚C, at average ambient temperature of -7.1, -18.4, -27.1 and -28.2˚C, respectively (Knezacek et al., 2010). Deep body temperatures were recorded by implanting sensors inside some birds, rectal temperatures were also collected using an electronic temperature probe. Presence of wets birds, condensation and frost were observed in some locations inside the semi-trailers. The heterogeneous temperature and humid environment found inside the transport system were non-ideal transport conditions for broilers.

At a later time, an additional 27 trips were monitored, where the ambient air temperature ranged from -27.2 to 21.9˚C. Data were collected from trailers using different ventilation vent configurations (with different loads of animals), which were representative of normal commercial practices. Temperature and relative humidity data were collected for air surrounding the broilers inside commercial 53-ft semi-trailers. Results of these tests and trailer configurations were reported in Knezacek (2005). These field tests confirmed thermal heterogeneity was found inside the cargo area of the transport vehicle. Broilers were subjected to more challenging transport conditions in winter than in summer (Knezacek, 2005).

Figure 1.2 summarizes data collected by Knezacek (2005) during the last 27 trips. As ambient temperature decreased, the range of heterogeneity widened. The maximum air temperature inside shipping drawers remained fairly constant, independent of ambient temperature. This may be caused by the fact that different vent configurations were used to ventilate the load. However, when ambient temperature decreased, the minimum air temperature inside shipping drawers also decreased. Figure 1.2 shows that in cold weather, broilers were subjected to more heterogeneous transport conditions, as indicated by the wider range of exposed temperatures. In winter, non-insulated side curtains were usually lowered in the hope of providing some protection to broilers against the severe cold temperature, wind or snow. The edges between the curtains and the trailer supporting structure were not sealed. Knezacek's work identified the presence of cold spots near these edges, which suggested cold air entered the load through these unintentional inlets. The presence of hot spots was also discovered near the front end of the trailer. Broilers were found wet, and on occasion, frost was accumulating on shipping drawers in positions near side curtains. In summary, Knezacek's work identified the presence of severe heterogeneous transport conditions in cold weather, and suggested that the ventilation in commercial semi-trailers was ineffective.

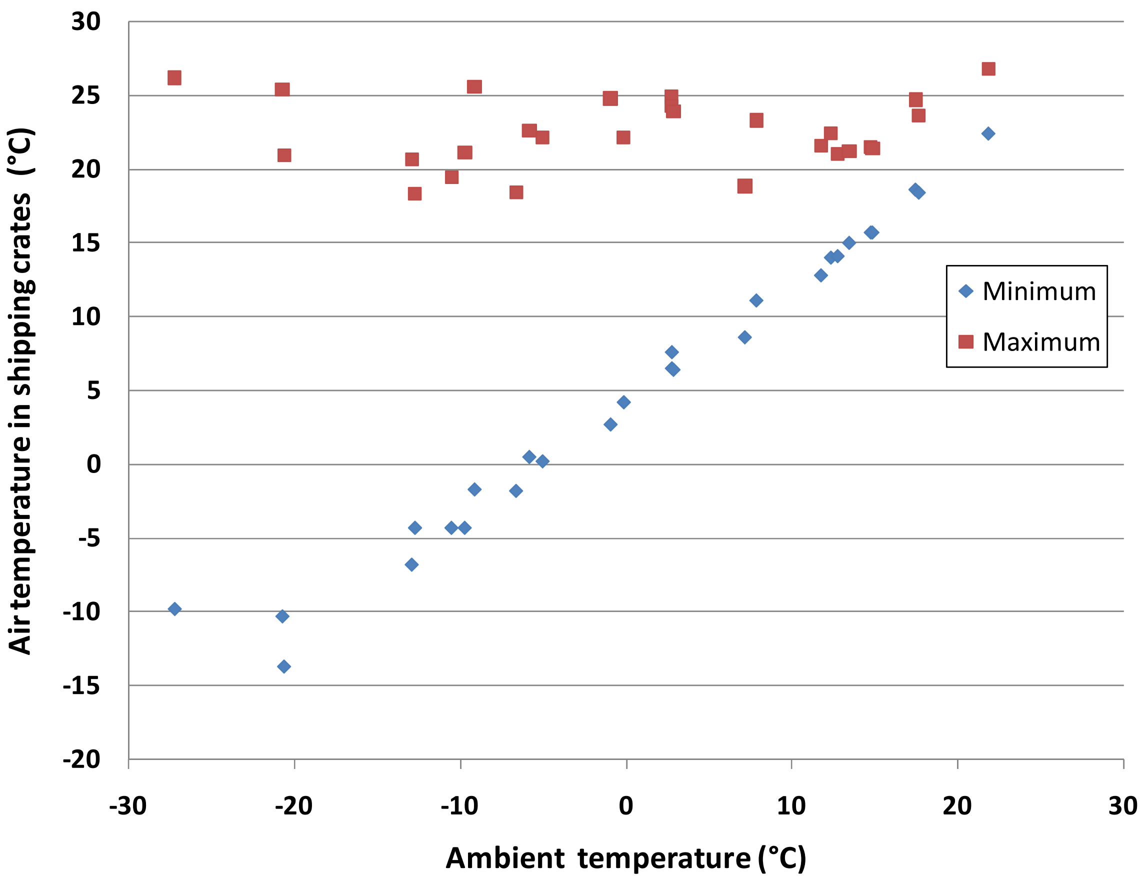

Figure 1.2. Air temperature during transport in shipping drawers as a function of ambient temperature (chart generated using data from Knezacek (2005)).

After examining the problem in phase one of the U of S broiler transport program, the second phase was initiated. The overarching goal of phase two was to investigate means to improve the transport conditions for broilers in winter. The approach was to design and build an experimental trailer that would allow the merits of active ventilation and supplemental heat to be evaluated. The research project documented in this dissertation is part of the phase two of the research program. Aside from evaluating the concept of utilizing active ventilation and supplemental heat in a transport system, this research project also examined the use of CFD to model the environmental conditions found inside the experimental trailer.

1.4 COMPUTATIONAL FLUID DYNAMICS

1.4.1 WHAT IS CFD?

CFD stands for Computational Fluid Dynamics. It is a technique which utilizes numerical method for solving partial differential equations which govern fluid dynamics and heat transfer. It can be used to study behaviour of fluid within or surrounding solid structures (internal or external flow). The development of CFD is closely linked to the development of computers. This modeling method was developed at the beginning of the 20th century. With the availability of faster and cheaper computers, it gradually gained popularity among researchers and engineers to use it as a modeling tool to study problems, design systems and processes. Historically, CFD followed in the developmental footsteps of numerical modeling for structural analysis. Relatively speaking, CFD is not as mature as structural analysis due to its higher computational demands and greater complexity in its governing equations.

The governing equations being solved by CFD are *Continuity*, *Navier-Stokes*, and *Energy* equations. These equations govern the fluid dynamics and heat transfer processes. These three equations can be simplified if the flow is incompressible, steady or one-dimensional. Depending on the complexity of the problem, other "secondary" equations such as turbulence models, porous media models, radiation models, natural convection models, and others are incorporated into these governing equations and must be solved. Within each category of the secondary equations, there are often different options available, and the theory behind some of them are not yet conclusive (such as for turbulent flow). In fact, one of the main challenges in CFD lies in selecting the secondary equations which best describes the problem. There is an entire field of research which focuses on testing these secondary equations in CFD problems to learn how they affect output results. Many of the governing and secondary equations are functions of the properties of the fluids involved in the process, and the solid materials which are in contact with the fluids. Therefore, values of the properties of the fluids and solids must be known in order to conduct a CFD analysis. Properties can specified as constants or variables. In cases where there are large variations of temperature or pressure in time or space, the properties become functions of other variables. Trying to determine the correct values of these properties certainly add another layer of complexity to the CFD analysis.

There are many different branches of CFD methods. The classical methods with the longest history are finite difference method (FDM), finite element method (FEM), and finite volume method (FVM). Within these branches, there are other sub-branches and hybrid modeling methods. The finite difference method and finite element method were first applied to the field of structural analysis and were later used to study the fields of fluid mechanics and heat transfer. Among the various CFD methods, one of the main differences is how the governing equations are transformed from continuous differential equations to discrete algebraic equations, a process known as "discretization". For example, the derivative is approximated by a truncated Taylor-series expansion in FDM, and it is approximated by a polynomial in FEM. As for FVM, the derivative is first approximated by a truncated Taylor-series expansion, and then it is integrated over a defined volume (thus the origin of the name "finite volume" method). There are other ways to discretize the equations within each category of FDM, FEM and FVM, some of them result in higher accuracy at the expense of higher computing power. Some CFD methods can handle complex, irregular geometries more readily than others. Many researchers devote their careers to developing and comparing these CFD methods.

In general, all these CFD methods follow a similar process in solving a problem. The first step is "*identification of the domain of interest*". The main considerations are the physical dimension (1-D, 2-D or 3-D), temporal dimension (steady or unsteady), the size and the boundaries of the problem. The higher the physical and temporal dimensions, the more computing power will be required as they affect the number of variables involved, the complexity of the governing equations and the complexity of the algorithm in solving them. The size of the problem will also affect the requirement of computational power. Problems involving larger physical dimensions require more computing power. Thus, it is common to study only half or a portion of a domain if symmetry exists. As for the boundaries of the domain, they need to be defined such that boundary conditions can be readily measured, known and applied. For internal flow, the domain of interest is usually an internal space which has well-defined boundaries, with inlets and outlets where the boundary conditions could be measured. However, if the boundary condition is not measurable because it is not accessible, a location further upstream or downstream where boundary conditions are known should be included in the domain of interest. Careful considerations are required to identify the domain of interest as it may affect the setup of the experiment and the CFD model.

Next, the physical domain has to be recreated in a virtual geometry: "*Geometry creation and clean-up*". Based on the physical dimensions of the domain, the virtual geometry is generated on a computer. The geometry can be created from scratch or based on CAD (computer-aided design) models. It can be done by writing computer codes or using software packages. In this step, assumptions are usually made to simplify the virtual geometry in order to simplify the meshing process. Of course, careful considerations should be taken when simplifications are made. In cases where geometry is created from scratch, it can be done using either a "bottom-up" or "top-down" approach. In the first approach, solids are built from points to lines to surfaces to volumes. In the later, volumes are created, then sliced, deleted or joined until the final shape is obtained. In cases where the geometry is created from CAD models, efforts are usually taken to "clean up" the CAD models to delete non-essential components, to repair broken lines, to fill in empty gaps, or to sub-divide volumes for meshing.

The third step in the CFD analysis is "*meshing*". It basically means the geometry is sub-divided into smaller cells, creating a grid or mesh. "Nodes", "nodal points" or "grid points" are also defined either at the intersections of gridlines or at the middle of a cell depending on the CFD method being employed. It is at these nodes where the algebraic equations are solved. Boundary conditions are applied at the boundary nodes. Meshing can be done by self-programming or using software package. Meshes come in different shapes, such as quadrilaterals (quads), triangles (tris), hexahedra (hexes), tetrahedral (tets), square pyramids, etc. (CFD Online 2007). They can be 2-D or 3-D, uniform or non-uniform, structured or unstructured or hybrid. Much effort has gone into developing algorithms to create meshing programs in the hope of requiring less input from users, nonetheless, it remains a time-consuming process for real-life problems. Both "geometry creation and clean-up" and "meshing" are commonly referred to as "pre-processing".

The next steps are known as "*discretization of governing equations*" and "*discretization of boundary conditions*". The governing equations and boundary conditions are transformed into algebraic equations. Different methods as mentioned earlier (FDM, FEM, FVM, etc.) are used to replace the derivatives in governing and secondary equations, thus transforming differential equations to algebraic forms. These equations are functions of variables of interest (velocity, temperature, pressure, etc.), properties, distances and time. The discretized governing equations are applied at the nodes inside the domain, whereas the discretized boundary conditions are applied at the boundaries. Ultimately, a system of algebraic equations, formatted in a matrix is developed. The system of equations includes constants and variables, and the variables are functions of other variables and constants. The system of equations also specifies how the values of the variables change with space and time.

The final steps are *"solving"* and *"post-processing"*. The algebraic equations are solved using various algorithms, sometimes iteratively for non-linear equations. In the iterative approach, initial values are applied at all internal nodes, the solving process is triggered by boundary values, and the program proceeds to calculate and recalculate values for the variables until the results meet the predefined convergence criteria. If the problem is non-steady, there will be second loop and second set of convergence criteria to handle the "time-step" progression. Finally, the massive amount of data is then "post-processed", i.e. plotted and analyzed. Many CFD data are presented as contour plots, line plots, histograms, scatter plots, animations, etc. Just like discretization, these two steps can be accomplished by self-programming or using a software package.

In summary, the seven steps in solving a CFD problem are "identification of the domain of interest", "Geometry creation and clean-up", "meshing", "discretization of governing equations", "discretization of boundary conditions", "solving" and "post-processing". Many researchers have devoted entire careers to improve one or several of these steps. In some cases, academics have written stand-alone computer code for research or teaching purposes. Indeed, writing one's own program is the best way to gain a deep understanding of CFD, how it works, its basic assumptions, the various techniques and options. Often these computer codes are usually limited to small-scale problems, simple geometry and simple physics. For more complex problems, many engineers are using commercial software. Nevertheless, it is still **essential** to acquire some theoretical background in order to use these commercial software packages intelligently.

When commercial software is used to conduct CFD analysis, it is common to use one package to generate the geometry, one to generate the mesh, another to solve the set of equations and several others to perform the post-processing. Therefore, in addition to having a good knowledge of fluid dynamics, heat transfer, CFD theories, and a comprehensive understanding of the problem; the analyst will need to learn multiple software packages (both technically and theoretically) in order to conduct a CFD analysis. Also, just like other modeling techniques, technical skills are required to collect experimental data, and analytical skills are required to calibrate and validate the model to ensure results generated by the CFD model reflect reality. Therefore, conducing CFD analysis is not an easy task.

Despite the considerable efforts and computing resources required to conduct CFD analyses, it is indisputable that CFD remains a very powerful modeling tool. Many engineering processes and natural phenomena involve fluid dynamics and heat transfer, thus engineers are encouraged to utilise CFD to study these problems. It is the collective efforts of the CFD users which will help to bring this modeling technique to its next level of maturity, to spread its popularity and to lower its cost.

1.4.2 CFD RESEARCH IN THE LITERATURE

Most of the CFD models developed for agricultural applications were devoted to ventilation and heat transfer studies for greenhouses, or to ventilation and air quality studies for animal-confinement buildings. One study used CFD to investigate the ventilation system within a day-old chick transport system (Quinn and Baker, 1997). No other research study has developed a CFD model to examine the conditions experienced by broilers while in transport.

The following paragraphs summarize some CFD research which either inspired the current work or examined broiler housing facilities.

One element of the CFD model developed for the current project was the use of a porous-media model to simulate the loading area of the experimental trailer filled with closely packed broilers. The experimental trailer can be filled with several thousands of individual animals, with the total head count and physical locations varying from tests to tests. Thus, some sort of simplification was required to eliminate the need for creating thousands of individual animals in the geometry and to prevent the need for using highly irregular and fine mesh between the air space and animals. Moureh et al. (2002) published a paper describing a CFD study of a refrigerated semi-trailer using the FLUENT commercial software. The model was validated by a 1/3.3 scale model in a lab setting. Although the setup of a refrigerated semi-trailer was very different from a poultry transport trailer, there are striking similarities between the two cargoes from the perspective of distributed small spaces within the loads. Moureh et al. (2002) eliminated the need to create a very fine mesh for these air spaces by simulating the load as a porous medium. A particular permeability coefficient was selected to match the airflow resistance as created by the air spaces (Moureh et al., 2002). Although the CFD model developed in the present study is different from the CFD model developed by Moureh et al. (2002), their research was an inspiration to investigate the various porous media models available in FLUENT to simulate the geometry in the experimental trailer.

Seo et al. (2006) developed several CFD models to compare the efficiencies of various ventilation systems in broiler housing units. Using the CFD models developed in FLUENT, the authors were able to quantitatively and qualitatively examine the air flow patterns and temperature uniformities among the various ventilation designs. The authors concluded that CFD analysis was an effective tool to study the design of ventilation systems in broiler housing units. Pawar et al. (2007) studied the airflow around and inside a laying hen facility using CFD models developed in FLUENT. This study examined the relationship between disease propagation and ventilation regime. Two 2-D CFD models were developed, using mostly rectangular cells to reduce the number of cells required, which also improved the speed of convergence. Triangular cells were used only in regions to provide smooth transitions between geometrical entities. While they were not validated with experimental data, the CFD models ranked ventilation regimes in their ability to reduce the spread of contaminant.

Saraz et al. (2010) developed a 3-D CFD model to study the temperature and airflow distributions in poultry housing units equipped with negative pressure ventilation and evaporative cooling systems, in Brazil. The geometry was meshed using ANSYS ICEM CFD using hexahedral cells, and the CFD analysis was conducted using ANSYS CFX. A normalized mean square error (NMSE) was calculated to compare experimental and simulated results. Twenty experimental data points were used and values of NMSE less than 0.25 were considered good for temperature measurements (Saraz et al., 2010). It was concluded that evaporative cooling within poultry housing units caused the temperature distributions to be less uniform.

Saraz et al. (2011) also presented a CFD model which studied ammonia emissions in a broiler barn with natural ventilation. The modeling exercise was intended to reduce the number of experiments required to study the emission problem in Brazil. Again, ICEM CFD was used for meshing, CFX was used to conduct the CFD analysis and NMSE was used to compare experimental and simulated data. The study looked at the air velocity and temperature distributions, as well as the ammonia flux distribution. In addition to using the CFD model to optimize the design of naturally ventilation broiler housing units, the authors concluded the model could be used to determine the appropriate distance between broiler houses to minimize ammonia gas transfer.

Quinn and Baker (1997) investigated the possibility of using CFD to study the ventilation system inside a day-old chick transport system. The chick transport system was 7.2-m long, 2.35-m high and 2.4-m wide. The ventilation system was located at the front end of the trailer and it circulated air from front to rear and back to the front. The ventilation system employed positive pressure to push air through the system, similar to the system employed in the refrigerated semi-trailer studied by Moureh et al. (2002). Quinn and Baker (1997) developed a CFD model using PHOENICS software and conducted a series of experiments to validate the air velocity data. It examined the 3-D velocity components in four loading configurations: no load, front half loaded, side half loaded and fully loaded (Quinn and Baker, 1997). The experiment was conducted in a stationary full scale model. Data were collected using a three component ultrasonic anemometer, and approximately 200 measurements were made in each of the first three loading configurations (75 measurements for the fully loaded configuration; Quinn and Baker, 1997). This study conducted statistical comparisons which looked at the percentage of the simulated data which fell within three standard deviations of the experimental mean (Quinn and Baker, 1997). The paper did not specify the number of replicates or the minimum sampling size. The model developed by Quinn and Baker (1997) was able to predict the mean ventilation flows, but it failed to successfully predict the turbulence measurements. The several studies presented above demonstrate CFD is a useful tool to complement experimental work in studying complex agricultural problems.

1.4.3 WHY USE CFD FOR THIS STUDY?

The study of some engineering systems involves trial-and-error iterations. It is common to build a prototype, test it under field conditions, modify it and retest the prototype until its performance is deemed satisfactory. The traditional "hands-on" approach is labour, cost and time consuming, especially in the case of large-scale experimental research. In case of this poultry transportation study, each test required several days to complete, involving half a dozen research personnel. Each test took at least one day for setting up the sensors and packing all required materials in the field. The experiment lasted 24 continuous hours. Afterward, it took at least half a day to clean up the sensors and download data. This did not include the time spent on logistics such as hiring students to assist with the experiment, scheduling among the various parties (processor, producer, university), getting approval from the animal care community to conduct the experiment, securing funding, and purchasing equipment and instrumentation, etc. In addition, the experimental trailer and equipment required regular maintenance to meet safety regulations, it needed to be refuelled and serviced.

Aside from the team of research personnel from the university, many other people were involved in each experiment. They included the poultry producer, loading crew and personnel from the processing company (truck drivers, unloading crew, veterinarian, managers, administrative staff). It was indeed cost, labour and time consuming to conduct an experiment in field conditions. It limited the number of replicates and the number of scenarios which could be tested. Furthermore, this research required the construction and building of a full-scale experimental trailer and the use of live animals. The cost of materials and labour required was considerably higher than the cost of purchasing computer equipment and software licenses.

Aside from cost, labour and time restrictions, conducting in-field tests also imposed other challenges. In this study, which involved live animals, there were risks involved. The risks associated with equipment failure or inclement weather are substantial. In addition, while it was ideal to gather data under real-life conditions, it did make the experimental conditions less "controlled". It was not possible to control the weather conditions, and it was not possible to reuse the same animals from test to test. The research team did not have control over the locations and conditions within which the animals were produced, nor was there any control over the timing of slaughter. Such variability created challenges in data analysis, making it impossible to isolate the variables and study one factor at a time. Furthermore, the presence of a research team may have modified the standard operating procedure and changed the practices of loading personnel. Special efforts were made to minimized disruptions from standard practices when implementing the experimental protocol, hoping not to modify the "real" field conditions.

This study also imposed special challenges from an instrumentation point of view. Because of the physical scale of the experimental and commercial trailers, sensor placement and quantity were carefully considered. While it would have been informative to install a sensor in each shipping drawer containing the animals, it was not economically feasible and it would have required considerably more time to install and retrieve the sensors, to process and analyze the data. On the other hand, the resolution of the data in a CFD model was largely dependent on the computational power which limited the mesh size. More "data points" existed in the CFD model than it was possible to collect during the experiment. The configuration of the systems also imposed restrictions on locations of sensors, possible types of sensors, and the type of data that could be collected. As most of the tests were conducted during the winter, and the trailers were washed after each use, the sensors were expected to withstand the outdoor environment and must be protected against water damage. These challenges created extra layers of complexity to the experimental setup, which is common in large-scale field experiments, but these challenges do not exist in CFD modeling.

One drawback of CFD modeling is that its accuracy is highly dependent on how well the model was calibrated and validated using experimental data. In general, a portion of experimental data sets are reserved to calibrate the model. The developer uses these data sets to evaluate equations, properties, or variables used to build the model. The goal of calibration is to determine what are the final settings of the model required to generate simulation results which match closely to the experimental data. Afterward, the remaining data sets would be used for validation, to evaluate the model's accuracy. Data used in calibration is not to be reused for model validation. Aside from the efforts required to develop a CFD model, calibration and validation require efforts to collect experimental data and analyse the results. Although not all researchers or engineers would (or are able to) invest resources to calibrate and validate their models, it is still desirable to do so, to ensure the accuracy of the CFD models.

In this particular research project, the CFD model was used as a tool to complement the experimental research. A number of tests were conducted to gain a basic understanding of how well the experimental trailer worked. After calibrating and validating the CFD model using the experimental data, it was used to study a variety of "what-if" scenarios. Using the CFD model reduced the amount of time and resources required to study different scenarios. It did not require the use of animals which eliminates any risk to them. Therefore, after calibrating and validating the CFD model with experimental data, it became a useful tool to simulate, understand and predict the environmental conditions to which the broilers were exposed during different transport conditions.

1.5 RESEARCH OBJECTIVES

A research program was developed aiming to improve the transportation conditions of broiler chickens. As part of the research program, a project was developed with the following research objectives:

1. design and construct an experimental trailer equipped with active ventilation and heating;
2. characterize the performance of the experimental trailer in field tests under Canadian Prairie winter conditions;
3. develop, calibrate and validate CFD models used for simulating the environmental conditions surrounding the broilers as found inside the experimental trailer; and
4. utilize one of the CFD models to predict the performance of the experimental trailer using conditions which may be encountered by the poultry transport industry.

A series of four papers were prepared, each one covering one of the objectives as listed above. These papers are presented as Chapters 2 to 5 in this dissertation. The last chapter, Chapter 6, summarizes major findings in this research project, discusses future work and presents final conclusions.

PREFACE TO CHAPTER 2

The following chapter is the first paper of a series of four papers. It focuses on the first objective of the research project: the design and construction of an experimental trailer equipped with active ventilation and heating.

This paper first reviews the designs of commercial poultry transport equipment and how they affected the design of the experimental trailer. The setup of the experimental vehicle is then discussed in detail, providing background information for the second paper, which discusses the performance of the experimental vehicle.

Documentation of the trailer designs was completed by K.P.C. Hui. The experimental vehicle was designed and constructed, using a team approach by M.R.L. Bantle, T.G. Crowe, K.P.C. Hui, E.M. Barber, H.L. Classen and staff members of the University of Saskatchewan. The instrumentation system was designed and installed by K.P.C. Hui, assisted by technical staff at the University. The electrical system was designed by K.P.C. Hui and installed by technical staff at the University of Saskatchewan.

2 DESIGN AND CONSTRUCTION OF AN ACTIVELY HEATED AND VENTILATED POULTRY TRANSPORT VEHICLE

K.P.C. Hui, T.G. Crowe, M.R.L. Bantle, E.M. Barber, H.L. Classen

The authors are K.P. Catherine Hui, **ASABE Member and Professional Engineer,** Graduate Student; Dr. Trever G. Crowe, Myles R.L. Bantle and Dr. Ernie M. Barber, **ASABE Members and Professional Engineers**; Dr. Hank L. Classen, University of Saskatchewan, Saskatoon, SK, Canada. **Corresponding author:** Dr. Trever Crowe, College of Graduate Studies and Research, University of Saskatchewan, C 180, 105 Administration Place, Saskatoon, Saskatchewan, S7N 5A2, Canada; phone: (306) 966-2229; fax: (306) 975-1026; e-mail: trever.crowe@usask.ca.

Abstract. *The harsh winter conditions on the Canadian Prairies impose special challenges in providing acceptable environmental conditions for broiler chickens during transport. Previous research conducted by the University of Saskatchewan demonstrated that broiler chickens were exposed to heterogeneous temperature and humidity conditions during transportation in extreme Canadian Prairie climates. Field observations indicated some animals were subjected to cold and wet conditions, while others on the same truck experienced warm moist conditions during transportation. These field results demonstrated passive (natural) ventilation systems employed in commercial vehicles were ineffective in removing large amounts of animal-produced heat and moisture from the loading area in the trailer. A multidisciplinary study was conducted by researchers of the University of Saskatchewan in collaboration with a commercial poultry processor. The overall objective of the research program was to improve the environmental conditions for chickens during transportation.*

In one of the early stages, a 13.7-m (45-ft) long experimental trailer equipped with active ventilation and supplemental heating was developed. This paper provides an overview of the economic, legislative, and logistical aspects surrounding the poultry transport industry in *western Canada. It also discusses the need to develop new innovative transport equipment in response to the climate and animal-specific demands. Furthermore, this paper reviews the design of some commercial transport equipment, and it provides a detailed description of the design and commissioning of an experimental trailer equipped with active ventilation and supplemental heating.*

Keywords. *Poultry, broiler, transport, ventilation, heating, animal welfare.*

2.1 INTRODUCTION

Two poultry processors currently exist in Saskatchewan. They are located in Wynyard and Saskatoon. Each processor services farms at different locations and use different styles of transport equipment. At the time when the U of S trailer was tested, only the Wynyard processing plant, owned by Lilydale Inc., existed. At that time, broiler chickens were transported for distances from 5 to 400 km, and the most common travel distance was about 200 km. Lilydale Inc. used 16.15-m semi-trailers known as a “53-ft semi-trailer”, and pairs of 8.53-m (28-foot) and 9.75-m (32-foot) trailers known as a “B-Train” to transport broilers from dispersed farms to the processing plant in Wynyard. These transport vehicles were not equipped with any active ventilation or sources of supplemental heat. Concept 2000 was the first commercially available poultry transport trailer equipped with mechanical ventilation. It was developed by a team of researchers based in the UK (Roslin Institute 2000, ASAE 2001, BBSRC 2002). The following sections review the designs of the 53-ft semi-trailer, B-train, Concept 2000, and how they inspired the design of the University of Saskatchewan’s experimental trailer.

2.1.1 COMMERCIAL HANDLING AND TRANSPORT EQUIPMENT

Different designs of broiler handling and transport equipment existed in the market. Many broilers were collected manually by loading personnel, and birds were placed either in individual crates or in a modular system. In the case of the older crate system, crates were stacked individually inside the transport vehicle. The crate and modular systems differed in their cost, holding capacity, the requirement for forklift accessibility in barns and the availability of other handling equipment. Some barns were built as a two-floor structure, making them more amenable to the crate system. The modular system facilitated the use of a forklift which can handle more birds within a palletized unit. In the modular system, a forklift could handle two modules at a time as they could be stacked one on top of the other. The modules could also be handled by an automatic truck unloading system, which lifted up to 22 units at a time. Meyn (2009) claimed, using such a system, it could empty the entire European size trailer in five minutes.

In some cases, broilers were collected from the barn floor using a mechanical harvester. A specific version of a mechanical harvester consisted of several large vertically-oriented rotating cylinders. Each cylinder had many rubber fingers protruding radially, making it look like a large brush. As the harvester moved around the barn, the rubber fingers gently brushed the broilers into a windrow and directed them to a series of conveying belts and bins. The birds could then be loaded into transport containers (crates or modules) or directly into the transport vehicle using conveyors. In a mechanical loading system (Peer system, 2006), the trailer was subdivided into multiple horizontal levels, and each level had a conveyer platform which moved birds from the rear of the truck to the front during loading; the direction of conveyance was reversed during the unloading process. When the mechanical harvester was used with the mechanical loading system, the broilers did not come in contact with loading personnel. These mechanical systems require a greater initial investment but they minimize the requirement for manually handling birds and reduce personnel costs.

2.1.1.1 Easyload Modules

The industrial collaborator in this research project employed “Easyload Modules”, as shown in Figure 2.1, in their transport fleet. These same modules were used in the design of the experimental trailer to simplify logistics involved in the loading, unloading and placement of the modules inside the vehicle.

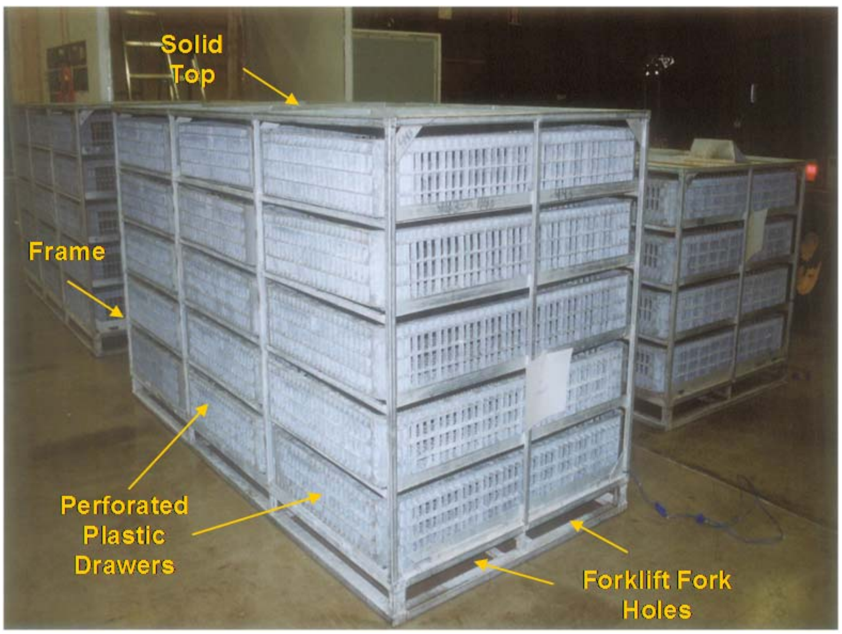

Figure 2.1. 5-Drawers and 4-Drawers high modules used for transportation of broiler chickens.

The Easyload modules were designed by Anglia Autoflow Ltd. based in England (Anglia Autoflow Ltd., 2002). Each module consisted of a steel frame with a set of perforated plastic drawers as shown in Figure 2.1. The module had a solid top surface, and openings at the bottom to allow handling by a forklift. Each module contained three drawers in width, and four or five levels of drawers in height. Thus, a single module held 12 or 15 drawers. The internal dimensions of each drawer were approximately 0.711 m (28 in.) wide, 1.118 m (44 in.) deep and 0.194 m (7.625 in.) high. Typically, each drawer was loaded with 22 to 26 birds, depending on their live weight, translating into 0.031 to 0.036 m^2 of area per bird. During loading, birds were deposited into the module by sliding open the drawers. The entire module was then loaded onto the trailer from either of the two sides using a forklift. A "stack" of modules was comprised of two modules, with one placed on top of the other.

2.1.1.2 53-ft Semi-Trailer

The "53-ft" semi-trailer was named after its length. It was 16.15 m (53 ft) long, and it had a step in the front, resulting in the rear portion being 0.46 m (18 in.) lower than the front portion as shown in Figure 2.2. With a total of 342 drawers, at a loading density of 22 to 26 birds per drawer, it could transport 7 524 to 8 892 chickens per trip. The envelope of the trailer consisted of a headboard, a tailboard and a roof. Retractable tarpaulins, which allowed the birds to be protected during transport in inclement weather, form the sides of the loading area (Figure 2.3). The position of the roof was fixed, and it was supported by metal beams along the length of the trailer. Ventilation openings were located along the centrelines of the headboard, tailboard and roof as shown in Figure 2.2. The sizes of the vent openings in the headboard and tailboard were variable and could be adjusted by manually sliding vent covers in horizontal tracks. The vents in the roof could also be adjusted manually. Roof vent covers were hinged along the length of the trailer and were either fully open or fully closed. Each vent covered a section of the roof and the pattern of vent openings was set by the truck driver upon loading of the birds. The fixed roof height required that free space be allowed above the top modules, as pallets had to be lifted up from the floor during loading and unloading. The height of the free space was approximately

0.33 m (13 in.) for modules on the front portion of the trailer and 0.53 m (21 in.) for modules on the rear portion. Additional photos of the 53-ft semi-trailer are included in Appendix B.

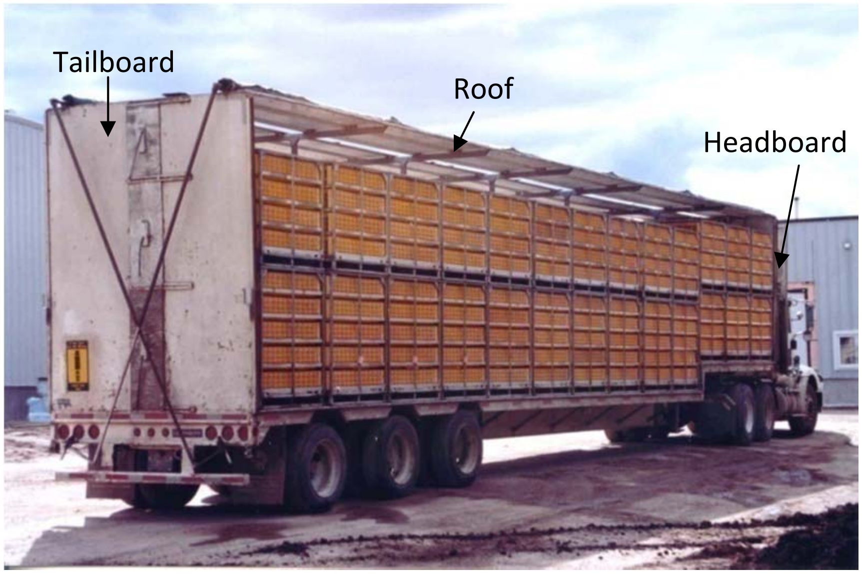

Figure 2.2. 53-ft semi-trailer with 13 Stacks of modules.

Figure 2.3. 53-ft semi-trailer covered with retractable tarpaulins.

2.1.1.3 B-Train Trailers

The "B-train" consisted of two trailers; the front one was 8.5 m (28 ft) and the rear one was 9.8 m (32 ft) long; they are connected in series as shown in Figure 2.4. This system had a higher load capacity than the single 53-ft semi-trailer. The B-train contained 441 drawers, and at a loading density of 22 to 26 birds per drawer, it could transport 9702 to 11,466 chickens per trip. The rear of the front trailer was 0.3 m (12 in.) lower than the front portion, while the deck of the second trailer was at the same height, from front to rear. Both trailers were equipped with headboards, tailboards and roofs. Similar to the 53-ft semi-trailer, the roofs on the B-train trailers were equipped with vents along the length of the trailer and hinged vent covers, which could be opened and closed manually. Headboards and tailboards were equipped with vents of similar design, which could be partially opened. The height of the roofs on B-Train trailers was not fixed. The roofs could be raised to facilitate loading of the modules, then lowered prior to transport (Figure 2.5). The trailers were designed as such that the tops of all modules were at the same height. Thus, when the roofs were lowered, there was virtually no space between the underside of the roofs and tops of the modules along the entire length of both trailers, making this design different from the 53-ft semi-trailer. The B-train was also equipped with side tarpaulins, which could be rolled up or down manually, similar to the 53-ft semi-trailer. Additional photos of the B-train trailer can be found in Appendix B.

Figure 2.4. High capacity B-Train trailers.

Figure 2.5. Raised roof on B-Train trailers for loading or unloading.

2.1.1.4 Passive Ventilation in Commercial trailers

Both the 53-ft semi-trailer and B-train trailers were ventilated by passive (natural) ventilation, meaning there is no mechanical system installed on these trailers to remove heat and moisture produced by the animals. The passive ventilation is driven by the movement of the vehicle. When the vehicle is in motion, positive and negative pressure zones are generated around the vehicle due to its aerodynamic design, similar to Figure 2.6. In commercial trailers, tarpaulins were loosely strapped along the two sides of the trailers. There were also vent openings on the roof, headboards and tailboards. Driven by the pressure differences surrounding the body of the trailers, air would move in and out of the loading area through the openings caused by the pressure gradients (from a relatively higher pressure zone to a lower pressure zone), generating passive ventilation for the animals.

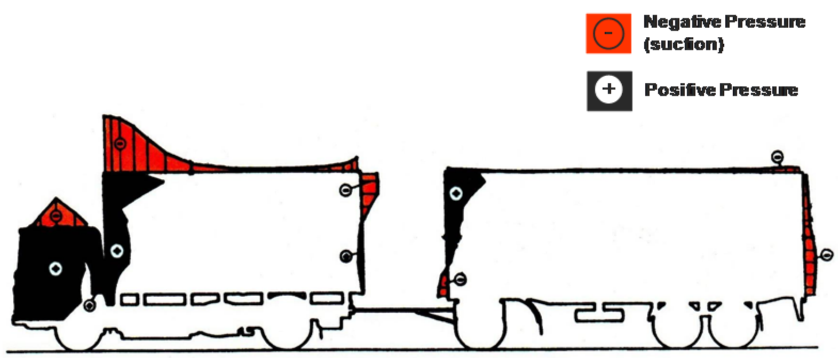

Figure 2.6. Pressure differences surrounding the trailers (adopted from Götz, 1987).

Previous experimental results indicated that cold temperatures existed along the edges of the 53-ft semi-trailer, and warmer temperatures could be found along the center and near the top of the load at the front of the trailer (Burlinguette et al., 2012). Negative pressure zones can be expected near the front and rear ends of the 53-ft semi-trailer, with the front end at greater negative pressure (Knezacek 2005). The experimental data suggested that air moved in from the sides, absorbing heat from the chickens and carrying it out through roof vents. Similar phenomena were observed in the front trailer of the B-train. For a B-train, as suggested by the temperature data, air probably traveled from rear to front in the front trailer. On the second trailer of the B-train, a hot spot was observed at the rear end. Thus, in the second trailer of the B-train, air probably traveled in the opposite direction, from front to rear, as driven by the negative pressure behind the second trailer.

These pressure differences around the trailers influenced the placement of ventilation fans on the experimental system. The main disadvantage of passive ventilation is it only functions when the trailer is in motion. When the trailer is stationary, no pressure gradient is created, thus no ventilation is provided. Thus, heat and moisture can accumulate within the load when the vehicle is stationary. Furthermore, the amount of ventilation is a function of travel speed, amount and location of vent openings, and the amount of air leakage. The ventilation cannot be easily controlled, making the system unreliable and resulting in large temperature gradients inside the load.

During transport, when there is a lack of facilities to protect animals against adverse weather conditions, it is recommended that trucks loaded with animals do not sit idle for more than 2 hours (Agriculture Canada, 1989). This recommendation is probably based on the fact that commercial vehicles utilize passive ventilation; there is no air movement or circulation when the vehicle is stationary. In summer, the broilers would become too hot. In fact, when there were delays in processing and the unloading dock was full, it was common to hear the processor asking their drivers to drive the vehicles around the processing plant to provide some ventilation for the birds in summer. In winter, the situation becomes more complicated, as side tarps are usually lowered to protect birds from cold weather, snow or wind. If the vehicle is held stationary for an extended period of time, bird heat and moisture will be trapped inside the trailer, and broilers will become wet. But, if the side tarps are raised, the broilers will be exposed to severe cold conditions. It is a delicate balancing act between providing adequate ventilation and protection from cold weather.

2.1.1.5 Concept 2000 Trailer

After several years of research in the transportation of broilers, a commercial transport vehicle equipped with mechanical ventilation was launched in May 1999 (BBSRC 2002). It was the final product of a multi-disciplinary research program led by Dr. Malcolm Mitchell and Mr. Peter Kettlewell. The Concept 2000 system was the first commercial-scale vehicle which employed ventilation fans to remove heat and moisture from within a poultry transport vehicle. The system could carry 11 stacks of modules (22 modules). It was equipped with its own generator to power its ventilation system, and it had sensors which monitored load conditions to provide warnings to drivers (Roslin Institute, 2000). A portion of the side curtains was made of perforated mesh, and there were extraction fans located on the front and rear headboards (ASAE 2001). During operation, the side curtains were lowered. Air would enter through the perforated mesh and was drawn forward or rearward, absorbing heat and moisture from the broilers, and exited from the front and rear fans. Both side curtains and the roof were insulated to reduce the effect of solar radiation, and the ventilation rate could be adjusted based on ambient conditions and the need of the birds (ASAE 2001). Additional photos of the Concept 2000 trailer are shown in Appendix B.

Figure 2.7. Concept 2000 developed by Drs. Malcolm Mitchell and Peter Kettlewell's research team in the UK (image taken from Roslin Institute (2000))

2.2 OBJECTIVE

This particular paper discusses the design and commissioning of the experimental trailer built for testing the merits of using active ventilation and supplemental heating for transportation of broilers in Western Canada's winter conditions.

2.3 EXPERIMENTAL TRAILER DESIGN

2.3.1 ACTIVE VENTILATION AND HEATING

In order to address some of the pitfalls of passive ventilation in commercial vehicles and to improve transport conditions for broilers in the Canadian Prairie's winter conditions, an experimental trailer was designed, built and tested by researchers at the University of Saskatchewan. The idea of adding supplemental heat to the ventilation air is original, as an approach to address the extreme winter conditions on the Canadian Prairies. According to ASHRAE (2001), the winter design temperatures in Western Canada are below -30˚C, which is much lower than the winter design temperatures in the UK (around -6 to -4˚C). Ambient air at -30˚C has little capacity to absorb moisture, thus the excess moisture (not absorbed by the ventilated air) may condense and freeze on the trailer infrastructure or animals in winter temperatures. Therefore, using active ventilation alone, as in Concept 2000, may not be suitable for Canadian Prairies' conditions. For the design of the experimental trailer, the research team decided to preheat the ventilation air to increase its moisture holding capacity prior to circulating it through the load. Preheating the air would also reduce the cooling effect of cold air coming in contact with the animals.

2.3.2 PHYSICAL STRUCTURE AND EQUIPMENT

The experimental unit was built on top of a 13.7-m (45-ft) long flatbed. It was approximately 2.5-m (8-ft) wide and 2.6-m (8.4-ft) high. The trailer was divided into three compartments: (1) instrumentation room, (2) heating and mixing chamber, and (3) loading area as shown in Figure 2.8. The loading area could accommodate six stacks of modules, with top modules made up of four layers of drawers, and the bottom modules made up of five layers of drawers. This resulted in a holding capacity of 162 drawers. With a loading density of 22 to 26 birds per drawer, it could transport 3 124 to 4 212 broilers per trip.

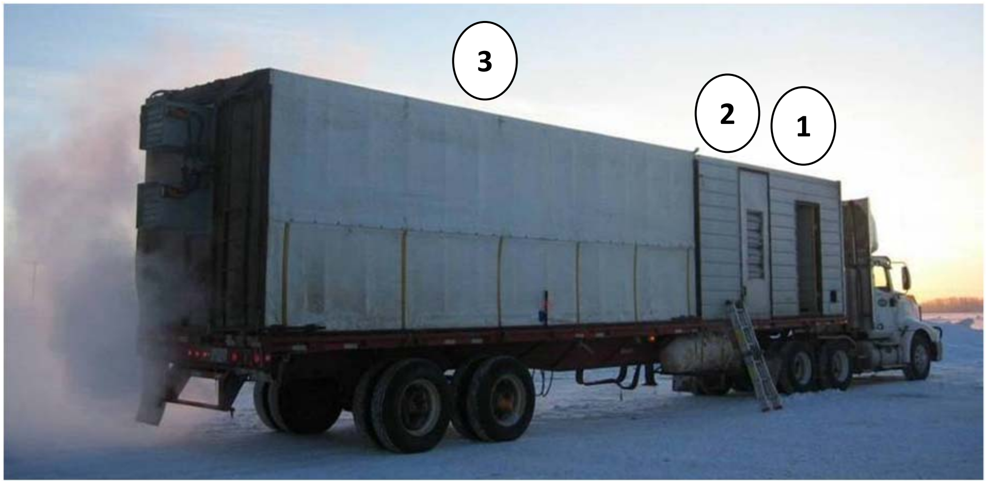

Figure 2.8. Experimental transport system with active ventilation and heating with (1) instrumentation room, (2) heating and mixing chamber, and (3) loading area.

The instrumentation room housed two gasoline powered electrical generators to power all the electrical systems on the trailer. The generators provided 120 and 240 VAC power to the trailer. It was also possible to power the trailer by plugging it into an electrical power outlet, which could come in handy for servicing. One programmable, multi-purpose controller (Supra 210000, Phason Inc., Winnipeg, Manitoba), two manual speed controls (MSC-4, Phason Inc., Winnipeg, Manitoba), one data acquisition system, and several 120-V power outlets were located inside the instrumentation room. The heating and mixing chamber was subdivided into two sections by a metal wall as shown in Figure 2.9. The section next to the instrumentation room included a programmable variable-inlet damper, two propane heaters, two manual-controlled mixing fans and several power outlets.

The inlet damper was installed on a side door, mounted on the right-hand side as viewed from the rear of the experimental trailer. The damper was connected to an actuator (AF24-MFT US, Belimo Americas (Canada), Mississauga, Ontario) to vary its opening area. This side door allowed easy access to the heaters as they needed to be turned on manually by pushing the start buttons. The heaters (S100, Sure Flame, Lethbridge, Alberta) and mixing fans (FC063-6EA.6F.1, Ziehl-Abegg AG, Künzelsau, Germany) were mounted on a metal frame on a pallet, with its dimensions similar to a stack of modules. The other side of the chamber was an empty space, acting like a plenum, providing additional empty area for air mixing. This area also housed a terminal box for the instrumentation system, and the necessary piping to supply propane to the heaters. The propane storage tank was mounted externally underneath the heating and mixing chamber, on the trailer chassis.

Figure 2.9. The heating and mixing chamber under construction (inlet damper not shown).

The loading area had three diffuser screens, two at its front entrance and one close to the tailboard. These diffuser screens had 25.4-mm (1-in) and 50.8-mm (2-in) opening slots on them which allowed air to pass through (as shown in Figure 2.10 and Appendix C). The 25.4-mm (1-in) opening slots were designed to direct air to the headspace above the animals inside each row of drawers, whereas the 50.8-mm (2-in) slots were directed to the perforated sidewalls of the drawers (Figure 2.1). Two diffuser screens were installed 50.8 mm (2 in) apart at the front end of the trailer, and the opening slots on these two screens were staggered, such that when the loading area was being washed, water could not easily pass through and enter the mixing chamber.

The loading area also had a set of three variable-speed exhaust fans (FC045-4EQ.4F.3, Ziehl-Abegg AG, Künzelsau, Germany) mounted at the tailboard of the trailer. The exhaust fans were wired to utilize 240 V power. These fans were positioned in a region where a negative pressure zone would develop behind the tailboard when the trailer is in motion. Therefore, placing the exhaust fans in the tailboard would take advantage of the aerodynamic characteristics of a moving trailer, facilitating the work of fans. The bottom fan was designed to operate continuously to provide the minimum ventilation to the load, while the middle and top fans were equipped with outlet dampers to seal the outlets to prevent short-circuiting of air flow when these fans were not in use (Figure 2.8). Each outlet damper was connected to an actuator to control its open/closed status (NF120-S US, Belimo Americas (Canada), Mississauga, Ontario). A second terminal box for instrumentation was placed in the empty space between the last diffuser screen and the tailboard for sensor connections.

Figure 2.10. The third diffuser screen located in front of the exhaust fans.

Different materials were used to construct the three compartments. Some surfaces were insulated, while others were not. The construction materials used for each compartment are summarized in Table 2.1. For the loading area, its floor and roof were both insulated with 50.8-mm (2-in) of pink Styrofoam to minimize heat loss. The tailboard was constructed from 19.05-mm (0.75-in) plywood and was not insulated. Similar to the commercial trailers, the two sides of the loading area were covered by tarpaulins. The tarpaulin on the left-hand side (viewed from the rear) was fixed to a metal frame. The tarpaulin on the right-hand side could be rolled up or down for loading and unloading of modules. Unlike the commercial trailers where the tarpaulins are loosely strapped along the bottom edges of the trailer, a special sealing system was designed to properly seal all edges of the tarpaulin on the right-hand side. Metal bars on hinges were installed along the three edges. After rolling down the tarpaulin, the edges of the tarpaulin were clamped tightly between these metal bars and the trailer frame.

Table 2.1. Materials used in constructing the experimental trailer.

Surface(s)	Construction material(s)
Three Diffuser screens	steel
Tailboard	plywood
Two Sidewalls	tarpaulin
Floor	plywood, insulation, plywood
Roof	tarpaulin, insulation, painted corrugated metal

The experimental trailer was equipped with roof vents, however, they were sealed. The roof vents were intended for use only in emergency situations. Similar to the B-train design, the experimental trailer was equipped with a mechanical roof which could be raised or lowered by the hydraulic system during loading and unloading. The use of the mechanical roof system eliminated the air space between the top of the modules and the bottom of the roof. This ensured the ventilation air would travel through the load, rather than short-circuiting through vacant space above the load, as would be expected with the 53-ft semi-trailer. Additional photos of the experimental trailer are presented in Appendix B.

2.3.3 AIR MOVEMENT

Air first enters the load through the variable-inlet damper at the heating and mixing chamber as shown in Figure 2.11 and Figure 2.12. A portion of the air travels through the propane heaters (located behind the inlet damper), being warmed by them; while the rest moves past the heaters. The hot and cold air is then mixed by the mixing fans inside the chamber, and the mixture turns 90-degree and travels through the empty portion of the mixing chamber. Air then enters the inlet diffuser screens, travels through the load and outlet diffuser and exits through the fans.

Figure 2.11. Air movement through the experimental trailer.

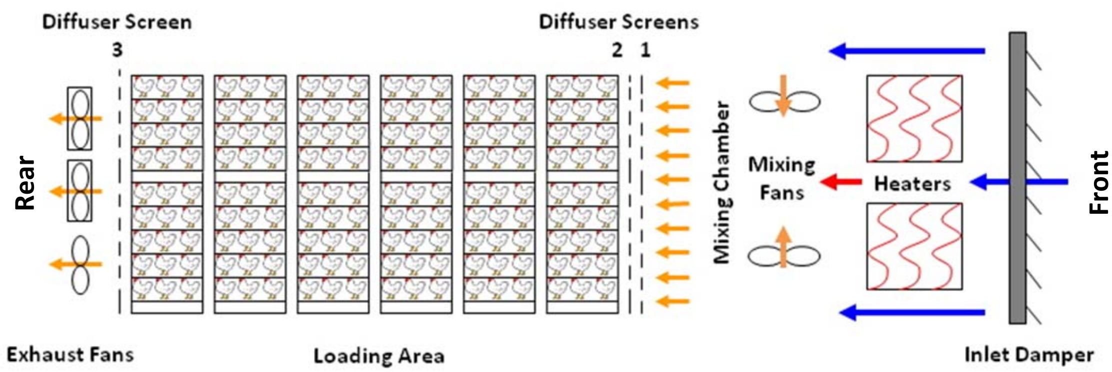

Figure 2.12. Conceptual diagram of the heating and ventilation systems inside the experimental trailer.

2.3.4 INSTRUMENTATION SYSTEM

The experimental trailer was equipped with an on-board instrumentation system to collect data at the inlet and outlet diffuser screens of the loading area. Data collected at these boundaries helped to quantify the performance of the heating and ventilation systems. The same data were used in the development of a Computational Fluid Dynamics (CFD) model, which is discussed in a separate paper. A total of 15 thermocouples (Type-T, OMEGA Engineering, INC., Stamford, Connecticut) and nine relative humidity sensors (HIH-3610 series, Honeywell International Inc., Morristown, New Jersey) were permanently installed on each of the inlet and outlet diffuser screens (first and third screens). The locations of these sensors on the two diffuser screens are shown in Appendix C.

Each relative humidity sensor was placed inside a tee fitting to protect it from light and physical damage as shown in Figure 2.13. Mosquito screens were used to cover both ends of the elbow, to block dust but allow air to pass though the sensor. During sanitation of the trailer, both ends of the T-elbows were covered with plastic caps to prevent water damaging the relative humidity sensors. Multiple temperature and relative-humidity sensors were installed on each diffuser screen to study spatial profiles of the data. Data from some of the thermocouples at the outlet diffuser were also used to activate a safety alarm system when the average outlet temperature exceeded 28°C. These sensors were wired to two terminal boxes located near the front and rear diffuser screens. Inside the terminal boxes, sensors were connected to extension wires running through conduits underneath the trailer. These extension wires carried signals from the sensors, through a piping system, to the data logging system located inside the instrumentation room.

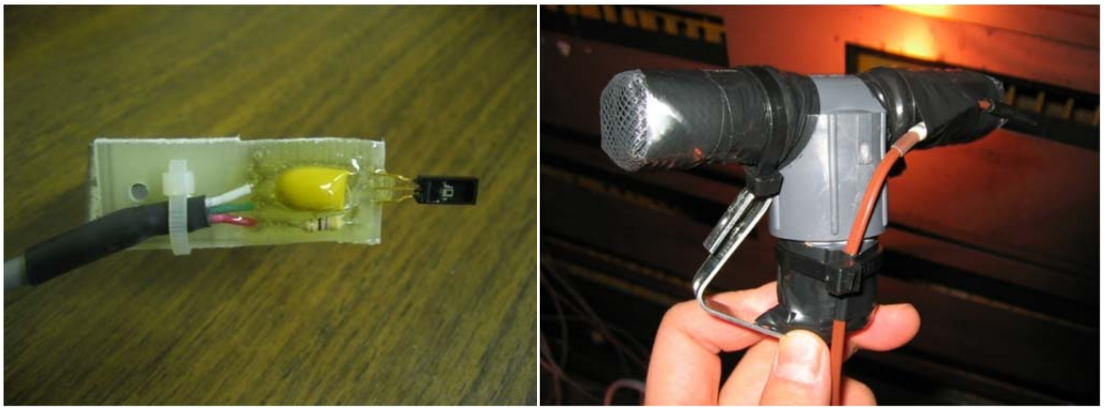

Figure 2.13. Relative humidity sensor mounted on a custom-made circuit board (left), and placed inside the protective casing (right). A thermocouple wire was mounted to the casing.

Inside the instrumentation room, additional terminal boxes were used to house the data acquisition system. The top terminal box housed a multi-channel relay multiplexer (AM416, Campbell Scientific Canada Corp., Edmonton, Alberta) to multiplex the thermocouple signals to the data logger. It also had a custom-made multiplexer to direct the relative humidity signals. The bottom terminal box housed a programmable, multi-purpose data logger (CR10X, Campbell Scientific Canada Corp., Edmonton, Alberta) to record all sensor signals. The entire on-board instrumentation system was powered by two rechargeable batteries. The data logger was programmed to operate without the use of the laptop computer. However, the system could be connected to the laptop computer to allow in-situ monitoring.

An RTD temperature sensor (MT-P3A/30, Phason Inc., Winnipeg, Manitoba) was installed at the outlet diffuser screen to provide an input signal to the multi-purpose controller installed inside the instrumentation room. The programmable controller controlled the operation mode (variable/fixed) and the speed of exhaust fans based on specified set-point temperatures. The bottom fan was set to operate at a very low setpoint resulting in continuous operation, it provided the minimum ventilation. The controller would activate the second and the third fans in the event that the exhaust air temperature exceeded the specific level defined for each fan. The inlet and outlet dampers, and the electrical wall plugs for the propane heaters were also controlled by this programmable controller. Both the laptop computer and the programmable controller were connected to the 120-V power outlets via an Uninterrupted Power Supply (UPS). The UPS system provided surge protection for the electronic equipment. It also served as a backup battery to provide emergency power to the computer and programmable controller in case of power failure. In addition, two manual speed controls could be found inside the instrumentation room. They allowed the user to manually switch on and adjust the speed of mixing fans. Additional photos of the instrumentation system can be found in Appendix B.

2.4 EXPERIMENTAL TRAILER COMMISSIONING

Prior to installation, the exhaust fans were sent to a third party (Agricultural Technology Centre, Lethbridge, Alberta) for calibration to determine their capacities. Each fan or fan with damper combination (in case of the top and middle fans) were tested in a setup shown in Figure 2.14.

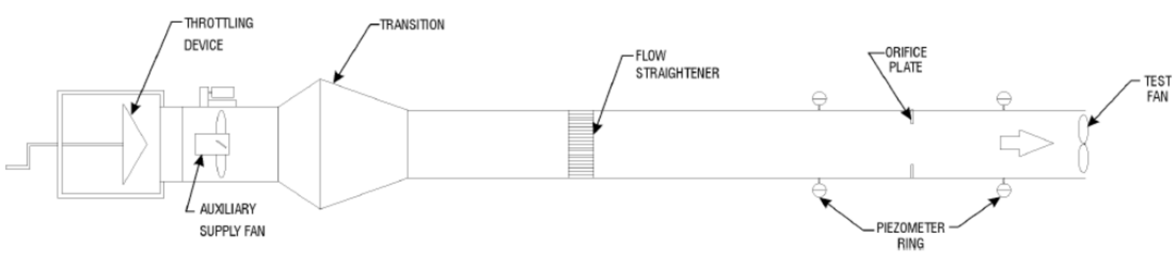

Figure 2.14. Experimental setup used for fan calibration (Atkins and Slingerland, 2004).

Based on the data from the fan calibration report (Atkins and Slingerland, 2004), the maximum flow rate a fan could generate was approximately 1.53 m^3/s (3 250 cfm). The propane heaters used in the experimental trailer could produce 29.30 kW of heat per heater. Using these values, it was possible to estimate the increase in air temperature based on flow rate, using

$$Q = \dot{m}Cp\Delta T \tag{2.1}$$

where

Q = amount of heat produced by heater (W),

$\dot{m}$ = mass flow rate (kg/s) calculated by volumetric flow rate x air density (assumed to be 1.205 kg/m^3),

Cp = specific heat of air (J/kg-K) assumed to be 1005 J/kg-K and

ΔT = change in air temperature due to heating (°C).

Figure 2.15 shows the calculated results based on the number of heaters in use. In both cases, ΔT decreases exponentially with increasing flow rate. The higher the flow rate, the lower the value is for ΔT. At the same flow rate, ΔT is higher when two heaters are being used. Such a relationship is logical as there is more heat to be absorbed. Referring to the winter design temperature from ASHRAE (2001), the winter conditions in Saskatoon could go as low to -34.8°C. Figure 2.15 shows the experimental trailer has the capacity to bring this inlet air up to 0°C by setting the flow rate to 0.7 m^3/s with one heater, or 1.4 m^3/s if two heaters are used. Although this theoretical calculation does not take into account of the efficiency of the propane heaters, field conditions (such as cross wind), nor heat losses to the ambient environment, Figure 2.15 suggests that the ventilation and heating systems in the experimental trailer could potentially handle the coldest design temperature.

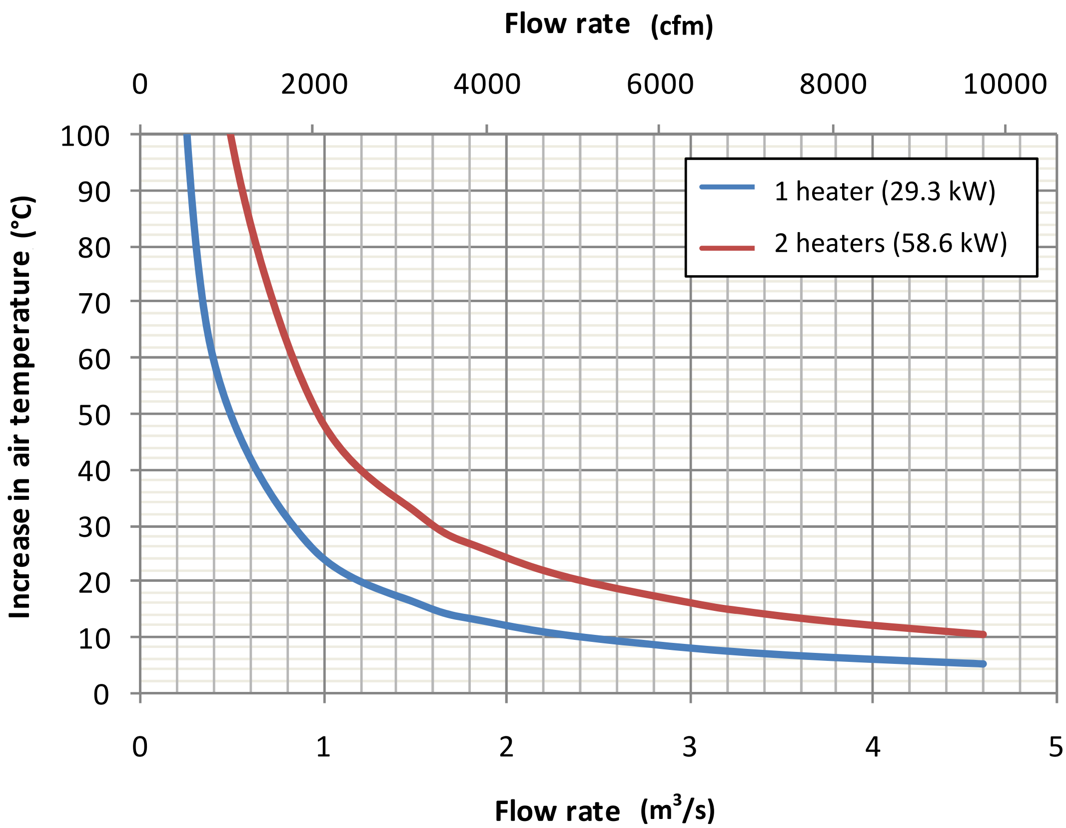

Figure 2.15. Theoretical relationship between flow rate, heater usage and increase in air temperature.

After installing the exhaust fans, their performances were verified by a series of indoor, stationary tests. The experimental trailer was connected to a wall outlet to obtain a steady source of power. The trailer was filled with empty modules without any birds. The side curtain was lowered, and the fans and inlet damper were adjusted to operate at various settings. Nine velocity data points were collected at the first diffuser in 3-second intervals using anemometers. The velocity data were then converted to flow rates by multiplying their values to their corresponding surface areas. This data served as background information to establish initial guest values of inlet velocities in the development of CFD models. It also provided an indication on how flow rates could vary with different fan and inlet damper settings. Most importantly, these tests helped to commission all the electrical components and the instrumentation system.

2.5 SUMMARY

This paper reviewed the design of some commercial transport equipment, and it provided a detailed description of the design and commissioning of an experimental trailer equipped with active ventilation and supplemental heating.

2.6 ACKNOWLEDGEMENT

The authors acknowledge financial support provided by the Natural Sciences and Engineering Research Council of Canada, Agriculture and Agri-Food Canada, the Chicken Farmers of Saskatchewan, Le Fonds Québécois de la Recherche sur la Nature et les Technologies and the University of Saskatchewan in this project. The authors also acknowledge support received from Lilydale Inc. and its personnel, especially Mr. Sunny Mak and Mr. Melvin Karakochuk. The authors thank Mr. Peter Kettlewell for his input in the design process of the experimental trailer. Special thanks also go to Ms. Agnes Northeast and Ms. Sherry Cochran for their help in the design and construction of the trailer. The authors are grateful to the following staff members from the University of Saskatchewan for their contributions during the construction and commissioning of the experimental trailer: Mr. Randy Lorenz, Mr. Wayne Morley, Mr. Mike Miller, Mr. Louis Roth and Ms. Toni Schleicher.

PREFACE TO CHAPTER 3

This paper is the second of a series of four papers. The previous paper examined the first objective of the research project: the design and construction of an actively heated and ventilated experimental vehicle. This paper focuses on the second objective of the research project, which was to characterize the performance of the experimental trailer in field tests under Canadian Prairie winter conditions.

In this paper, after a brief review of the vehicle's design, it discusses the experimental procedure used in testing its performance in field conditions. Results obtained from this study were used to develop and validate the Computational Fluid Dynamics (CFD) model, which will be discussed in the third paper.

The experimental work was conducted by K.P.C. Hui and S. Cochran. Data analyses were conducted by K.P.C. Hui with input from T.G. Crowe.

3 Performance of an Actively Heated and Ventilated Poultry Transport Vehicle

K.P.C. Hui, T.G. Crowe, S. Cochran

The authors are K.P. Catherine Hui, **ASABE Member and Professional Engineer,** Graduate Student; Dr. Trever G. Crowe, **ASABE Member and Professional Engineer**; Sherry Cochran. **Corresponding author:** Dr. Trever Crowe, College of Graduate Studies and Research, University of Saskatchewan, C 180, 105 Administration Place, Saskatoon, Saskatchewan, S7N 5A2, Canada; phone: (306) 966-2229; fax: (306) 975-1026; e-mail: trever.crowe@usask.ca.

Abstract. *In an effort to improve transport conditions for broiler chickens in winter, a 13.7-m (45-ft) long experimental trailer equipped with active ventilation and supplemental heating was constructed. The performance of this experimental trailer was evaluated in a series of field tests conducted under commercial loading practices, in winter conditions on the Canada Prairies. The average load temperature varied from 7.1 to 15.6°C in the nine sets of data. The system was able to maintain an environment above -1°C. As for the humidity level inside the trailer, the majority of sensors had "representative relative humidity" (RH*) values between 10 and 40%, with the rest having RH* values below saturation. The 3-D plots, showing temperature and humidity spatial distributions, suggested the presence of air leakage near the side tarpaulins. The front section was generally colder than the rear, and the longitudinal mid-planes were warmer than the sides. The front of the trailer was drier than the rear. Results from this study suggested that the concept of active ventilation and heating is a promising option to improve the transport conditions for broiler chickens during cold ambient conditions.*

Keywords. *Poultry, broiler, transport, ventilation, heating, animal welfare.*

3.1 INTRODUCTION

The harsh winter conditions on the Canadian Prairies impose special challenges in providing acceptable environmental conditions for broiler chickens during transport. Previous research conducted by the University of Saskatchewan demonstrated that broilers were exposed to heterogeneous temperature and humidity conditions during transportation in extreme Canadian Prairie climates. Field observations indicated some animals were subjected to cold and wet conditions, while others on the same truck experienced warm moist conditions. These field results showed that the passive (natural) ventilation systems employed in commercial vehicles were ineffective in removing large amounts of animal-produced heat and moisture from the loading area in the trailer when the trailers were fully covered with side tarps. As a result of such findings, a multidisciplinary study was conducted by researchers of the University of Saskatchewan in collaboration with a commercial poultry processor. The overall objective of the research program was to develop a better understanding of and improve the environmental conditions for chickens during transportation.

In order to evaluate the merits of active ventilation and supplemental heat, a 13.7-m (45-ft) long experimental trailer was developed. The idea of using active ventilation to remove heat and moisture was inspired by research conducted in the UK on a mechanically ventilated poultry transport vehicle (Roslin Institute 2000, ASAE 2001, BBSRC 2002). The idea of adding supplemental heat to the ventilation air is original, as an approach to address the extreme winter conditions on the Canadian Prairies. According to ASHRAE (2001), the winter design temperatures in Western Canada are below -30˚C. At such low temperatures, ambient air has little capacity to absorb moisture, thus the excess moisture (not absorbed by the ventilated air) may condense and freeze on the trailer infrastructure or animals in winter temperatures.

Consequently, the experimental trailer was designed such that ventilation air could be heated prior to entering the load to increase its moisture-holding capacity, and to reduce the cooling effect of cold air coming in contact with the birds. In addition to the mechanical ventilation and heating systems, the experimental trailer was also equipped with a number of sensors to monitor its performance. In this study, the experimental trailer was integrated into the commercial fleet, to be tested under field conditions.

3.2 Objective

The objective of this study was to characterize the performance of the experimental trailer in field tests under Canadian Prairie winter conditions, by monitoring the conditions (temperature and relative humidity) next to the broilers. Data collected from the field tests were used to evaluate the effect of active ventilation and supplemental heat on the environmental conditions to which broiler chickens were subjected to during transportation. The acquired data were also used to develop a Computational Fluid Dynamics (CFD) model which is discussed in a subsequent paper.

3.3 Materials and Methods

This section provides an overview of the experimental trailer used in field tests. Additional details on the design of the trailer can be found in the previous chapter. The experimental procedure employed in field tests are described in detail in this section.

3.3.1 Experimental Trailer

The experimental unit (Figure 3.1) was built on top of a 13.7-m (45-ft) long flatbed. It was approximately 2.5-m (8-ft) wide and 2.6-m (8.4-ft) high. The trailer was divided into three compartments: instrumentation room, heating and mixing chamber, and loading area.

Figure 3.1. Experimental transport system with active ventilation and heating.

The instrumentation room housed two gasoline powered electrical generators, a hydraulic system, a data acquisition system, a programmable multi-purpose controller (Supra 210000, Phason Inc., Winnipeg, Manitoba), and two manual speed controls (MSC-4, Phason Inc., Winnipeg, Manitoba) to control the ventilation and heating equipment. The heating and mixing chamber was sub-divided into two sections. On one side, it housed a motorized variable-inlet damper which controlled the amount of ambient air entering the loading area. It also contained a palletized metal frame mounted with two propane heaters (S100, Sure Flame, Lethbridge, Alberta) and two mixing fans (FC063-6EA.6F.1, Ziehl-Abegg AG, Künzelsau, Germany) for heating and mixing ambient air (Figure 3.2). On the other side of the chamber, it consisted of an empty space, acting like a plenum, providing additional empty area for air mixing.

Figure 3.2. The heating and mixing chamber under construction (inlet damper not shown).

Following commercial practices of the industrial collaborator, broiler chickens were transported using palletized Easyload modules designed by Anglia Autoflow Ltd. based in England (Anglia Autoflow Ltd., 2002), as shown in Figure 3.3. Inside the experimental trailer, the loading area could hold six stacks of modules. Each stack of modules consisted of two modules, with one placed on top of the other. The top modules consisted of four layers of drawers, and the bottom modules had five layers of drawers. This resulted in a holding capacity of 162 drawers. With a loading density of 22 to 26 birds per drawer, the experimental trailer could transport 3 124 to 4 212 broilers per trip.

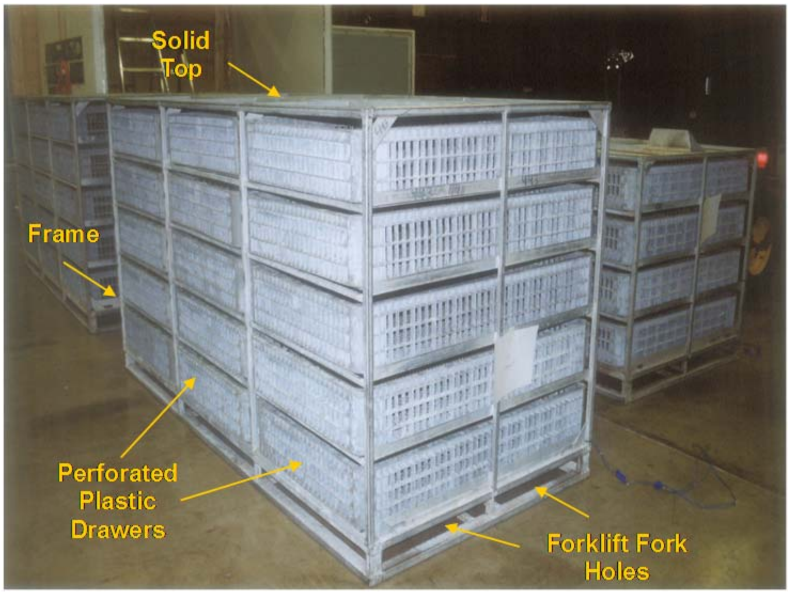

Figure 3.3. 5-Drawers and 4-Drawers high modules used for transportation of broiler chickens.

The loading area had three diffuser screens, two at its front entrance and one close to the tailboard. These diffuser screens had 25.4-mm (1-in) and 50.8-mm (2-in) opening slots on them which allowed air to pass through as shown in Figure 3.4. Two diffuser screens were installed 50.8 mm (2 in) apart at the front end of the trailer, and the opening slots on these two screens were staggered, such that when the loading area was being washed, water could not easily pass through and enter the mixing chamber. The loading area also had a set of three variable-speed exhaust fans (FC045-4EQ.4F.3, Ziehl-Abegg AG, Künzelsau, Germany) mounted at the tailboard of the trailer. The operation of these fans was controlled by the multi-purpose controller located in the instrumentation room and a RTD temperature sensor (MT-P3A/30, Phason Inc., Winnipeg, Manitoba) installed at the outlet diffuser screen. The fans were programmed to run in on/off mode (100% or 0%), they would switch on one after the other when the outlet temperature (measured by the RTD sensor) exceeded the user-defined set-points in the program. Hence, the three fans were staged at three set-point values. The bottom fan was designed to run continuously by programming it to switch on at a very low set-point temperature (well below what the load temperature could be). The fans could have been programmed to operate at variable speeds (variable % instead of 0 and 100%), however, it was decided to operate in the on/off mode such that the air flow rate would remain constant when the same number of fans was in use. This strategic was applied to simplify the modeling work. The middle and top fans were equipped with motorized dampers to seal off the outlets, to prevent short-circuiting of air flow when these fans were not in use. These outlet dampers were also controlled by the multi-purpose controller, which opened up the dampers fully just before turning on the fans.

Figure 3.4. The third diffuser screen located in front of the exhaust fans.

Different materials were used to construct the three compartments. Some surfaces were insulated, while others were not. The materials types are summarize in Table 3.1. Similar to the commercial trailers, the two sides of the loading area were covered by tarpaulins. The tarpaulin on the left-hand side (viewed from the rear) was fixed to a metal frame. The tarpaulin on the right-hand side could be rolled up or down for loading and unloading of modules. Unlike the commercial trailers where the tarpaulins are loosely strapped along the bottom edges of the trailer, a special sealing system was designed to properly seal all edges of the tarpaulin on the right-hand side for winter operations. Metal bars on hinges were installed along the three edges. After rolling down the tarpaulin, the edges of the tarpaulin were clamped tightly between these metal bars and the trailer frame. The experimental trailer was also equipped with a mechanical roof which could be raised or lowered by the hydraulic system during loading and unloading.

Table 3.1. Materials used in constructing the experimental trailer.

Surface(s)	Construction material(s)
Three diffuser screens	steel
Tailboard	plywood
Two Sidewalls	tarpaulin
Floor	plywood, insulation, plywood
Roof	tarpaulin, insulation, painted corrugated metal

A conceptual diagram of the air movement inside the experimental trailer is presented in Figure 3.5. The unit was designed such that air would first enter the load through the variable-inlet damper at the heating and mixing chamber. A portion of the air travels through the propane heaters, being warmed by them; while the rest moves past the heaters. The hot and cold air is then mixed by the mixing fans inside the chamber, and the mixture travels through the empty portion of the mixing chamber. It then enters the inlet diffuser screens (#1 and #2), travels through the load and outlet diffuser screen (#3) and exits through the fans. Additional details about the design of the experimental trailer can be found in the previous chapter.

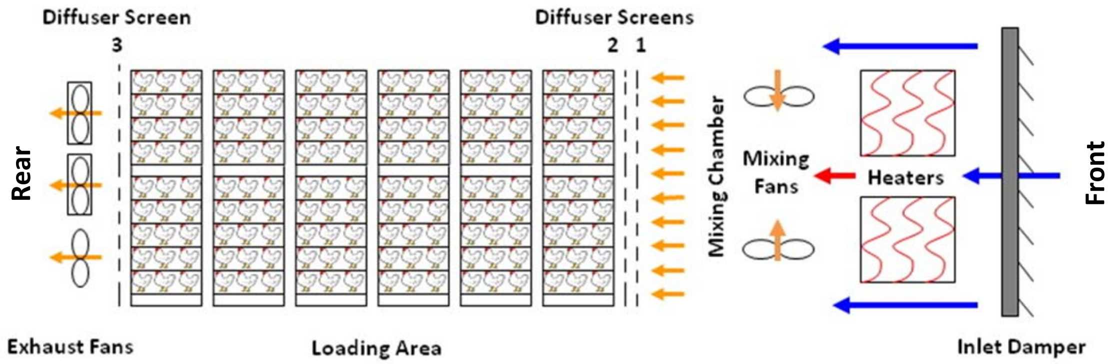

Figure 3.5. Conceptual diagram of the heating and ventilation systems inside the experimental trailer.

3.3.2 ON-BOARD INSTRUMENTATION SYSTEM

The experimental trailer was equipped with sensors that were permanently installed on the diffuser screens. These on-board sensors measured conditions at the inlet and outlet boundaries of the loading area. A total of 15 thermocouples (Type-T, OMEGA Engineering, INC., Stamford, Connecticut) and nine relative humidity sensors (HIH-3610 series, Honeywell International Inc., Morristown, New Jersey) were permanently installed on diffuser screens one and three as named in Figure 3.5. The accuracy of the humidity sensors was ±2% at 0 to 100%. The thermocouples were installed at five different heights and at three positions across the width of the trailer, collecting data in a grid of five by three. The relative humidity sensors were installed at three different heights and at three positions across the width, collecting data in a grid of three by three. These sensors were placed at the middle of the 50.8-mm (2-in) opening slots through which ventilation air passed. The locations of these sensors on the two diffuser screens are summarized in Appendix C.

As shown in Figure 3.6, each relative humidity sensor was placed inside a plumbing tee connector to shield it from light and protect it from physical damage. Mosquito screens were used to cover both ends of the tee, to block large dust particles but allow air to pass through the sensor. During sanitation of the trailer, both ends of each tee were covered with plastic caps to prevent water damaging the relative humidity sensors. Data from these sensors were used to establish spatial profiles at the boundaries of the load. Some data from the thermocouples at the outlet diffuser screen were also used by the data acquisition system to compute the average outlet temperature. A safety alarm would be activated if the temperature of the air exiting the load exceeded 28°C. All on-board sensors were wired to either one of two terminal boxes located near the front and rear diffuser screens. Extension wires carried their signals to the data acquisition system located inside the instrumentation room, through a piping system.

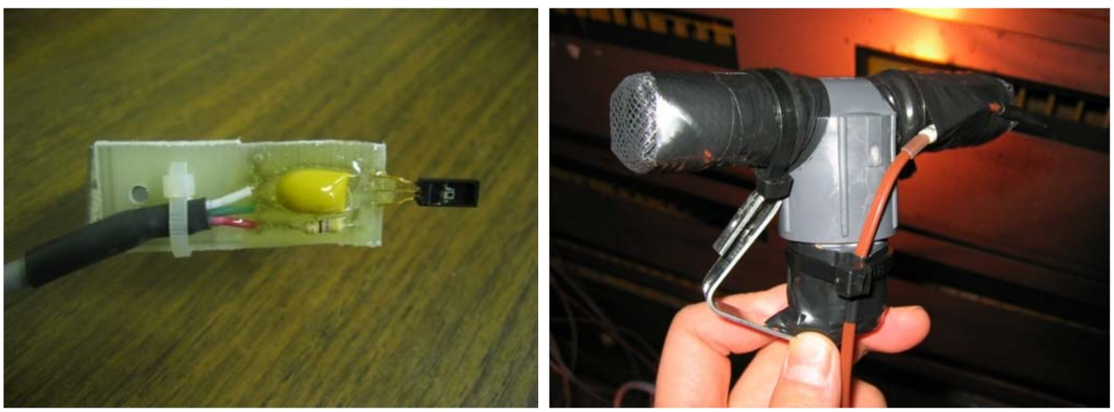

Figure 3.6. Relative humidity sensor mounted on a custom-made circuit board (left), and placed inside the protective casing (right). A thermocouple wire was mounted to the casing.

3.3.3 DATA LOGGERS

In each field test, additional data loggers were installed inside module drawers to monitor the conditions inside the load, and on the tractor to record ambient air conditions. Two types of data loggers were used, the first type recorded only temperature (Flashlink model 20200, DeltaTRAK, Pleasanton, California), it had an accuracy of ±0.5°C at 0 to 66°C and ±1°C over the entire range of -40 to 66°C. The second type of data logger, as shown in Figure 3.7, recorded both temperature and relative humidity (Flashlink model 20203, DeltaTRAK, Pleasanton, California). Flashlink model 20203 had the same temperature accuracy as model 20200, its accuracy on relative humidity was ±5% between 20 to 90% relative humidity from 0.5 to 66°C, its operating humidity range was 1 to 99%. These loggers were battery operated, programmable by computer and output data files in text format. Over 30 data loggers were installed in each test. The data loggers were randomly assigned to pre-determined drawer positions at the farm. The data loggers were labelled individually, which facilitated the recording and identification of their locations inside the load. In addition, two air velocity transducers as shown in Figure 3.7 (Model 8450-20M-V and 8450-50M-V, TSI Incorporated, St. Paul, Minnesota) were installed at the outlet diffuser screen to collect air velocity readings. These anemometers were connected to portable batteries for power and the signal wires were connected to the multi-purpose data logger in the instrumentation room through extension wires. The air velocity transducers were not installed permanently inside the experimental trailer due to their fragile nature.

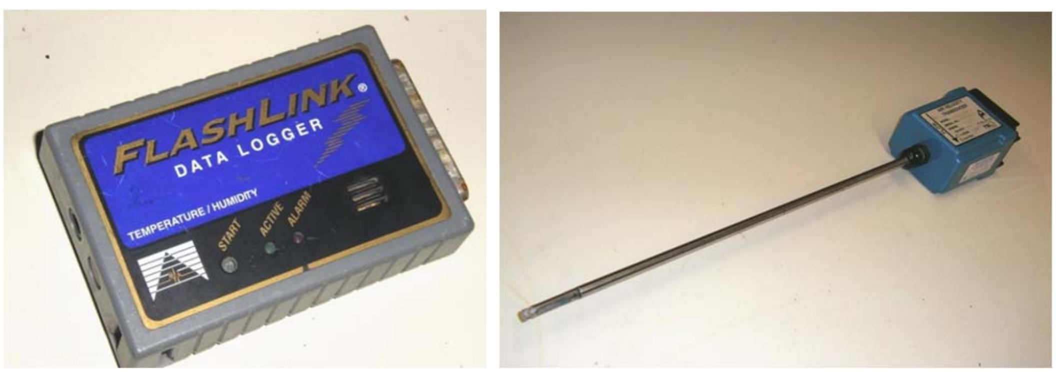

Figure 3.7. Data logger (left) and air velocity transducer (right) used in field tests.

3.3.4 FIELD TEST PROCEDURE

A series of field tests were conducted to collect temperature, relative humidity and air velocity data from the experimental trailer. Sensors connected to the multi-purpose data logger (thermocouples, relative humidity sensors and anemometers) were programmed to collect data at intervals of 30 seconds. As for the data loggers, they were programmed to collect data each minute. All sensors were programmed to commence collecting data prior to farm departure and terminate after arriving at the processing plant. The experimental trailer traveled mostly on highways at typical travel speeds (~100 km/h). Most of the field tests occurred during the early morning, after midnight. Data were collected while en route from farms near Saskatoon to the processing plant in Wynyard, with a typical travel time of two hours. One to two stops were made en route to inspect the electrical equipment and instrumentation system to ensure they were functioning properly and there was no failure. In some tests, changes were made during a stop to modify the ventilation and heating regime such that a different set of experimental data could be collected for the new regime.

The experimental procedure used to collect the field data can be summarized as follows. At the farm, after starting the generators, the mechanical roof of the experimental trailer was raised. Air velocity sensors were then installed at the outlet diffuser screen. The empty modules were unloaded by forklift, and each module was labelled with a tag on its right-hand side (viewed from the rear) to ensure sensors would be installed in the correct locations. Data loggers were pre-programmed and pre-tied in mesh wire cages in the lab, and they were installed inside specific drawer locations at the farm as shown in Figure 3.8. They were installed in empty drawers prior to loading of broilers. Care was taken to have the data loggers facing the outside of the drawers as shown in Figure 3.8, to ensure the data loggers would monitor air conditions surrounding the broilers, but not conditions of the body of animals. The position of each data logger was manually recorded to permit 3-D mapping of data. A single data logger was also mounted on the mirror of the tractor to record ambient air conditions.

Figure 3.8. Installing data logger inside an empty drawer using cable tie (left). Orientation of the data logger inside a drawer loaded with broilers (right).

Figure 3.9. Data logger installed on the right-hand side mirror of the experimental trailer to monitor ambient air conditions.

After installing all data loggers inside the drawers, each module was brought inside the barn and loaded with chickens by the catching crew. The module was then loaded onto the experimental trailer according to a pre-assigned order as shown in Figure 3.10. After loading all modules, the mechanical roof was lowered, the right-hand side tarpaulin was rolled down and clamped tightly between the metal bars on hinges and the trailer frame as shown in Figure 3.11.

The on-board data acquisition system was then initiated. The exhaust fans were also activated based on the average outlet temperature and control program input into the multi-purpose controller. The mixing fans were manually switched on. Depending on the ambient temperature, one or two heaters may be switched on manually after turning on the propane gas line. After verifying all the electrical components and the on-board sensors were functioning properly, the driver would then be given the signal to depart. The research team followed the experimental trailer closely en route. Any special event, such as activation of the second or third fans by the multi-purpose controller, or malfunction of equipment was duly recorded. The driver would make one or two stops at predetermined locations. These stops allowed research personnel to verify all electrical and electronic components were still working properly, or apply a new ventilation and heating regime. The times of departure, rest stops and arrival were duly recorded.

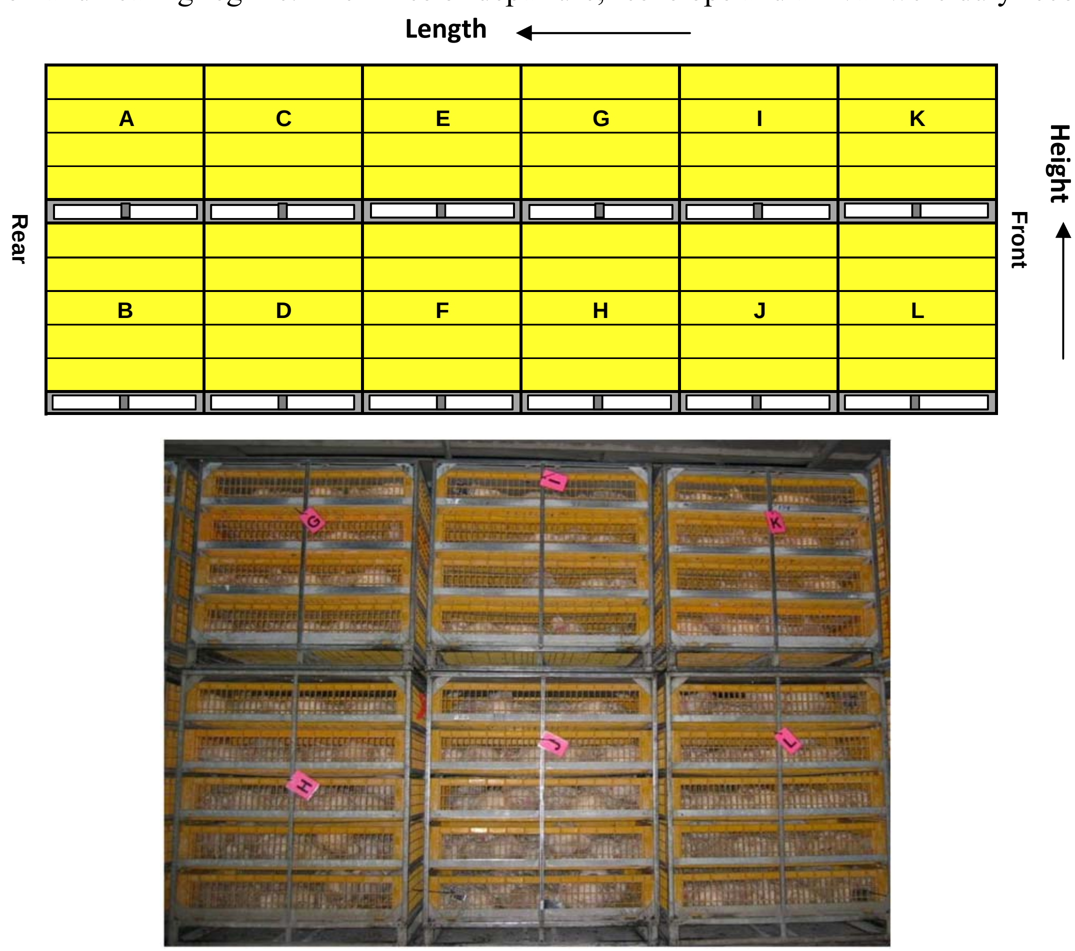

Figure 3.10. Arrangement of modules inside the experimental trailer (side view).

Figure 3.11. Right-hand side tarpaulin sealed against the modules.

After arriving at the processing plant, the exhaust fans and heaters were turned off. The right-hand side tarpaulin was then unsealed, rolled up and the mechanical roof was raised. The modules were unloaded into the indoor unloading dock, the air velocity transducers were retrieved, and the data acquisition system was shut off. Small protective caps were installed on both ends of the relative humidity sensors before power washing the loading area. The roof was then lowered and the generators shut off. The data logger on the tractor was collected. At the unloading dock, another crew collected data loggers from the drawers and removed any chickens which died during transit. The data loggers were counted and the dead chickens were given to the veterinarian to determine cause of death. All the sensors were sanitized and data were downloaded from the loggers after returning to the lab.

The field tests were completed during the months of February and March. Each field test required 12-h of field work, plus pre-planning and clean-up. Only one to two tests could be conducted per week. Field tests were scheduled based on the availability of the broilers (which is based on shipping schedule from the collaborator), the locations of farms (near Saskatoon) and the availability of cold weather conditions. Efforts were made to carry out as many field tests as possible during the two-month period, with different fan and heater settings to test the capability of the system (when weather permitted). Under these restrictions, it was not possible to apply an experimental design on the entire experiment itself. On the other hand, the locations of sensors (on-board or in shipping drawers) followed a pre-determined experimental design aiming to collect data in a distributed manner to capture data throughout the load.

3.4 DATA ANALYSIS

3.4.1 TEMPERATURE GAIN IN AMBIENT AIR AT DIFFUSER SCREEN

The experimental data collected by the on-board instrumentation system or data loggers were temporally and spatially dependent. Raw data were processed by calculating their time-averages. Each data set obtained from a test were first plotted over time using the Excel software (Microsoft Office Excel 2007, Microsoft Corporation, Redmond, Washington). In some tests, the numbers of exhaust fans and heaters used by the experimental trailer changed during the journey. These raw data sets were therefore subdivided based on these changes. For each set of data, a relatively steady state period was visually identified from the raw data plots, and time averages were calculated for each data logger over a time period of 30 min (except for one test where 20-min time averages were calculated). These time averages were used as the "base data" in data analysis. For example, the symbol, $\bar{T}$, was used to denote time-averaged temperatures.

As mentioned previously, the inlet diffuser screen 1 had 15 thermocouples installed on it, data of each thermocouple were averaged over time to generate a set of base data. Furthermoe, one data logger was installed on the exterior of the truck to record ambient conditions, its data were also averaged over the same period of time used by the thermocouples. Using these base data, the temperature difference between the inlet air for thermocouple i and the ambient air was calculated using

$$\Delta\bar{T}_{inlet\ i} = \bar{T}_{inlet\ i} - \bar{T}_{ambient} \tag{3.1}$$

where

i = index of thermocouple,

$\Delta\bar{T}_{inlet\ i}$ = time-averaged temperature gain in ambient air at diffuser screen 1, for thermocouple i (°C),

$\bar{T}_{inlet\ i}$ = time-averaged temperature at diffuser screen 1 for thermocouple i (°C) and

$\bar{T}_{ambient}$ = time-averaged temperature of ambient air measured outside the vehicle (°C).

After computing the $\Delta\bar{T}_{inlet\ i}$ values for the 15 thermocouples, they were averaged over space using

$$\Delta\bar{T}_{inlet} = \frac{\sum_{i=1}^{15}\Delta\bar{T}_{inlet\ i}}{15} \tag{3.2}$$

where

$\Delta\bar{T}_{inlet}$ = temperature gain in ambient air at diffuser screen 1 (°C),

i = index of thermocouple and

$\Delta\bar{T}_{inlet\ i}$ = time-averaged temperature gain in ambient air at diffuser screen 1, for thermocouple i (°C).

3.4.2 Representative Relative Humidity

It is known in the literature that wet birds are more easily subject to hypothermia than dry birds (Hunter et al., 1999). Therefore, it is important to examine the humidity level inside the experimental trailer. Much thought was put into identifying the correct parameter to quantify "humidity". The data loggers record values in percentage of relative humidity. Relative humidity is dependent on temperature. For the same amount of moisture contained by moist air, a lower value of relative humidity would be obtained at higher temperatures (ASHRAE, 2005). The raw data obtained from the data logger were time dependent. Although much care was taken to identify a time period in which the data were steady, the temperature data could still vary during the time period when time-averages were computed. Due to the varying nature of the recorded temperature and the dependency of relative humidity on temperature, it could be misleading to compute time-average relative humidity (*RH*) values based on the arithmetic mean of the raw relative humidity data. The actual amount of moisture contained in the air as indicated by the arithmetic mean *RH* could be under or over-estimated, at the calculated average temperature.

There are two measures commonly used to quantify humidity in absolute terms: wet-bulb temperature and humidity ratio. The wet-bulb temperature is dependent on the moisture content, but also on the dry-bulb temperature, thus it is not the appropriate measure to be used in this case. The humidity ratio is defined as "the ratio of the mass of water vapour per mass of dry air" by ASHRAE (2005). It is an absolute value, independent of temperature. Unfortunately, using the humidity ratio alone does not provide an indication of the potential for the air to become saturated; it does not answer the question of the susceptibility of broiler chickens to becoming wet. After much consideration, it was decided to combine the concepts of humidity ratio and relative humidity to develop a new variable "*RH**" to analyze the humidity data collected by the data loggers. This new variable takes advantages of the temperature independency of humidity ratio and the ability to quantify the closeness to saturation from relative humidity.

The concept behind *RH** is relatively straight forward. First, temperature and relative humidity raw data at a given time from a data logger were used to compute its corresponding humidity ratio. After compiling the humidity ratio values at every minute, a time-averaged value was calculated using the humidity ratio values. A time-averaged temperature was also computed for the same time interval. The time-averaged humidity ratio and time-averaged temperature were then used to compute its *representative relative humidity*, thus *RH**. It is a time-averaged relative humidity value derived from the time-averaged humidity ratio and time-averaged temperature. The reason for not naming this new value as $\overline{RH}$ is to highlight the fact which it is not a simple arithmetic mean. All the equations used to compute the *RH** for a data logger are summarized in Appendix D. At the end of the calculations, each logger would have one *RH** value representative of the average humidity level over a 30-min (or 20-min) time interval .

3.4.3 3-D VOLUMETRIC CONTOUR PLOTS

In order to obtain a better visual picture of the spatial distributions of base data, data were also plotted as volumetric contour plots in three-dimensional space using the Tecplot software (Tecplot 10, Tecplot, Inc., Bellevue, Washington). The first step in creating such 3-D plots involved assigning 3-D spatial coordinates (for *x, y, z* positions) to each base data point. The base data set (which included the spatial coordinates and the variable of interest of all data loggers) was then imported into the Tecplot software using a special Excel Add-In program.

Each base data set was spatially varying, discrete data; the data points were not linked by a mesh structure as shown in Figure 3.12a. They are considered as “irregular data”, and they had to be interpolated to a “regular, IJK-ordered zone” to allow the creation of the volumetric contour plots (Amtec Engineering, Inc. 2003). Thus, a uniform, structured, quadrilateral mesh of 10 x 28 x 10 (width x length x height) was created as shown in Figure 3.12b. This mesh was scaled to the actual dimensions of the experimental trailer, yielding a nodal point (for data interpolation) at roughly every 0.254 m (10 in). The base data were then interpolated over this quadrilateral mesh. Using the Kriging algorithm, the software computed new values at each nodal point based on values of the base data. The resulting “interpolated” data were then used to create the 3-D plots (Figure 3.12c), “slicing planes” with constant *x*-, *y*- or *z*-coordinates (Figure 3.12d) were also created to allow visualization of data distribution at different cross-sectional areas inside the experimental trailer. The origin of the *x, y, z* coordinates (0,0,0) was defined at the bottom-right front corner of the loading area.

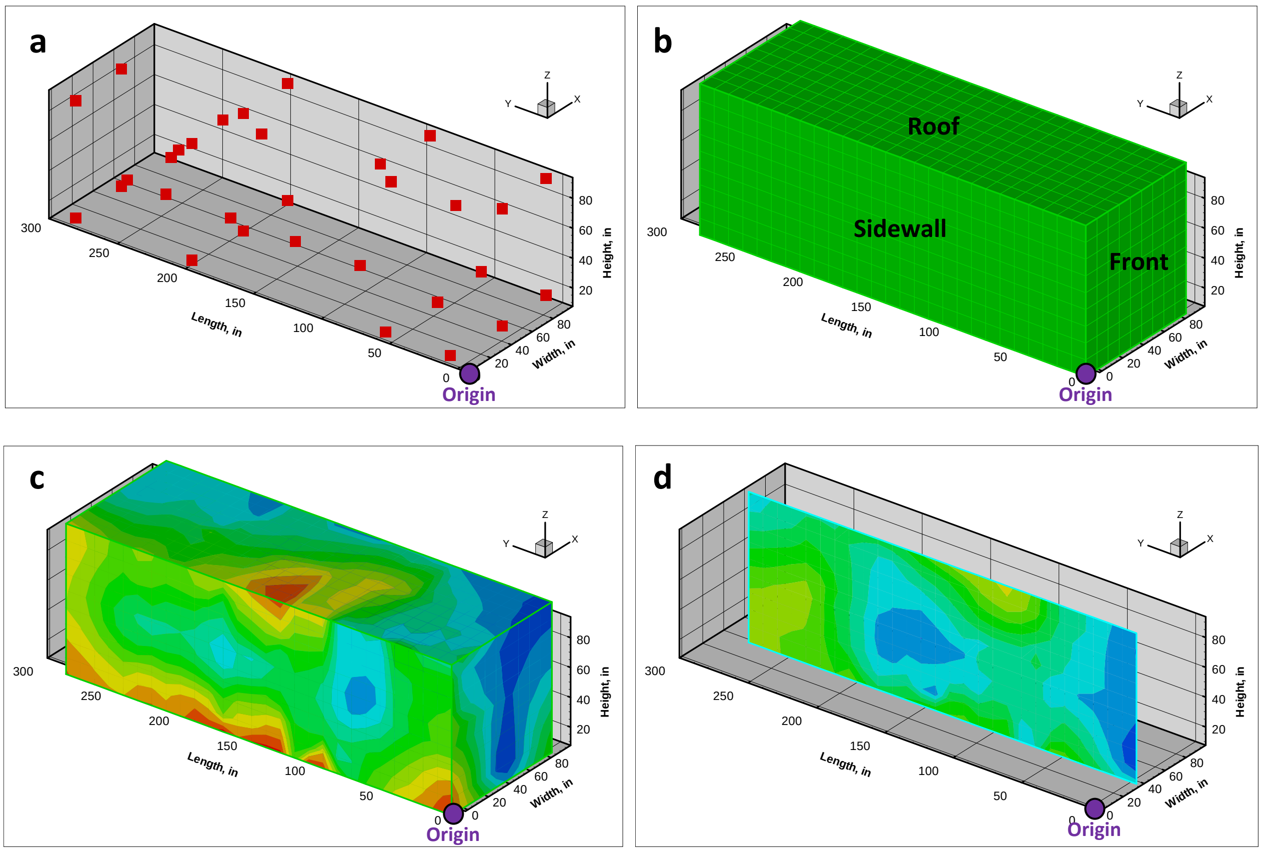

Figure 3.12. Procedure involved in creating 3-D plots using the Tecplot software: a) import discrete experimental data, b) create a quadrilateral mesh for data interpolation, c) interpolate data and create 3-D plot, d) create a cross-section area from the 3-D plot.

For temperature data collected by data loggers, a derived temperature variable was used to create the 3-D plots instead of using the time-averaged load temperature ($\overline{T}$). The nine data sets were collected under different ambient conditions, fan and heater settings. In order to study the effect of fan settings, $\overline{T}$ had to be processed to eliminate the effect of ambient conditions and heater setting. One simple way to achieve this goal was to calculate the difference between each $\overline{T}$ value and the average temperature at the inlet using

$$\overline{\overline{T}}_{inlet} = \frac{\sum_{i=1}^{15} \overline{T}_{inlet\ i}}{15} \tag{3.3}$$

and

$$\Delta \overline{T}_j = \overline{T}_j - \overline{\overline{T}}_{inlet} \tag{3.4}$$

where

i = index of thermocouple,

$\overline{T}_{inlet\ i}$ = time-averaged temperature at diffuser screen 1 for thermocouple i (°C),

$\overline{\overline{T}}_{inlet}$ = overall averaged temperature at diffuser screen 1 from 15 thermocouples (°C),

j = index of data logger,

$\overline{T}_j$ = time-averaged load temperature of data logger j (°C) and

$\Delta\overline{T}_j$ = temperature gain in inlet air for data logger j (°C).

3.5 RESULTS AND DISCUSSION

3.5.1 CAPACITY OF HEATING AND VENTILATION SYSTEMS

In the field tests, different numbers of heaters and exhaust fans were used to create different heating and ventilation settings for the load. Minimum ventilation was provided by the bottom fan. The second and the third fans would turn on automatically when the outlet temperature reached the second and the third set-point temperatures. Therefore, three fan settings were possible: one, two or three fans. The heaters were controlled manually, three settings were possible for the heating system: no heater, one heater (either top or bottom unit) and two heaters.

Figure 3.13 shows the temperature gain in ambient air ($\Delta\overline{T}_{inlet}$) based on various fan and heater settings. A total of nine sets of data were obtained from the field tests. However, results from only five sets of data are presented in Figure 3.13. Ambient air temperature was not available for the other data sets due to malfunction of sensor or missing record of sensor identification. Without data for the ambient air, it was not possible to compute the value of $\Delta\bar{T}_{inlet}$ of these tests.

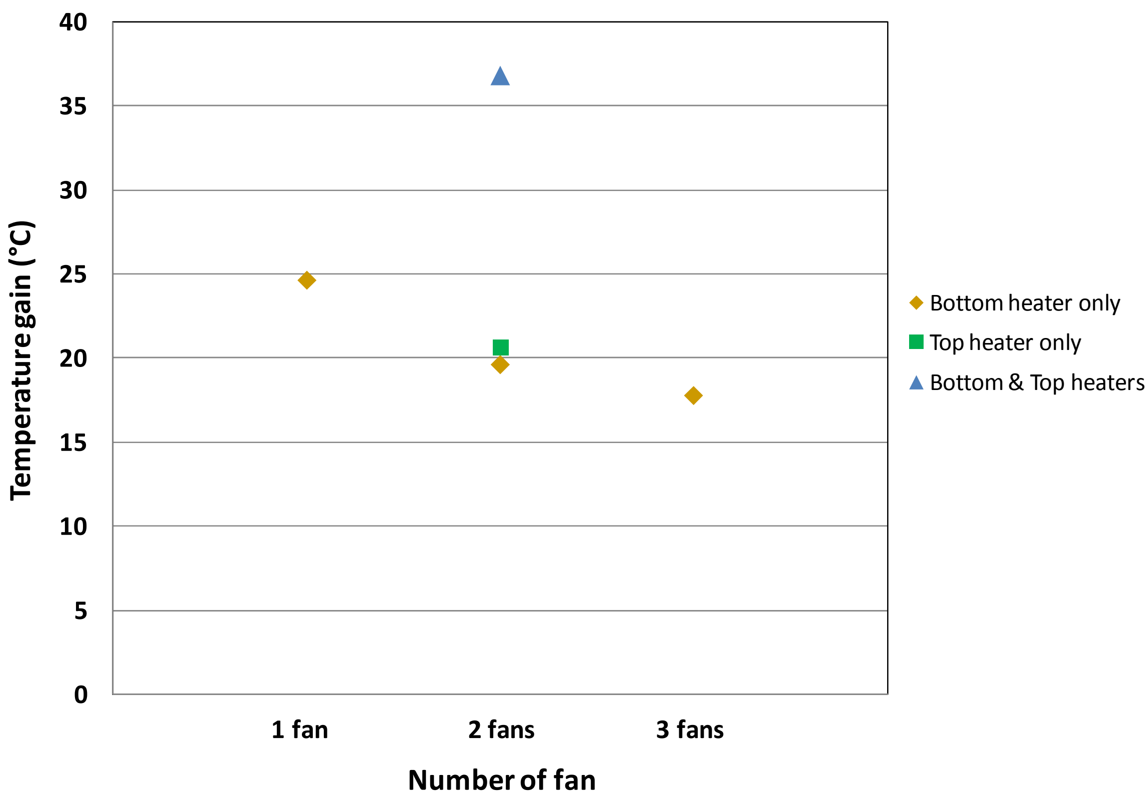

Figure 3.13. Temperature gain in ambient air as a function of fan and heater settings.

As shown in Figure 3.13, for the same number of heaters, the temperature gain in ambient air decreased with increasing number of fans. This trend is logical, when more fans were used, a larger amount of air travelled through the load and each unit of air would absorb less heat. When one heater was used, the temperature gain dropped by approximately 7°C in the case of one fan versus three fans. When one heater was used, the temperature gain was almost 25°C for one fan, near 20°C when two fans operated and at around 18°C for three fans. In the case of one heater and two fans, using the top or the bottom heater made minimal difference in temperature gain (19.6°C versus 20.6°C). Such results were anticipated as both heaters had the same nominal heating capacity. Figure 3.13 also illustrates the effect of two heaters versus one when two fans were used. Using two heaters increased the magnitude of the temperature gain as compared to the one-heater setting. However, it did not exactly double the temperature gain when two heaters were used (~20°C versus ~36°C). In some tests, when two heaters were switched on, one of them would shut off automatically. The incidents occurred when the inlet damper was opened too large or when the heating chamber became overheated. In the latter case, it is possible that when two heaters were used, some heat would accumulate in the heater chamber if the fan setting was too low or if the ambient temperature is not low enough. Therefore, it is not ideal to use two heaters unless the weather is extremely cold and three exhaust fans are used.

3.5.2 CHARACTERISTICS OF THE LOAD

Table 3.2 summarizes the heater, fan and inlet damper settings for the nine sets of data. Some data sets (e.g. 1 and 2) were taken from the same field test, but different heating and ventilation regimes were used at different time intervals which resulted in two sets of usable data. The data sets are ranked by the number of heaters, then by the number of fans in Table 3.2. The table also lists the time-averaged ambient temperatures recorded by the truck's data loggers. The time-averaged temperatures at the Saskatoon airport are also included. There were some discrepancies between the data logger's ambient temperatures and airport values. The data logger values were collected during transportation and may have been affected by road weather conditions. The airport values were collected at a stationary observation station, but they did provide an idea of the ambient conditions when no data logger values were available. These airport values were solely for reference and they were not used to compute any secondary values in data analysis. In general, the nine data sets were collected when the ambient temperatures were approximately between -17 and -3°C.

Table 3.2 also summarizes the temperature values in each load: its spatial average, standard deviation, minimum and maximum values. All these values were computed using the time-average data from data loggers installed inside the drawers. Each field test used more than 30 data loggers. After computing the time-averaged temperature value ($\overline{T}$) for each data logger, the spatial average, standard deviation, minimum and maximum values were computed using all the $\overline{T}$ data in each load. These "macro" data were meant to provide a general perspective of the load condition, but not the spatial distribution of temperature within the load. At this stage, it is not possible to examine the effect of heater and fan settings on the load temperatures. The load temperatures were affected by the heater and fan settings, but also the ambient air conditions. The average load temperature varied from 7.1 to 15.6°C.

Table 3.2. System settings and load conditions.

Date	Data set #	Number of heaters	Number of fans	Inlet opening	Ambient temperature (°C)		$\bar{T}$ (°C)				*RH** (%)		Number of loggers
					Data logger	Airport	Avg	Stdev	Min	Max	Min	Max	RH data n.a.
Feb 2nd 2005	6	0	1 (B)	40%	n.a.	-2.6	12.7	8.9	1.2	30.0	9.1	66.1	0
Feb 4th 2005b	8	0	1 (B)	60%	n.a.	-11.9	9.9	5.7	-0.8	24.3	10.0	67.9	1
Feb 15th 2005	3	1 (B)	1 (B)	50%	-14.4	-17.1	12.2	6.0	0.0	25.4	9.4	62.2	2
Feb 4th 2005a	7	1 (B)	1 (B)	60%	n.a.	-9.8	11.5	4.9	2.3	24.5	10.0	75.3	0
Feb 23rd 2005a	1	1 (T)	2 (B & M)	50%	-14.9	-15.4	7.1	3.9	0.7	17.0	10.8	93.2	4
March 24th 2005	9	1 (B)	2 (B & M)	50%	n.a.	-16.4	9.8	6.4	2.0	26.8	9.9	74.8	0
March 17th 2005	5	1 (B)	2 (B & T)	50%	-12.8	-10.8	7.6	5.3	0.6	20.7	8.1	85.1	1
Feb 23rd 2005b	2	1 (B)	3 (B,M,T)	50%	-11.7	-13.1	9.6	4.1	2.7	19.4	10.1	74.7	0
Feb 18th 2005	4	2 (B, T)	2 (B & M)	50%	-15.6	-15.4	15.5	5.3	4.6	26.3	9.0	75.3	2

Notes:

- For data set #3, base data were obtained by averaging raw data over 20 min instead of 30 min.
- "B" denotes "bottom", "M" denotes "middle" and "T" denotes "top".
- "n.a." denotes data "not available"
- "Airport" ambient temperatures were calculated based on hourly data at Saskatoon airport from Environment Canada (http://www.climate.weatheroffice.gc.ca)

Furthermore, looking at the minimum $\overline{T}$ values in Table 3.2, it is encouraging to see the experimental trailer was capable of providing an environment above 0°C, or more specifically above -1°C for broiler chickens at different heater and fan settings. The highest maximum $\overline{T}$ value was around 30°C. According to the study conducted by Knezacek (2005) on commercial trailers, for ambient temperatures ranging from -12.9 to -5.0^{o}C, the lowest crate temperature among the eight tests was -6.8^{o}C and the highest crate temperature was 25.6^{o}C. Knowing the design of the commercial trailers was different from that of the experimental trailer, and the positions of sensors in the two studies were different, it is still encouraging to see the experimental trailer was able to provide a warmer environment than commercial trailers at the similar range of ambient temperatures.

Table 3.2 summarizes the minimum and maximum *RH** values for each data set. In general, the *RH** values varied from 8.1 to 93.2%. In Figure 3.14, *RH** is divided into a number of ranges. The *y*-axis indicates the percentage of data loggers (count) which had the *RH** value fall into each range. Figure 3.14 shows that the majority of sensors had *RH** values between 10 and 40%, with the rest having *RH** values below saturation. It is important to point out there were a few sensors from which relative humidity data were not available. In these cases, the loggers recorded erroneous signals suggesting the data loggers had either malfunctioned or were near saturation. The number of sensors which contained erroneous relative humidity signals was listed in Table 3.2. These sensors were not included in the calculations of the percentiles of data loggers for Figure 3.14. During the experiment, all chickens transported on the experimental trailer were observed to be dry at the receiving dock.

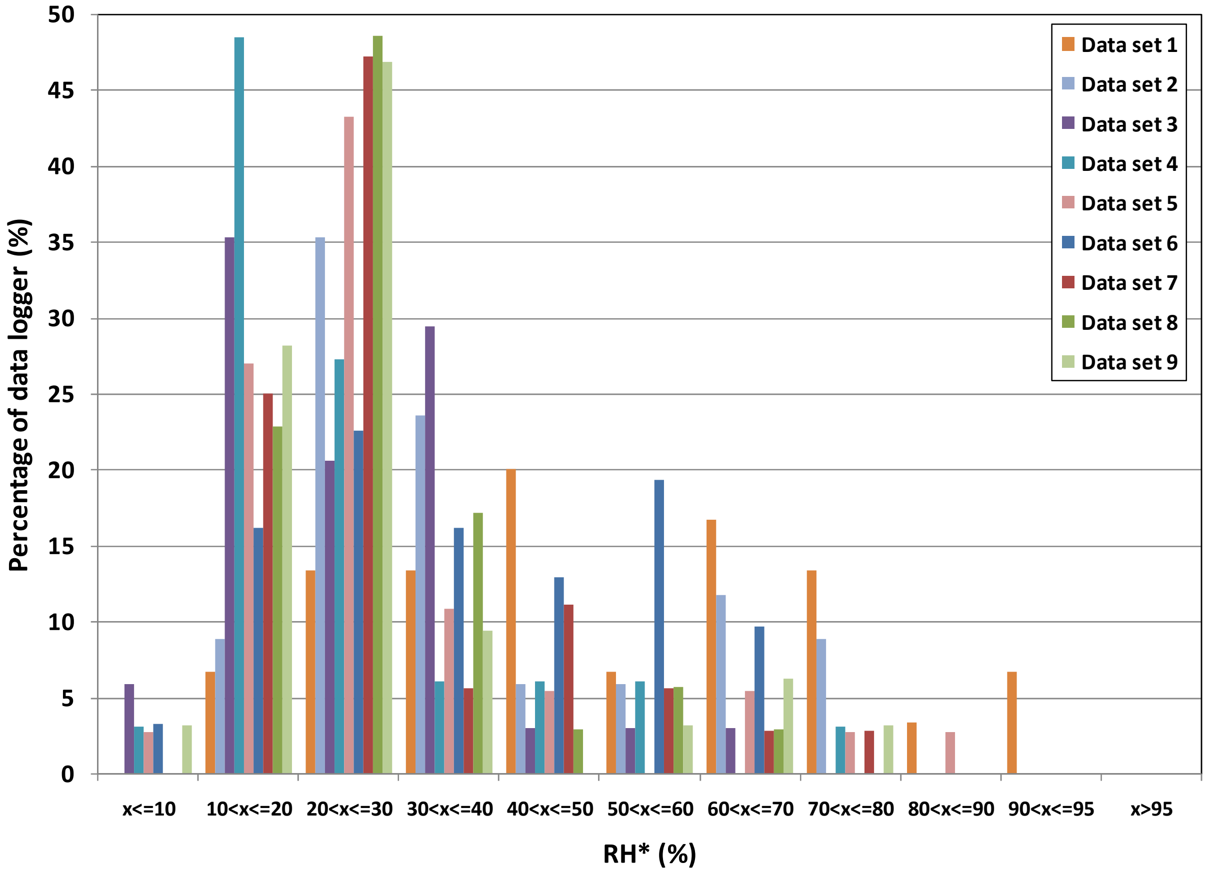

Figure 3.14. Percentage of data loggers found in different ranges of *RH values (refer to Table 3.2 for system settings of the nine sets of data).**

Hunter et al. (1999) concluded that broiler chickens subjected to an air velocity of 0.7 m/s could be safely transported at crate temperatures as low as –4°C, if they are dry. However, with wetting, moderate hypothermia would occur at temperatures as high as 8°C. Based on the lowest averaged load temperature ($\overline{T}$) at around -1°C (Table 3.2) and the majority (except those which gave error signals) of the data loggers giving a *RH** value below 95% (Figure 3.14), these data suggest that the experimental trailer was able to provide safe transportation conditions for broiler chickens.

As for the upper limit, Webster et al. (1993) suggested that well-feathered broilers or laying hens would be comfortable at temperatures ranging between 15 and 26°C. Mitchell and

Kettlewell (1998) measured the physiological response of broiler chickens in transport drawers under a range of temperature and humidity conditions. They discovered high levels of relative humidity (70-80%) in commercial transport vehicles, therefore, heat stress can be expected when temperatures reach 25°C. In the experimental trailer, the maximum load temperature did exceed 26°C in some cases (26.3°C to 30.1°C in data set 4, 6, 9). The maximum level of *RH** of these data sets were between 66.2 to 75.4%. These three cases employed one or two fans. Table 3.2 does not provide information on whether the high temperature and the high *RH** levels occurred at the same position. However, these data pointed out that although the research focus was on preventing cold stress in birds, it is important to pay close attention to prevent the occurrence of over-heating when programming the set points of the fans, and selecting the number of heaters to be used. It may be worthwhile to investigate the feasibility of connecting the heaters to a programmable controller or replacing the existing heaters if they are not programmable. By having both types of components programmable, and examining the data obtained from this research, the operator can then develop a regime to optimize the ventilation and heating system.

3.5.3 DISTRIBUTION OF LOAD CONDITIONS

Volumetric contour plots of temperature gain in inlet air for data loggers ($\Delta\overline{T}$) of eight data sets were created using Tecplot. The plots were not created for data set 6 because the locations of some data loggers were not properly recorded, thus making it impossible to obtain the coordinates of the data loggers and generate the 3-D plots. The eight data sets can be sub-divided into three groups based on the number of fans that were used. Group 1 included data sets 8, 3 and 7 which used the bottom fan only. Group 2 used two fans, which included data sets 1, 9, 4 and 5, the first three data sets used the bottom and middle fans, while data set 5 used the bottom and top fans. Group 3 used three fans which included data set 2. All the temperature plots are presented in Appendix E, and Figure 3.15 shows one example.

As shown in Figure 3.15, each plot shows six temperature profiles, the left side of the figure shows three longitudinal planes: the right-side (viewed from the rear), the centerline and the left-side of the experimental trailer. The right side of Figure 3.15 shows three cross-sectional planes width-wise: the front, the mid-plane and the rear of the trailer. Each plane has its own set of axes, and the origin of the *x, y, z* coordinates (0,0,0) is positioned at the bottom-right front corner of the experimental trailer. Each plot has its own legend, covering the minimum and maximum $\Delta\overline{T}$ values. Because the minimum and maximum $\Delta\overline{T}$ values were not the same for all data sets, different legends were used. This was intentional in order to view the contours at the highest resolution.

Looking at these plots, a few general trends can be identified. In general, the temperature profiles were longitudinal, they varied from the front to the rear end of the experimental trailer. The front planes were generally colder than the rear planes, the experimental trailer was circulating air longitudinally, collecting heat from front inlet and carrying it to the rear outlet. In addition, the longitudinal mid-planes were warmer than left and right planes near the tarpaulins. The longitudinal left- and right-planes were not perfectly symmetrical. It is interesting to see some readings were negative. They were located near the inlet and the side planes. For the locations near the inlet, it can be explained by the fact which $\Delta\overline{T}$ were calculated based on the "averaged" inlet temperature. The individual inlet temperatures were not uniform as indicated by the standard deviation of the averaged inlet temperature presented in Table 3.3. Therefore, it is logical to see some data loggers near the inlet read lower than the averaged inlet temperature.

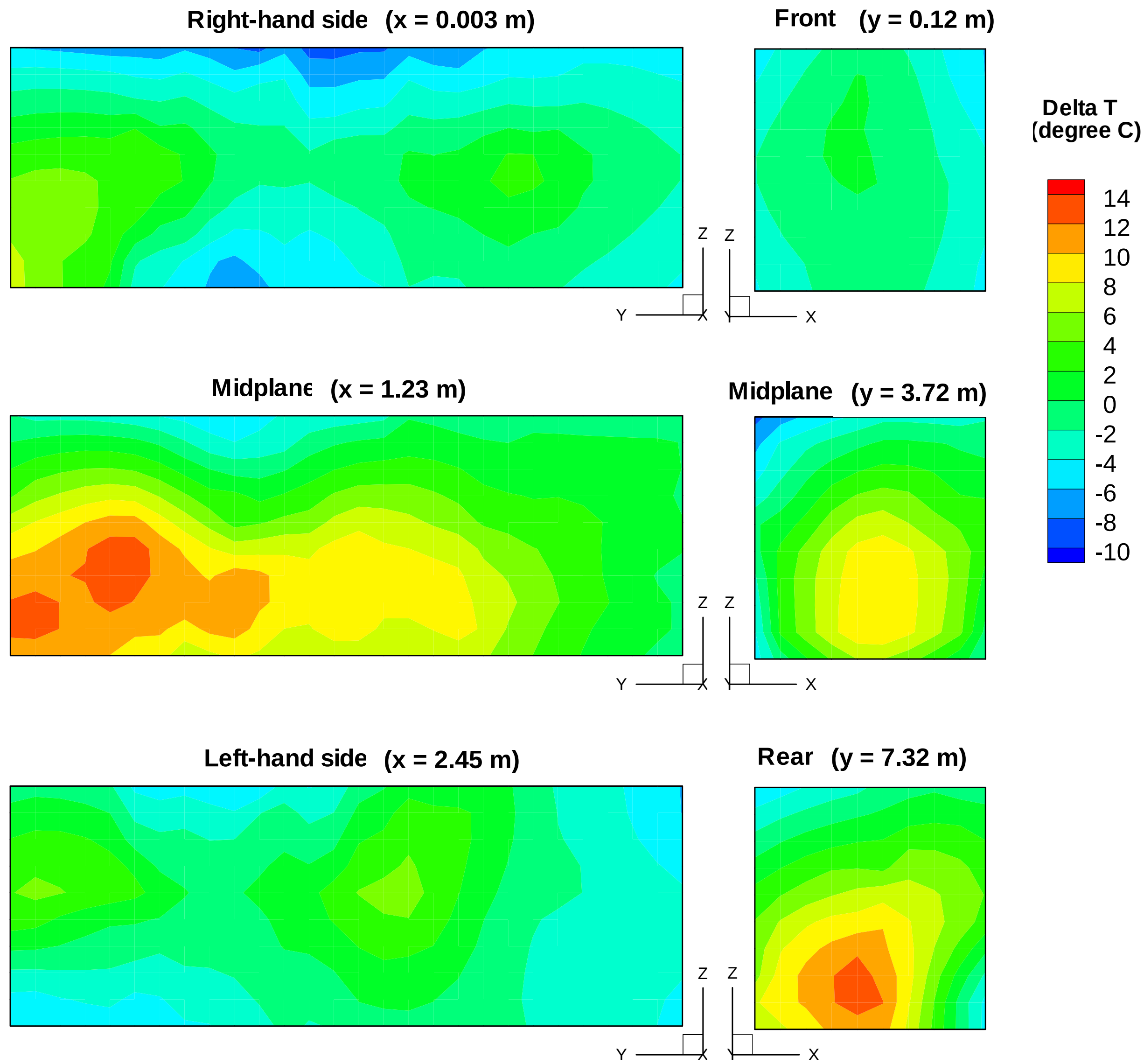

Data set #	5
Amb. T at Saskatoon airport, degree C	-10.83
Nb. fans used	2 (Btm & Top)
Nb. heaters used	1 (Btm)
Inlet opening, %	50%
Date	17-Mar-05

Figure 3.15. Profiles of temperature gain in inlet air for data loggers $\left(\Delta\overline{T}\right)$ of data set 5, the origin of the *x*, *y*, *z* axis (0,0,0) indicates the bottom-right front corner of the experimental trailer (viewed from the rear).

As for the side planes, the negative values were likely caused by heat loss (conduction and convection of a moving vehicle) through the sidewalls or leakage at the edges. Knowing the ambient temperatures were lower than the averaged inlet temperatures (Table 3.3), for sensors located near the non-insulated sidewalls, they would approach the ambient temperatures, resulting in negative $\Delta\overline{T}$ values. In many cases, the lowest $\Delta\overline{T}$ values occurred at the top-left and/or the bottom-right edge, locations which presented the most difficulty for sealing in the field tests. The longitudinal plots suggested the presence of air leakage near the edges, which in turn may have caused the lack of symmetry between the left and right sides of the experimental trailer.

The 3-D plots in Appendix E did not differentiate the effect of one, two or three fans on the temperature distributions. Table 3.3 summarizes the average, minimum, maximum and the range of $\Delta\overline{T}$ values. The average, minimum and maximum values did not reveal much difference between the three groups of fan settings. The range of $\Delta\overline{T}$ (difference between maximum and minimum values) did suggest that when more fans were used, the range of $\Delta\overline{T}$ narrowed. Such a trend is logical as when more fans were used, more air would be pulled through the load and each unit of air would pick up less heat (assumed the total heat production from broilers was similar from load to load). As this trend was not very strong, it is recommended to collect additional data to better support this observation.

Table 3.3. Inlet conditions and temperature gain in inlet air for data loggers $\left(\Delta\bar{T}\right)$ from field tests, during transport.

	Data set #	Number of heaters	Number of fans	Temp at Diffuser 1 (TC1-25) Avg (°C)	Stdev (°C)	Ambient temperature (°C) Data logger	Airport	$\Delta\bar{T}$ (°C) Avg	Min	Max	Range
Group 1											
Feb 4th 2005b	8	0	1 (B)	7.4	0.2	n.a.	-11.9	2.4	-8.3	16.8	25.2
Feb 15th 2005	3	1 (B)	1 (B)	10.1	4.3	-14.4	-17.1	2.0	-10.0	15.3	25.4
Feb 4th 2005a	7	1 (B)	1 (B)	10.3	0.7	n.a.	-9.8	1.1	-8.0	14.1	22.1
Group 2											
Feb 23rd 2005a	1	1 (T)	2 (B & M)	5.7	1.4	-14.9	-15.4	1.3	-4.9	11.2	16.2
March 24th 2005	9	1 (B)	2 (B & M)	6.0	0.9	n.a.	-16.4	3.7	-4.0	20.7	24.8
Feb 18th 2005	4	2 (B, T)	2 (B & M)	21.2	5.0	-15.6	-15.4	-5.6	-16.6	5.1	21.7
March 17th 2005	5	1 (B)	2 (B & T)	6.7	1.1	-12.8	-10.8	0.9	-6.0	13.9	20.0
Group 3											
Feb 23rd 2005b	2	1 (B)	3 (B,M,T)	6.0	1.1	-11.7	-13.1	3.5	-3.2	13.3	16.6

Appendix F summarizes the *RH** volumetric contour plots from the eight data sets. These plots have the same layout as those showing the temperature data, but they all use the same legend, because the range of *RH** did not vary much among the data sets. In general, the front end of the trailer was drier than the rear. In some cases, the floor of the trailer had much higher humidity levels than the rest of the trailer. This occurred in all data sets for two and three fans, and one data set where one fan was used.

3.6 CONCLUSIONS AND RECOMMENDATIONS

A series of field tests were conducted to study the performance of an actively ventilated and heated poultry transport vehicle. The experimental data were collected when the ambient temperatures were between -17 and -3°C approximately. The average load temperature varied from 7.1 to 15.6°C in the nine sets of data. The system was able to maintain an environment above -1°C. As for the humidity level inside the trailer, the majority of sensors had *RH** values between 10 and 40%, with the rest having *RH** values below saturation. The highest maximum load temperature was around 30°C, which identified that although the research focus was on preventing stress to birds caused by cold conditions, it is important to pay attention to the possibility of over-heating when programming the fans, and deciding the number of heaters to be used.

The 3-D temperature profiles showed that temperatures varied longitudinally. The front end was generally colder than the rear end. In addition, the longitudinal mid-planes were warmer than left and right planes near the tarpaulins. The longitudinal plots also suggested the presence of air leakage, which in turn may have caused the non-symmetric conditions between the left and right sides of the experimental trailer. In general, the front end of the trailer was drier than the rear end. In some cases, the floor of the trailer was much wetter than the rest of the trailer. The experimental data did not clearly differentiate the effect of various fan settings. It is possible that using more fans lowered the variability of temperatures within a load, but more experimental data are needed to confirm this observation.

The field tests were conducted in stressful circumstances for researchers. Data were collected in journeys after midnight, at cold outdoor conditions, with lots of traffic and under a tight schedule. As a result, there was missing sensor placement information in one of the field tests. It is recommended to pay extra attention when taking field notes under the stressful circumstances. In some tests, ambient temperatures at the tractor were missing due to poor record keeping or malfunction of the sensor. It is recommend to install an additional data logger outside the load to record ambient temperature to prevent the occurrence of missing data. Using more data loggers inside the modules may improve the spatial resolution of the data. Of course, conducting more replicates at each fan and heater setting will further strengthen the conclusions observed in this study.

Results from this study allowed the characterization of the performance of the experimental trailer in field conditions. As a first attempt in testing the system, the data also helped to develop confidence while using the system. The results suggested that the concept of active ventilation and heating is realizable. It is a promising option to improve the transport conditions for broiler chickens in cold conditions.

3.7 ACKNOWLEDGEMENT

The authors acknowledge financial support provided by the Natural Sciences and Engineering Research Council of Canada, Agriculture and Agri-Food Canada, the Chicken

Farmers of Saskatchewan, Le Fonds Québécois de la Recherche sur la Nature et les Technologies and the University of Saskatchewan in this project. The authors also acknowledge support received from Lilydale Inc. and its personnel, especially Mr. Sunny Mak and Mr. Melvin Karakochuk. The authors thank the following staff members from the University of Saskatchewan for their help during the construction and testing of the experimental trailer: Mr. Wayne Morley, Mr. Mike Miller, Mr. Louis Roth, Ms. Toni Schleicher and especially Mr. Randy Lorenz.

PREFACE TO CHAPTER 4

This paper is the third of a series of four papers. The previous two papers focused on the design, construction and experimental evaluation of an actively heated and ventilated vehicle. This paper examines the third objective of the research project: to develop, calibrate and validate CFD models used for simulating the environmental conditions surrounding the broilers as found inside the experimental trailer.

This paper begins by briefly reviewing the design of the experimental trailer, it then discusses the development of a Computational Fluid Dynamics (CFD) model which simulated this trailer. The paper then discusses the calibration and validation of the CFD model using experimental data described in the previous paper. The CFD model's performance, limitations and effect of input parameters are also discussed in detail in this paper.

The model was developed by K.P.C. Hui with input from T.G. Crowe.

4 DEVELOPMENT, CALIBRATION AND VALIDATION OF A CFD MODEL OF A POULTRY TRANSPORT VEHICLE EQUIPPED WITH ACTIVE VENTILATION

K.P.C. Hui, T.G. Crowe

The authors are K.P. Catherine Hui, **ASABE Member and Professional Engineer,** Graduate Student; Dr. Trever G. Crowe, **ASABE Member and Professional Engineer**; **Corresponding author:** Dr. Trever Crowe, College of Graduate Studies and Research, University of Saskatchewan, C 180, 105 Administration Place, Saskatoon, Saskatchewan, S7N 5A2, Canada; phone: (306) 966-2229; fax: (306) 975-1026; e-mail: trever.crowe@usask.ca.

Abstract. *Computational Fluid Dynamics (CFD) is a numerical method used to study processes which involve fluid dynamics and heat transfer. Three 3-D CFD models were developed to simulate the environmental conditions inside an experimental poultry transport vehicle, driven by three different ventilation regimes. This study employed GAMBIT for meshing a 7.95-m long by 1.23-m wide by 2.57-m high geometry. Working in the ANSYS Workbench Framework, ANSYS DesignXplorer was setup to run the simulations as parametric studies inside FLUENT. Post-processing was completed using CFD-Post, Tecplot and Excel. This paper reviews the geometric simplifications and assumptions made in developing the models. It discusses some of the properties and sub-models used in building the models and examines the processes of model calibration and validation using experimental data. During calibration, sensitivity studies revealed that inlet velocities as well as heat and moisture production had a great impact on the results obtained from the CFD models. The levels of porosity investigated did not play a significant role. The standard error of estimate (σ_{est}) was selected as a statistical measure to evaluate the accuracy of the CFD models against experimental data during model* *validation. For temperature data, σ_{est} varied from 3.2 to 7.3°C. For humidity ratio, σ_{est} varied from 1.6 to 5.0 g of water vapour per kg of dry air. The models tended to be less accurate at the boundaries. The CFD models were able to accurately recreate the temperature trends as observed from experiments, and they provided additional information in regions where experimental data were not available or difficult to collect. These models would be most effective when conducting comparative studies involving the experimental trailer.*

Keywords. *Computational Fluid Dynamics, CFD, poultry, broiler, transport, ventilation, calibration, validation.*

4.1 Introduction

In Canada, transporting broiler chickens from dispersed farms to a central slaughter facility is an essential step of broiler production. The harsh winter conditions on the Canadian prairies impose special challenges for providing acceptable environmental conditions for broiler chickens during transport. In an effort to improve transport conditions for broiler chickens in winter, a 13.7-m (45-ft) long experimental trailer equipped with active ventilation and supplemental heating was constructed. After studying its performance in a series of field tests, the acquired data were used to develop a Computational Fluid Dynamics (CFD) model.

4.2 Objective

This paper discusses the development, calibration and validation of CFD models used for simulating the environmental conditions to which broilers are exposed within an experimental trailer.

4.3 MATERIALS AND METHODS

4.3.1 OVERVIEW OF THE CFD MODEL DEVELOPMENT

This section reviews the process, reasoning and settings employed in the development of the CFD models. The process followed the seven steps outlined in the introduction: identification of the domain of interest, geometry creation and clean-up, meshing, discretization of governing equations, discretization of boundary conditions, solving and post-processing. Commercial software packages were used to develop the CFD model. After reviewing the physical setup, the virtual geometry was created and meshed using GAMBIT 2.4.6. The governing equations and boundary conditions were then assigned in, discretized by and solved by the ANSYS FLUENT 12.0.16 software. ANSYS FLUENT was used within the ANSYS Workbench 2.0 Framework (version 12.0.1), which provided additional features such as ANSYS DesignXplorer to conduct parametric studies in FLUENT, and CFD-Post 12.0.1 to post-process the results. In addition, Tecplot 10 (version 10.0-3-66) and Microsoft Office Excel 2007 (version 12. 0.6514.5000) were also used to plot and analyze the results.

4.3.2 EXPERIMENTAL TRAILER

Before discussing the CFD model, it is important to review the configuration of the experimental trailer. It will help to understand the setup, assumptions and simplifications that were made to create the virtual geometry.

The experimental unit was built on top of a 13.7-m (45-ft) long flatbed. It was approximately 2.5-m (8-ft) wide and 2.6-m (8.4-ft) high. The unit was divided into three compartments: instrumentation room, heating and mixing chamber, and loading area. The instrumentation room housed two generators to power the electrical equipment, one hydraulic system to control the mechanical roof, three ventilation controllers, two mixing fans, one data acquisition system, and electrical boxes and conduits to connect the electrical components. In the heating and mixing chamber, there was a variable-inlet damper which controlled the amount of ambient air entering the loading area, two propane heaters and two mixing fans to heat and mix incoming air. There was also a large empty space which acted as a plenum for air mixing. A terminal box for sensor connection was also found in this empty space to connect sensors to extension wires.

The loading area was adjacent to the heating and mixing chamber. At its inlet, there were two diffuser screens with openings designed to direct air to the modules. The loading area could accommodate six stacks of modules. Each module housed multiple layers of plastic drawers. During loading, the drawers were slid out and filled with broilers. When all the drawers were filled, the operator would stack a module on top of another and load the entire stack of modules inside the loading area. Next to the six stacks of modules, there was a 229-cm (9-in) empty area, and then the third diffuser screen. Behind the diffuser screen was another 455-cm (17.9-in) gap which housed the second terminal box for sensors, followed by the tailboard of the trailer with three exhaust fans installed in a vertical pattern. Two grids of sensors, installed on the second and third diffuser screens, sensed and recorded boundary conditions. An array of data loggers was also installed inside the modules' drawers to record the environmental conditions which the broilers experienced. The roof and the floor of the loading area were insulated. The diffuser screens were made of steel, and the two sidewalls of the loading area were covered with tarpaulin curtain.

4.3.3 VIRTUAL TRAILER – BOUNDARIES, ASSUMPTIONS AND SIMPLIFICATIONS

4.3.3.1 Defining the Boundaries of the Virual Trailer

The first task in developing the CFD model was to define the boundaries of the virtual trailer, to determine if the virtual trailer should be in 2-D or 3-D, and to decide where simplifications could be made. These decisions were made based on the purpose of the CFD model, the physical setup of the trailer and observations from experimental data. The purpose of the CFD model was to simulate the environmental conditions surrounding the broilers. The inlet boundary of the model was set at the second inlet diffuser; data recorded by sensors located on this diffuser would be used to define the inlet conditions and to run the model. The top and the bottom boundaries of the area were defined by the inner surfaces of the roof and floor. Because the movement of air was driven by the exhaust fans, the tailboard of the experimental trailer was chosen to be the outlet boundary.

Experimental data showed that the environmental conditions inside the loading area were three-dimensional. The temperature and humidity profiles varied longitudinally, from front to rear. The profiles also varied across the width, from left to right. The left versus right profiles exhibited some degree of symmetry, but they were not perfectly symmetrical. The experimental data suggested that there was some air leakage, which in turn may have caused the non-symmetrical conditions between the left and right sides of the experimental trailer as discussed in Chapter 3. Based on the experimental data and field observations, it was concluded that the virtual trailer has to be three-dimensional to capture the three-dimensional data profiles. As leakage was not quantified, it was impossible to simulate leakage in the model. Therefore, it was assumed that environmental conditions on the left and right side of the virtual trailer were symmetrical. With this symmetry assumption, only half of the trailer (at full scale) was simulated. The right side (viewed from rear) of the trailer was chosen as it was quite probable leakage occurred on the left side of the trailer based on field observations. Simulating only half of the trailer, instead of the entire trailer, considerably reduced the amount of computing resources and time required to mesh and run the simulations. While it was clear that the trailer was not symmetrical, it was assumed there is perfect symmetry between the left and right sides of the trailer and the geometry of the virtual trailer would consist of the right side of the physical trailer. In summary, the boundaries of the virtual trailer were defined by the second inlet diffuser screen, the tailboard, the inner surface of the roof, the inner surface of the floor, the right tarpaulin curtain and a symmetry vertical plane which ran along the trailer's midline, from the front to its rear.

4.3.3.2 Simplifing the Geometry of the Virtual Trailer - Modules

After defining the scale, dimensions and boundaries of the virtual trailer, it was necessary to consider if simplifications could be made in recreating the modules, the exhaust fans and third diffuser screen in the virtual geometry. The experimental trailer contained six stacks of modules as shown in Figure 4.1. A stack of modules was made of two modules, the top module had four layers of drawers, the bottom module had five layers of drawers. Each layer of drawers had three drawers which spread across the width of the trailer as shown in Figure 4.2. There were 12 drawers in the top module and 15 drawers in the bottom module, with a total of 162 drawers for all six stacks of modules. In a module, the drawers were arranged on a metal frame, with a small head space above each layer of drawers. The module had a solid metal top surface, and openings at the bottom to allow handling by a forklift. The drawers were made of thick heavy plastic, with sidewalls and bottom surface (there is no top cover) made of perforated surfaces as shown in Figure 4.3. Each drawer could hold 22 to 26 birds depending on the loading density.

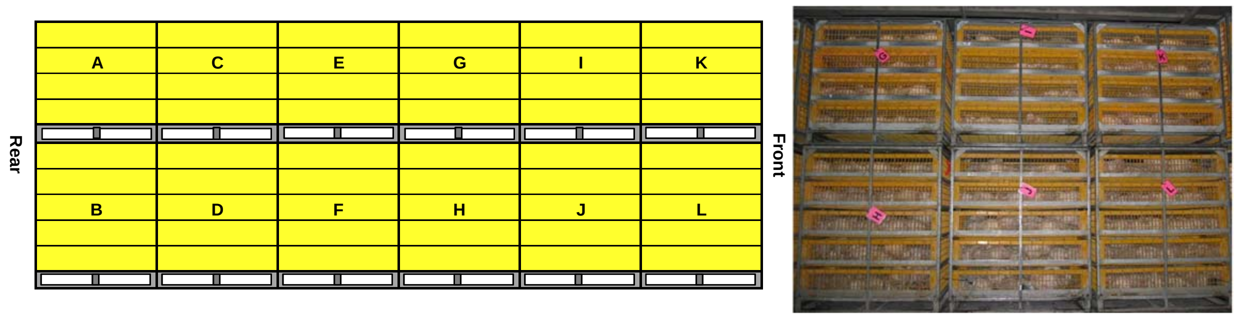

Figure 4.1. Schematic diagram and modules filled with broilers in the experimental trailer (side view).

Figure 4.2. Three columns of drawers sitting across the width of the experimental trailer.

Figure 4.3. Perforations on the sidewalls and bottom of a plastic drawer.

In the modules, the metal structure, the perforated drawer surfaces and the animals within drawers created unique challenges for meshing the irregular air space between these solid materials (Figure 4.4). Further examination confirmed the chicken modules have to be simplified in the virtual geometry in order to proceed. First of all, the scale of the air spaces on the perforated surfaces of the drawers was very small compared to the air space which existed above, below and in-between the individual drawers. It would be difficult to create a reasonable size of mesh which contained both length scales, with high-quality transitional cells joining the fine and large cells. Secondly, even if an unlimited amount of resources was available and all the details of the metal structure and the perforated walls could be recreated, it would still be difficult to know the exact position of the animals to determine the shape and size of the air space inside the drawers. The broilers may not remain at the same positions during the same test, or from test to test. Thirdly, if individual broilers were drawn into the virtual geometry, different geometry (and mesh) would be required when there is a change of loading density.

From an application point of view, it would be better to have one geometry and mesh which can handle the various changes in loading density, instead of multiple geometries and meshes. Inputting a different loading density into the model is a relatively simple task, but re-drawing a geometry and re-creating a mesh is very time consuming. Therefore, in order to work within the limits of the computing resources available, to not make any assumptions on how animals would position themselves in the drawers, and to avoid creating multiple geometries and meshes, it was decided to look for a modelling approach which would permit simplification of the modules.

Figure 4.4. Irregular air space between the broilers, and against perforated sidewalls and bottom of a drawer.

Research conducted by Moureh et al. (2002) provided inspiration in resolving the problem. Their work focused on studying the airflow pattern inside a refrigerated truck. In their research, their truck was densely loaded with pallets of boxes surrounded by small empty air gaps. The dimensions of their pallets were much bigger than the air spacing between the pallets, making it difficult to create a high-quality mesh without exceeding computing power. To resolve their problem, they replaced the thin air spacing by a fictitious porous medium with properties which generated the same resistance for the airflow (Moureh et al., 2002). Their work inspired the use of a porous media model in the chicken modules and simplifying the modules with rectangular boxes instead of drawing in all the details (metal structure, perforated drawers and individual broilers). It is important to point out the work by Moureh et al. (2002) only provided inspiration for using a porous media model. Their geometry and treatment of the porous media model were different than what was used in the current study.

In the virtual geometry, a top module was simplified to one solid surface and four layers of drawers as shown in Figure 4.5. One large, single drawer occupied each layer which spanned the width of the trailer. Above each drawer, a headspace was recreated as presented in Figure

4.6. The metal frame was not recreated as it was assumed that most of the restriction would come from the perforations of the drawers and presence of broilers instead of the metal frame. The simulated drawer was essentially a "floating" rectangular box. The porous media model was applied to the box to simulate the perforations and presence of broilers. At the bottom of each module, a large space was recreated to represent the forklift opening. A bottom module was similar to the top module, except it had five layers of "floating" drawers instead of four. In total, there were 54 drawers in the virtual geometry.

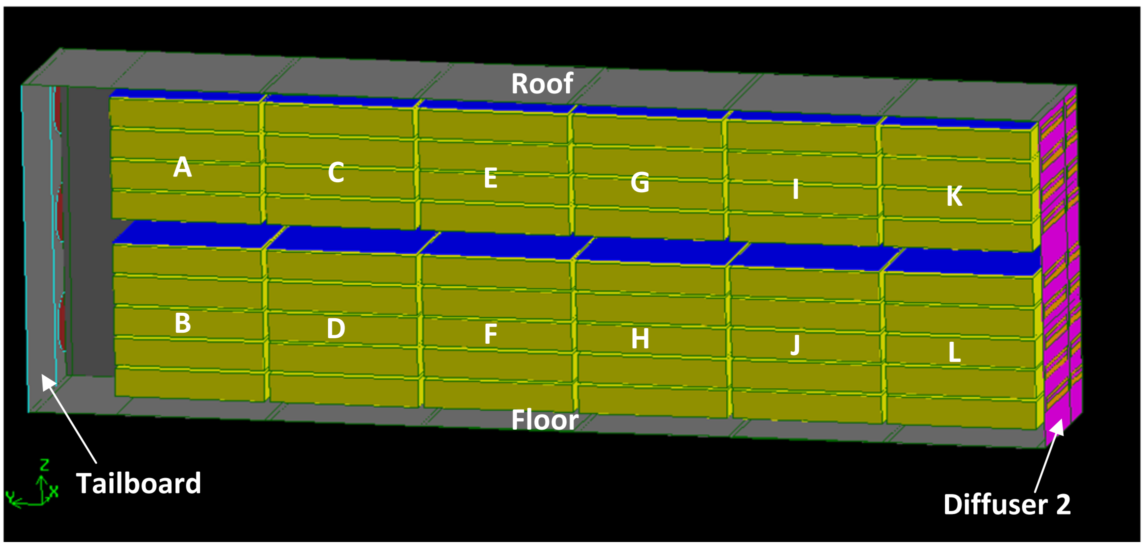

Figure 4.5. The virtual geometry showing the simplified drawers in yellow and metal surfaces in blue (viewed at mid-plane).

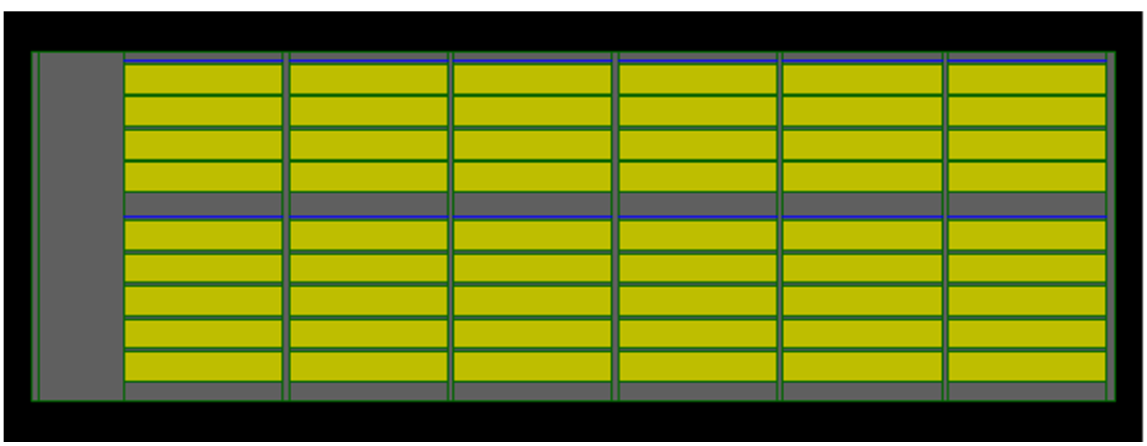

Figure 4.6. Side view of the six stacks of modules, showing headspace in grey above the drawers and larger space underneath each module (viewed at mid-plane).

4.3.3.3 Simplifing the Geometry of the Virtual Trailer – Exhaut Fans

The experimental trailer had three fans mounted on its tailboard. The top and middle fans were covered by dampers. The dampers were programmed to open when these two fans were in use. The bottom fan did not have a damper as it was designed to operate constantly to provide minimum ventilation to the load. During the experiment, the top and middle fans were set at on/off mode to operate at either 100 or 0% of their capacities. Due to space limitation, it was not possible to set up straight air ducts and flow straighteners to properly measure static pressure of the fans and to use the fan curves to obtain the fan flow rates. In the virtual trailer, the three fans were simplified to simple outlets, looking like three semicircular holes (circular holes cut into halves as only half of the trailer was simulated). The middle and top holes were defined as solid surfaces in the CFD model when these fans were not in operation, simulating the outlet dampers being closed in the experimental trailer.

4.3.3.4 Simplifing the Geometry of the Virtual Trailer – Diffuser Screen

The last simplification applied on the virtual trailer was to eliminate the third diffuser screen situated near the tailboard as shown in Figure 4.2. Assuming the air would mostly travel horizontally through the headspace just above the broilers, the presence or absence of the third diffuser screen should have minimal effect on the air flow movement and heat transfer. This decision was made after analyzing results obtained from some preliminary CFD simulations. The removal of the third diffuser screen helped to simplify meshing of the rear section of the virtual trailer, and reduce the required computing resources.

4.3.4 VIRTUAL TRAILER – FINAL SPECIFICATIONS

After analyzing the setup of the experimental trailer, reviewing the experimental data, and applying assumptions and simplifications discussed in the previous section, a 3-D virtual trailer was created using the GAMBIT software.

The virtual trailer measured 7.95 m (313.15 in) in length along the *y*-axis, 1.23 m in width (48.25 in) along the *x*-axis and 2.57 m in height along the *z*-axis (101 in). The trailer was created using the "bottom-up" approach as illustrated by Figure 4.7. The origin of the coordinates was defined at the bottom-right front corner, as shown in Figure 4.8. Individual coordinates of the experimental trailer were input into the software to create points. Points were then joined into lines. Lines were linked to create 2-D surfaces, and finally, surfaces were fused into volumes. The key points, surfaces and volumes were named as they were being created in order to keep track and reuse them. Figure 4.8 shows an isometric view of the right-hand side of virtual trailer with the second inlet diffuser screen (solid surfaces in pink, inlet holes in yellow), the inner surface of the roof and the tarpaulin curtain are in grey. The rectangular boxes with green outlines indicate the locations of the module drawers situated behind the tarpaulin curtain. The blue lines represent the solid surfaces above each module. Figure 4.9 shows the left side of the virtual trailer, with the brown holes located at the tailboard. Figure 4.9 also shows clearly the module drawers in yellow.

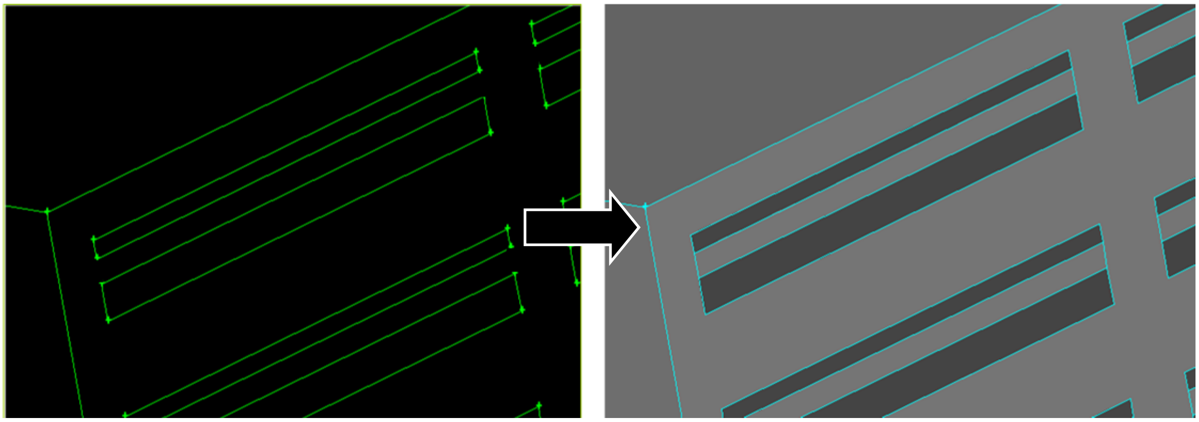

Figure 4.7. Constructing the geometry using the “bottom-up” approach.

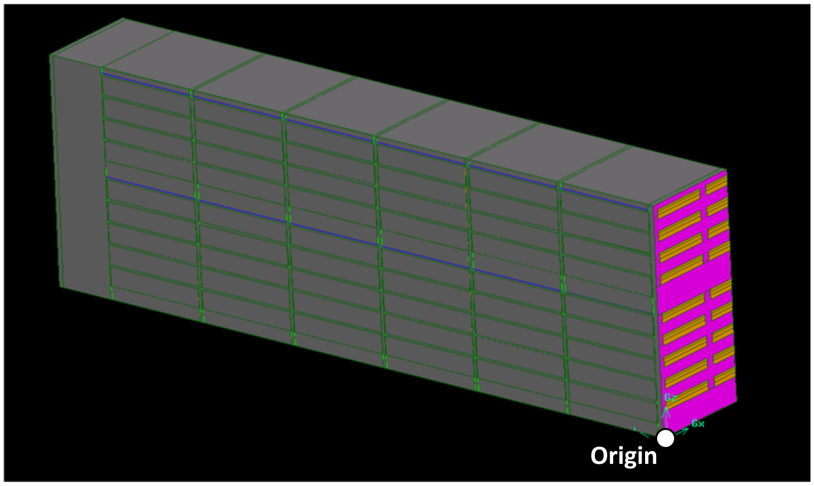

Figure 4.8. The right side (with tarpaulin sidewall) of the virtual trailer as viewed from the front.

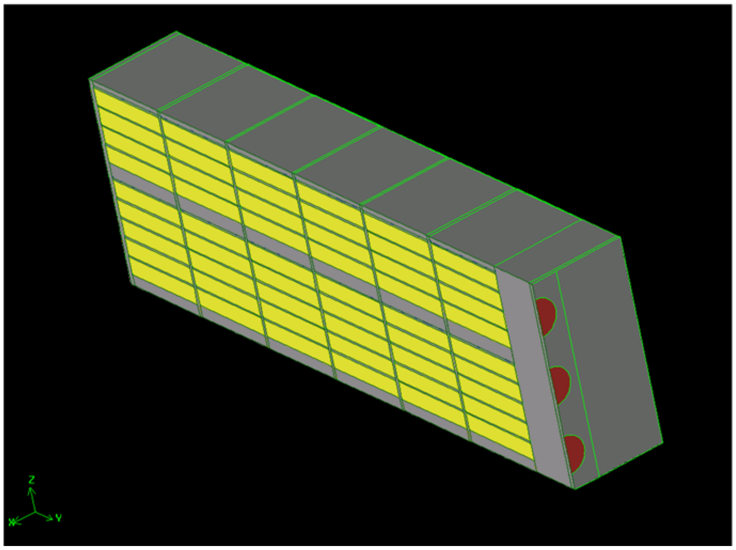

Figure 4.9. The left side (mid-plane) of the virtual trailer as viewed from the rear.

As shown in Figure 4.8 and Figure 4.9, the geometry was broken down into multiple sections. The break-down was necessary because different properties would be assigned to various sections in FLUENT. However in some cases, such as for the roof surface, the break-down was required to allow GAMBIT to create a regular mesh of higher quality, and to use fewer cells which required less computing power and time. Some of these sub-divided sections were grouped (but not fused), and they would be assigned the same properties in FLUENT. For example, the inlet diffuser was divided into many sections as defined by the green lines in Figure 4.10. After meshing, just before exporting the model to FLUENT, some of these sections were grouped together as they would share the same properties. Each group was given a name to make it easily identifiable in FLUENT. The inlet diffuser was sub-divided into 12 groups, as indicated by the different colors in Figure 4.10. There were six groups of inlet vents, giving the user the freedom to assign different boundary conditions to each group (air velocity, relative humidity and temperature). The reason for having only six groups of inlet vents was because only six humidity sensors were installed in this section of the inlet (see Appendix C). Similarly, there were six groups of solid surfaces, giving the user the flexibility to assign different wall properties to each group.

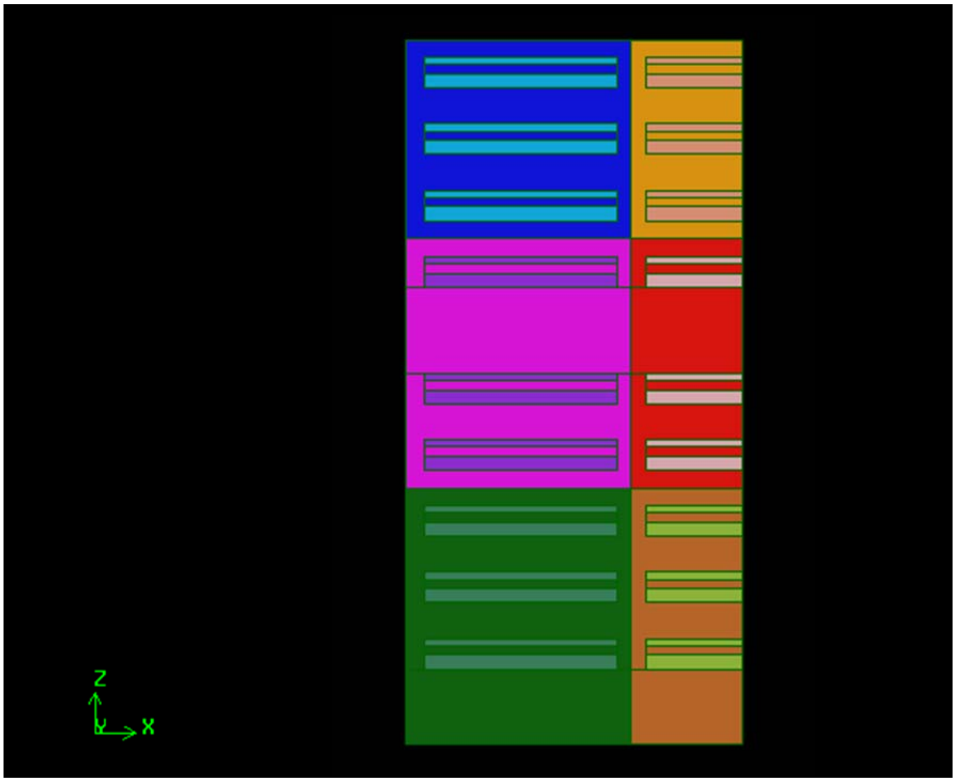

Figure 4.10. Different groups of the inlet diffuser as shown in different colors.

The tailboard consisted of five groups, as shown in Figure 4.11: two groups of solid wall in grey, and the three holes in green, blue and brown. Each hole could be set as "outflow" to simulate the fan in use, or set as a solid "wall" if the fan was not in use with the outlet damper being closed. All the small sections of the roof were grouped into one single surface. Similarly, the small sections of the floor were grouped as one. However, the tarpaulin curtain was composed of six groups, giving the user the freedom to define different boundary conditions for each group.

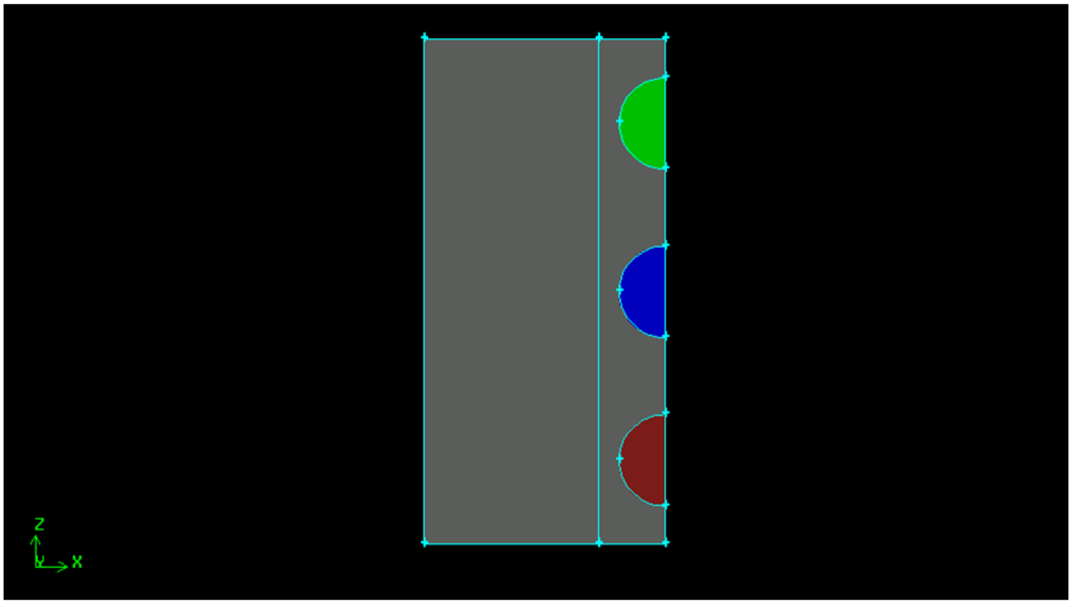

Figure 4.11. Different groups in tailboard as viewed from the outside of the trailer.

As for modules, all solid plates at the top of upper and lower modules were grouped as one (Figure 4.12). The module drawers themselves were divided into six groups representing the six stacks of modules. Figure 4.13 highlights an example of one group of modules in red. Table 4.1 summarizes all the groups as defined in GAMBIT.

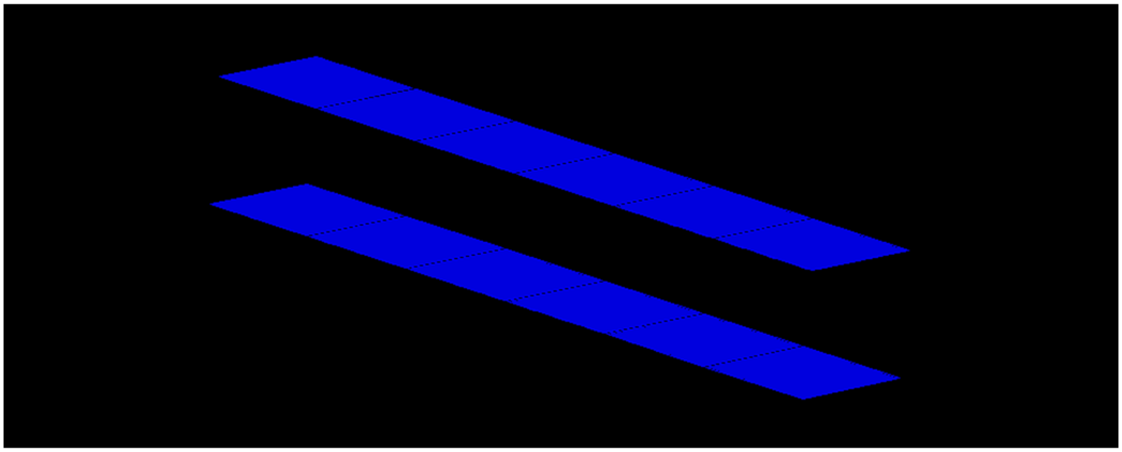

Figure 4.12. One group of solid plates on top of module drawers.

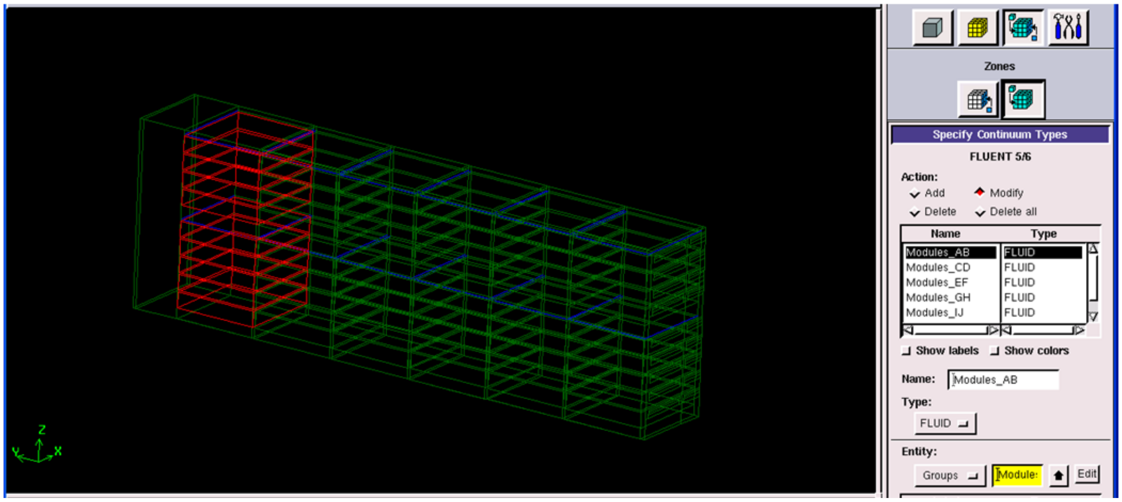

Figure 4.13. One group of module drawers as highlighted in red.

Table 4.1. Various groups existing in the virtual trailer.

Surfaces and volumes on the virtual trailer	Name of groups defined in GAMBIT
Inlet diffuser 2 - solid surface	Wall 11 to Wall 16
Inlet diffuser 2 – vents	Inflow 1 to Inflow 6
Tailboard – solid surface	Wall 2
Roof	Wall 3
Floor	Wall 4
Tarpaulin sidewall	Wall 5_ab to Wall 5_kl
Modules' solid plates	Wall 6
Module drawers	Modules_ab to Modules_kl
Tailboard - top hole	Outflow 1
Tailboard - middle hole	Outflow 2
Tailboard - bottom hole	Outflow 3

4.3.5 MESHING

The geometry of the virtual trailer was meshed in GAMBIT, then imported to FLUENT. The meshed geometry consisted of hexahedral and mixed cells. There was a total of 724,953 cells, 2,047,710 faces and 618,193 nodes. The meshing of the virtual trailer was challenging. It required many iterations of trial and error to create a mesh which passed through the "Mesh Check" in FLUENT. To successfully create a mesh in GAMBIT, it was necessary to sub-divide some regions into smaller sections, especially in regions where the geometry was irregular or there was a significant change in scales (long versus short length). In addition, it was necessary to perform the meshing in a certain sequence to control the mesh sizes in different sections and the type of transitional cells. Most regions had hexahedral cells, which required fewer cells and resolved "out of memory" problems. However, regions near the inlet diffuser and the tailboard required mixed cells to capture the inlet openings and circular hole. Following a specific sequence helped to create high-quality cells in the transitional regions which joined the hexahedral and the mixed cells successfully.

Meshes were first created on the faces (2-D surfaces) then the surface meshes were extended to create volume meshes (3-D geometry). This method controlled the size of the resulting 3-D mesh. To specify the size of the mesh, an "interval size" was defined in GAMBIT. In general, an interval size of 3 was used to mesh the length of the geometry, an interval size of 1 was used to mesh the wide and height of the geometry. These settings resulted in a cell length of approximately 76.20 mm (3 in) along the y-axis (length of trailer), and a length of around 25.4 mm (1 in) along the x- and z-axes (width and height of trailer). For example, a module drawer with a length of 1.17 m (45.87 in) and the setting of an interval size of 3 generated 15 cells along the length, with a distance of 77.67 mm (3.06 in) between each pair of nodes. Figure 4.14 shows an example of these mesh settings applied to a forklift hole. More surface cells were created along the width of the trailer (x coordinate direction) than the length (y coordinate direction). The cells along the width resembled squares, whereas the cells along the length were rectangular. These interval size settings were applied everywhere in the geometry, except the small gaps between the module drawers (an interval size of 1 was used) and the regions with irregular geometry (such as the tailboard). It was important to carefully consider the size of cells, as it would affect the accuracy of the results. A coarse mesh would reduce the resolution and accuracy of the results, but having a very fine mesh would be taxing on computer resources (power and running time). The maximum mesh size used in this study was limited by the computing power available to the project.

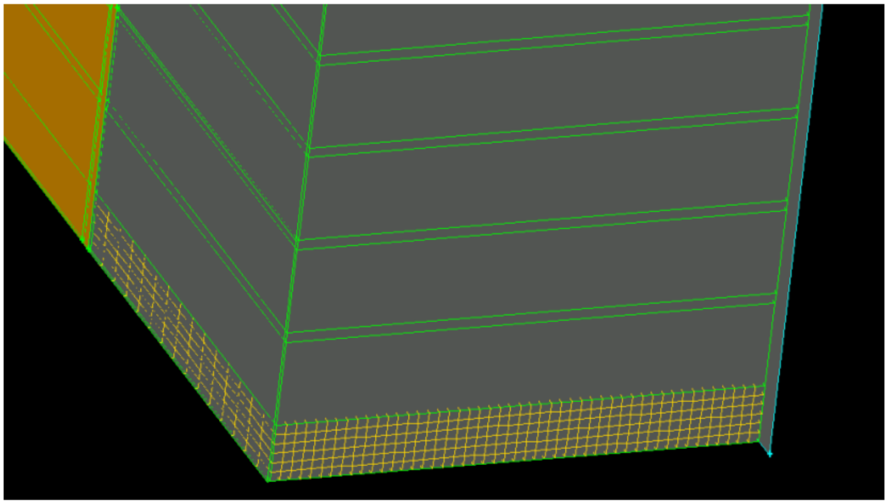

Figure 4.14. Close-up of the mesh on the forklift hole under a bottom drawer.

Table 4.2 summarizes the procedure used to mesh the virtual trailer. It also contains the settings specified in GAMBIT to create the mesh. Column two specifies if it was for a face or volume mesh. Column three lists the locations of sections which were meshed. The rest of the information included settings to create the mesh. Various “schemes” were available in GAMBIT to mesh a section. The “Quad” scheme created a mesh made of only quadrilateral elements. The “Hex” scheme was used to create a volume mesh with only hexahedral elements, and the “Tet/Hybrid” scheme generated a mesh mostly made up of tetrahedral elements but would also have hexahedral, pyramidal and wedge elements if needed (Fluent Inc., 2007). The “Map” type created a structured mesh. “Submap” first broke up a section into mappable sections and generated structured mesh. “Pave” created an unstructured mesh, and “TGrid” was a specialized meshing scheme. Figure 4.15 to Figure 4.17 show details of the mesh created in GAMBIT.

Table 4.2. Procedure and settings used to mesh the virtual trailer (refer to Figure 4.5).

Step	Faces (F) or volumes (V)	Sections	Elements	Type	Smoother	Interval size
1	F	Space2 - top & floor, between modules K/L & tarp)	Quad	Map	None	3
2	F	Space1 - top & floor, between modules K/L & diffuser 2	Quad	Map	None	1
3	V	Modules K/L (entire stack)	Hex	Map	None	1
4	V	Space 2	Hex	Submap	-	1
5	F	Diffuser 2 - all openings	Quad	Map	None	1
6	F	Diffuser 2 - plates between openings	Quad	Map	None	1
7	F	Space 1 - tarp & mid-plane	Quad	Submap	-	1
8	F	Diffuser 2 - rest of solid wall				
		• D2-face1 & 1b	Quad	Pave	-	1
		• D2-face2 a to 2d	Quad	Submap	-	1
		• D2-face3 & 3b	Quad	Pave	-	1
		• D2-face4a to 4d	Quad	Pave	-	1
9	V	Space1	Tet/Hybrid	TGrid	-	1
10	F	All space lengthwise between modules & tarp - top & floor	Quad	Map	None	3
11	F	All space widthwise between modules - top & floor	Quad	Map	None	1
12	V	• Modules I/J	Hex	Map	None	1
		• Space widthwise between modules	Hex	Map	None	1
		• Space lengthwise between modules & tarp	Hex	Map	None	1
13	V	Repeat step 12 for all other modules (G/H, E/F, C/D, A/B), one by one				
14	F	Rear - floor1 (1st section of floor located just behind module A/B)	Quad	Map	None	3
15	V	Rear - floor 1	Hex	Map	None	1
16	F	Tailboard openings - all 3	Quad	Pave	-	1
17	F	Rear - 2nd section – sidewalls, floor & roof (connected to tailboard)	Quad	Map	None	1
18	F	Tailboard 1 - solid surface, larger section	Quad	Map	None	1
19	F	Tailboard 2 - solid surface, smaller section around the circular openings	Quad	Pave	-	1
20	V	Rear - 2nd section	Tet/Hybrid	TGrid	-	1

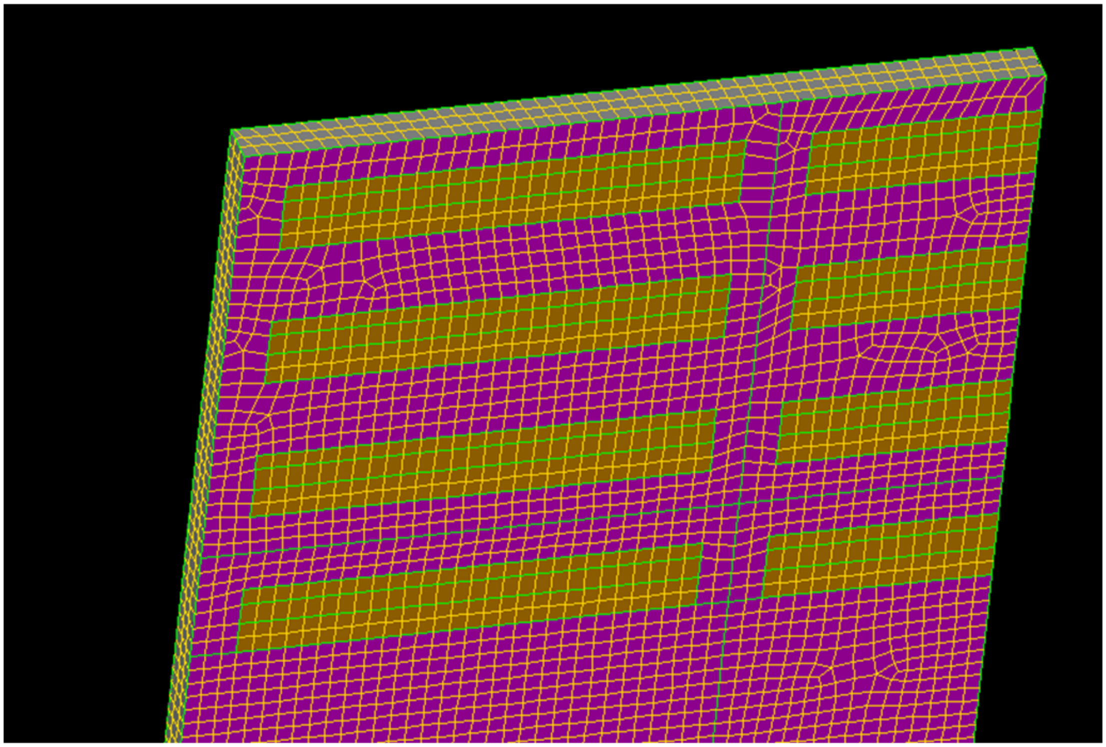

Figure 4.15. Close-up of mesh at Diffuser 2.

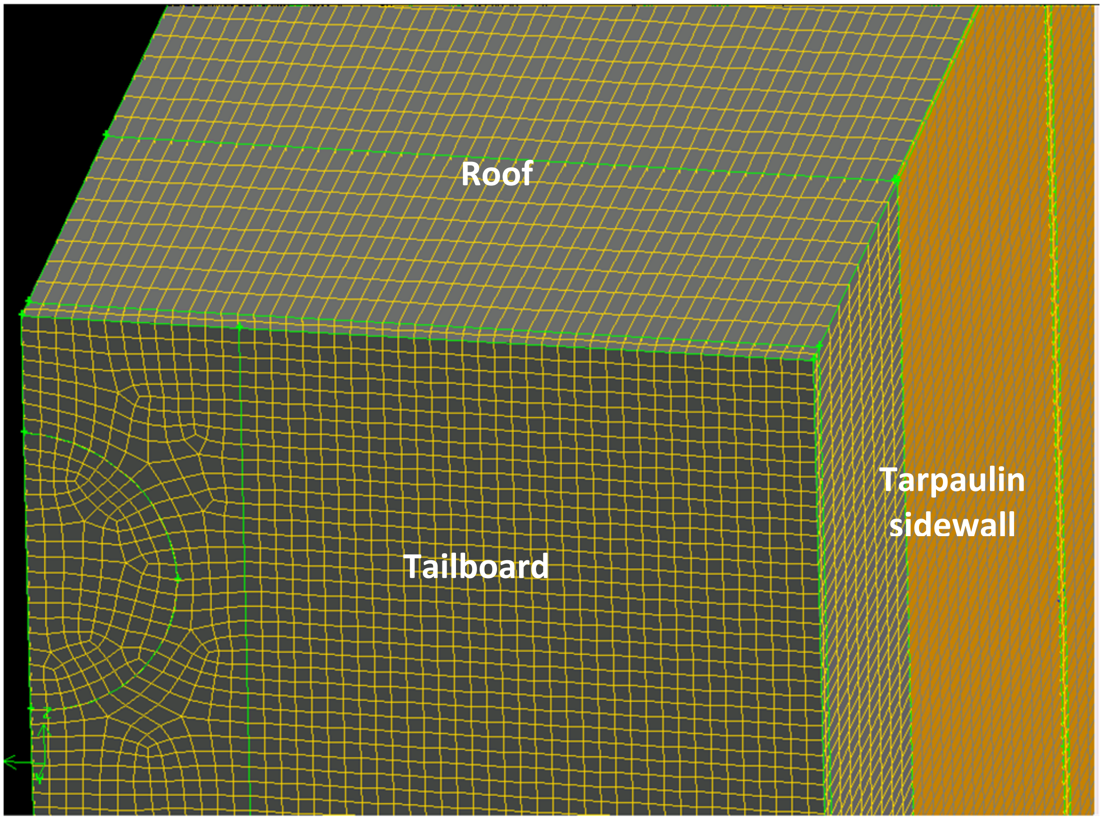

Figure 4.16. Structured mesh used along the tarpaulin sidewall, roof and part of tailboard.

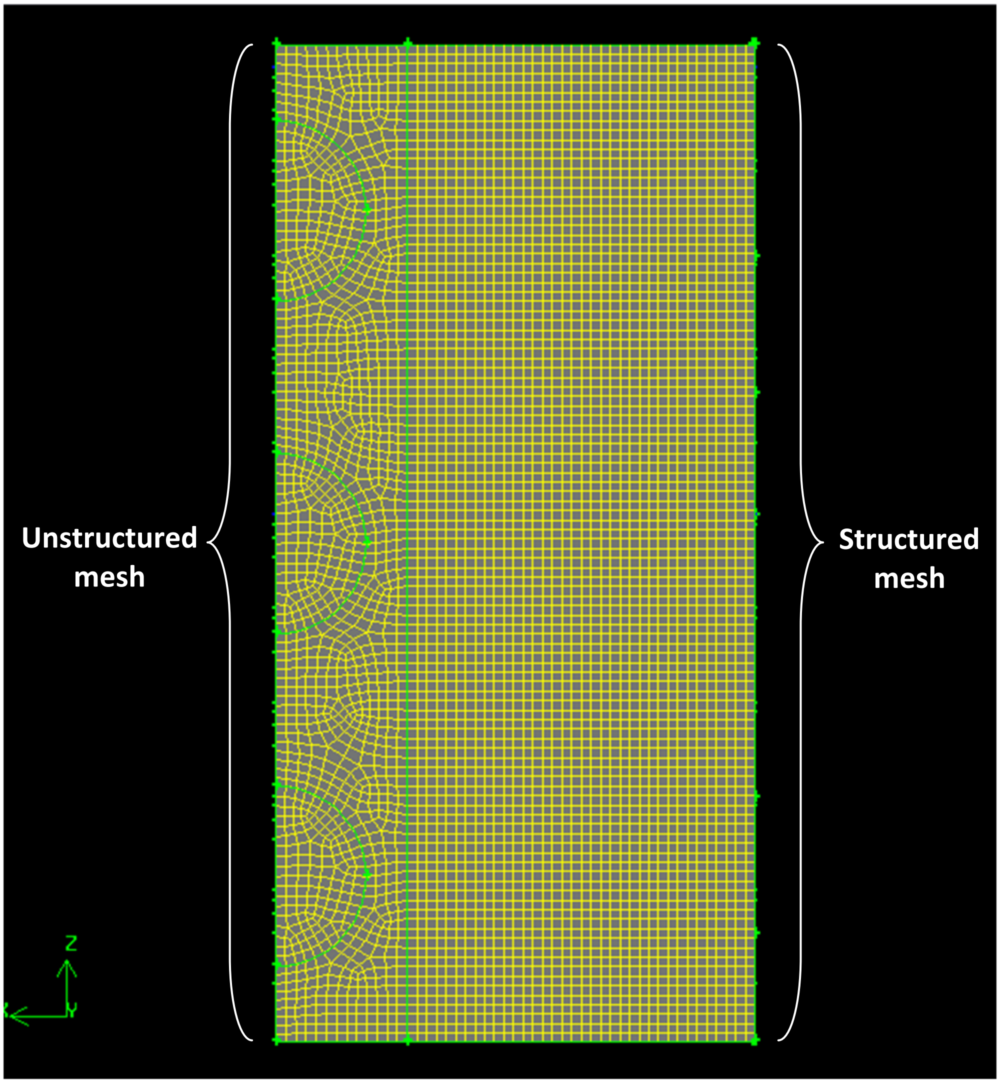

Figure 4.17. Structured mesh used in the large section of the tailboard, and unstructured mesh used around the circular openings and on the openings.

After completing the mesh, each group listed in Table 4.1 was specified as either boundary or "continuum" with fluid running in it. Boundary groups were specified within GAMBIT as wall, velocity inlet, outlet vent, or symmetry plane (for the longitudinal plane which ran along the trailer's midline). These boundary types could later be modified in FLUENT. Module drawers were specified as continuums. At this point, no properties were assigned to these boundaries or continuums. After making these specifications, the GAMBIT file was exported to a specific file format, making it readable in FLUENT.

4.3.6 CFD MODEL – PARAMETRIC STUDY

A total of three CFD models were developed and solved using FLUENT. The first model simulated the trailer using 1-fan: the bottom circular hole set as “outflow”, with the other 2 holes closed and defined as “walls”. The second model simulated the 2-fan ventilation regime, and the third model simulated the 3-fan regime. The models were set up such that FLUENT would execute within the Workbench Framework. A screen shot of this application is shown in Figure 4.18. Within Workbench, it was possible to connect FLUENT with DesignXplorer to conduct a “parametric study”.

Running simulations as parametric studies has gained popularity in the last few years. Many CFD software packages now offer this feature to design analysts. It does take extra effort to set up a simulation, but it reduces the amount of time to run multiple scenarios. In the past, an input value (such as inlet velocity) was treated as a constant with a numerical value assigned to it inside FLUENT. To test the effect of an input value, it was necessary to go into the model, underneath several levels of sub-menus to modify its value. Each CFD model developed here employed over two dozen input values, and it would be a tedious task to update and to keep track of changes in input values if they were manually updated one-by-one.

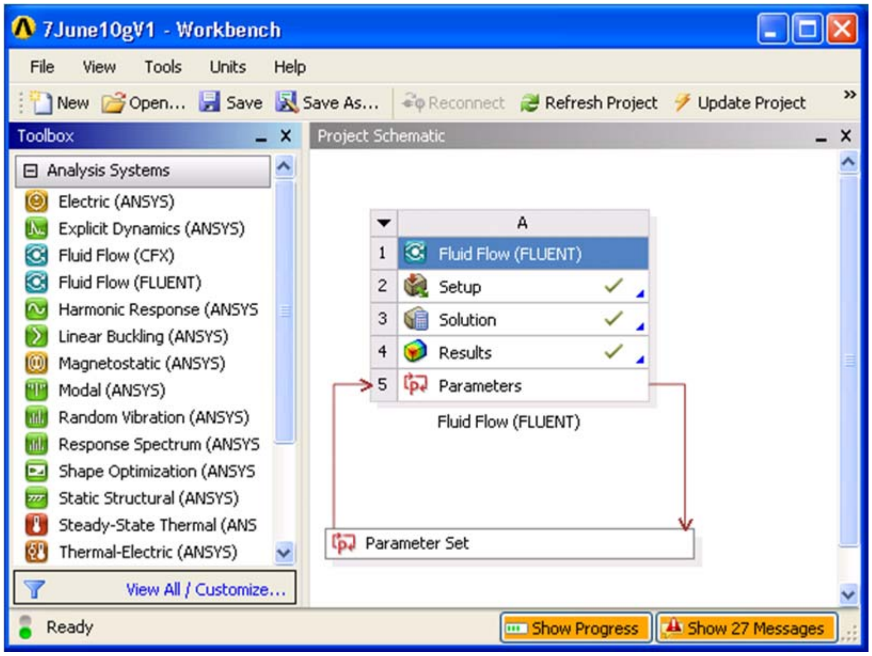

Figure 4.18. Using FLUENT in the Workbench Framework.

In the case of a parametric study, input values (such as inlet velocity) were defined as variable "parameters" instead of constants. In this present study, an input value was set as a parameter by giving it a name inside FLUENT, as shown in Figure 4.19. Input values were then no longer treated as constants but as variables by the software. Once all parameters were identified, their values could then be updated inside DesignXplorer in a spreadsheet format (Figure 4.20). The use of FLUENT and DesignXplorer also allowed the creation and use of "output parameters". It was set up to extract results of the output parameters from FLUENT and summarize them in a tabulated format inside DesignXplorer. It was also possible to set a few test cases (called "design points") with different values assigned to each parameter and let the software run the cases in batch mode. The use of FLUENT with DesignXplorer in Workbench simplified the logistics required to modify input variables and extract results, and saved time by running simulations in a batch mode.

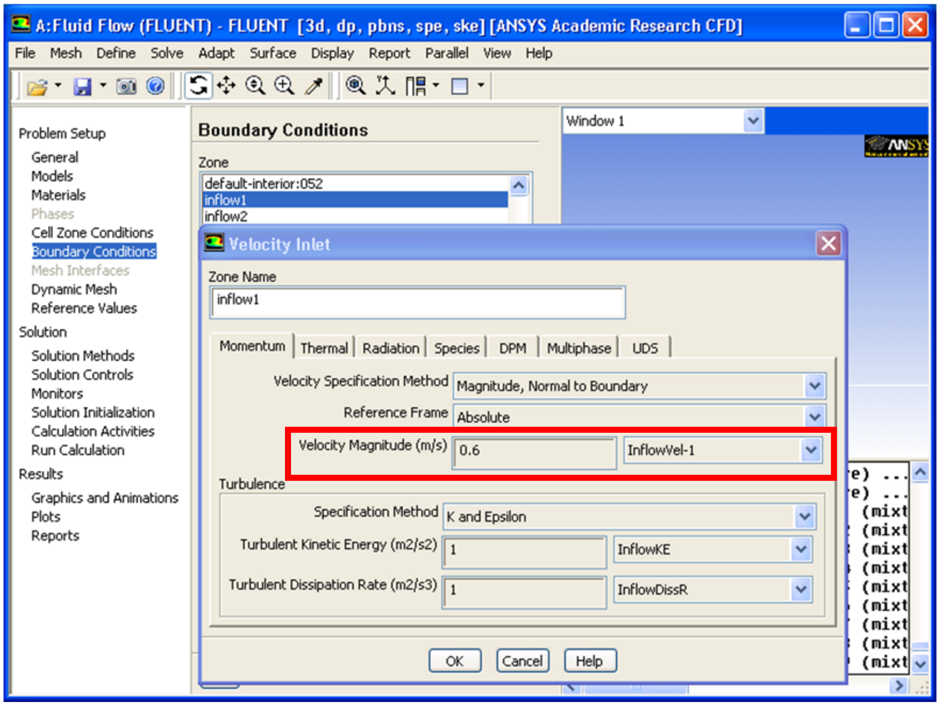

Figure 4.19. Defining “Velocity Magnitude” as a parameter “InflowVel-1”.

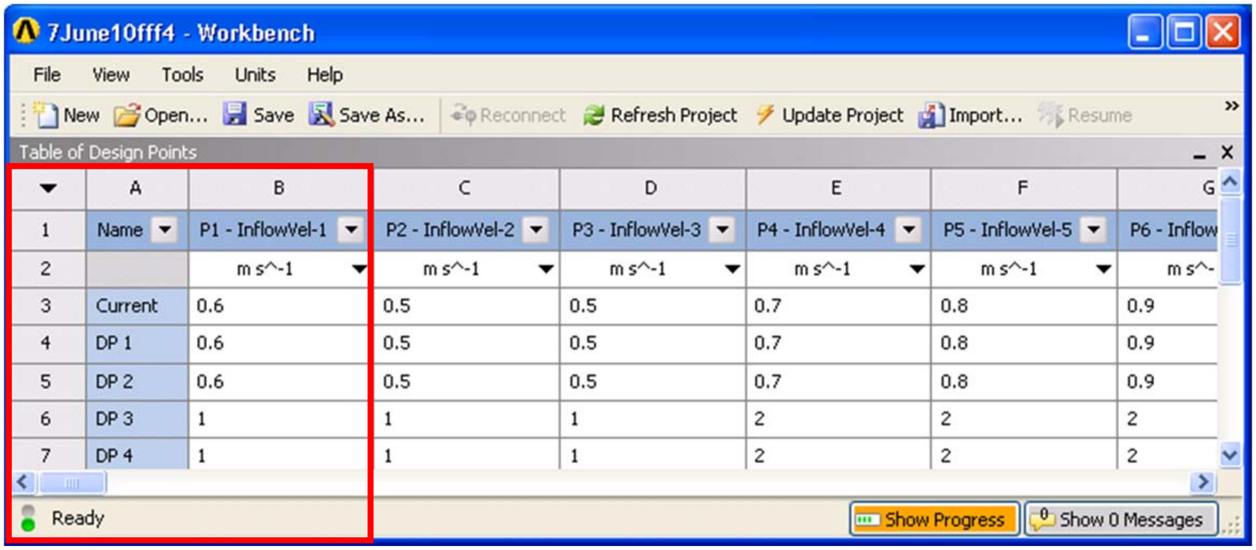

Figure 4.20. Creating 4 test cases with different values assigned to “InflowVel-1”.

4.3.7 CFD Model – The Basic Setup

In FLUENT, the solver was set up to run in 3-D, double precision and serial (instead of parallel) mode. Running the simulations in double precision could help to reduce round-off error from iterative calculations. The solver used was pressure-based, steady, with the velocity formulation set to be absolute. The viscous model was set to turbulent, using the standard k-epsilon model and standard wall functions. In addition, several additional models particular to this research project were activated: the energy model, the species transport model and the porous media model.

In order to calculate one of the primary variables of interest, temperature, the energy model was activated to calculate heat transfer. Heat and moisture sources as generated by the broilers were defined as "cell zone conditions" in the module drawers. By grouping the module drawers separately from the empty space in the loading area in GAMBIT, it was possible to instruct FLUENT that heat and moisture originated only from the drawers, but not from the other regions in the loading area. Specifying the amount of heat produced by the broilers was relatively simple. It was simply a matter of inputting the volumetric heat source in W/m^3 in one of the sub-menus. However, adding a moisture source was less straight forward. It was necessary to activate the species transport model to instruct FLUENT to simulate another type of fluid: moist air. The species transport model is commonly used to model multi-phase processes; it can be used to simulate chemical reactions. In this case, water was defined as one component of the mixture, and dry air as the second component. After setting up the species transport model, the moisture source can then be specified as "mass fraction of water", another cell zone condition for the module drawers.

FLUENT does not model relative humidity as the primary variable. Therefore, to add "relative humidity" in the module drawers or define the inlet air conditions, it was necessary to calculate the corresponding "mass fraction" of water vapour and use this as an input in FLUENT. Mass fraction for water vapour is defined as the mass of water vapour per unit mass of moist air (dry air and water vapour). It is a function of temperature, relative humidity and atmospheric pressure. After consulting the ASHRAE Fundamental Handbook (2001) and FLUENT support personnel, a series of equations were identified to convert relative humidity values to mass fraction as presented in Appendix G.

Lastly, the porous media model was implemented as part of the cell zone conditions for the module drawers. One way to define this model was to specify the viscous resistance and inertial resistance coefficients inside the media. After comparing different examples in the FLUENT manual (Fluent Inc., 2006), it was decided that the packed bed example most closely resembled the current case. One technique used to derive the input coefficients is to apply the Ergun equation along with Darcy's Law. The viscous resistance coefficient ($1/\alpha$) and inertial resistance coefficient (C_2) were then calculated using these equations (Fluent Inc., 2006),

$$\alpha = \frac{D_p^2}{150} \frac{\varepsilon^3}{(1-\varepsilon)^2} \tag{4.1}$$

and

$$C_2 = \frac{3.5}{D_p} \frac{(1-\varepsilon)}{\varepsilon^3} \tag{4.2}$$

where

α = inverse of viscous resistance coefficient (m^2),

ε = void fraction = porosity (in decimal),

C_2 = inertial resistance coefficient (m^{-1}) and

D_p = mean particle diameter (m).

For the treatment of the energy equation in porous media, effective conductivity was used in the conduction term, and the thermal inertia of the solid region was added in the transient term (Fluent Inc., 2006). The energy equation now became dependant on conductivity and density of solid particles, in addition to the properties of the fluid. The effective conductivity of the porous medium was computed by FLUENT using the following equation (Fluent Inc., 2006),

$$k_{eff} = \gamma k_f + (1-\gamma)k_s \tag{4.3}$$

where

k_{eff} = effective thermal conductivity in the porous medium (W/m-K),

γ = porosity of the porous medium (in decimal),

k_f = thermal conductivity of fluid including the turbulent contribution (W/m-K) and

k_s = thermal conductivity of solid medium (W/m-K) .

During the development, each of the above models was implemented one after another, using some approximate, bulk-value boundary conditions and properties. All solid wall surfaces were left as adiabatic walls. At each step, FLUENT was able to generate a converged solution.

4.3.8 CFD Model – Properties and Boundary Conditions

In order to set properties and boundary conditions to values which closely reflected experimental conditions, the following parameters were examined closely: heat and moisture production rates, porosity and related coefficients, and solid wall boundary conditions.

4.3.8.1 Heat and Moisture Production Rates

In 2002, Pedersen and Sallvik published a CIGR report which reviewed various models for estimating heat and moisture production rates. As part of the report, several equations were available for broiler chickens. These equations are summarized in Appendix A. The total heat loss can be sub-divided into sensible and latent heat losses. The sensible heat loss is driven by temperature difference between the animal's deep body temperature and the ambient conditions. The latent heat is the heat released during moisture evaporation (CIGR, 2002). Thus, the heat production rate originates solely from sensible heat loss, while the latent heat value is related to the moisture production rate. By calculating the total and sensible heat production from the equations, the latent heat value can be obtained from their difference. The resulting latent heat can then be divided by the enthalpy of vaporization to obtain the moisture production rate.

The equations in Appendix A are valid for temperatures ranging from 0 to 30°C and possibly higher (CIGR, 2002). The two main equations for total and sensible heat production yield results in W/hpu. The heat production unit (hpu) is defined as the quantity of animals producing 1000 W of total heat at 20°C (Pedersen and Thomsen, 2000). The CIGR report did not provide a clear explanation on how to convert these values to W for a different temperature. After confirming with Dr. Pedersen (personal communication), a method presented in Appendix A was developed to convert the results as FLUENT requires heat rates expressed in W per volume.

The air temperature varies inside the experimental trailer. Thus, the heat and moisture production rates would also be spatially different. It was assumed the air temperature inside the trailer would vary from 0 to 30°C, and broilers weighted 1.75 kg/bird. Heat and moisture production rates for this range of temperatures are listed in Table 4.3. As expected, values of the total and sensible heat production rates decreased with increasing temperatures.

Heat production is a function of the body weight, physiology of the animal, its level of activities as affected by feeding intake/routines and photoperiod, and the environmental conditions (air temperature, air velocity, radiation from surfaces and bedding conditions) which surround the animal (CIGR, 2002). The equations used to estimate the heat and moisture production in this study were developed for “normal” production conditions in the barns. Knowing that transport conditions were quite different than barn conditions, these equations were still chosen due to the fact that they were the best models available in the literature at the time the CFD model development was carried out.

Table 4.3. Heat and moisture production rates for one broiler at 1.75 kg (refer to Appendix A for method of calculation).

Temperature T (°C)	Enthalpy of vaporization h_{fg} (kJ/kg)	Total heat Φ_{tot} (W)	Sensible heat Φ_s (W)	Latent heat Φ_l (W)	Modified moisture dissipation F^* (kg/s)
0	2 501.4	22.6	13.8	8.8	3.53E-06
5	2 489.6	21.0	12.7	8.3	3.33E-06
10	2 477.7	19.4	11.5	7.9	3.20E-06
15	2 465.9	17.8	10.0	7.8	3.15E-06
20	2 454.1	16.2	8.4	7.8	3.17E-06
25	2 442.3	14.5	6.6	8.0	3.27E-06
30	2 430.5	12.9	4.6	8.4	3.44E-06

FLUENT required volumetric heat and moisture production rates as input. To compute such values, one needed to multiple the individual production rates from Table 4.3 by the total number of birds inside all modules, then divide the values by the total volume of all modules. In reality, at each layer of module, there were three individual drawers as shown in Figure 4.21. These three drawers were grouped as one rectangular box in GAMBIT, as part of the geometry simplification. Its external dimensions were used to calculate the total volume of the modules. The total volume was slightly overestimated, as the air gaps between the three drawers at each layer, and the wall thickness of plastic drawers were neglected.

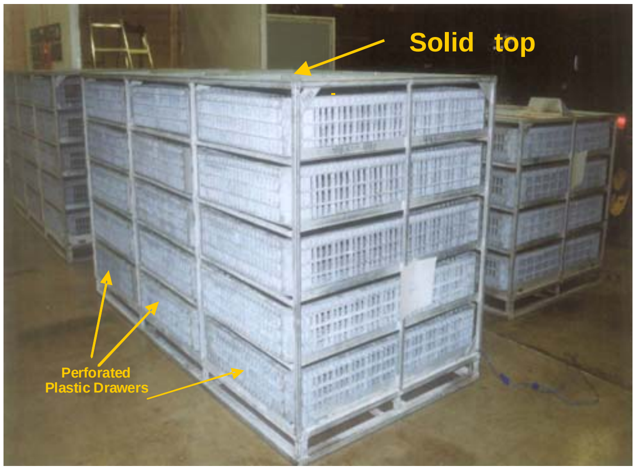

Figure 4.21. Set of three drawers per layer of module.

The volume of each simulated box was 0.61 m^3. For 54 boxes, the total volume was 33.12 m^3. In the case of a loading density of 24 birds per drawer, there were 3,888 birds per trailer. The calculated volumetric heat and moisture production rates are summarized in Table 4.4. When comparing the minimum and maximum values against the average values, the heat source varied by $\pm$ 50.3%, and the moisture source varied by $\pm$ 5.7%. The CFD software only accepted constant heat and moisture production rates. For each CFD simulation, the heat and moisture production rates were calculated based on the actual loading density encountered during the experiment, at a constant temperature value identified in the calibration process.

Table 4.4. Volumetric heat and moisture production rates for FLUENT.

Temp (°C)	Heat source (W/m^3)	Moisture source ($kg/s\text{-}m^3$)
0	1 619.8	0.000414
5	1 493.3	0.000391
10	1 345.2	0.000376
15	1 175.4	0.000369
20	984.1	0.000372
25	771.0	0.000383
30	536.4	0.000404
min	536.4	0.000369
max	1 619.9	0.000414
average	1 078.1	0.000387

4.3.8.2 Porosity and Related Coefficients

The viscous resistance and inertial resistance coefficients for the porous media are functions of mean particle diameter and porosity. The body of a broiler chicken could be viewed as an ellipsoid. For a broiler chicken of 1.75 kg, it measured approximately 0.20 m by 0.15 m by 0.12 m (semi-axis: $a \times b \times c$). To obtain the same volume as this ellipsoid, the equivalent spherical diameter was calculated to be 0.1557 m. During transportation, broilers usually assume a sitting position. Their body size did not occupy the entire height of the drawers (2.44-m by 1.17-m by 0.22-m externally). There was an available "headspace" above the heads of chickens. By assuming the chickens were spherical particles with a 0.1557-m diameter, there was a headspace of 0.0602 m (difference of 0.22 m and 0.1557 m).

Porosity was calculated according to

$$\varepsilon = 1 - \frac{V_{solid}}{V_{total}} \tag{4.4}$$

where

ε = porosity (in decimal),

V_{solid} = total volume of all solid particles within one rectangular box (m^3) and

V_{total} = total volume of one rectangular box (set of 3 drawers plus adjoining space) (m^3).

With the mean particle diameter assumed to be 0.1557 m for each broiler, and a rectangular box holding 24 x 3 chickens, the porosity of the box at the full height (H = 0.22 m) was

$$\varepsilon = 1 - \frac{V_{solid}}{V_{total}} = 1 - \frac{4/3\pi r^3 \times 24 \times 3}{L \times W \times H} = 0.768 \tag{4.5}$$

where

r = equivalent spherical radius of a broiler chicken (m),

L = length of the rectangular box (m),

W = width of the rectangular box (m) and

H = height of the rectangular box (m).

When calculated at the reduced box height (H = 0.1557 m with no headspace), the porosity was 0.678. The related coefficients of the porous media model at the two different drawer heights are summarized in Table 4.5. For each CFD model simulation, the porosity was calculated based on the actual number of broilers during the experiment. A sensitivity study was carried out during the calibration process to identify which drawer height should be used to calculate the porosity and its coefficients.

Table 4.5. Porosity, viscous resistance and inertial resistance coefficients at two drawer heights.

	Full height (0.2159 m)	Reduced height (0.1557 m)
ε	0.768006	0.678307
α (m^2)	0.001360	0.000487
C_2 (m^{-1})	11.51	23.17

4.3.8.3 Solid Wall Boundary Conditions

Within the FLUENT model, there were different types of solid walls as summarized in Table 4.1. These surfaces were assigned with adiabatic boundary conditions when testing the first version of the CFD model. In reality, some of the walls should not be adiabatic, as they did not have any insulation. In the final version of the CFD models, the type of boundary condition applied to each wall are summarized in Table 4.6.

Table 4.6. Material types and boundary conditions for solid walls.

Description	Group name in FLUENT	Material/ Insulation	Boundary condition(s)
Inlet diffuser 2 (six solid sub-surfaces)	Wall 11 to Wall 16	Steel	Constant temperature (a different value applied to each sub-surface)
Tailboard (solid surface)	Wall 2	Plywood	External radiation
Roof	Wall 3	Insulated	Adiabatic (fixed heat flux = 0)
Floor	Wall 4	Insulated	Adiabatic (fixed heat flux = 0)
Tarpaulin sidewall (six sub-surfaces)	Wall 5_ab to Wall 5_kl	Polyvinyl-chloride (assumed)	Convection with external radiation (same parameters for all six sub-sections)
Modules' solid plates	Wall 6	Steel	Coupled (between two regions)

For the tarpaulin sidewall, the user needed to supply convective heat transfer coefficient to the model. The outdoor temperature, surface temperature and traveling velocity varied from test to test, it was important to capture the effect of such variations on the heat transfer coefficient. Therefore, a customized heat transfer coefficient was calculated for each simulation. The traveling velocity was assumed to be 100 km/h. For forced convection, assuming this corresponded to the situation of parallel flow over a flat plate with mixed boundary layer (laminar, then transitioned to turbulent), the following equations were used to calculate the heat transfer coefficient of the tarpaulin sidewall (Incropera and De Witt, 2002),

$$\mathrm{Re}_L = \frac{u_{\inf} L_{tarp}}{\nu} \tag{4.6}$$

$$\overline{Nu}_L = 0.037\,\mathrm{Re}_L^{4/5}\,\mathrm{Pr}^{1/3} \tag{4.7}$$

$$\overline{h} = \frac{\overline{Nu}_L k}{L_{tarp}} \tag{4.8}$$

$$T_{film} = \frac{T_s + T_{\inf}}{2} \tag{4.9}$$

where

Re_L = Reynolds number based on the length of the tarp sidewall,

u_{inf} = traveling velocity (m/s) ,

L_{tarp} = length of the tarp sidewall (m),

ν = kinematic viscosity at T_{film} (m^2/s),

$\overline{Nu}_L$ = average Nusselt number of the tarp sidewall,

Pr = Prandtl number at T_{film},

$\overline{h}$ = average convection heat transfer coefficient of the tarp surface (W/m^2-K),

k = thermal conductivity at T_{film} (W/m-K),

T_{film} = film temperature (K),

Ts = surface temperature of the tarp sidewall based on the surface temperatures at the inlet and outlet (K) and

T_{inf} = outdoor temperature (K).

4.3.9 CFD Model - Calibration and Validation

4.3.9.1 Input and Output Parameters

As mentioned previously, each CFD model was set up to conduct a parametric study, and it required a number of input parameters to run. The values of these input parameters were calculated from the properties and measurements collected from the experimental trailer. Some of the properties were certain, others were based on assumptions. For those which were based on assumptions, it was necessary to conduct sensitivity studies to verify how changes in these input parameters affected the output parameters during the model calibration process. At the end of this calibration process, it would then be possible to identify appropriate values for these “less certain” input parameters. After determining the values of these input parameters, they were applied to the model and the model is being validated through another series of simulations. The validation process was used to evaluate the accuracy of the model.

In addition, it was also necessary to identify the output parameters required to calibrate and validate the model against experimental data. The main purpose of this CFD model was to simulate the environmental conditions inside the load, and the variables of interest were temperature and relative humidity within the load. To allow direct comparisons between simulated and experimental data, it was decided to extract temperature and relative humidity data at the same positions as where the sensors were installed in the field tests.

A number of steps were followed in the calibration of a CFD model:

- identify input parameters which required calibration,
- identify the range of values for each of these “less certain” input parameters, and
- set up these input parameters in the model.

Furthermore, it was also important to

- identify output parameters of interest,
- obtain geometrical coordinates (*x, y, z*) of the output parameters based on actual locations of the field tests’ sensors, and set up the model to extract output parameters at these specific locations.

Figure 4.22 summarizes the properties and measurements from the experimental trailer, and input parameters required to run a CFD simulation. As the input parameters vary from test to test, their values were re-calculated for each simulation based on the experimental data obtained from each field test. The list of output parameters (i.e. simulation results) is also presented in Figure 4.22.

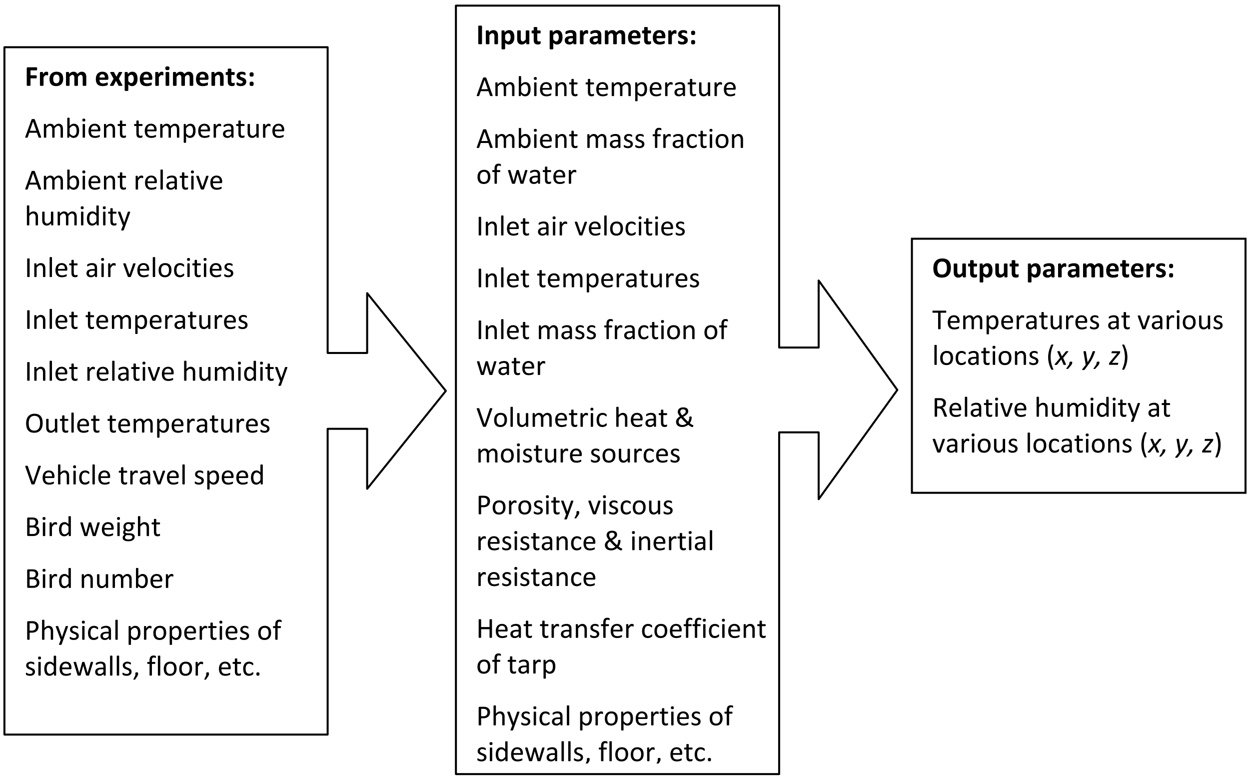

Figure 4.22. Properties, measurements and parameters required to run a CFD simulation.

4.3.9.2 Number of Simulations

Table 4.7 shows the input parameters that were examined in the sensitivity studies during the calibration process. The number of levels tested for each parameter are also listed in the same table. The values of each level are discussed in the next section, they varied by the number of fans. At these settings, a total of 54 simulations were required to calibrate a set of field data. The purpose of model calibration was to conduct sensitivity studies to determine the values of inlet velocities, porosity (and associated parameters), heat and moisture sources to be used in the final version of the CFD models.

Table 4.7. List of input parameters examined in calibration.

Parameters	Number of levels
Inlet velocities	6
Porosity and associated parameters (viscous & inertial resistances)	3
Heat and moisture sources	3
Total number of simulations (6x3x3)	54

Once calibration was completed, the model was validated to examine its accuracy. The values of inlet velocities, porosity (and associated parameters), heat and moisture sources were set at levels chosen from the calibration process. Simulations were run at these values during the validation process, and new sets of experimental data were used to compare with these results. Figure 4.23 show the procedure used to compute the simulation results in FLUENT.

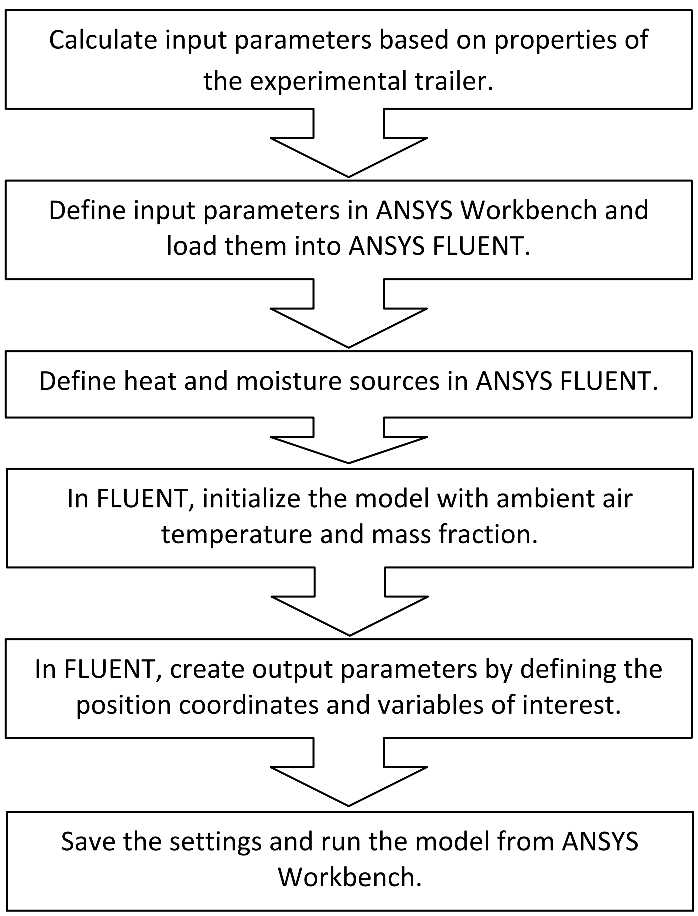

Figure 4.23. Procedure employed for validation of the numerical model.

From the experiment, a total of nine sets of data were obtained for the 1-fan, 2-fan and 3-fan configurations. One-third of the data set was used to calibrate the model (data set 4Feb2005b, 23Feb2005a, 23Feb2005c), whereas two-thirds of the data set was used to validate the model (data set 4Feb2005a, 15Feb2005, 18Feb2005, 23Feb2005b, 17March 2005, 24March2005). Data used in calibration were not re-used in validation. The data sets were chosen randomly for either the calibration or the validation process. Table 4.8 summarizes how the data sets were divided in the two processes. One data set from each fan configuration was used in the calibration. For three sets of experimental data, running 54 simulations per data set as sensitivity studies, resulted in a total of 162 simulations for calibration. In the case of validation, two data sets for the 1-fan configuration, three data sets for the 2-fan configuration and one data set for the 3-fan configuration were used. In total, six simulations were executed in the validation (as sensitivity studies were no longer required).

Table 4.8. Number of data sets used in calibrating and validating the model.

Fan configuration	No. of data sets used in calibration	No. of data sets used in validation
1 fan	1	2
2 fan	1	3
3 fan	1	1
Total	3	6
Grand total	9	

4.3.9.3 Standard Error of Estimate

There was a general lack of information from the literature on how to quantify the accuracy of results obtained from 3-D CFD models. In this study, it is proposed to evaluate the performance of the numerical models using "standard error of estimate". By adopting this statistical measure in the study, standard error of estimate helped to compare two sets of simulated and experimental data which varied spatially, in a quantitative manner. Thus, instead of comparing each pair of simulated and experimental data at location by location in the 3-D space, a single value was computed which quantified the overall accuracy of a CFD model. The standard error of estimate, σ_{est}, was calculated using

$$\sigma_{est} = \sqrt{\frac{\sum_{1}^{n}\left(Y_{sim} - Y_{\exp}\right)^2}{n}} \tag{4.10}$$

where

σ_{est} = standard error of estimate,

Y_{sim} = result from simulation,

$Y_{\exp}$ = result from field experiment and

n = number of data points.

Originated from regression analysis, the standard error of estimate indicated how closely the simulated data fitted the experimental data in this case. If the simulated data perfectly matched the experimental data, the standard error of estimate would yield zero, thus a smaller error is preferred. The use of standard error of estimate permitted direct comparisons of the two sources of data without spatial interpolation, without averaging out the values. For example, temperature obtained in position *x, y, z* from the field test was compared to the temperature obtained from the numerical model at the same position. More than twenty data points were used to calculate the standard error of estimate in each simulation.

4.4 RESULTS AND DISCUSSION

4.4.1 MODEL CALIBRATION - SENSITIVITY STUDIES

Results obtained from the sensitivity studies in the calibration process are summarized in Figure 4.24 to Figure 4.29. The various levels of porosity are shown on the *x*-axis, along with the level of inlet velocities below. The three levels of volumetric heat and moisture sources are indicated by different colors. For example in Figure 4.24, the first red column on the left was obtained by running the model at a porosity of 0.6, at inlet velocities set at the "lab level", with heat and moisture sources at "level 1". Figure 4.24, Figure 4.26 and Figure 4.28 summarize the standard errors of estimate for temperature data. Figure 4.25, Figure 4.27 and Figure 4.29 summarize the standard errors of estimate for humidity ratio. The unit of the *y*-axis in these plots is g_w/kg_{da}, which stands for "g of water vapour per kg of dry air". Initially, the numerical model generated temperature and relative humidity as results. It was decided to convert the relative humidity values to humidity ratios so that they would be independent of temperature (see Appendix D).

The yellow star symbol in Figure 4.24 to Figure 4.29 indicates the values of inlet velocities, porosity, and heat and moisture sources selected to be used in the final models. Results from these graphs indicated that the levels of porosity examined had little effect on the standard error of estimate. The error was affected mostly due to the levels of the inlet velocities, and heat and moisture sources. In the graphs, when an inlet velocity of 0.5-1 m/s was specified in the *x*-axis, it means 0.5 m/s was applied to Inflow 1 to 3, and 1 m/s was applied to Inflow 4 to 6 (Table 4.1). The higher velocity value was applied to the inlet vents near the mid-plane of the trailer (Figure 4.10). For the 1- and 2-fan configurations, the errors first decreased with increasing air velocities and eventually stabilized. For the 3-fan configuration, the errors stabilized immediately after the "lab level" velocities. The lab level velocities for the 3-fan configuration were 0.5, 0.5, 0.4, 0.6, 0.7 and 0.8 m/s, applied to the six inflow groups. These values were much smaller than the other levels of velocity tested, which may explain the sudden reduction and stabilization of errors. After deliberating what would be realistic levels of inlet velocities and heat and moisture sources, and considering the magnitude of the standard error of estimate, it was decided to employ the levels of parameters specified in Table 4.9 in the final models, for validation and prediction.

Table 4.9. Levels of input parameters used in model validation and prediction.

	Inlet velocities	**Porosity**	**Heat and moisture sources**
1-fan configuration	1.5 m/s for all six inlet sections	Level 2 (based on number of birds, an "average" height of the drawer)	Level 2 (based on the averaged inlet and outlet temperatures from thermocouples)
2-fan configuration	2.5 m/s for all six inlet sections	Level 2 (based on number of birds, an "average" height of the drawer)	Level 2 (based on the averaged inlet and outlet temperatures from thermocouples)
3-fan configuration	3.0 m/s for all six inlet sections	Level 2 (based on number of birds, an "average" height of the drawer)	Level 2 (based on the averaged inlet and outlet temperatures from thermocouples)

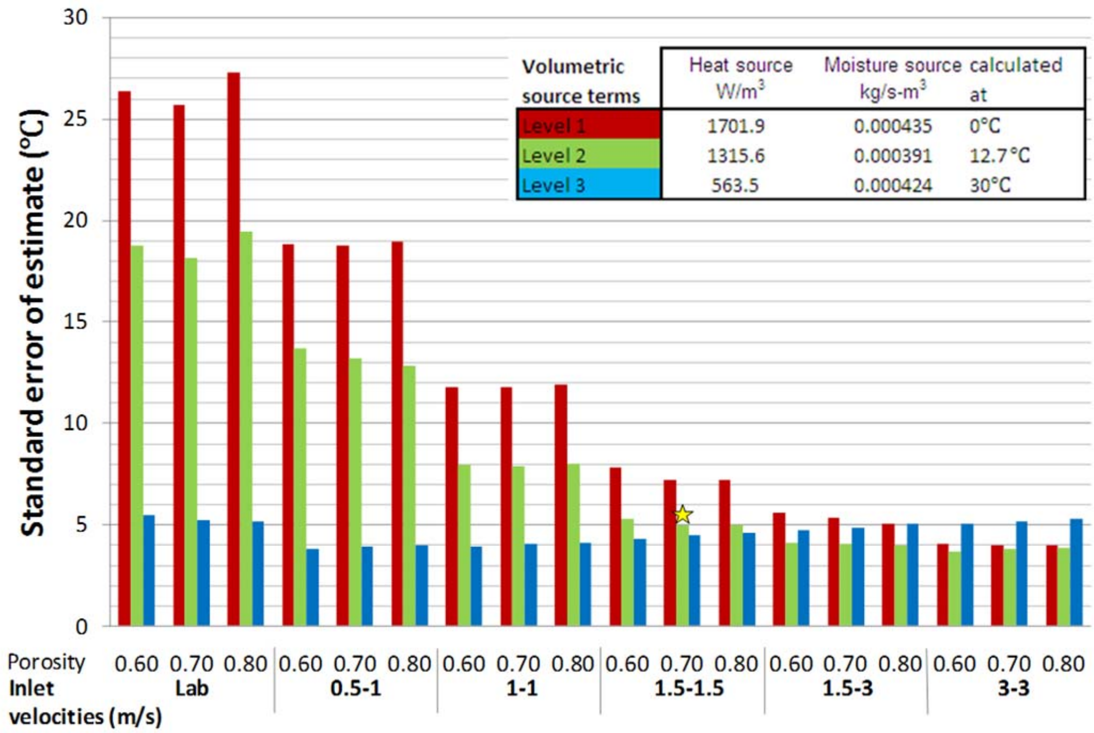

Figure 4.24. Standard error of estimate for temperature data for 1-fan configuration.

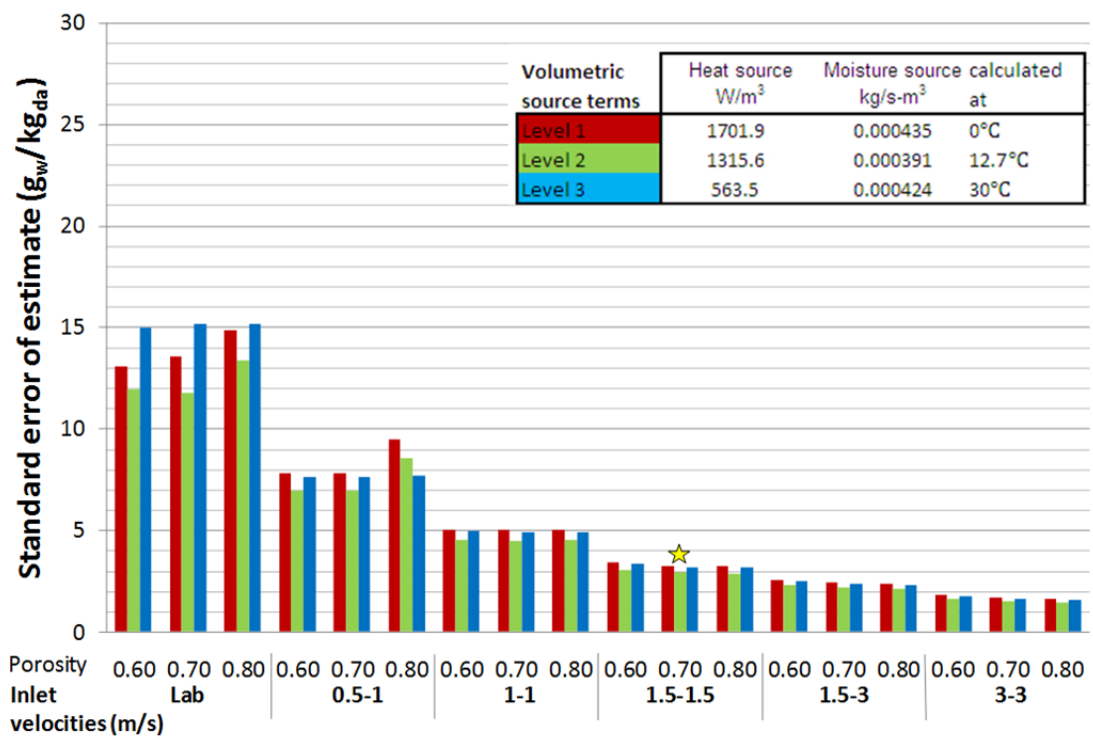

Figure 4.25. Standard error of estimate for humidity ratio data for 1-fan configuration.

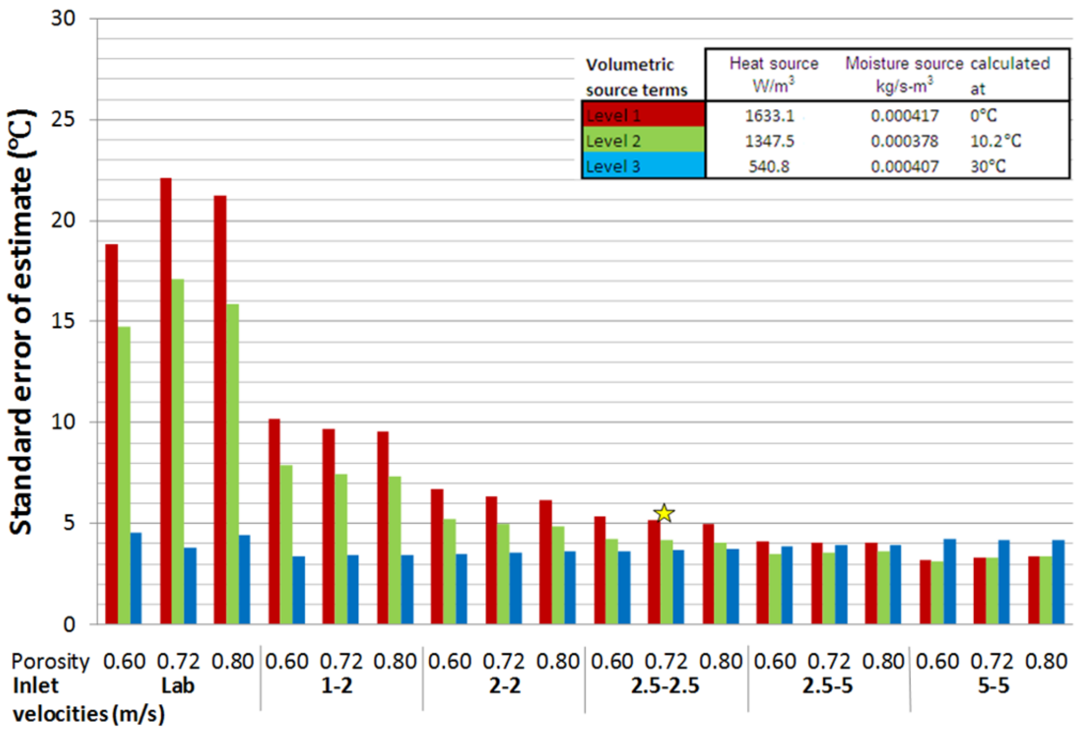

Figure 4.26. Standard error of estimate for temperature data for 2-fan configuration.

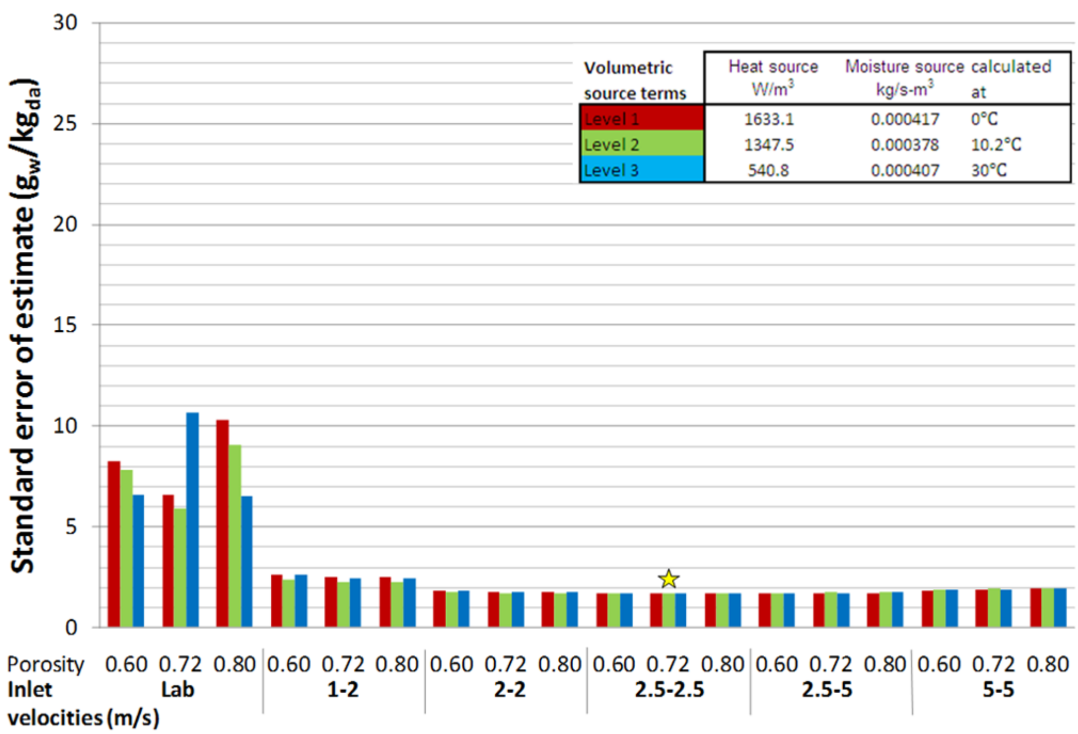

Figure 4.27. Standard error of estimate for humidity ratio data for 2-fan configuration.

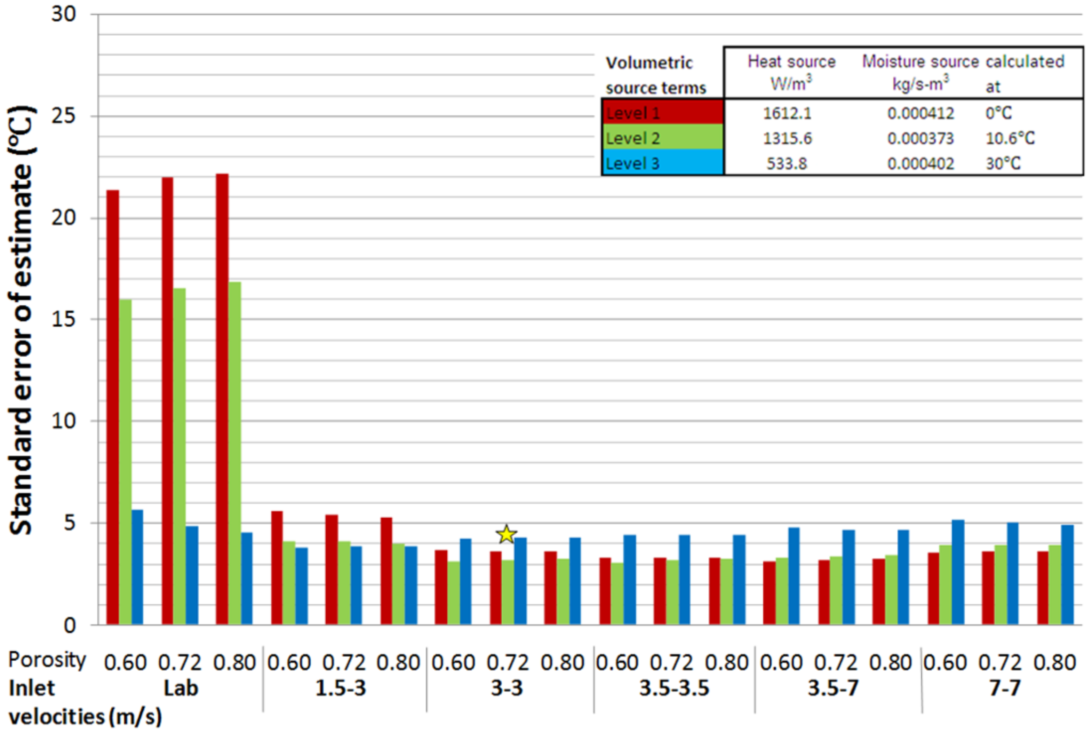

Figure 4.28. Standard error of estimate for temperature data for 3-fan configuration.

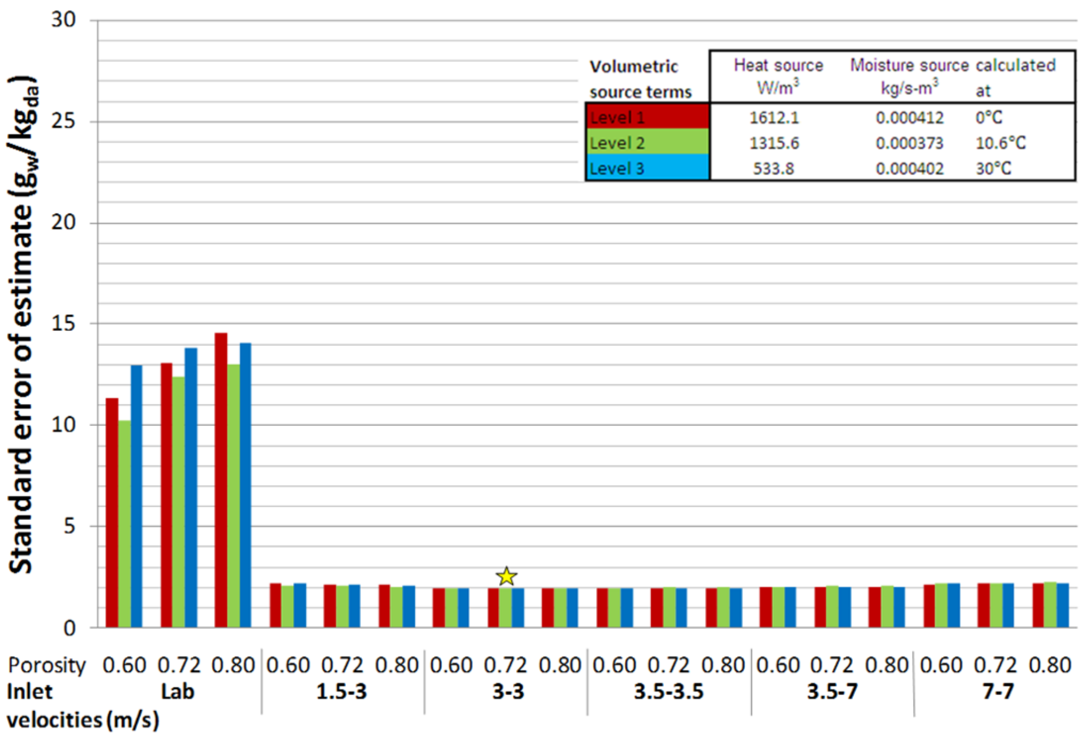

Figure 4.29. Standard error of estimate for humidity ratio data for 3-fan configuration.

4.4.2 MODEL VALIDATION VERSUS MODEL CALIBRATION

Table 4.10 summarizes the range of experimental versus simulated data obtained from the calibration and validation of the three CFD models (using the same final settings). It is encouraging to see the simulated data were in the same order of magnitude as the experimental data. For each set of spatially varying data (experimental or simulated), standard error of estimates were computed for temperature and humidity ratio using equation 4.10.

As show in Table 4.11, the numerical model generated standard errors of estimates which varied from 3.2 to 7.3°C for temperature, and 1.7 to 5.0 g of water per kg of dry air for humidity ratio in the load. Each standard error of estimate was calculated using 20 to 24 data points. The σ_{est} values were lower in the calibration cases, which was expected as the CFD models were adjusted to obtain low σ_{est} values. However, it was encouraging to see the σ_{est} values were not much higher in the validation cases, which gave confidence in using these CFD models as prediction tools.

There is no established standard which dictates the threshold value for a good CFD model of a large-scale animal transport system. In fact, there is a general lack of information on how to quantify the performance of 3-D CFD models. Furthermore, every CFD model developed is applicable to a specific situation, a threshold value established for a research field would be meaningless when applied to another field. This research is a first attempt to study an animal transportation system using CFD. Contributions from future research will help to establish standards in quantifying the goodness of the CFD models across this field of research.

Table 4.10. Range of experimental versus simulated data obtained from calibration and validation.

		Temperature (°C)		Humidity ratio (g_w/kg_{da})	
		Experimental (min to max)	Simulated (min to max)	Experimental (min to max)	Simulated (min to max)
1 Fan	**Calibration**	3.7 to 24.4	4.2 to 23.0	3.0 to 58.0	2.1 to 7.6
	Validation 1	6.6 to 24.6	8.2 to 25.2	1.4 to 6.2	2.6 to 8.1
	Validation 2	4.4 to 25.5	6.6 to 25.2	0.9 to 5.6	3.3 to 9.9
2 Fan	**Calibration**	0.8 to 17.0	4.4 to 15.6	1.0 to 8.9	2.1 to 5.6
	Validation 1	2.0 to 26.8	4.9 to 16.3	0.9 to 4.7	2.1 to 5.5
	Validation 2	7.4 to 26.3	19.0 to 28.9	1.1 to 12.6	2.7 to 6.5
	Validation 3	0.7 to 20.7	5.8 to 16.8	0.9 to 4.8	2.1 to 5.5
3 Fan	**Calibration**	5.4 to 19.6	7.5 to 16.2	1.3 to 9.6	2.4 to 5.5
	Validation 1	4.1 to 19.4	5.9 to 14.7	1.2 to 8.5	2.2 to 5.2

Table 4.11. Standard error of estimates obtained from calibration and validation.

		Standard error of estimate, σ_{est}		No. of data points used to calculate σ_{est}
		Temperature (°C)	Humidity ratio (g_w/kg_{da})	
1 Fan	**Calibration**	4.9	2.9	22
	Validation 1	5.9	3.0	22
	Validation 2	6.2	5.0	24
2 Fan	**Calibration**	4.1	1.7	21 / 20 *
	Validation 1	4.9	2.3	21
	Validation 2	7.3	3.0	21 / 20 *
	Validation 3	6.1	2.4	24 / 23 *
3 Fan	**Calibration**	3.2	1.9	21
	Validation 1	3.4	1.7	21

* Missing one humidity ratio experimental datum, thus one fewer data point was used to calculate the standard error of estimate of humidity ratio.

4.4.3 Differences Between Simulated and Experimental Data

Table 4.12 and Table 4.13 examine the differences in results obtained from simulations versus field tests. The tables summarize the locations in the trailer where the largest differences existed. Table 4.12 presents results for temperature, and Table 4.13 presents results for humidity ratio. A positive difference indicates the CFD models overestimated the experimental data, where a negative difference indicates the model underestimated the data.

The “average value” in Table 4.12 and Table 4.13 represents the mean value of arithmetic difference between simulated and experimental data. Thus, the averaged temperature difference between simulated and experimental data ranged from -0.8 to 6.1°C (Table 4.12). The averaged humidity ratio difference between simulated and experimental data ranged from 0.5 g_w/kg_{da} to 4.8 g_w/kg_{da}.

For the temperature data, the largest positive difference ranged from 6.0 to 17.7°C as shown in Table 4.12. The overestimation mostly occurred near the right-hand side tarpaulin (as viewed from the rear), at the rear of the load, close to the floor. The largest negative temperature difference ranged from -11.8 to -0.2°C. The underestimation most often occurred at the mid-plane, at the 2nd module from the front , and close to the floor. For the humidity ratio data, the largest positive difference ranged from 3.0 g_w/kg_{da} (g of water vapour per kg of dry air) to 7.1 g_w/kg_{da} as shown in Table 4.13. The overestimation mainly occurred at the mid-plane across the width, at either the 5th or 6th module, and anywhere from the bottom to the top of the load. The largest negative difference ranged from -7.8 g_w/kg_{da} to -1.4 g_w/kg_{da}. These underestimations occurred everywhere, without a pattern of occurrence along the width, length or height of the load. For the one fan configuration, the CFD model overestimated the results in all locations, thus there was no negative differences.

Table 4.12. Locations in the trailer where largest differences existed between simulated and experimental temperature data.

		Average value (°C)	Largest positive difference				Largest negative difference			
			Temperature (°C)	Location (m)			Temperature (°C)	Location (m)		
				x	y	z		x	y	z
1 Fan	**Validation 1**	4.0	15.8	0.06	7.22	0.30	-4.5	1.23	2.44	0.30
	Validation 2	2.2	14.2	0.06	7.22	0.30	-11.8	1.23	2.44	0.30
2 Fan	**Validation 1**	-0.8	9.7	0.06	7.22	0.30	-11.7	1.23	6.06	1.26
	Validation 2	6.1	17.7	0.06	7.22	0.30	-0.2	1.23	2.44	0.30
	Validation 3	2.9	11.6	0.06	5.05	0.30	-5.7	1.23	2.44	0.30
3 Fan	**Validation 1**	-0.8	6.0	1.23	7.27	2.29	-9.9	1.23	2.44	0.30

Table 4.13. Locations in the trailer where largest differences existed between simulated and experimental humidity ratio data.

		Average value (g_w/kg_{da})	Largest positive difference				Largest negative difference			
			Humidity ratio (g_w/kg_{da})	Location (m)			Humidity ratio (g_w/kg_{da})	Location (m)		
				x	y	z		x	y	z
1 Fan	**Validation 1**	2.7	5.7	1.23	7.27	1.26	no negative data	-	-	-
	Validation 2	4.8	7.1	1.23	5.00	0.30	no negative data	-	-	-
2 Fan	**Validation 1**	2.0	3.7	1.23	7.27	1.26	-1.4	1.23	2.44	0.30
	Validation 2	0.8	4.3	0.06	5.05	2.29	-7.8	0.06	3.12	1.26
	Validation 3	1.9	4.1	1.23	7.27	0.30	-2.5	1.23	0.17	0.30
3 Fan	**Validation 1**	0.5	3.0	1.23	5.00	2.29	-3.3	0.06	7.22	1.26

In general, the largest positive differences were greater in magnitude than their corresponding negative differences, for both temperature and humidity ratio data. This means the CFD models tended to overestimate experimental data in greater magnitude. It is interesting to see that the temperature overestimation occurred at floor positions which were opposite to the floor positions where the underestimation occurred: rear tarp side versus front mid-plane. As for humidity ratio, the differences occurred in a more random fashion in the 3-D space. For temperature, the largest positive and negative differences are far away from their mean. As for humidity ratio, the largest positive and negative differences are not as far away from their mean.

Many factors may have caused the differences between the simulated and experimental data. Possible errors may have occurred during field testing (sensor accuracy and placement, measurement errors for distances, etc.), and during the CFD modeling (modeling assumptions, geometry simplifications, inaccuracy of sub-models and/or properties, round-off errors, etc.). These errors occurred at different layers, interacting with each other. It is difficult to quantify the contribution of each factor.

Nevertheless, the inlet conditions may be one of the factors which contributed to the overestimation of temperature values near the tarpaulin sidewall, and the underestimation near the mid-plane. In order to understand how this may be the case, it is important to review how the inlet conditions were measured experimentally and implemented in the CFD models. Appendix C illustrates where the inlet conditions were measured. These data were then later applied in six inflow groups inside the CFD models; the same conditions were applied to each Inflow group (inlet vents sharing the same color in Figure 4.10). During the experiment, the inlet conditions were not measured near the tarpaulin sidewall, but at the centre of the first column of inlet vents, and these inlet conditions were later applied from the sidewall to the entire surface of the inlet vents. It is reasonable to assume in reality the inlet temperatures near the sidewall should be lower than what was used as boundary condition at the sidewall in the model. Because the boundary temperature was overestimated at the sidewall, it is logical to conclude it would overestimate temperature values in locations near the tarpaulin sidewall. That was exactly what happened.

As for the underestimation of the mid-plane value, the magnitude of the underestimation at the mid-plane was not as great as the overestimation at the sidewall. That may be due to the fact that the experimental data were collected at the mid-plane (Appendix C). Errors still existed, probably because the spatial resolution of the inlet conditions was still not great and point data were applied over large surfaces.

The inlet conditions is the driving force behind the CFD models. In future studies, it is recommended to refine the measurement grid of the inlet conditions. More data points at higher spatial resolution should be collected along the width and height of the inlet diffuser. Furthermore, in the CFD models, more inflow groups (vents only) should be created to utilize the experimental data of higher resolution. In addition, the current CFD model applied the same temperature value over the entire solid portion of the inlet diffuser. It is recommended that the solid portion of the diffuser should also be sub-divided into a large number of groups and each group should use its own temperature value.

4.4.4 3-D PROFILES

Aside from comparing the simulated and experimental data quantitatively, it would be useful to verify if the numerical models also yielded the same temperature distributions as observed in experimental data. The CFD models generated more data points than the field tests in the 3-D space. Figure 4.30 shows a summary of contour plots extracted from the 1-fan CFD model for the calibration simulation (using the final settings). There was a total of nine calibration and validation simulations which used the final settings. The graphs of the other simulations are presented in Figure 4.31 to Figure 4.38. Similar to the grouping of experimental data, there are three groups of graphics, Group 1 for one fan, Group 2 for two fans and Group 3 for three fans. Results from the calibration simulation appear before the validation data. All the contour plots were plotted using the same legend to facilitate comparisons. On each page, the top portion shows the temperature distribution from the front to rear of the trailer. The left bottom section shows the profiles of the sidewall and mid-plane. It is important to remember CFD simulations were conducted only on the right half of the trailer, which explains why there is no data on the left sidewall. The right bottom section of each figure shows the top cross-sectional views, from the floor to the roof. These temperature plots were created based on the actual temperature values calculated by the CFD models. They did not use the derived temperature values such as the $\Delta\overline{T}$ temperature profiles presented in Appendix E for experimental values. Therefore, it is important not to directly compare the numerical values. However, the trends of the temperature distributions should be similar if the CFD models were set up properly.

Several general trends could be observed from these temperature profiles. Similar to the experimental data plots, the temperature profiles varied longitudinally from the front to the rear end of the trailer. Air picked up heat from the animals, getting warmer and warmer towards the rear of the trailer, especially near the exhaust fan holes. The right tarpaulin sidewall was always colder than the mid-plane of the trailer, which matched the observations from the field tests (Chapter 3).

Experimental data suggested that the number of fans used had an effect on the temperature range. As discussed in Chapter 3, when more fans were used, the range of $\Delta\overline{T}$

(difference between maximum and minimum values) become narrower, but the trend was not very noticeable. The temperature profiles of the 1-fan configuration were noticeably less uniform than the 2- or 3-fan configurations in general. There were no distinguishable differences between the 2- and 3-fan configurations in terms of temperature uniformity.

When comparing the 1-, 2-, and 3-fan configurations in the CFD data, it can be observed that the hot spot at the fan openings migrated upward when more fans were used. In the 1-fan configuration, the bottom opening was hottest. When two fans were used, the hot spot expanded and covered both the bottom and middle openings. When three fans were used, the hot spot was spread out covering all three openings.

Overall, the CFD models generated results which shared the common trends with the experimental data. Because more data points were available, the CFD models allowed conditions to be explored in regions where no experimental data were available or difficult to obtain in the field tests.

Group 1 – one fan, calibration (test g3dp4)

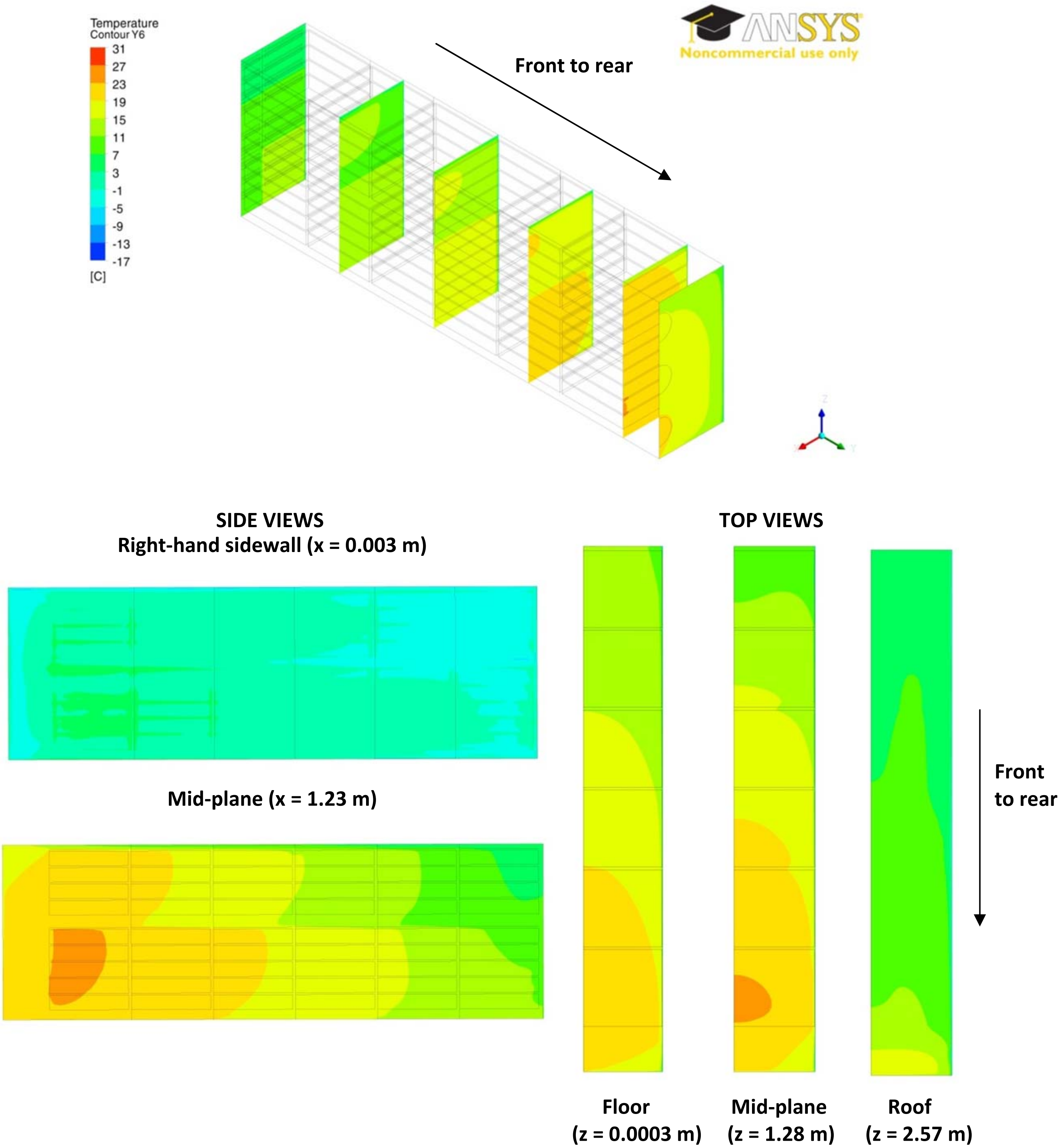

Figure 4.30. Temperature contour plots extracted from the 1-fan CFD model of the calibration test.

Group 1 – one fan, validation 1 (test gv1)

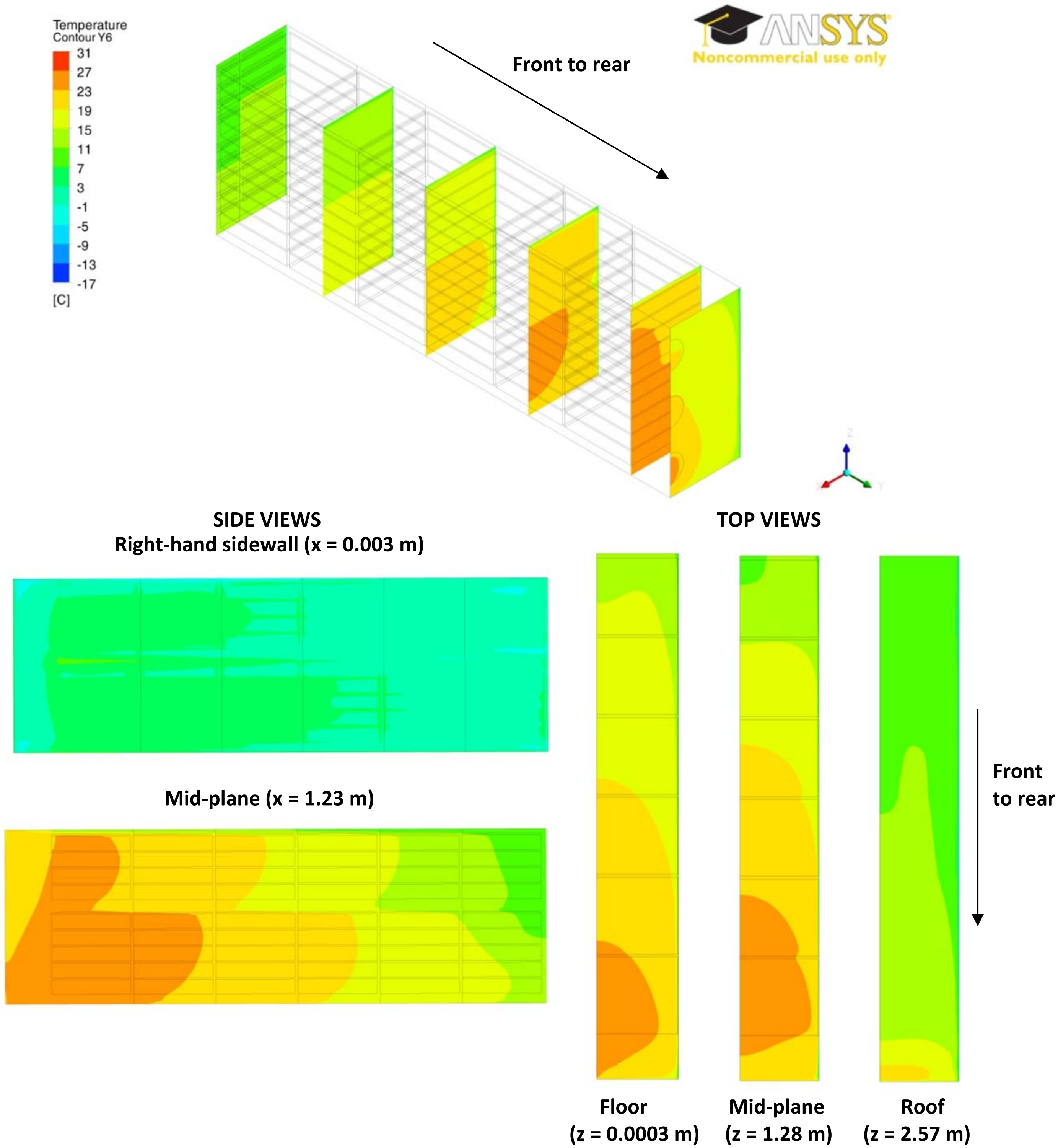

Figure 4.31. Temperature contour plots extracted from the 1-fan CFD model of the first validation test.

Group 1 – one fan, validation 2 (test gV2)

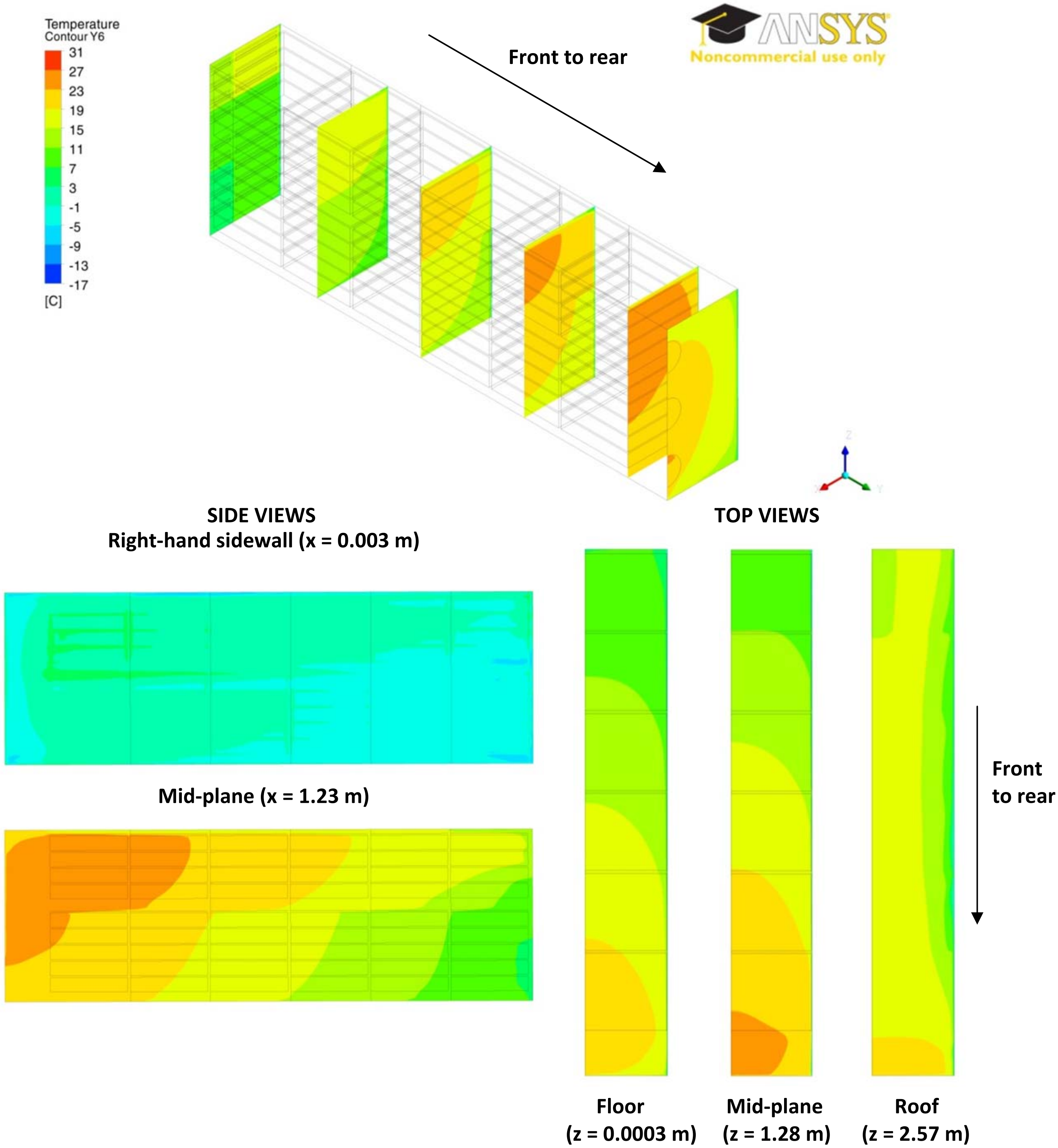

Figure 4.32. Temperature contour plots extracted from the 1-fan CFD model of the second validation test.

Group 2 – two fans, calibration (test fff2dp10)

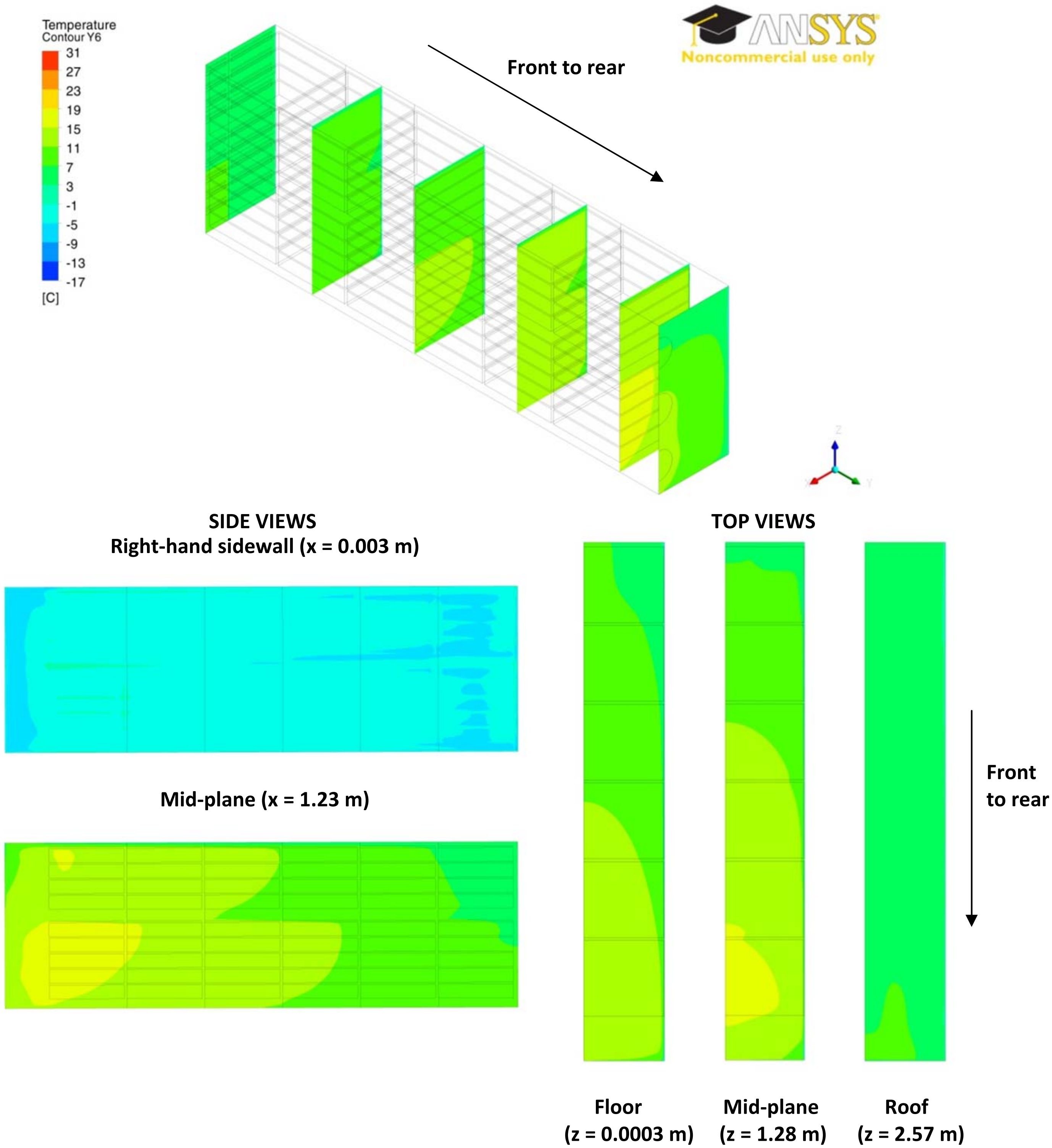

Figure 4.33. Temperature contour plots extracted from the 2-fan CFD model of the calibration test.

Group 2 – two fans, validation 1 (test fffv1)

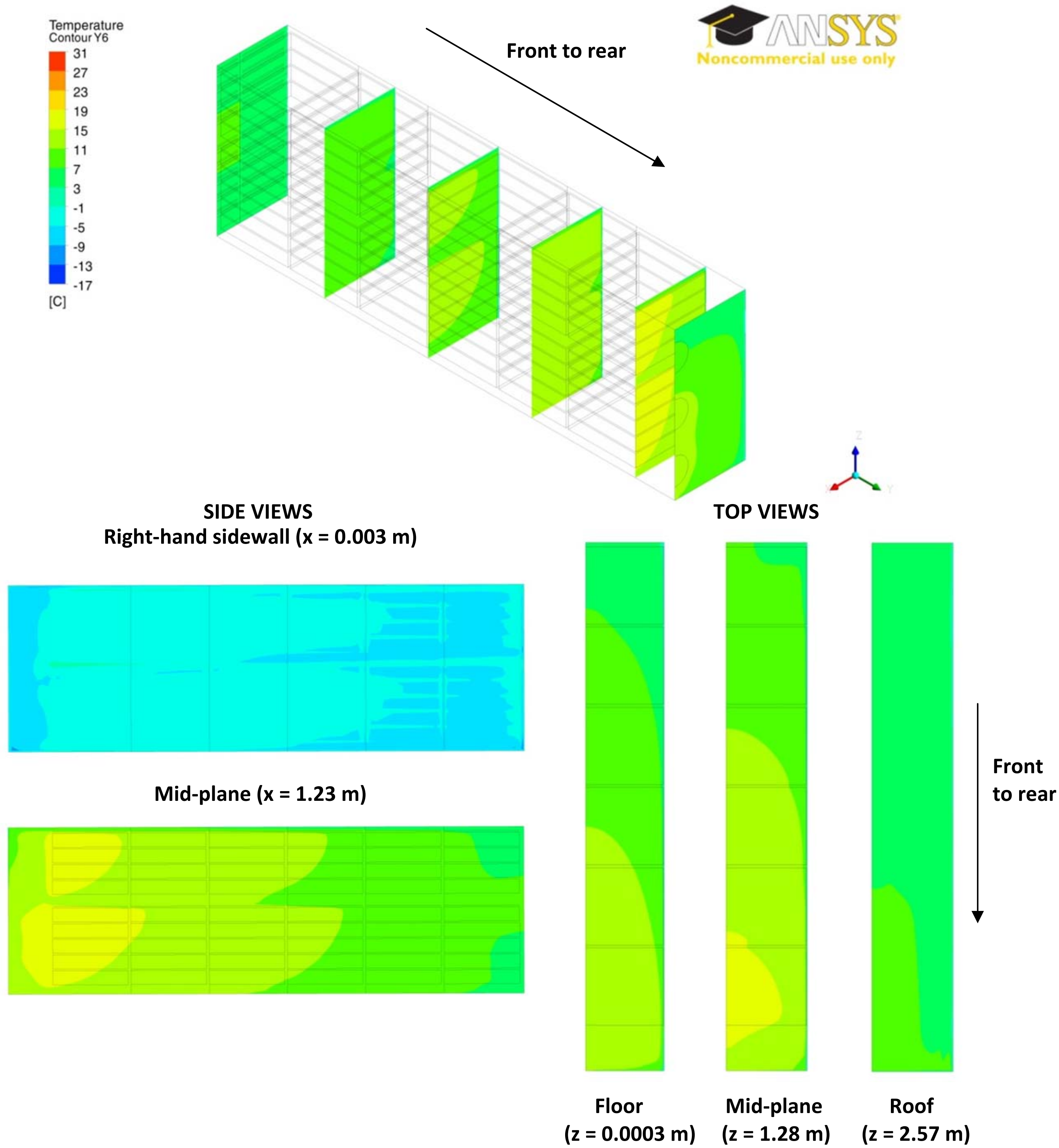

Figure 4.34. Temperature contour plots extracted from the 2-fan CFD model of the first validation test.

Group 2 – two fans, validation 2 (test fffv2)

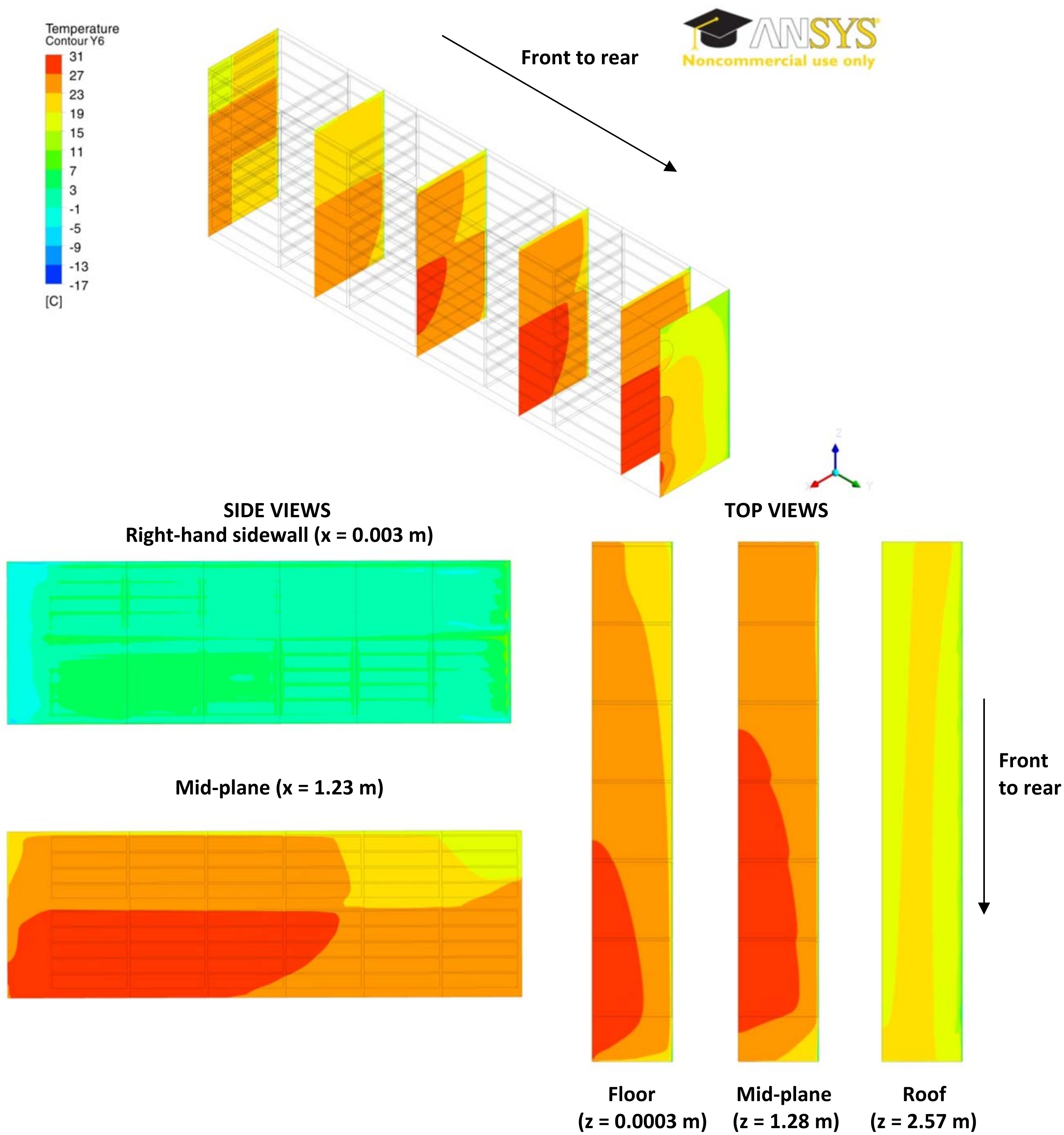

Figure 4.35. Temperature contour plots extracted from the 2-fan CFD model of the second validation test.

Group 2 – two fans, validation 3 (test fffv3)

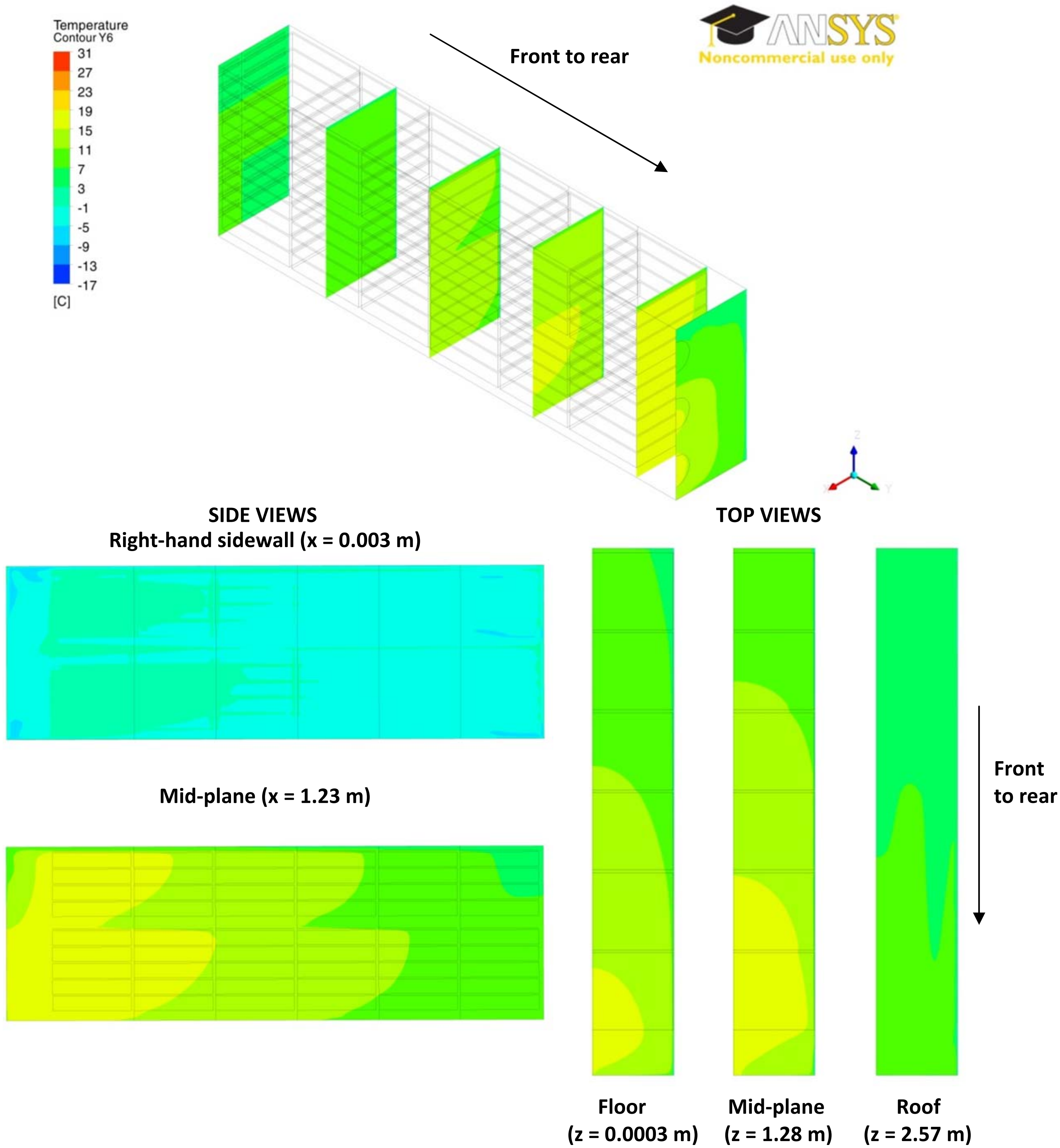

Figure 4.36. Temperature contour plots extracted from the 2-fan CFD model of the third validation test.

Group 3 – three fans, calibration (test h3dp1)

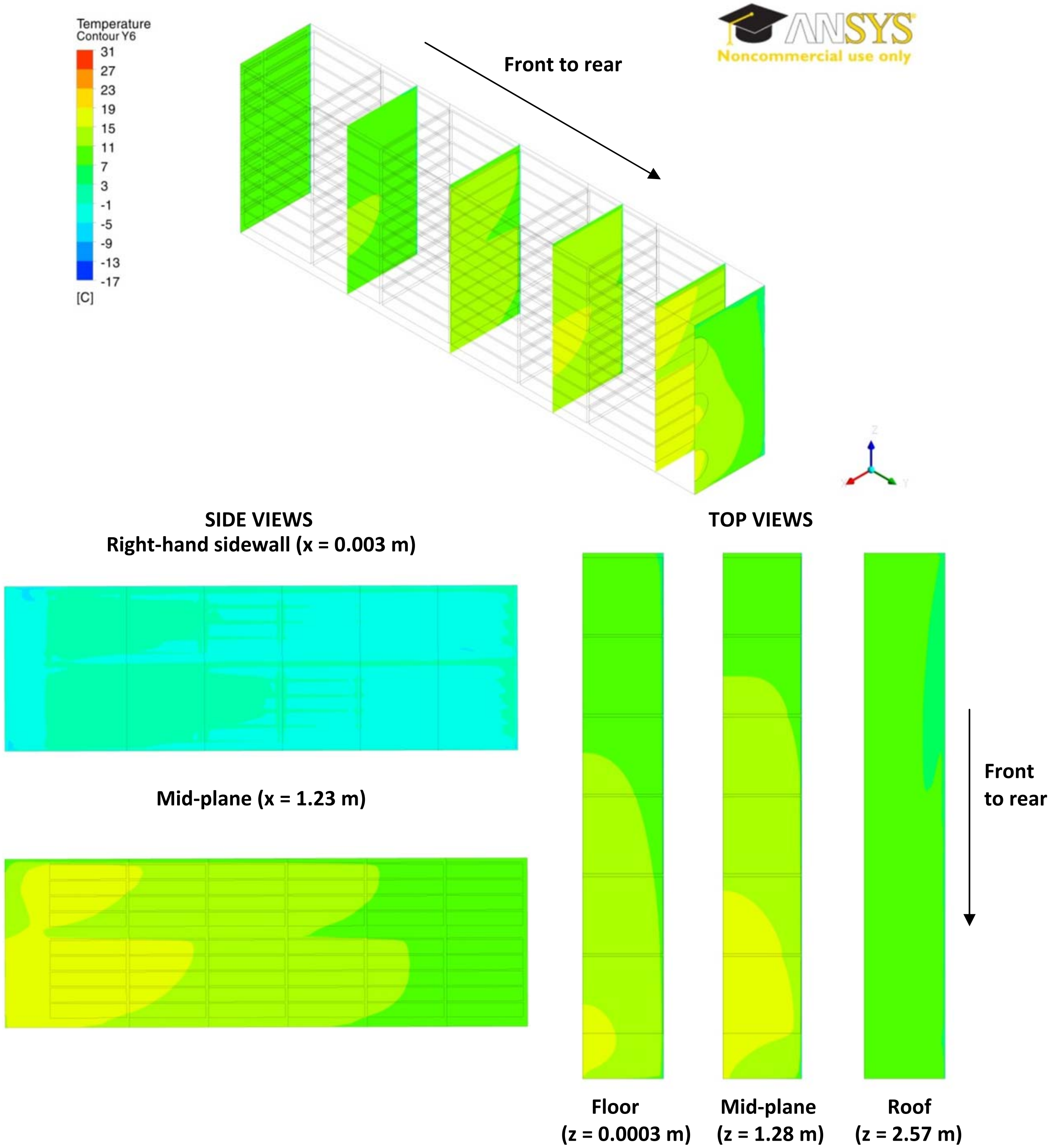

Figure 4.37. Temperature contour plots extracted from the 3-fan CFD model of the calibration test.

Group 3 – three fans, validation (test hv1)

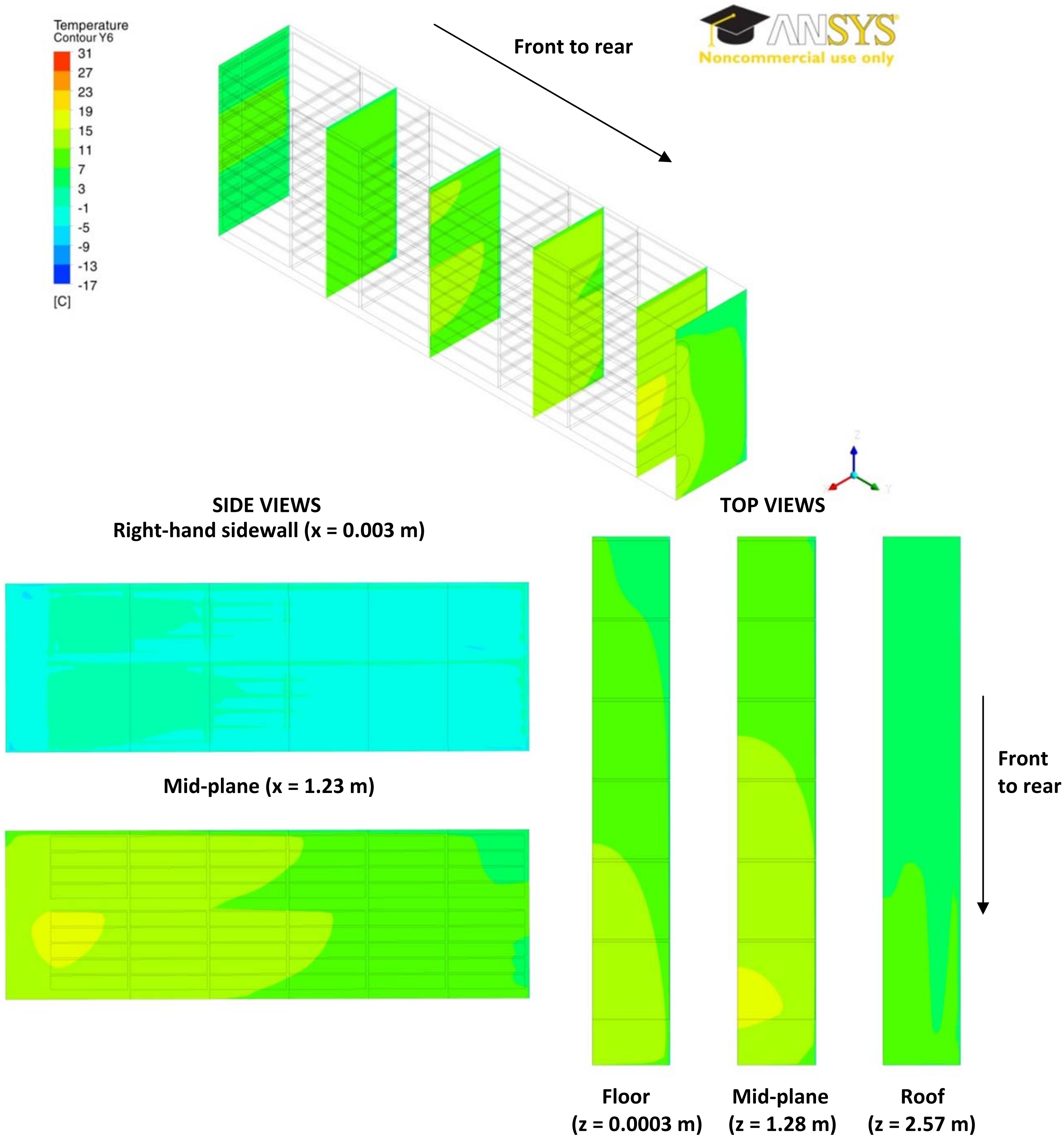

Figure 4.38. Temperature contour plots extracted from the 3-fan CFD model of the validation test.

4.5 CONCLUSIONS AND RECOMMENDATIONS

Three 3-D CFD models were developed to simulate the environmental conditions surrounding broilers within an experimental trailer. The models were calibrated and validated against experimental data presented in a previous chapter. These models are applicable to cold and dry weather conditions similar to Canadian Prairie's winter conditions, and they were specifically developed for a unique experimental trailer built at University of Saskatchewan.

The three models simulated the three fan configurations as encountered during the field tests. Several assumptions were made to simplify the geometry of the virtual trailer. The model did not take into account leakage in the experimental trailer. Because leakage was not simulated, it was assumed the left side of the trailer was symmetrical to the right side of the trailer, thus only half the trailer was studied by the CFD models. The geometry of the chicken modules was simplified with the use of a porous media model. The exhaust fans were replaced by circular openings and the third diffuser screen was eliminated in the virtual trailer.

This project was unique as the trailer contained a large number of animals in a relatively small space as compared to a regular poultry barn. Some of the animals were subjected to cold ambient temperature, they did not have access to water and feed, and they were confined within plastic drawers which restricted their movement. At the time when the models were being developed, there were no heat or moisture production data for these conditions available in the literature, there was little choice but to use data derived from broilers within production facilities. After modeling work was completed, Watts et al. (2011) published some heat and moisture production rates for temperatures between -8 to -18°C and at +20°C (as the control condition), for broilers which were fasted, confined in transport drawers and exposed to an air flow rate of 0.35 m^3/s. The experiment was conducted in a laboratory setting, and the setup was stationary.

The authors concluded the amount of heat and moisture produced by the broilers was significantly greater under Western Canadian winter transport conditions, as compared to in a heated barn (Watts et al., 2011). It would be interesting to incorporate this latest data in the CFD models to verify if the active ventilation could still handle the additional heat and moisture, if the temperature profiles would become less uniform, and how would the standard error of estimates change.

During calibration, sensitivity studies revealed that inlet velocities, heat and moisture production had a great impact on the results obtained from the CFD models. The levels of porosity examined did not play a major role. This information is useful as it helps to focus the efforts in data collection in areas which matter most in future studies.

The standard error of estimate was selected as a statistical measure to evaluate the accuracy of the CFD models against experimental data. When calibrating and validating the models, it was found that σ_{est} varied from 3.1 to 7.3°C for temperature data, and varied from 1.7 to 5.0 g of water vapour per kg of dry air for humidity ratio. In the literature, there was a lack of standardized method to validate 3-D CFD models developed for animal transport system similar to the one examined in this study. Thus, more research is required to establish these validation methods.

Temperature and humidity ratio data were further analyze to identify locations in the trailer where the largest errors occurred between simulated and experimental data. It is suggested a possible factor which contributed to these errors was the low spatial resolution of inlet experimental data and how they were applied to the CFD models as boundary conditions. It is recommended that a more refined grid of experimental data should be collected at the inlet of the loading area, and the data should be applied into a more refine grid at the inlet of the virtual trailer inside the CFD models.

Temperature profiles obtained from the simulations were compared to experimental data profiles (presented in Chapter 3). Similar to experimental data, the temperature profiles were longitudinal from the front to the rear end of the trailer. The right tarpaulin sidewall was always colder than the mid-plane of the trailer, which matched the observations from the field tests. Because more data points were available, the CFD models allowed conditions to be explored in regions where no experimental data were available or difficult to obtain in the field tests.

Three 3-D CFD models were successfully developed to simulate the environmental conditions surrounding broilers within an experimental trailer. By examining the standard errors of estimate, the profiles and the largest differences between simulated and experimental data, the following conclusions can be made. These models were developed for a specific system and it should be used to evaluate the condition of this experimental trailer only. The models were validated and are valid only for winter conditions, for an ambient temperature down to -13.5°C. They do not take into account the effect of air leakage. The models were able to recreate temperature trends observed in field tests and their standard errors of estimate were at reasonable levels. However, the models tended to overestimate or underestimate temperature and humidity ratio values at the boundaries. For the above reasons, it can be concluded that these models are suitable to be used in comparative studies (such as comparing operating conditions), but not for determining the absolute values of temperature and relative humidity inside the trailer.

4.6 ACKNOWLEDGEMENT

The authors acknowledge financial support provided by the Natural Sciences and Engineering Research Council of Canada, Agriculture and Agri-Food Canada, the Chicken Farmers of Saskatchewan, Le Fonds Québécois de la Recherche sur la Nature et les Technologies, Saskatchewan Chicken Industry Development Fund and the University of Saskatchewan in this project. The authors also thank staff members from the Engineering Computer Center of the University of Saskatchewan for their support in the setup of the software and the usage of the Xi simulation lab. Special thanks go to the staff members of ANSYS and FLUENT in providing training materials and answering many questions regarding the usage of their software. The authors also thank Lilydale Inc. and its personnel for their support in the collection of experimental data which were used to calibrate and validate the CFD models.

PREFACE TO CHAPTER 5

This is the last paper of a series of four papers. The first two papers focused on the design, construction and field evaluation of an actively heated and ventilated trailer. After reviewing the Computational Fluid Dynamics (CFD) model developed in the third paper, this paper focuses on the last objective of the research project: to utilize one of the CFD models to predict the performance of the experimental trailer using conditions which may be encountered by the poultry transport industry.

Using the CFD model as a tool, this paper discusses the settings and results obtained from the predictive simulations. It also identify the parameters which mattered most to the operation of the experimental trailer.

The modeling work was conducted by K.P.C. Hui with input from T.G. Crowe.

5 PERFORMANCE PREDICTION OF AN ACTIVELY VENTILATED POULTRY TRANSPORT VEHICLE USING CFD

K.P.C. Hui, T.G. Crowe

The authors are K.P. Catherine Hui, **ASABE Member and Professional Engineer,** Graduate Student; Dr. Trever G. Crowe, **ASABE Member and Professional Engineer**; **Corresponding author:** Dr. Trever Crowe, College of Graduate Studies and Research, University of Saskatchewan, C 180, 105 Administration Place, Saskatoon, Saskatchewan, S7N 5A2, Canada; phone: (306) 966-2229; fax: (306) 975-1026; e-mail: trever.crowe@usask.ca.

Abstract. *A Computational Fluid Dynamics (CFD) model was developed to simulate the environmental conditions within an experimental poultry transport vehicle. After calibration and validation, the model was used to examine several "what-if" scenarios. Three cases were investigated, based on conditions which may be encountered by the poultry transport industry. The first case examined the effects of vehicle travel speed and ambient temperature. The second case looked at the effects of bird size, loading density and ambient temperature. The last case studied the effects of side tarp insulation and ambient temperature.*

In the first case, for travel speeds at 90, 100 and 110 km/h, coupled with an ambient temperature of 5°C and 10°C, with a total bird weight of 8113 kg at 18 birds/drawer, the range of travel speeds tested had minimal effect on the minimum, maximum, and range (max minus min) of load temperatures. In the second case, the ambient temperatures investigated were -13.5, -10, -5, 0 and 5°C. The bird types examined were small (1.8 kg at 22, 24 or 26 birds/drawer), and large (2.3 kg at 16, 18 or 20 birds/drawer). Results indicated minimum load temperature was closely related to the ambient temperature, and a colder ambient temperature widened the range of temperature inside the load. For the same bird size, a higher loading density increased the *maximum load temperature but did not affect the minimum temperature. In the last case, the effect of three insulated tarps were compared with the original tarp, at two ambient temperatures (-13.5 and 5 °C). It was found that for the types of insulated tarp tested, insulation helped to raise the minimum load temperature, but it also raised the maximum load temperature. It is recommended not to use an insulated tarp (at the insulation value examined) for ambient temperatures greater than 5 °C.*

Keywords. *Computational Fluid Dynamics, CFD, poultry, broiler, chicken, transport, ventilation, prediction.*

5.1 INTRODUCTION

In Canada, transporting broiler chickens from dispersed farms to a central slaughter facility is an essential step of broiler production. In transit, broilers are exposed to a wide range of ambient climatic conditions. Presently, commercial broiler transport vehicles are not actively ventilated. In cold weather, previous studies indicated the passive ventilation system resulted in severe heterogeneous transport conditions within the load of broilers, and suggested the ventilation in commercial semi-trailers was ineffective (Knezacek, 2005).

An experimental trailer was developed to test the merits of using active ventilation and supplemental heating for transportation of broilers in Western Canada's winter conditions (Chapter 2 and 3). In order to gain a better understanding of what goes on inside this experimental trailer, a CFD (Computation Fluid Dynamics) model was developed to simulate the environmental conditions within the trailer. After calibrating and validating three CFD models (Chapter 4), it was decided to use one of the models as a tool to predict the effect of operational parameters on the environmental conditions generated inside the experimental trailer.

The tasks associated with commercial poultry transportation are varied and complex. Effective management of the conditions within trailers transporting broiler chickens requires the knowledge of various factors. The number of broilers and their body weight may vary from shipment to shipment, affecting the amount of heat and moisture which need to be ventilated from the experimental trailer. In addition, the load is subjected to a range of ambient temperature and the trailer could travel at different speeds. Such factors would affect the amount of heat loss through the non-insulated side tarps. Both the commercial and experimental trailers had non-insulated sidewalls, and it would be interesting to examine the degree to which insulating the sidewalls would reduce the amount of heat loss and the effect on the interior load temperatures.

In order to study the various conditions which may be encountered in the field, a CFD model was used as a tool to evaluate several realistic scenarios. Simulations were conducted to examine what would happen if the vehicle travels at different speeds at different ambient temperatures; if the drawers were loaded with different sizes of birds at different loading densities exposed to different ambient temperatures; or if the side tarp is insulated. The use of the CFD model would allow the study of these cases without endangering animals, while varying operational parameters and eliminating the high cost associated with conducting field tests. Results of these predictions will help to gain a better understanding of the various factors which govern the performance of the experimental trailer, aiming to establish guidelines for best management practices and to better advise the poultry transport industry.

5.2 OBJECTIVE

The objective of this study was to use a CFD model to study combined effects of travel speed, ambient temperature, bird size, loading density and side tarp insulation on conditions within the experimental trailer transporting broiler chickens.

5.3 MATERIALS AND METHODS

5.3.1 OVERVIEW OF THE CFD MODEL

The CFD model was developed using GAMBIT 2.4.6. and ANSYS FLUENT 12.0.16 software. FLUENT was used within the ANSYS Workbench 2.0 Framework (version 12.0.1), utilizing the feature ANSYS DesignXplorer to conduct parametric studies in FLUENT.

The virtual trailer was three-dimensional; its geometry represented the right half of the experimental trailer as shown in Figure 5.1. Air entered the inlet slots (orange sections in Figure 5.1) of the inlet diffuser and travelled through the load . After picking up heat and moisture from the simulated drawers of broilers (yellow boxes in Figure 5.2), air exited through the semi-circular fan holes (brown half-circles in Figure 5.2). In reality, the drawers were supported by metal frames. In the virtual model, the metal frames were eliminated as part of the simplification of the geometry, leaving gaps in-between the simulated drawers. Another simplification of the geometry was to replace the 3 exhaust fans and 2 exhaust dampers (for top and middle fans) by semi-circular holes. After creating the geometry, it was meshed with a combination of hexahedral and mixed cells in GAMBIT. There was a total of 724,953 cells, 2,047,710 faces and 618,193 nodes in the model.

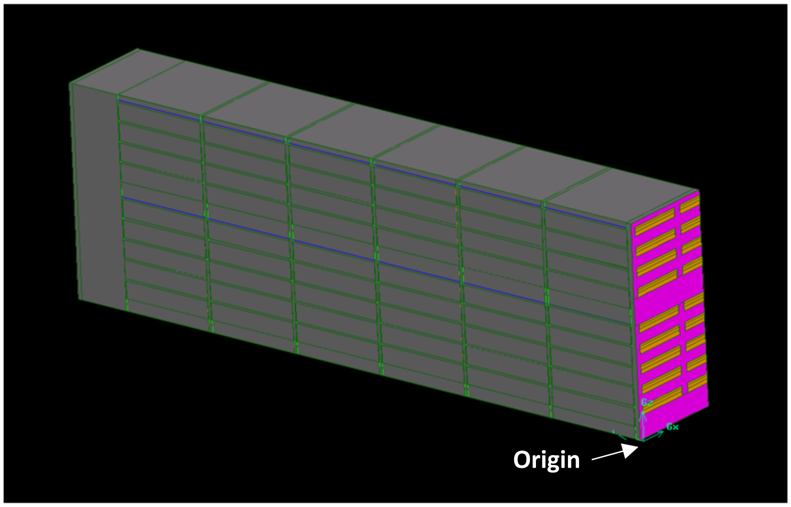

Figure 5.1. The right side of the virtual trailer viewed from the front.

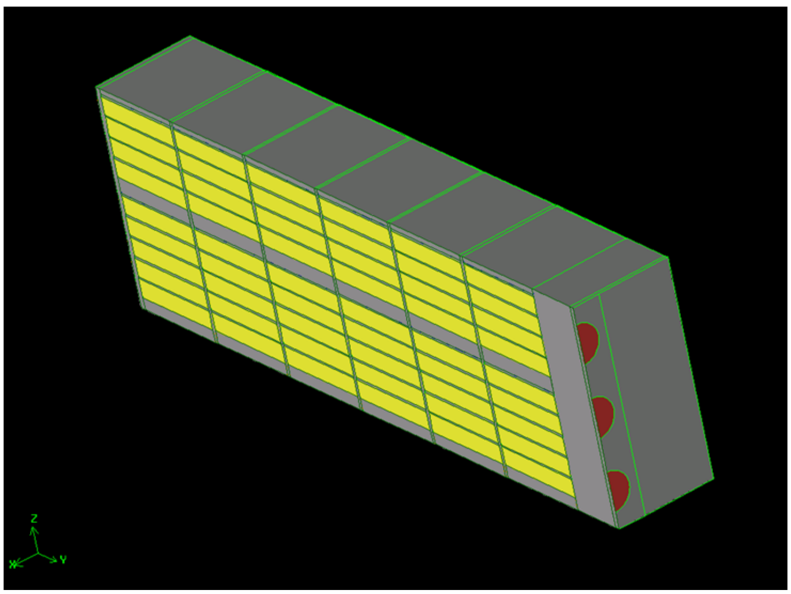

Figure 5.2. The left side of the virtual trailer viewed from the rear.

5.3.2 PROPERTIES AND BOUNDARY CONDITIONS REQUIRED TO USE THE MODEL

It was decided to use the 1-fan CFD model to run the predictions, as it was the configuration which can potentially cause the most heat build-up if the side tarp was insulated. The model had been calibrated and validated using experimental data. Details of the settings used in FLUENT can be found in Chapter 4. One important element of this model was the fact that it was set up to run a “parametric study” in the ANSYS Workbench 2.0 Framework. Several properties or boundary conditions were set as “input parameters” inside FLUENT. It allowed users to assign and vary their values in a spreadsheet format outside FLUENT in DesignXplorer. This setup allowed the software to run multiple simulations in batch mode, assigning new values to the input parameters as required. If desired, “output parameters” can be set up in FLUENT which automatically export specific results back to DesignXplorer, saving time that would otherwise be required to extract results individually. At the end of a batch of simulations, values of the input parameters and the results of output parameters would all be summarized in a spreadsheet format. The use of FLUENT in conjunction with DesignXplorer reduced the amount of time to run simulations and facilitated post-processing of the results.

The first step in using the CFD model for predictions was to identify which properties and boundary conditions should be set fixed, and which should be set variable. Table 5.1 summarizes the settings and values applied to them in the predictive simulations. The first column listed the properties and boundary conditions of concern. Some of them were straight forward, while others had to be calculated. The range of the “variable” properties and boundary conditions will be specified in the next few sections, they varied from case study to case study based on their objectives.

Table 5.1. Properties and boundary conditions used in predictions.

	Setting/Value
Ambient temperature (ambient T)	variable
Ambient mass fraction of water	
- ambient T	variable
- ambient RH	95%
Inlet air velocities	1.5 m/s
Inlet temperature	ambient T + 4°C
Inlet mass fraction of water	ambient mass fraction of water
Heat & mositure prod rates	
- bird loading density	variable
- bird weight	variable
- avg T_{inlet} (10 pts)	ambient T + 4°C
- avg T_{outlet} (10 pts)	ambient T + 23°C
Porosity	0.7
Viscous resistance	1623.54/m^2
Inertial resistance	19.66/m
Convective heat transfer coeff for tarp	
- avg T_{inlet} (5 pts)	ambient T + 4°C
- avg T_{outlet} (5 pts)	ambient T + 21°C
- ambient T	ambient T
- vehicle travel speed	variable
Side tarp properties	
- thermal conductivity	variable
- thickness	variable
- specific heat	900 J/kg-K
- density	variable

Ambient temperature was one of the factors being studied in case 1 and case 2 of the predictions, thus it was set as a variable. For the ambient mass fraction of water, it was a function of the ambient temperature and ambient relative humidity. A value of 95% was chosen as the relative humidity level. For the range of ambient temperatures of -13.5 to 5°C, it would typically result in very high relative humidity values in real life scenarios. The inlet air velocities were set at 1.5 m/s for all inlet holes for 1-fan operation as determined in the calibration of the CFD model (Chapter 4). From data collected experimentally, the inlet temperature at the boundary of the virtual trailer was found to be 4°C higher than the ambient temperature, on average. The inlet mass fraction of water was assumed to be the same as the ambient mass fraction of water.

The number of broilers per drawer (loading density) and the bird weight affected the values of the heat and moisture production rates, and they were set as variables. In addition, these volumetric heat and moisture source terms were functions of the environmental temperature surrounding the birds. This temperature was estimated as the average of the inlet and outlet temperatures. When using the model for predictions, neither the inlet nor outlet temperatures were available for calculations of properties. These properties were required by FLUENT. Thus, it became necessary to estimate these values based on the ambient temperature. During the experiment, there were 10 thermocouples at the inlet and 10 thermocouples at the outlet. After analyzing the experimental data, it was decided to assume that the 10-point average inlet temperature would equal the ambient temperature plus 4°C, and the average outlet temperature would be ambient temperature plus 23°C for the sole purpose of calculating the properties. The environmental temperature used to calculate the heat and moisture production rates was then assumed be the average of the 10-point average of the inlet temperature and the 10-point average of the outlet temperature.

Porosity was used in the porous media sub-model in FLUENT, applied solely to the simulated drawers to represent resistance created by the physical presence of broilers. Its value depends on the loading density and the size of broilers in each drawer. During the calibration of the model, it was discovered that a porosity in the range of 0.6 to 0.8 had little effect on the temperature and relative humidity levels inside the load. Thus, for the purpose of the predictions, it was set as constant at 0.7. The viscous and inertial resistances were functions of the porosity and the mean particle diameter (Chapter 4). For a porosity of 0.7 and assuming the equivalent diameter of a broiler was 0.16 m, the viscous and inertial resistances were equal to $1623.54/m^2$ and 19.66/m, respectively.

The convective heat transfer coefficient of the side tarp was a function of the averaged inlet temperature from five thermocouple readings (closest to the edge of the tarp), the averaged outlet temperature from five thermocouple readings, the ambient temperature and the vehicle travel speed. After analyzing the experimental data, this 5-point average inlet temperature was assumed to be 4°C higher than the ambient temperature and the outlet temperature to be 21°C higher than the ambient temperature. The 5-point average outlet temperature was lower than the 10-point average outlet temperature, because the 5-point average looked at the conditions near the sidewall, whereas the 10-point average also considered the condition at the mid-plane which was warmer. The vehicle travel speed was set to be variable. Lastly, various thermal conductivity, thickness and density values were assigned to the tarp sidewall to study the effect of insulation in the last case study.

In order to take advantage of the "parametric study" setup in ANSYS Workbench 2.0 Framework, the ambient temperature, inlet air velocities, inlet temperature, inlet mass fraction of water, porosity, viscous resistance, inertial resistance and convective heat transfer coefficient of the side tarp were set up as input parameters, with values assigned to them outside of FLUENT, and the simulations were ran in batch mode. As for the heat and moisture production rates and the sidewall properties, version 12.0.16 of FLUENT did not allow these variables to be created as input parameters, thus they were updated manually inside FLUENT and ran one-by-one.

5.4 RESULTS AND DISCUSSION

Three cases were studied to examine various scenarios most commonly encountered by the poultry transport industry. Results from these simulations predicted the performance of the experimental trailer, which helped to set operational guidelines for users of the experimental trailer and set design parameters for the next generation of a poultry transport vehicle equipped with active heating and ventilation. The use of a CFD model helped to study a multitude of scenarios without risking the lives of the broilers and at a lower research cost.

5.4.1 EFFECTS OF VEHICLE TRAVEL SPEED AND AMBIENT TEMPERATURE

Generally, commercial trailers are ventilated by passive (natural) ventilation, meaning there is no mechanical system installed on these trailers to remove heat and moisture produced by the animals. The passive ventilation is driven by the movement of the vehicle. When a vehicle is in motion, positive and negative pressure zones are generated around the vehicle caused by its aerodynamic design. Because the tarpaulins are loosely strapped along the two sidewalls of the trailers and there are vent openings on the roof, headboards and tailboards, air is able to move in and out of the loading area, driven by pressure gradients surrounding the body of the vehicles. For example, in the case of the 53-ft semi-trailer, previous experimental results suggested that air moved in from the sides, absorbed heat from the chickens and carried it out through roof vents (Chapter 2).

The main disadvantage of passive ventilation is it only functions when the trailer is in motion. When the trailer is stationary, no pressure gradients are created, thus no ventilation is provided. Heat and moisture can accumulate within the load when the vehicle is stationary. Furthermore, the amount of ventilation is a function of travel speed, amount and location of vent openings, and the amount of air leakage. The ventilation rate cannot be easily controlled, making the system unreliable and resulting in large temperature gradients inside the load.

During the transportation process, when there is a lack of facilities to protect animals against adverse weather conditions, it is recommended that trucks loaded with animals do not sit idle for more than 2 hours (Agriculture Canada, 1989). This recommendation is probably based on the assumption that commercial vehicles utilize passive ventilation; there is no air movement or circulation when the vehicle is stationary. In summer, the broilers would become too hot. In fact, when there were delays in processing and the unloading dock was full, it was common to hear the processor asking their drivers to drive the vehicles around the processing plant to provide some ventilation for the birds in summer. In winter, the situation becomes more complicated, as side tarps are usually lowered to protect birds from cold weather, snow or wind. If the vehicle is held stationary for an extended period of time, heat and moisture would be trapped inside the trailer, and broilers would become wet. However, if the side tarps are raised, the broilers would be exposed to severe cold conditions. It is a delicate balancing act between providing adequate ventilation and protection from cold weather.

Contrary to commercial trailers, the experimental trailer simulated by the CFD model utilized active ventilation. If all the edges were sealed and there was no air leakage, the performance of the ventilation system should not be a function of the vehicle travel speed, regardless of the ambient temperature. If such was the case, the experimental trailer would provide more independent and reliable ventilation to broilers during transport. In order to examine such a hypothesis, it was decided to study the effect of vehicle travel speed and ambient temperature on load conditions, using the CFD model.

Table 5.1 summarizes the settings applied in the first series of simulations. The objective was to study the effects of vehicle travel speed and ambient temperature on load conditions. The CFD model was programmed to run at two ambient temperatures (-5 and -10℃), and three vehicle travel speeds (90, 100, 110 km/h), resulting in six simulations. As summarized in Table 5.2, the heat and moisture production rates were based on the bird loading density which was set at 18 birds per drawer, with the bird weight set to the maximum level of 2.78 kg per bird, giving a total bird weight of 8113 kg. As for the side tarp properties, it was not possible to determine the specific material properties from the supplier, therefore, the properties of polyvinyl chloride were used.

Table 5.2. Variable settings used to study effects of vehicle travel speed and ambient temperature.

Prediction 1 - Variable settings

Ambient temperature	-5, -10 °C
Heat & mositure production rates	
- bird loading density	18 per drawer
- bird weight	max of guideline (2.78kg)
Vehicle travel speed	90, 100, 110 km/hr
Side tarp properties	
- thermal conductivity	0.16 W/m-K
- thickness	0.0015875 m
- specific heat	900 J/kg-K
- density	1380 kg/m^3

Figure 5.3 summarizes results obtained from the six simulations. The label on the *x*-axis indicates the setting for the ambient temperature and travel speed. The blue bars denote the minimum temperatures found inside the load, and the red bars denote the maximum temperatures. The green bars represent the ranges of temperature by subtracting the minimum from its corresponding maximum value. These results indicated that traveling speed has little

effect over the minimum, maximum or range of temperatures found inside the load, at an ambient temperature of -5°C or -10°C, for a vehicle travel speed of 90, 100 or 110 km/h.

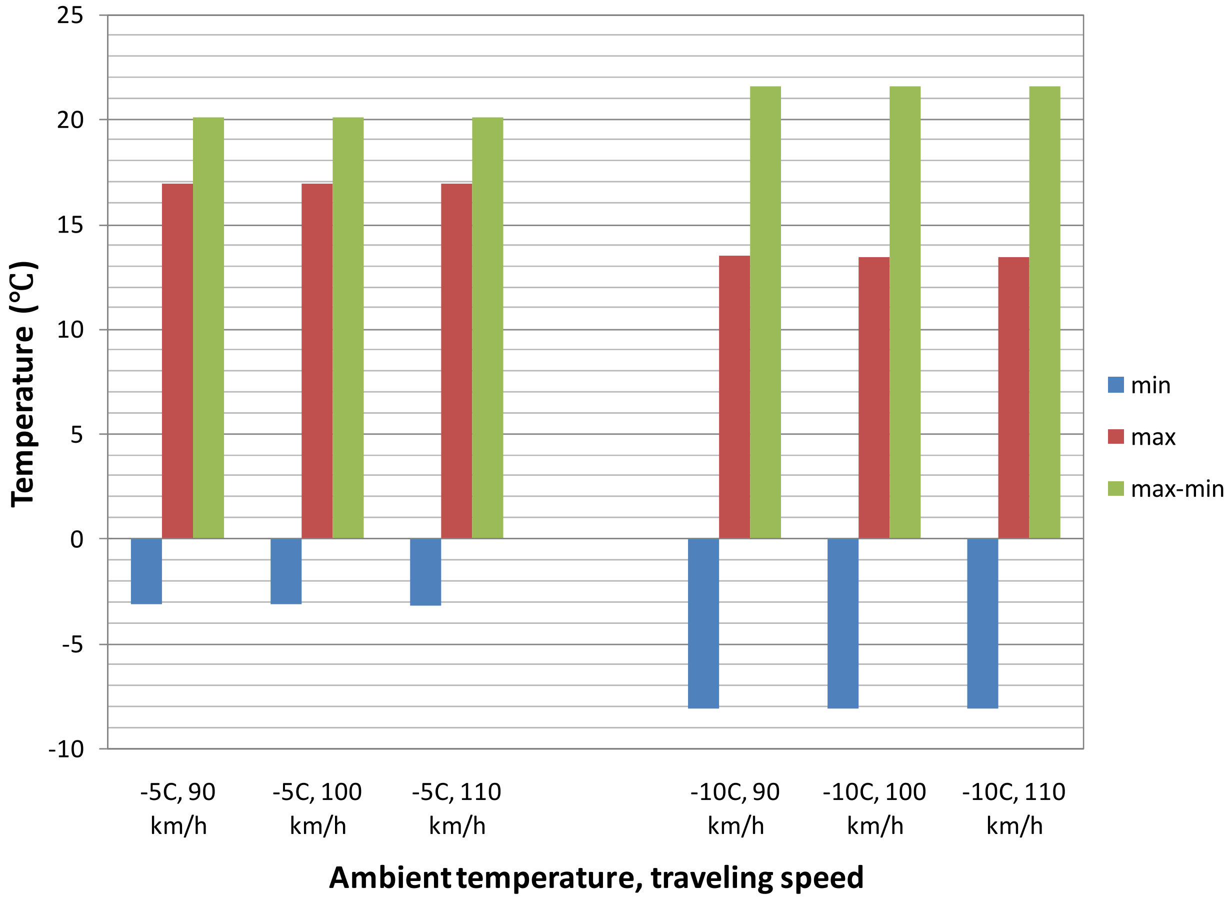

Figure 5.3. Effects of ambient temperature and traveling speed at a loading density of 18 birds/drawer, with a total bird weight of 8113 kg.

These results suggested driving the experimental trailer at a different speed has minimal effect on the load conditions for travel speeds ranging from 90 to 110 km/h. It is important to point out the CFD model did not take air leakage into account, which existed in the experimental trailer. As the amount of leakage in the experimental trailer was not quantified, it is difficult to estimate how much these prediction results would deviate from reality. However, it is certain that the experimental trailer had much less leakage than the commercial trailers in which the side tarp was loosely secured with rubber tie down straps, with roof vents opened occasionally in winter.

Results from Figure 5.3 showed that the experimental trailer equipped with active ventilation with no air leakage was able to provide more independent and reliable ventilation to broilers, which is independent of the highway travelling speeds between 90 to 110 km/h.

5.4.2 EFFECTS OF BIRD SIZE, LOADING DENSITY AND AMBIENT TEMPERATURE

The bird size (i.e. weight) and loading density affect the total amount of heat and moisture to be ventilated from the experimental trailer. In commercial practices, it is very common to have bird size and loading density varying from one shipment to another, depending on final weight and number of broilers grown. In the CFD model, the bird size and loading density affected the heat and moisture source terms. The second series of predictive simulations were conducted to examine the effects of bird size, loading density and ambient temperature.

Table 5.3 summarizes the variable settings used in the second series of simulations. There were five settings for the ambient temperature (5, 0, -5, -10 and -13.5°C) and two types of birds (1.8 kg for small birds, 2.3 kg for large birds). For each bird weight, there were three types of loading density (22, 24 and 26 birds/drawer for small birds, and 16, 18 and 20 birds/drawer for large birds). The vehicle travel speed was set at 100 km/h as the most common highway speed. The same side tarp properties were used as in the first series of predictions.

Table 5.3. Variable settings used to study effects of bird size, loading density and ambient temperature.

Prediction 2 - Variable settings	
Ambient temperature	5, 0, -5, -10, -13.5 °C
Heat & mositure production rates	
- bird loading density	small (22, 24, 26 per drawer), large (16, 18, 20 per drawer)
- bird weight	small (1.8kg), large (2.3kg)
Vehicle travel speed	100 km/hr
Side tarp properties	
- thermal conductivity	0.16 W/m-K
- thickness	0.0015875 m
- specific heat	900 J/kg-K
- density	1380 kg/m^3

Figure 5.4 and Figure 5.5 summarize the effects of ambient temperature and loading density for two sizes of birds (1.8 and 2.3 kg). For both sizes of birds, the minimum and maximum load temperatures decreased with ambient temperature. The minimum values were related to the ambient temperature. The range (max minus min) of load temperatures increased with decreasing ambient temperature. The colder the temperature, the wider the range of temperatures existed around the birds. For the same bird size, loading more birds in a drawer increased the maximum temperature, but did little to affect the minimum temperature as shown in Figure 5.6 and Figure 5.7.

The heat and moisture production rates were a function of temperature, individual bird size and total number of birds. At the same temperature, if a load of small birds had higher loading density than another load of larger birds at lower loading density, this load could still result in greater heat and moisture production rates. Therefore, it is important not to only consider loading density or bird size alone. Both factors are inter-related and they have to be considered together.

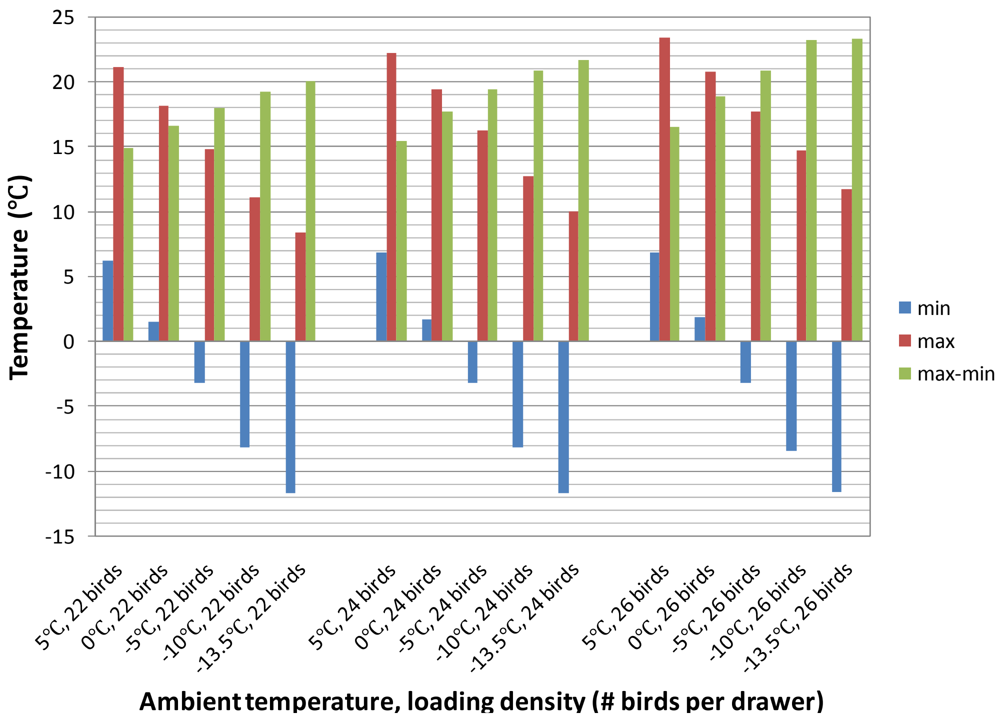

Figure 5.4. Effects of ambient temperature and loading density for small birds at 1.8 kg.

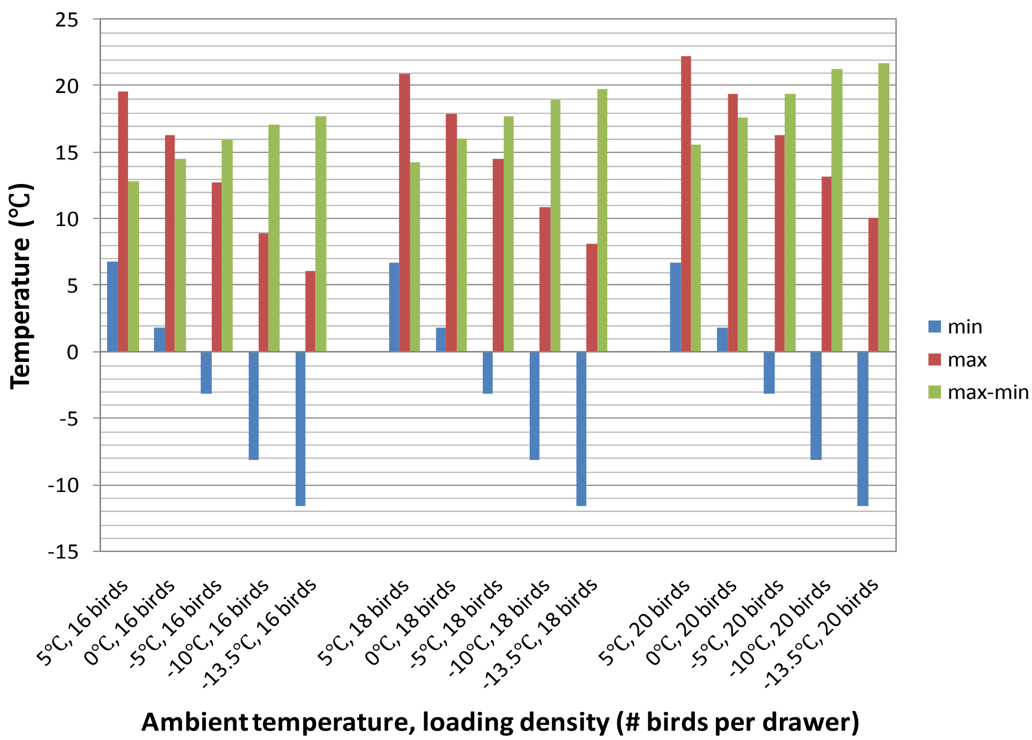

Figure 5.5. Effects of ambient temperature and loading density for large birds at 2.3 kg.

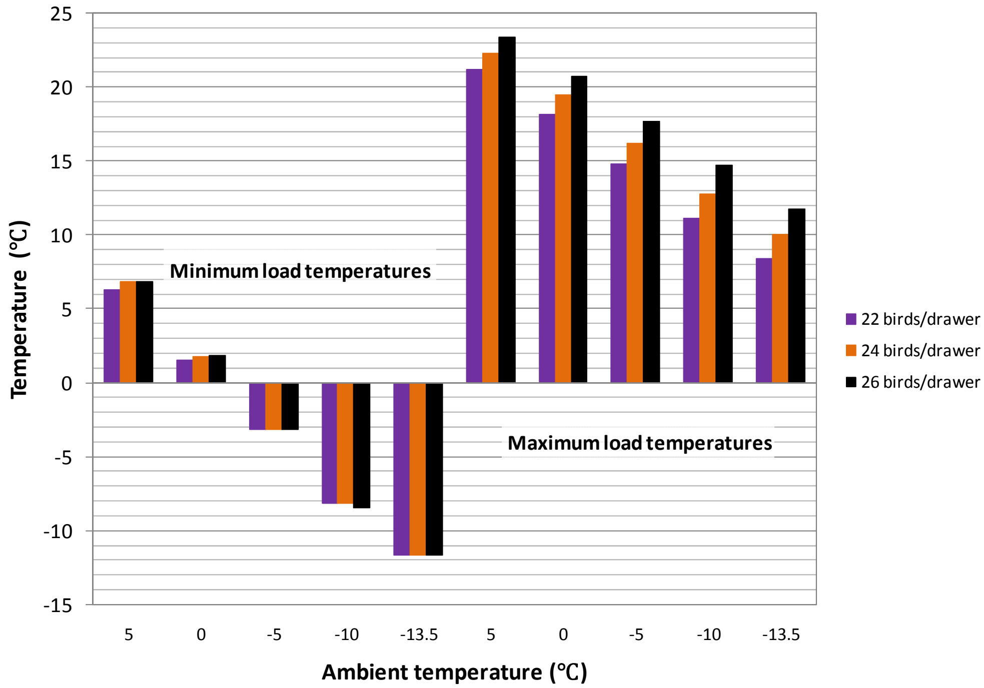

Figure 5.6. Minimum and maximum load temperatures inside the trailer at various loading density of small birds at 1.8 kg.

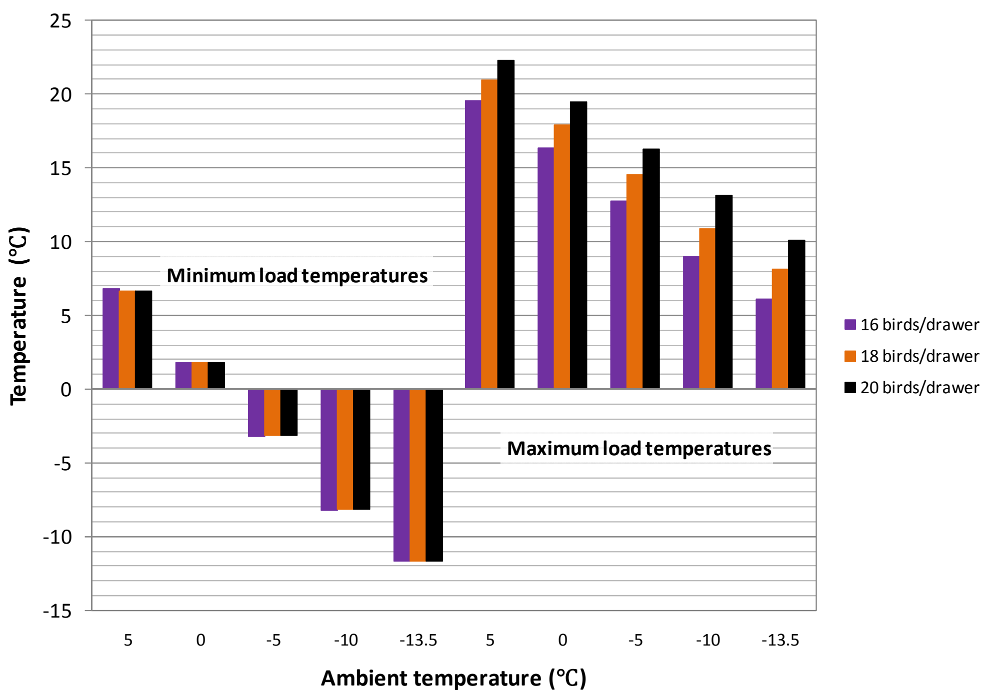

Figure 5.7. Minimum and maximum load temperatures inside the trailer at various loading density of large birds at 2.3 kg.

5.4.3 EFFECTS OF SIDE TARP INSULATION AND AMBIENT TEMPERATURE

The side tarp used in the experimental trailer was not insulated. With the minimum load temperature varying with the ambient temperature, the question of how an insulated side tarp may affect the load temperature arose.

Table 5.4 summarizes the model setup and properties of three types of insulated tarps. These properties were assumed, based on values from tarps available commercially which could be used in the current application. As the insulation value changes with thermal conductivity and/or material thickness, it was decided to set the thickness to a constant value and simply vary the value of thermal conductivity. Specific heat is the amount of heat required to raise the temperature of a unit mass of substance by one degree Celsius. It was not possible to know the specific heat value of commercially available insulated side tarp, thus it was assumed to be the same as the original non-insulated one. The goal of this series of predictive simulations was to examine the concept of adding insulation to the side tarp, rather than designing an insulated side tarp.

Table 5.4. Variable settings used to study effects of side tarp insulation and ambient temperature.

Prediction 3 - Variable settings	
Ambient temperature	5, -13.5°C
Heat & mositure production rates	
- bird loading density	26 per drawer
- bird weight	small (1.8kg)
Vehicle travel speed	100 km/hr
Side tarp properties*	
- thermal conductivity	0.02, 0.04, 0.08 W/m-K
- thickness	0.0184912 m
- specific heat	900 J/kg-K
- density	145.946 kg/m^3

*The original non-insulated side tarp had properties of 0.16 W/m-K, 0.0015875 m, 900 J/kg-K and 1380 kg/m^3.

Figure 5.8 shows the load temperatures obtained from simulations for the three types of insulated side tarps. Results from the second series of simulations for the original side tarp were also plotted in the same graph to compare their performances. Using an insulated tarp with a lower thermal conductivity, higher thickness and lower density increased the minimum and maximum load temperatures. For an insulated tarp of 0.02W/m-K as thermal conductivity, the minimum load temperature increased by 2.1°C as compared to using the original tarp, for both categories of ambient temperature (5°C and -13.5°C). For the same insulated tarp, it also increased the maximum load temperature by 1.0°C when the ambient temperature was 5°C, or by 1.3°C when the ambient temperature was -13.5°C. Using the insulated tarp slightly narrowed the range of temperatures inside the load when more insulation was added. Results of these simulations suggested that using an insulated tarp was desirable in winter, as it could better protect animals against cold temperatures. It would be useful to run the model at ambient temperatures below -13.5°C (temperature limit imposed by the broiler heat and moisture production equations). It is not recommended to use an insulated tarp at ambient temperatures greater than 5°C, as the maximum temperature in the load was approaching the upper limit of 25-26°C (Webster et al. 1993, Mitchell and Kettlewell 1998), which may expose the broilers to heat stress.

As a common practice, the poultry industry rolled down the side tarp in winter, but rolled it up in summer in the commercial trailers (not equipped with fans). However, if active ventilation is desired in the new design of commercial trailers (to reduce temperature and humidity levels), the side tarp must remain rolled down for all four seasons for the fans to create front-to-rear airflow. Two sets of side tarps may be required: an insulated tarp for winter operation and a non-insulated tarp for summer operations. It is important to point out only one fan was used in the predictive simulations, therefore, it may be possible to use only one type of tarp, the insulated one, for all seasons if more ventilation is provided to the load. Although using one type of tarp would reduce the capital cost, it would also increase the operating cost for the additional ventilation. This assumption can be verified by setting up the 2- and 3-fan CFD models to re-run this analysis to verify how much the maximum temperature would be lowered if higher flow rates are applied. When additional experimental data for summertime become available, the CFD models can be calibrated and validated for summer conditions, and use to determine the required ventilation rates for summer when an insulated tarp is used. Once the desirable levels of flow rate are determined for different seasons, a cost analysis can be conducted to estimate the operating costs. Further cost analysis can then be carried to estimate the potential benefit (such as reduction of death-on-arrival or increase in marketable weight) to determine which is the most viable option (1 or 2 types of tarp) from the financial point of view.

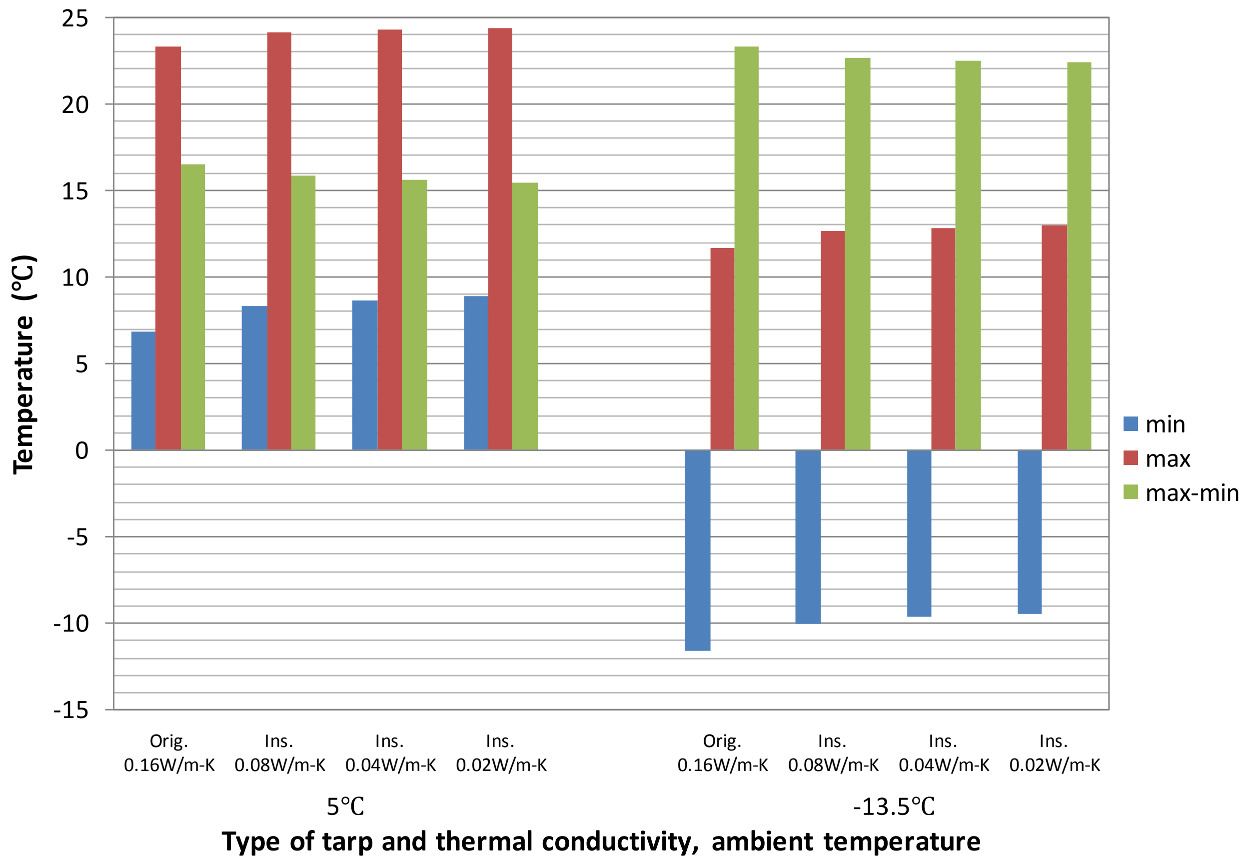

Figure 5.8. Effects of insulating the side tarp and ambient temperature on load temperatures, for small birds at 1.8 kg, 26 birds per drawer.

5.5 Conclusions and Recommendations

A CFD model using one fan was used to predict the performance of an experimental trailer equipped with active ventilation. Three cases were investigated, based on conditions which may be encountered by the poultry transport industry. The first case examined the effects of vehicle travel speed and ambient temperature. The second case looked at the effects of bird size, loading density and ambient temperature. The last case studied the effects of side tarp insulation and ambient temperature.

For travel speeds of 90, 100, 110 km/h, subjected to ambient temperatures of -5°C and -10°C, with a total bird weight of 8113 kg at 18 birds/drawer, the travel speeds tested had little effect on the minimum, maximum, or range (max minus min) of load temperatures. The travel speed affected the simulated value of the convective heat transfer coefficient of the side tarp, but the model did not take air leakage into consideration. It can be conclude that for the experimental trailer equipped with active ventilation, it was able to provide more independent and reliable ventilation to broilers, without being affected by typical highway travelling speeds.

The ambient temperature played a key role in the load temperatures in all three cases studied. The second case examined this parameter in detail, along with bird size and loading density. The ambient temperatures tested were -13.5, -10, -5, 0 and 5°C. The bird types examined were small (1.8 kg at 22, 24 or 26 birds/drawer), and large (2.3 kg at 16, 18 or 20 birds/drawer). The travel speed was set at 100 km/h. The minimum load temperatures were about 1-2 °C higher than the ambient temperatures. Colder ambient temperature widened the range of temperatures surrounding the birds, effectively causing the load temperature to be less uniform. As expected, for the same bird size, a higher loading density increased the maximum load temperature, but it did not affect the minimum temperature. These simulations were set up by assuming broilers are loaded uniformly across the trailer, as in current commercial practices. Based on the results obtained from this case study, there may be potential benefit in loading the broilers in a non-uniform matter in winter, helping to shift the minimum load temperature to a higher level, keeping the broilers at the boundaries warmer and narrowing the temperature range across the load.

In the last series of simulations, performances of three insulated tarps were compared with the original tarp, at two ambient temperatures (-13.5 and 5°C). The travelling speed was set at 100 km/h, with bird size at 1.8 kg and 26 birds/drawer. Results of these simulations suggested that using an insulated tarp was desirable in winter, as it could better protect animals against cold temperatures by shifting the minimum temperature upward (1-2°C for the insulation value tested). It is not recommended to use an insulated tarp at ambient temperatures greater than 5°C, as the maximum temperature in the load was approaching the upper limit of 25-26°C (Webster et al. 1993; Mitchell and Kettlewell 1998), which may expose the broilers to heat stress.

This study identified that ambient temperature, bird sizes, loading density and side tarp insulation value were important factors to consider in the design of an actively ventilated poultry transport vehicle. For a well-sealed vehicle, travel speed did not play a role. Among all the factors, ambient temperature had the most effect on the minimum, maximum and range of load temperatures. The CFD model, based on data acquired using the experimental trailer, proved to be a valuable tool, permitting the study of different scenarios, identifying parameters which played a significant role and eliminating those which did not in the design of a poultry transport vehicle. It helped to answer a number of "what if" questions, and enhanced the understanding of the performance of the experimental trailer. Results from this study will help to design the next generation of the actively ventilated poultry transport vehicles.

5.6 ACKNOWLEDGEMENT

The authors acknowledge financial support provided by the Natural Sciences and Engineering Research Council of Canada, Agriculture and Agri-Food Canada, the Chicken Farmers of Saskatchewan, Le Fonds Québécois de la Recherche sur la Nature et les Technologies, Saskatchewan Chicken Industry Development Fund and the University of Saskatchewan in this project. The authors also thank staff members from the Engineering Computer Center of the University of Saskatchewan for their support in the setup of the software and the usage of Xi simulation lab. Special thanks go to the staff members of the ANSYS and FLUENT in providing training materials and answering many questions regarding the usage of their software. The authors also thank Lilydale Inc. and its personnel for their support in the collection of experimental data which were used to calibrate and validate the CFD models.

6 GENERAL DISCUSSION

6.1 SCOPE OF THE RESEARCH PROJECT & DISSERTATION

A research program was developed aiming to improve the transportation conditions of broiler chickens. As part of this research program, a research project was developed which had the following 4 objectives:

1. design and construct an experimental trailer equipped with active ventilation and heating;
2. characterize the performance of the experimental trailer;
3. develop, calibrate and validate CFD models used for simulating the environmental conditions surrounding the broilers as found inside the experimental trailer; and
4. utilize one of the CFD models to predict the performance of the experimental trailer using conditions that may be encountered by the poultry transport industry.

This dissertation consists of six chapters. The first chapter serves as the introductory chapter which provide background information to the readers. The following four chapters cover each of the research objectives as listed above, one after another. This last chapter summarizes major findings in this research project, discusses future work and presents final conclusions.

6.2 SUMMARY OF MAJOR FINDINGS

The first introductory chapter reviewed economical, logistical and legislative aspects surrounding the poultry transport industry. It summarized important parameters for the design of an experimental transport system, including limits of environmental conditions suitable for housing chickens, their heat and moisture production rates, climatic conditions in Southern Saskatchewan and conditions found within commercial transport systems. This chapter also reviewed some fundamental concepts of the Computational Fluid Dynamics (CFD) modeling method and why it was chosen as a tool to complement the experimental work in this project.

The second chapter examined the first objective of this research project. It included a comprehensive review of the designs of some commercial poultry transport equipment which were not previously documented in the literature. It discussed how these commercial systems inspired the design of an actively heated and ventilated experimental vehicle. The setup of the experimental trailer was discussed in detail, providing background information for the third chapter, which discussed the performance of the vehicle.

The third chapter examined the second objective of this research project. After briefly reviewing the experimental trailer, it discussed the experimental procedure used to evaluate the performance of the experimental trailer. The performance of the system was evaluated in a series of field tests conducted under commercial loading operations, in winter conditions on the Canada Prairies. Results obtained from the field tests showed the average load temperature ranged from 7.1 to 15.6°C in the nine sets of data. The experimental trailer was able to maintain an environment above -1°C. As for the humidity level inside the trailer, the majority of the sensors had representative relative humidity (RH^*) values between 10 and 40%, with the rest having RH^* values below saturation. The 3-D plots suggested the presence of air leakage near the side tarpaulins. The front section was generally colder than the rear, and the longitudinal mid-planes were warmer than the sides. The front end of the trailer was drier than the rear. Results from the field tests suggested that the concept of active ventilation and heating is a promising option to improve the transport conditions for broiler chickens during cold ambient conditions.

The fourth chapter of this dissertation reviewed the development, calibration and validation of the 3-D CFD models developed to simulate the environmental conditions inside an experimental trailer. A total of three CFD models were developed to simulate the three different ventilation regimes encountered in field tests. GAMBIT was used to mesh a 7.95-m long by 1.23-m wide by 2.57-m high geometry. Working in the ANSYS Workbench Framework, ANSYS DesignXplorer was set up to run the simulations as parametric studies inside FLUENT. Post-processing was completed using CFD-Post, Tecplot and Excel. This chapter reviewed the geometrical simplifications and assumptions made to simplify the problem. It discussed some of the properties and sub-models used in building the models. It examined the processes of model calibration and validation using experimental data.

During calibration, sensitivity studies revealed that inlet velocities, and production rates of heat and moisture had a great impact on the results obtained from the CFD models. The levels of porosity investigated did not play a significant role. The standard error of estimate (σ_{est}) was selected as a statistical measure to evaluate the accuracy of the CFD models against experimental data. For temperature data, σ_{est} varied from 3.2 to 7.3°C. For humidity ratio, σ_{est} varied from 1.7 to 5.0 g of water vapour per kg of dry air. The models tended to overestimate or underestimate temperature and humidity ratio values at the boundaries. The CFD models were able to accurately recreate the temperature trends as observed, and they provided additional information in regions where experimental data were not available or difficult to collect. It is recommended to use these models for comparative studies, but not for determining the absolute values of temperature and relative humidity inside the experimental trailer.

The fifth chapter examined the last research objective of this project, the 1-fan CFD model developed in previous chapter was used to study several “what-if” scenarios. Three cases were investigated, based on conditions which may be encountered by the poultry transport industry. The first case examined the effects of vehicle travel speed and ambient temperature. The second case looked at the effects of bird size, loading density and ambient temperature. The last case studied the effects of side tarp insulation and ambient temperature.

In the first case, for travel speeds at 90, 100, 110 km/h, coupled with ambient temperature of -5°C and -10°C, with a total bird weight of 8113 kg at 18 birds/drawer, the range of travel speeds tested had minimal effect on the minimum, maximum, and range (max minus min) of load temperatures. In the second case, the ambient temperatures tested were -13.5, -10, -5, 0 and 5°C, and the bird types examined were small (1.8 kg at 22, 24 or 26 birds/drawer) and large (2.3 kg at 16, 18 or 20 birds/drawer). Results indicated the minimum load temperature was closely related to the ambient temperature, and a colder ambient temperature expanded the range of temperature inside the load. For the same bird size, a higher load density increased the maximum load temperature but did not affect the minimum temperature. In the last case, the effect of three insulated tarps was compared with the original tarp, at two ambient temperatures (-13.5 and 5°C). It was found that for the types of insulated tarp tested, insulation helped to raise the minimum load temperature, but it also raised the maximum load temperature. It is recommended not to use an insulated tarp (at the insulation value examined) for ambient temperatures greater than 5°C.

6.3 FUTURE WORK

It is recommended to use the CFD models as a design tool for comparative studies (such as comparing operating conditions), but not for determining absolute values of temperature and relative humidity inside the experimental trailer (see Chapter 4). A few things could be done to improve the accuracy of the CFD models and facilitate the research work.

First of all, it was an ambitious plan to collect data on the experimental trailer which was in motion. It took a significant amount of resources to gather each set of data. The research team did not have any control over the ambient conditions which the field tests were carried out, nor the availability of animals. The field tests were scheduled around a commercial operation. The research team had to work almost 12 hours continuously to obtain one set of data (at the barn, travelling, and at the processing facility). Looking back, it would have been much easier if the CFD models were first developed for a stationary vehicle in a lab setting, rather than for a moving vehicle. Such an approach would have eliminated many of the logistical issues and allowed the researcher to focus on data collection and model development. The only obstacle is to determine where to obtain animals to run stationary tests which would still be marketable afterward. It will require negotiations with the processor. Another possibility is to use artificial “broilers” (for example light sources and humidifiers) to simulate the heat and moisture load. The trailer could be put inside a wind tunnel with the artificial broilers to simulate the effect of forced convection outside the trailer.

Secondly, if experiments are conducted in a stationary setup, it would facilitate the collection of flow rate data from the fans. Conduits could be mounted at the fan outlets to properly measure static pressures, just like in fan calibration setup. Hall effect sensors could be used to measure rotational speed and the flow rates could be obtained from fan curves. Such elaborated setup was not feasible in a moving trailer. If fan flow rates were available, they could be used as boundary conditions instead of inlet velocities in the CFD models.

Thirdly, leakage was not quantified in this study. It would be easier to control leakage if the experimental data were collected in a stationary setup. There will be more time to properly seal off the trailer and the trailer would not be subject to wear as much as in the current study.

Fourthly, as mentioned in Chapter 4, a more refined grid of temperature and relative humidity data is required for inlet boundary conditions, and such data should be implemented in a more refined grid inside the CFD models. The instrumentation system will need to be modified; more sensors will need to be wired, installed and programmed. As for implementing them in the CFD models, the geometry will have to be further sub-divided in small groups such that more inlet boundary conditions could be applied on them.

Fifthly, during the development of the CFD models, it was discovered the heat and moisture production models available at that time were not developed for transport conditions and they were for broilers subjected to 0 to 30℃. Because heat and moisture production rates are important variables in the heat transfer equations, future work is required to examine the latest heat and moisture production models developed for broilers at lower temperatures during transport conditions, and testing them in the CFD models.

Lastly, aside from the tremendous efforts put into learning how to and developing the CFD models, it was discovered there is a lack of literature on how to compare simulated results against experimental data. A statistical measure commonly used in regression analysis, standard error of estimate, was proposed and adopted to evaluate the accuracy of the CFD models. More research is required to develop methodology, and establish standards on how to compare a large set of data which varies spatially and over time, for any CFD application. Specific standards should be established to determine the acceptable level of errors for poultry transport research. These are interesting topics for engineers, poultry scientists, CFD researchers and statisticians.

6.4 FINAL CONCLUSIONS & SCIENTIFIC CONTRIBUTIONS

The work included in this dissertation achieved the four research objectives as outlined at the beginning of this chapter. This dissertation documented the commercial practices and equipment, information that is rare in the scientific or non-scientific literature. It discussed the design and construction of a new, experimental trailer equipped with active ventilation and heating, fulfilling the first research objective. The dissertation also described the field work and analysis conducted to characterize the performance of the experimental trailer, meeting the second research objective. The third research objective was met by presenting the development, calibration and validation of new CFD models used for simulating the environmental conditions surrounding the broilers as found inside the experimental trailer. Lastly, the fourth research objective was achieved by using one of the CFD models to predict the performance of the experimental trailer using conditions which may be encountered by the poultry transport industry.

In addition to achieving these four research objectives, this research project also answered two key questions for the poultry transport research program. Firstly, the experimental work proved that the concept of active ventilation and heating is a promising option to improve the transport conditions for broiler chickens during cold ambient conditions. The experimental trailer helped to provide a warmer and drier environment for broilers during transportation. Secondly, the CFD work proved that CFD modeling is a valuable tool to simulate what happened inside the experimental trailer, and allow different operating conditions to be studied.

Considering the only CFD study on chicken transportation was conducted for a day-old chick transport system, and there is a limited number of scientific literature which discuss chicken transportation from an engineering perspective, this dissertation fulfilled an important void in the current scientific literature. The most significant scientific contributions presented by the author of this dissertation include: a comprehensive review of the designs of various poultry transport systems (commercial and experimental); characterization the performance of an actively heated and ventilated poultry transport system; development, calibration, validation, and application of CFD models developed for a 3-D, large-scale poultry transport system; and presentation of a unique, quantitative method to analyse large set of experimental and simulated data which vary spatially and over time.

In conclusion, the research work presented in this dissertation has provided significant contributions to the knowledge advancement of poultry transport and applied CFD research.

REFERENCES

AAFC. 2010. Annual Poultry Slaughter Report (for chicken, eviscerated weight). Poultry Section, Animal Industry Division, Agriculture and Agri-Food Canada. Ottawa, ON, Canada. Available at: www.agr.gc.ca/poultry/sla-aba_eng.htm#poultry. Accessed 15 February 2010.

AAFC. 2009. Canadian Poultry Slaughter Plants (all poultry, Saskatchewan). Agriculture and Agri-Food Canada. Ottawa, ON, Canada. Available at: www.agr.gc.ca/volaille/esta-entr_s1_eng.htm#. Accessed 15 February 2010.

AAFC. 2008. Canada's Poultry Industry at a glance. Poultry Section, Animal Industry Division, Agriculture and Agri-Food Canada. Ottawa, ON, Canada. Available at: www.ats-sea.agr.gc.ca/pro/3315-eng.htm. Accessed 15 February 15 2010.

Agriculture Canada. 1989. Recommended code of practice for the care and handling of poultry from hatchery to processing plant. Agriculture Canada Publication 1757/E. Communications Branch, Agriculture Canada, Ottawa, ON, Canada. Available at: www.agr.ca/poultry/pub1757e.pdf. Accessed 21 January 2010.

Amtec Engineering, Inc. 2003. Tecplot User's Manual Version 10. Amtec Engineering, Inc. Bellevue, Washington, USA.

Anglia Autoflow Ltd. 2002. Product catalogue: Easyload - leading the world in live bird handling systems. Anglia Autoflow Ltd., Wortham Ling, Diss, Norfolk, England.

ASAE. 2001. Comfortable ride – Concept 2000 provides climate control during poultry transport. Resource: Engineering and Technology for a Sustainable World, vol. 8, no. 9. American Society of Agricultural Engineers (ASAE), St. Joseph, MI, USA.

ASHRAE. 2005. Chapter 6 – Psychrometrics. In *ASHRAE Handbook: Fundamentals (SI)*. American Society of Heating, Refrigerating and Air-Conditioning Engineers, Inc. Atlanta, GA, U.S.A.

ASHRAE. 2001. Chapter 27 – Climatic Design Information. In *ASHRAE Handbook: Fundamentals (SI)*. American Society of Heating, Refrigerating and Air-Conditioning Engineers, Inc. Atlanta, GA, U.S.A.

Atkins R. P. and D. Slingerland. 2004. Ventilation Fan Testing (Development Project DL0903). Agricultural Technology Centre, Lethbridge, AB, Canada.

Barbosa Filho, J. A. D., F. M. Corrêa Vieira, I. J. Oliveira da Silva, D. de Brito Garcia, M. A. Neves da Silva and B. H. Fernandes Fonseca. 2009. *Poultry transport: microclimate characterization of the truck during the winter*. Revista Brasileira De Zootecnia, 38(12): 2442-2446.

Bayliss P.A. and M.H. Hinton. 1990. *Transportation of broilers with special reference to mortality rates*. Appl. Anim. Behav. Sci., 28:93-118.

BBSRC 2002. Science and animal welfare. Biotechnology and Biological Sciences Research Council (BBSRC), Swindon, Wiltshire, UK Available at: www.bbsrc.ac.uk/organisation/policies/position/public_interest/animal_welfare.pdf. Accessed 23 January 2010.

Bianchi, M., M. Petracci and C. Cavani. 2005. *Effects of transport and lairage on mortality, liveweight loss and carcass quality in broiler chickens*. Italian Journal of Animal Science 4 (SUPPL. 2): 516-518.

Burlinguette N.A., M. L. Strawford, J. M. Watts, H. L. Classen, P. J. Shand and T. G. Crowe. 2012. *Broiler trailer thermal conditions during cold climate transport.* Can. J. Anim. Sci. 92: 109-122.

CARC. 2001. Recommended code of practice for the care and handling of farm animals – Transportation. Canadian Agri-Food Research Council (CARC), Ottawa, ON, Canada. Available at: www.nfacc.ca/code.aspx. Accessed 21 January 2010.

CFC. 2011. Chicken Data Booklet 2011. Chicken Farmers of Canada (CFC), Ottawa, ON, Canada. Available at http://publications.gc.ca/site/eng/404274/publication.html. Accessed 4 March 2011.

CFD Online. 2007. Mesh Classification. Available at http://www.cfd-online.com/Wiki/Mesh_classification. Accessed 4 March 2011.

Chauvin, C., S. Hillion, L. Balaine, V. Michel, J. Peraste, I. Petetin, C. Lupo and S. Le Bouquin. 2011. *Factors associated with mortality of broilers during transport to slaughterhouse.* Animal 5 (2): 287-293.

CIGR. 2002. 4th Report of Working Group on Climatization of Animal Houses - Heat and Moisture Production at Animal and House levels. Eds. S. Pedersen and K. Sallvik., Research Centre Bygholm, Danish Institute of Agricultural Sciences. Horsens, Denmark. Available at: www.cigr.org/CIGRWorkingGroupReports.htm. Accessed 28 October 2008.

Classen, H.L., T. Knezacek, G.P. Audren, S. Stephens, T. Crowe, E.M. Barber, A.A. Olkowski, M.A. Mitchell and P.J. Kettlewell. 2002. Final Report, Project SDAF#19990246-24BX, Studies on Broiler Chicken Transportation in Saskatchewan. Regina, SK: Saskatchewan Agriculture and Food.

Dadgar, S., E. S. Lee, T. L. V. Leer, N. Burlinguette, H. L. Classen, T. G. Crowe and P. J. Shand. 2010. *Effect of microclimate temperature during transportation of broiler chickens on quality of the pectoralis major muscle*. Poultry Science 89 (5): 1033-1041.

Environment Canada 2005. Hourly Data Report for March 24, 2005. Available at: http://www.climate.weatheroffice.gc.ca/climateData/hourlydata_e.html?timeframe=1&Prov=CA&StationID=3328&Year=2005&Month=3&Day=24. Accessed 24 April 2010.

Fluent Inc. 2007. GAMBIT 2.4 Modeling Guide - Volume 2. Fluent, Incorporated, Lebanon, NH, U.S.A.

Fluent Inc. 2006. FLUENT 6.3 User's Guide. Fluent, Incorporated, Lebanon, NH, U.S.A.

Götz, H. 1987. Chapter 8: Commercial vehicles. In *Aerodynamics of Road Vehicles: from Fluid Mechanics to Vehicle Engineering*, 295-354. W.H. Hucho, ed. Butterworth & Co. (Publishers) Ltd. London, UK

Haslam, S. 2008. Chapter 7: Legislation and poultry welfare. In *Poultry diseases*, sixth edition, 94-108. M. Pattison, P.F. McMullin, J.M. Bradbury and D.J. Alexander, eds. Elsevier Limited.

Hunter, R.R., M.A. Mitchell and A.J. Carlisle. 1999. *Wetting of broilers during cold weather transport: a major source of physiological stress?* British Poultry Science, Supplement 40: S48-S49.

Incropera F. P. and D. P. De Witt. 2002. Fundamentals of Heat and Mass Transfer, 5th edition. John Wiley & Sons. New York.

Kettlewell, P.J., R.P. Hoxey and M.A. Mitchell. 2000. *Heat produced by broiler chickens in a commercial transport vehicle.* J. Agric. Eng. Res. 75: 315-326.

Knezacek, T. D., A. A. Olkowski, P. J. Kettlewell, M. A. Mitchell and H. L. Classen. 2010. *Temperature gradients in trailers and changes in broiler rectal and core body temperature during winter transportation in Saskatchewan.* Canadian Journal of Animal Science 90 (3): 321-330.

Knezacek, T. D. 2005. Broiler Transportation in Saskatchewan. M.Sc. thesis. Saskatoon, Saskatchewan: University of Saskatchewan, Department of Animal and Poultry Science.

Meyn. 2009. Meyn News. Issue 1-2009. Meyn Food Processing Technology B.V., The Netherlands. Available at: http://www.meyn.com/index.php/es/meynnews. Accessed 13 May 2012.

Minister of Justice. 2009. Health of Animals Regulations. C.R.C., c. 296. Minister of Justice, Canada. Available at: http://laws.justice.gc.ca/PDF/Regulation/C/C.R.C.,_c._296.pdf. Accessed 21 January 2010.

Mitchell, M.A. and P.J. Kettlewell. 1998. *Physiological stress and welfare of broiler chickens in transit: solutions not problems!* Poultry Science 77: 1803-1814.

Moureh, J., N. Menia and D. Flick. 2002. *Numerical and experimental study of airflow in a typical refrigerated truck configuration loaded with pallets*. Computers and Electronics in Agriculture 34 (Issues 1-3): 25-42.

Pawar, S. R., J. M. Cimbala, E. F. Wheeler and D. V. Lindberg. 2007. *Analysis of Poultry House Ventilation Using Computational Fluid Dynamics.* Transactions of the ASABE 50(4): 1373-1382.

Pedersen, S. and M. G. Thomsen. 2000. *Heat and Moisture Production of Broilers kept on Straw Bedding*. J. agri. Engng. Res. 75: 177-187.

Peer system. 2006. The chicken-friendly transport system (video clips). Peer system B.V., The Netherlands.

Quinn, A. D. and C.J. Baker. 1997. *An investigation of the ventilation of a day-old chick transport vehicle*. Journal of Wind Engineering and Industrial Aerodynamics 67&68: 305-311.

Ritz, C. W., A. B. Webster and M. Czarick III. 2005. *Evaluation of hot weather thermal environment and incidence of mortality associated with broiler live haul*. Journal of Applied Poultry Research 14 (3): 594-602.

Roslin Institute. 2000. Concept 2000: a New Generation of Poultry Transport Vehicle. Annual Report 1998-1999, Roslin Institute of the University of Edinburgh, Scotland, UK Available at: http://epublications.roslin.ac.uk/9899annrep/annrep9899.html. Accessed 23 January 2010.

Sallvik K. and S. Pedersen. 1999. Animal Heat and Moisture Production. In CIGR handbook of agricultural engineering, vol. II, animal production and aquacultural engineering. Eds. E. H. Bartali, A. Jongebreur, D. Moffitt and F. Wheaton, Ch. 2.2: 41-54. St Joseph, MI: American Society of Agricultural Engineers.

Saraz, J. A. O., K. S. Rocha, I. de F. F. Tinôco, R. S. Gates, L. B. Mendes, O. L. Z. Marin, and F. A. Damasceno. 2011. Use of CFD modeling for determination of ammonia emission in non-insulated poultry houses with natural ventilation. Paper number 1110781, 2011 ASAE Annual Meeting.

Saraz, J. A. O., F. A. Damasceno, R. S. Gates, K. S. Rocha, I. de F. F. Tinôco and O. L. Z. Marin. 2010. 3D-CFD Modeling of a Typical Uninsulated and Internal Misting Tunnel

Ventilated Brazilian Poultry House. Paper number 1009150, 2010 ASAE Annual Meeting.

Seo, I.-H., I.-B. Lee, P.-W. Chang, H.-S. Hwang, S.-W. Hong and S.-Y. Lee. 2006. Study on Ventilation System of Naturally ventilated Broiler House by Aerodynamic approach. Paper number 064013, 2006 ASAE Annual Meeting.

Vecerek, V., S. Grbalova, E. Voslarova, B. Janackova, and M. Malena. 2006. *Effects of travel distance and the season of the year on death rates of broilers transported to poultry processing plants.* Poultry Science 85 (11): 1881-1884.

Vieira, F. M. C., I. J. O. Silva, J. A. D. Barbosa Filho, A. M. C. Vieira and D. M. Broom. 2011. *Preslaughter mortality of broilers in relation to lairage and season in a subtropical climate.* Poultry Science 90 (10): 2127-2133.

Vieira, F. M. C., I. J. O. da Silva, J. A. D. B. Filho and A. M. C. Vieira. 2010. *Productive losses on broiler preslaughter operations: effects of the distance from farms to abattoirs and of lairage time in a climatized holding area.* Revista Brasileira De Zootecnia 39 (11): 2471-2476.

Wark, Kenneth. 1988. Thermodynamics, 5th edition. McGraw-Hill, Inc. New York.

Warriss, P. D., A. Pagazaurtundua and S. N. Brown. 2005. *Relationship between maximum daily temperature and mortality of broiler chickens during transport and lairage.* British Poultry Science 46 (6): 647-651.

Watts, J.M., L. J. Graff, M. L. Strawford, T. G. Crowe, N. A. Burlinguette, H. L. Classen , and P. J. Shand. 2011. *Heat and moisture production by broilers during simulated cold weather transport*. Poultry Science 90: 1890–1899.

Webster, A.J.F., A. Tuddenham, C.A. Saville and G.B. Scott. 1993. *Thermal stress on chickens in transit.* British Poultry Science 34: 267-277.

Yalçin, S. and H. C. Güler. 2012. *Interaction of transport distance and body weight on treslaughter stress and breast meat quality of broilers*. British Poultry Science 53(2): 175-182.

APPENDIX A - EQUATIONS TO CALCULATE HEAT AND MOISTURE PRODUCTION RATES OF POULTRY

According to CIGR (2002), the total heat production for poultry can be calculated using

$$\Phi_{tot(hpu)} = 1000 + 20 \times (20 - T) \tag{A.1}$$

where

$\Phi_{tot(hpu)}$ = total heat production per hpu (W/hpu) and

T = temperature (ºC).

The unit "hpu" stands for "heat production unit", it is defined as the quantity of animals producing 1000 W of total heat at 20°C (Pedersen and Thomsen, 2000).

The sensible heat production for broilers on litter can be determined as follows based on CIGR (2002),

$$\Phi_{s(hpu)} = 0.61\Phi_{tot(hpu)} - 0.228 \times T^2 \tag{A.2}$$

where

$\Phi_{s(hpu)}$ = sensible heat production per hpu (W/hpu),

$\Phi_{tot(hpu)}$ = total heat production per hpu (W/hpu) and

T = temperature (ºC).

At 20°C, CIGR (2002) recommends this equation to calculate the total heat production for broilers based on weight

$$\Phi_{tot(mass)} = 10.62 m^{0.75} \quad for \quad T = 20^{\circ}C \tag{A.3}$$

where

$\Phi_{tot(mass)}$ = total heat production in the barn based on mass (W) and

m = animal weight (kg).

According to Sallvik and Pedersen (1999), the moisture dissipation can be computed using

$$F = \frac{\Phi_l}{r} \tag{A.4}$$

where

F = moisture dissipation (g/h),

Φ_l = latent heat production (W) and

r = 0.680 for water at 20ºC (W-h/g).

Sallvik K. and S. Pedersen (1999) does not provide a value for r for temperatures different from 20°C. A closer examination indicates r is related to the enthalpy of vaporization. The enthalpy of vaporization is also known as latent heat of vaporization (h_{fg}), it represents the amount of energy required to vaporize a unit mass of saturated water at a given temperature or pressure (Wark, 1988). These values, as a function of temperature, are listed in steam tables. For saturated water at 20ºC, h_{fg} is equal to 2454.1 kJ/kg or 2454.1 J/g. If 2454.1 J/g is divided by 3600s/h, a result of 0.6817 is obtained. This value is very close to the r-value of 0.680 W-h/g given by Sallvik K. and S. Pedersen (1999).

Therefore, the above equation can be modified to the following to calculate the moisture dissipation, as a function of temperature,

$$F = \frac{\Phi_l}{r} = \frac{\Phi_l}{h_{fg}/3600} \tag{A.5}$$

where

F = moisture dissipation (g/h),

Φ_l = latent heat production (W),

r = 0.680 for water at 20ºC (W-h/g) and

h_{fg} = enthalpy of vaporization for saturated water as function of temperature (kJ/kg).

Moisture source in CFD simulations is usually expressed in kg/s-m^3, the above equation can be modified to obtain moisture dissipation in kg/s,

$$F^* = \frac{\Phi_l}{1000 h_{fg}} = \frac{\Phi_{tot} - \Phi_s}{1000 h_{fg}} \tag{A.6}$$

where

F^* = modified moisture dissipation (kg/s),

Φ_l = latent heat production (W),

h_{fg} = enthalpy of vaporization for saturated water as function of temperature (kJ/kg),

Φ_{tot} = total heat production (W) and

Φ_s = sensible heat production (W).

EXAMPLE OF CALCULATIONS

The following example demonstrate the use of above equation by calculating the heat and moisture production for 1 bird at 30°C.

According to equation A.3, for a broiler with a mass of m = 1.75 kg, the total heat at 20°C is

$$\Phi_{tot\,(mass)} = 10.62\, m^{0.75} = 10.62\ (1.75)^{0.75} = 16.16 \text{ W (for one bird).}$$

The number of birds producing 1000 W total heat at 20°C is

$$1000 \ / \Phi_{tot\,(mass)} = 61.9 \text{ birds.}$$

From equation A.1, the total heat production in W/hpu is

$$\Phi_{tot\,(hpu)} = 1000 + 20 \times (20 - T) = 1000 + 20 \times (-10) = 800\text{W/hpu.}$$

From equation A.2, the sensible heat production in W/hpu is

$$\Phi_{s\,(hpu)} = 0.61\Phi_{tot\,(hpu)} - 0.228 \times T^2 = 0.61\,(800) - 0.228 \times (30^2) = 282.8\text{W/hpu.}$$

Both $\Phi_{tot\,(hpu)}$ and $\Phi_{s\,(hpu)}$ are expressed as per unit of hpu. For m=1.75kg/bird, these heat production values are for 61.9 birds.

At 30°C, the total heat per bird is

$$\Phi_{tot\ at\,30} = 800\,/\,61.89 = 12.9\text{ W.}$$

At 30°C, the sensible heat per bird is

$$\Phi_{s\ at\,30} = 282.8\,/\,61.89 = 4.6\text{W.}$$

At 30°C, h_{fg} = 2 430.5 kJ/kg (Wark, 1988) and the moisture dissipation rate is

$$F^* = \frac{\Phi_l}{1000\,h_{fg}} = \frac{\Phi_{tot\ at\,30} - \Phi_{s\ at\,30}}{1000\,h_{fg}} = \frac{12.93 - 4.57}{1000 \times 2430.5} = 3.44 \times 10^{-6}\ \text{kg/s.}$$

In summary, the heat and moisture production rates for one 1.75-kg bird at 30°C are

$$\boxed{\begin{array}{c}\text{Heat production rate} = \Phi_{s\ at\,30} = 4.6\text{W} \\[1em] \text{Moisture production rate} = F^* = 3.44 \times 10^{-6}\ \text{kg/s}\end{array}}$$

The same procedure can be used to compute heat and moisture production rates at other temperatures or bird weights.

APPENDIX B – DESIGNS OF DIFFERENT POULTRY TRANSPORT SYSTEMS

53-FT SEMI-TRAILER

a b c

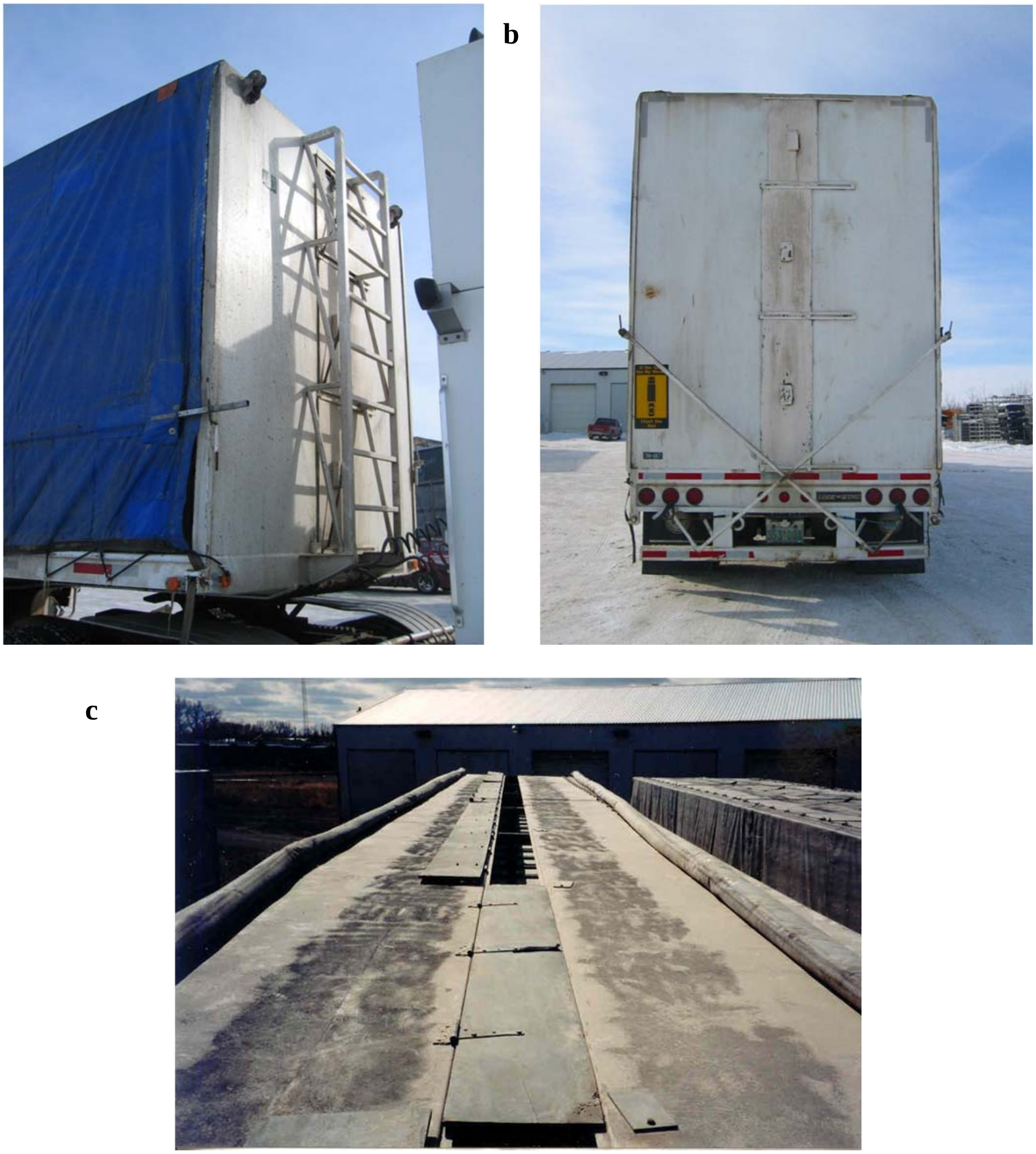

Figure B.1. Ventilation openings located along centerlines of the (a) headboard, (b) tailboard and (c) roof of the 53-ft semi-trailer.

Figure B.2. A 53-ft semi-trailer with its vertical support beams, ventilation vents on walls and roof, and pyramidal floor guides for module alignment.

B-TRAIN TRAILERS

Figure B.3. Side view of a B-train with a capacity to transport 30 modules.

Figure B.4. B-train covered with retractable tarpaulins.

Figure B.5. Roof vents on a B-train.

Figure B.6.Ventilation openings on the headboard of a B-train shown as (a) closed or (b) open. The vent configuration is secured by a butterfly nut and long screw (c). View from the tailboard when the roof is raised.

Figure B.7. Side view of the rear trailer in a B-train when the roof is raised.

Figure B.8. An empty B-train with a raised roof. No vertical support beams exist on the B-train.

Figure B.9. Metal guides are welded on the floor to assist forklift driver to align modules during loading.

CONCEPT 2000 TRAILER

Figure B.10. Concept 2000 with a hauling capacity of 22 modules (Roslin Institute, 2000).

Figure B.11. Concept 2000 with its side curtains lowered (BBSRC 2002).

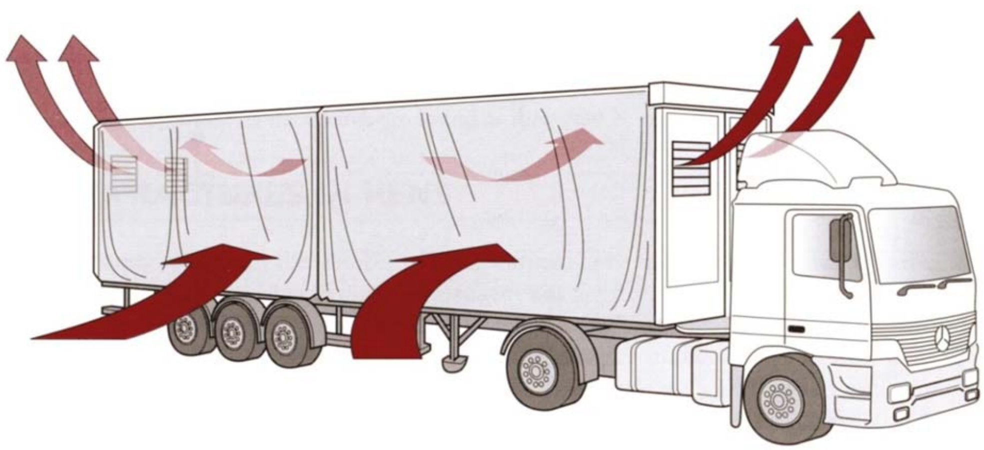

Figure B.12. Air flow regime in Concept 2000 (Haslam, 2008).

Figure B.13. Ventilation fans and system controller inside the headboard of Concept 2000 (Roslin Institute, 2000).

UNIVERSITY OF SASKATCHEWAN (U OF S) EXPERIMENTAL TRAILER

Figure B.14. Experimental poultry trailer constructed by University of Saskatchewan.

Figure B.15. Front view of the U of S experimental poultry trailer.

Figure B.16. Rear view of the U of S experimental poultry trailer.

Figure B.17. Rear fans in operation inside the U of S experimental poultry trailer.

Figure B.18. Roof vents on the U of S experimental poultry trailer.

Figure B.19. View from the tailboard when the roof is raised.

Figure B.20. View from the side when the roof is raised in the loading area.

Figure B.21. Sealing of the loading area with side curtain.

Figure B.22. The left-front end of the experimental trailer.

Figure B.23. The left-rear end of the experimental trailer.

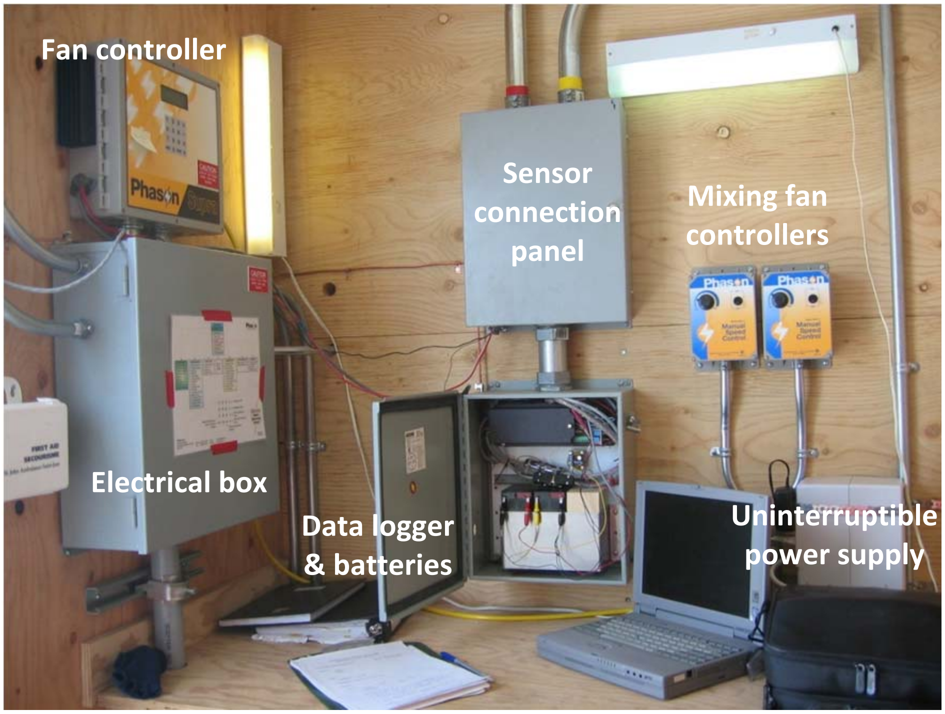

Figure B.24. Electrical and electronic equipment inside the instrumentation room.

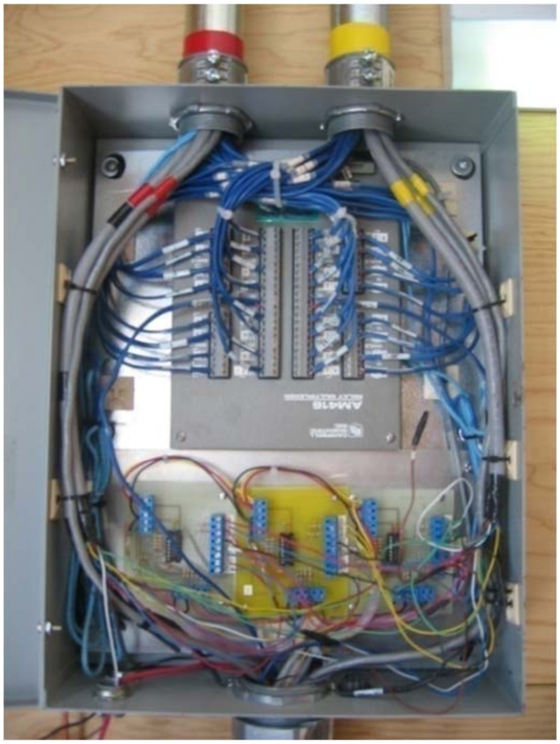

Figure B.25. Thermocouples and relative humidity sensors are connected to two types of multiplexers inside the sensor connection panel.

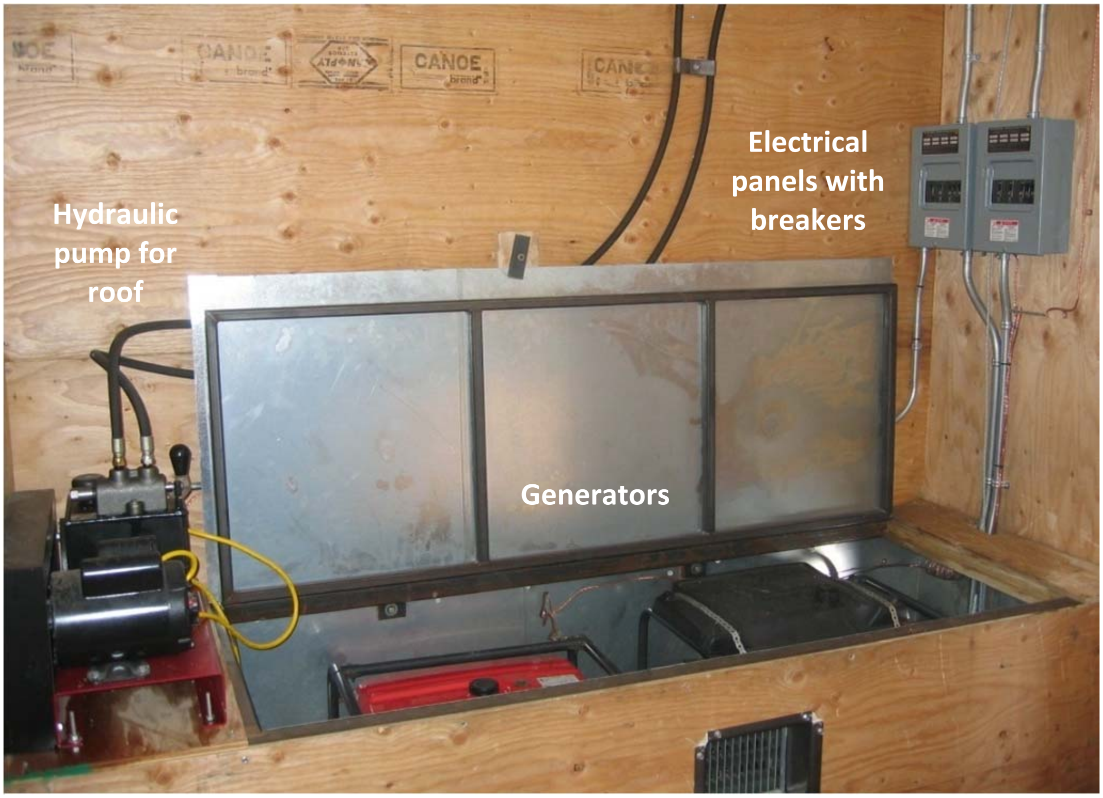

Figure B.26. Hydraulic pump for the mechanical roof (left) and two generators to supply power for the electrical equipment (housed inside the compartment).

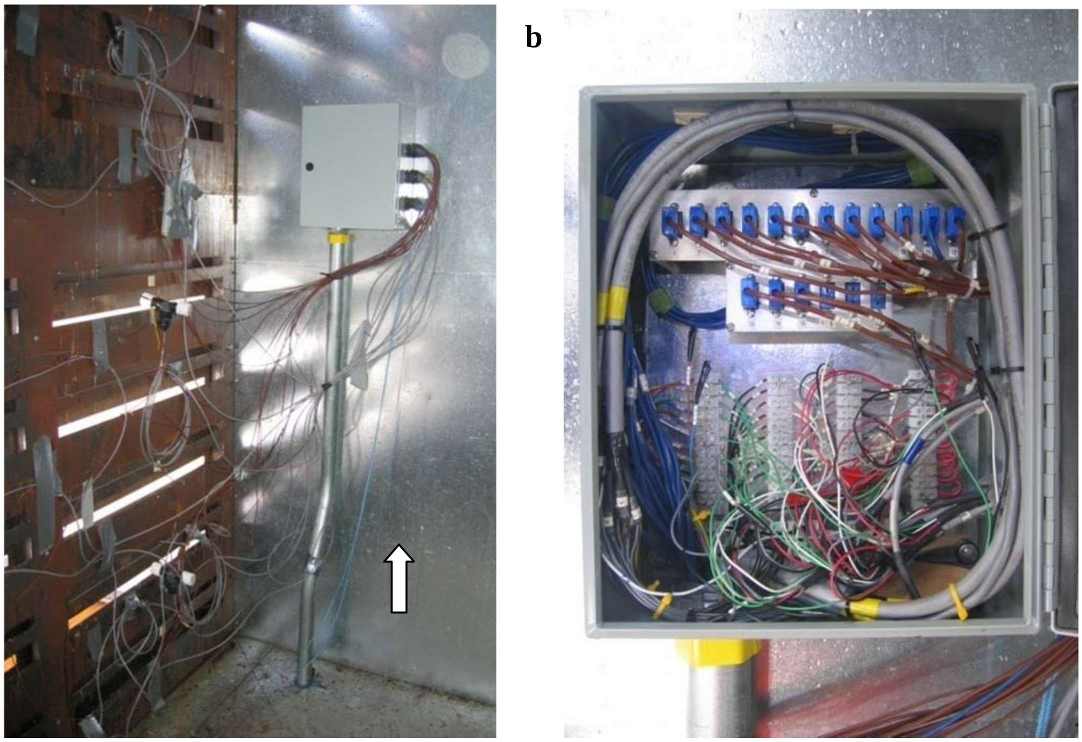

Figure B.27. Sensors' extension wires coming from the instrumentation room to (a) the junction box located near the front diffusers. The use of quick disconnect connectors facilitate servicing of sensors as shown inside junction box (b).

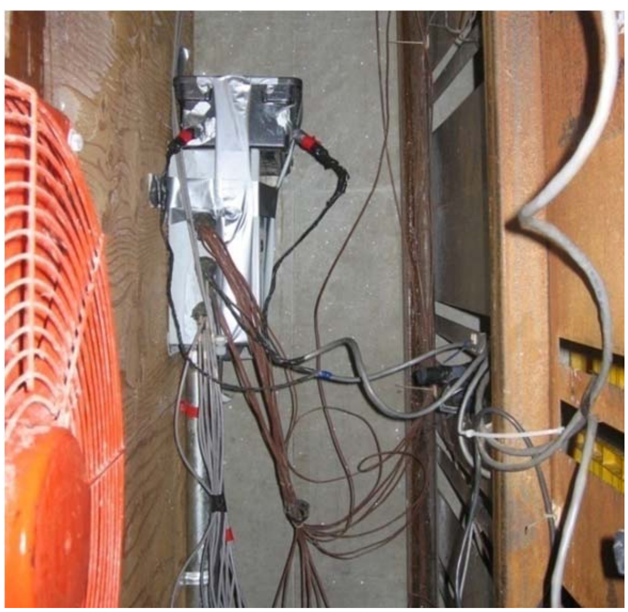

Figure B.28. A second junction box is located near the diffuser. Extra portable batteries are installed during field tests to power anemometers.

Figure B.29. Anemometers are installed just prior to field tests to avoid damage.

Figure B.30. A sets of 2 diffusers are installed at the load inlet, in off-set manner, to avoid water damaging sensors during cleaning.

Figure B.31. Rear diffuser with thermocouples and relative humidity sensors permanently installed on it.

Figure B.32. RTD temperature sensor at the rear diffuser to control the operation of exhaust fans.

Figure B.33. One of the propane heater in operation as viewed from the inside of the trailer.

Figure B.34. Data logger mounted on the mirror of the tractor to monitor ambient conditions.

Figure B.35. Data logger installed inside the drawer to monitor conditions next to the broilers.

APPENDIX C - ON-BOARD SENSOR LOCATIONS AND DIFFUSER SCREEN DIMENSIONS

The following figures illustrates the positions of on-board temperature and relative humidity sensors on the diffuser screens. They also shows the locations of the 25.4-mm (1-in) and 50.8-mm (2-in) opening slots on the diffuser screens.

x denote locations of temperature sensors

▲ denote locations of relative humidity sensors

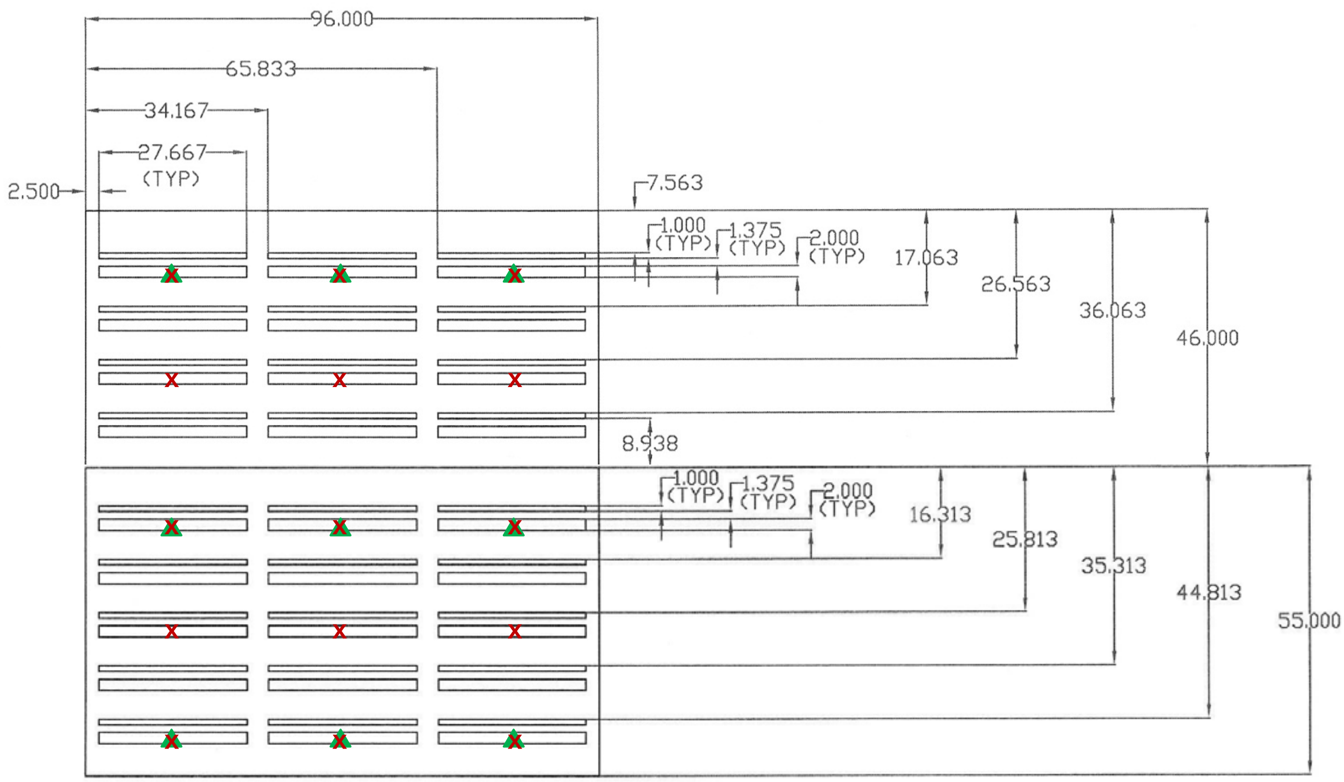

Figure C.1. Sensor locations and dimensions of diffuser screen 1.

x denote locations of temperature sensors (for diffuser screen 3 only)

▲ denote locations of relative-humidity sensors (for diffuser screen 3 only)

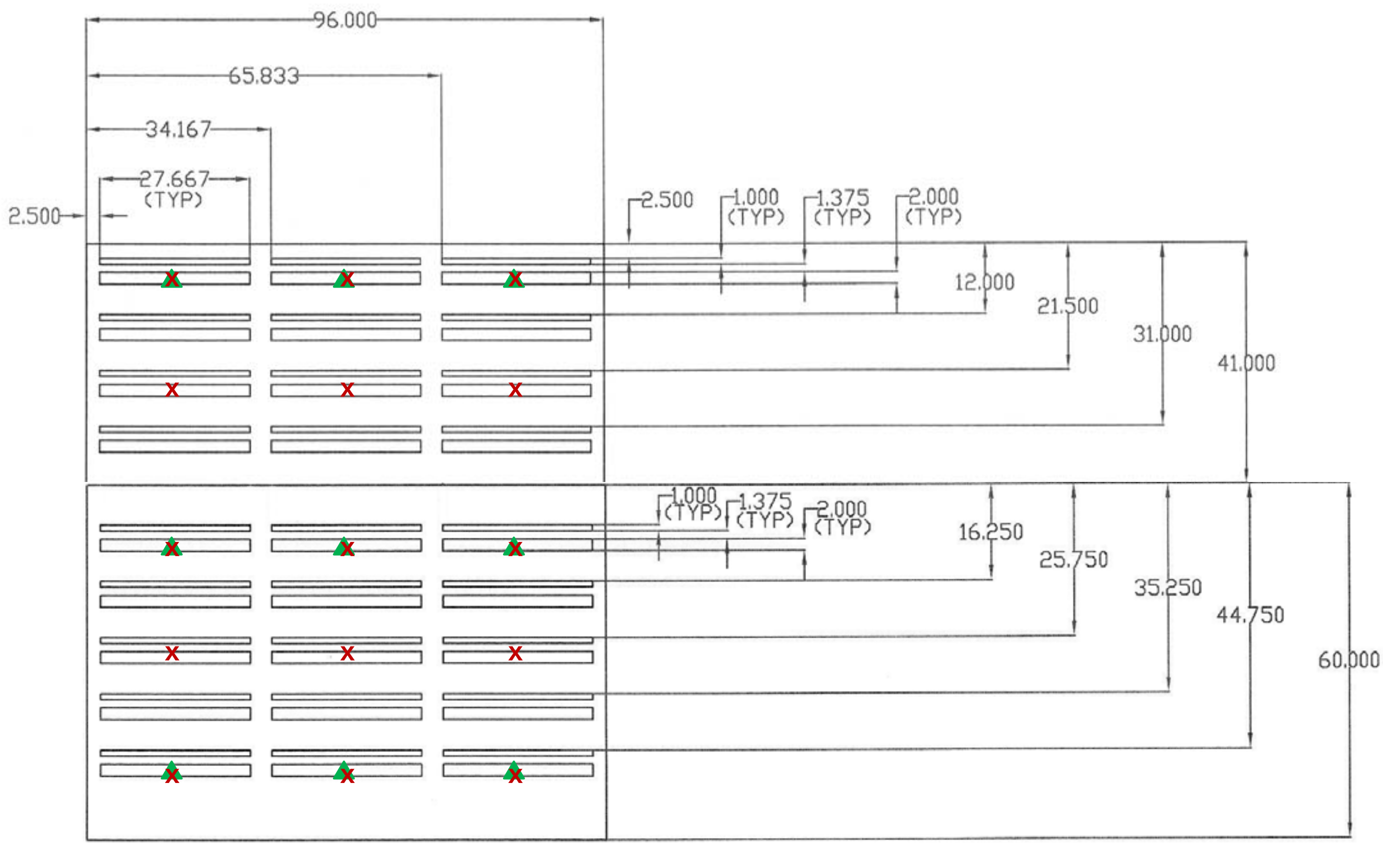

Figure C.2. Sensor locations and dimensions of diffuser screens 2 and 3.

APPENDIX D - CONVERSIONS BETWEEN RELATIVE HUMIDITY AND HUMIDITY RATIO

According to ASHRAE (2005), relative humidity can be converted to humidity ratio by using equations D.1 to D.3. First of all, the saturation pressure of water vapour in the absence of air has to be calculated. For temperature of 0 to 200ºC, this equation is recommended

$$\ln p_{ws} = C_8 / T + C_9 + C_{10} T + C_{11} T^2 + C_{12} T^3 + C_{13} \ln T \qquad \text{(D.1)}$$

where

C_8 = constant = -5.800 220 6 E+03,

C_9 = constant = 1.391 499 3 E+00,

C_{10} = constant = -4.864 023 9 E-02,

C_{11} = constant = 4.176 476 8 E-05,

C_{12} = constant = -1.445 209 3 E-08,

C_{13} = constant = 6.545 967 3 E+00,

p_{ws} = pressure of saturated pure water (Pa) ≈ p_s (vapour pressure of water in moist air at saturation) and

T = absolute temperature (K).

The humidity ratio is also a function of the partial pressure of water vapour at constant temperature and pressure, it can be calculated using

$$p_w = \phi \, p_{ws} \qquad \text{(D.2)}$$

where

p_w = partial pressure of water vapour in moist air (Pa),

ϕ = relative humidity (in decimal point) and

p_{ws} = pressure of saturated pure water (Pa).

Finally, the humidity ratio can be calculated using

$$W = 0.62198 \frac{p_w}{p - p_w} \tag{D.3}$$

where

W = humidity ratio (in decimal point),

p = total pressure of moist air (Pa) and

p_w = partial pressure of water vapour in moist air (Pa).

In the present analysis, the total pressure of moist air (p) was assumed to be equal to the atmospheric pressure at the Saskatoon Diefenbaker International airport (also called "station pressure"). According to ASHRAE (2005), the atmospheric pressure can be calculated using

$$p_{atm} = 101.325 \ (1 - 2.25577 \times 10^{-5} Z)^{5.2559} \tag{D.4}$$

where

p_{atm} = atmospheric pressure assumed equal to total pressure of moist air p (Pa) and

Z = altitude (m).

According to Environment Canada (2005), the altitude of the Saskatoon Diefenbaker International airport is 504.10 m. Using this value for Z, it yields an atmospheric pressure of 95.41 Pa based on equation D.4.

For each logger, a humidity ratio can be computed at a specific time using its corresponding T and ϕ values. In the data analysis, after calculating humidity ratio for an x time interval, a time-averaged $\overline{W}$ can be calculated using

$$\overline{W} = \frac{\sum_{t=1}^{x} W_t}{x} \tag{D.5}$$

where

$\overline{W}$	=	time-averaged humidity ratio (in decimal point),
x	=	number of temporal data,
t	=	index for time and
W_t	=	humidity ratio at time t (in decimal point).

Furthermore, a time-average temperature can be computed using

$$\overline{T} = \frac{\sum_{t=1}^{x} T_t}{x} \tag{D.6}$$

where

$\overline{T}$	=	time-averaged temperature (ºC),
x	=	number of temporal data,
t	=	index for time and
T_t	=	temperature at time t (ºC).

The $\overline{T}$ and $\overline{W}$ then be used to calculate the RH^* by following a number of steps. First of all, the pressure of saturated pure water (p_{ws}) has to be determined using equation D.1 and $\overline{T}$. Secondly, by manipulating equation D.3, the partial pressure of water vapour in moist air (p_w) can be calculated using

$$p_w = \frac{\overline{W}\ p}{(\overline{W} + 0.62198)} \tag{D.7}$$

where

p_w = partial pressure of water vapour in moist air (Pa),

$\overline{W}$ = time-averaged humidity ratio (in decimal point) and

p = total pressure of moist air assumed equal to atmospheric pressure (Pa).

The relative humidity can then be determined by modifying equation D.2 to

$$\phi = \frac{p_w}{p_{ws}} \tag{D.8}$$

where

ϕ = relative humidity (in decimal point),

p_w = partial pressure of water vapour in moist air (Pa) and

p_{ws} = pressure of saturated pure water (Pa).

Finally, RH^* can be calculated using

$$RH^* = \phi \times 100 \tag{D.9}$$

where

RH^* = representative relative humidity (%) and

ϕ = relative humidity (in decimal point).

Appendix E - $\Delta\bar{T}$ Temperature Profiles from Field Tests

Group 1 – One Fan

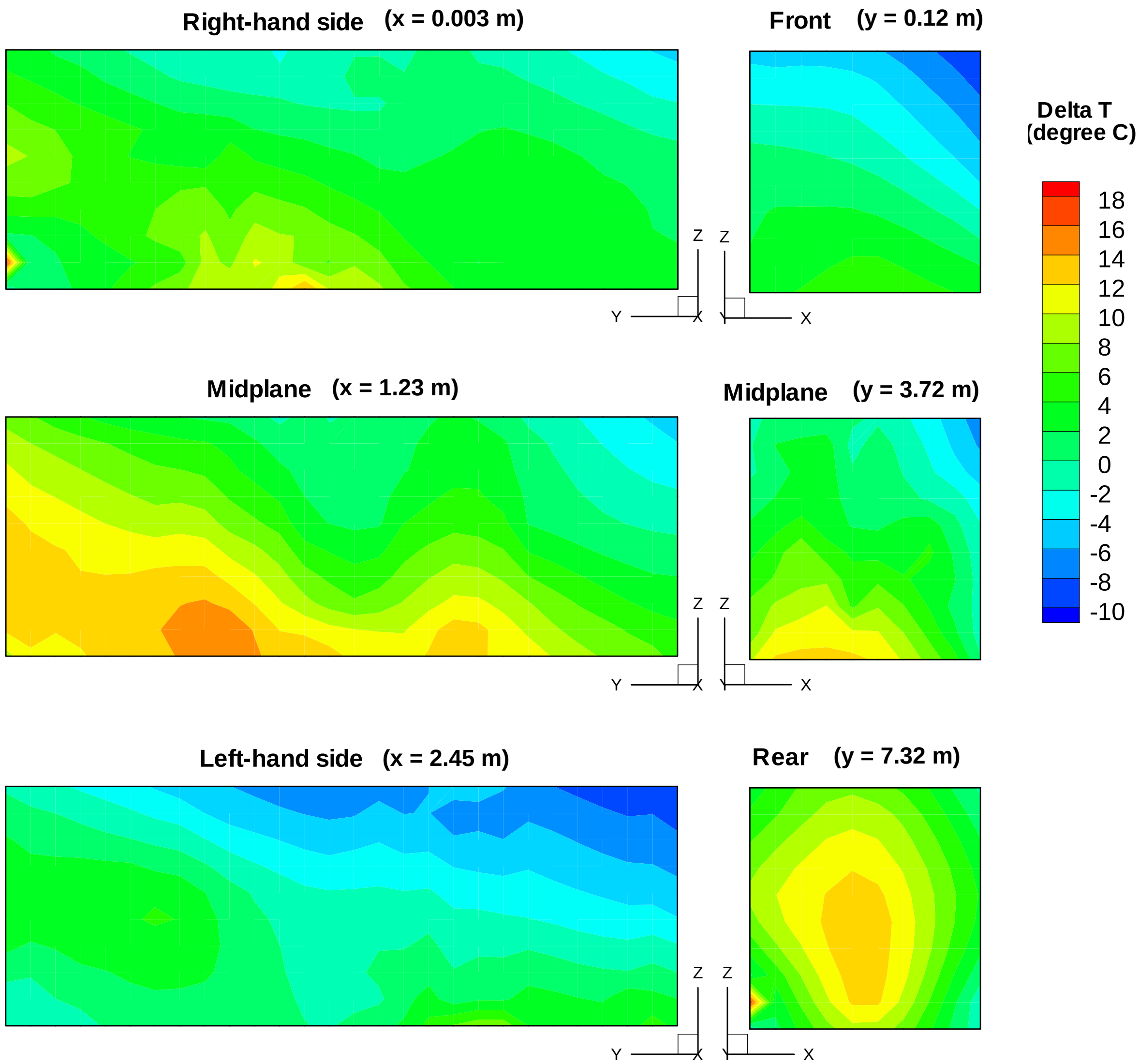

Data set #	8
Amb. T at Saskatoon airport, degree C	-11.90
Nb. fans used	1 (Btm)
Nb. heaters used	0
Inlet opening, %	60%
Date	4-Feb-05b

Figure E.1. Profiles of temperature gain in inlet air for data loggers $(\Delta\bar{T})$ of data set 8, the origin of the *x, y, z* axis (0,0,0) indicates the bottom-right front corner of the experimental trailer (viewed from the rear).

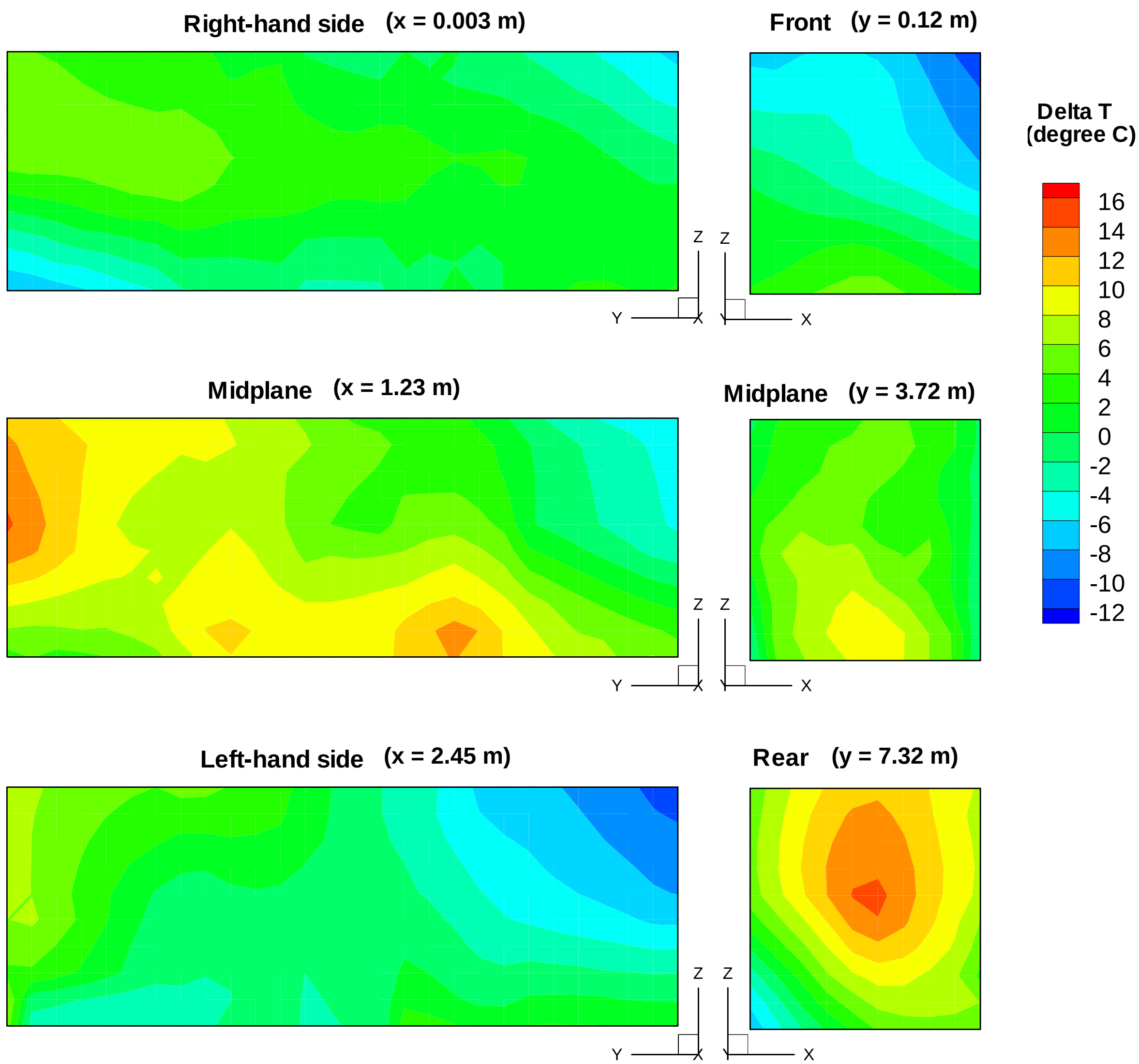

Data set #	3
Amb. T at Saskatoon airport, degree C	-17.10
Nb. fans used	1 (Btm)
Nb. heaters used	1 (Btm)
Inlet opening, %	50%
Date	15-Feb-05

Figure E.2. Profiles of temperature gain in inlet air for data loggers $\left(\Delta\overline{T}\right)$ of data set 3, the origin of the *x*, *y*, *z* axis (0,0,0) indicates the bottom-right front corner of the experimental trailer (viewed from the rear).

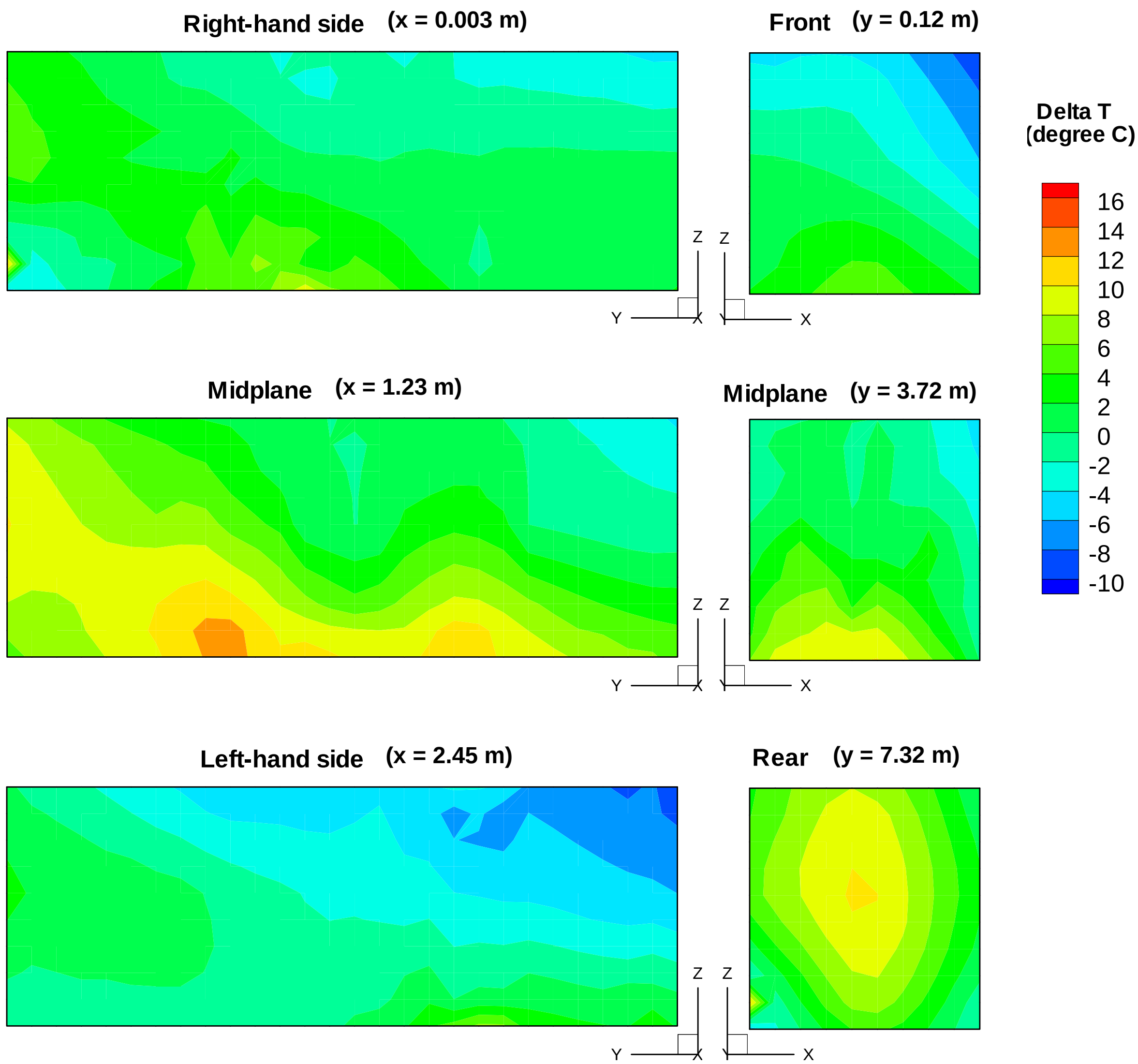

Data set #	7
Amb. T at Saskatoon airport, degree C	-9.80
Nb. fans used	1 (Btm)
Nb. heaters used	1 (Btm)
Inlet opening, %	60%
Date	4-Feb-05a

Figure E.3. Profiles of temperature gain in inlet air for data loggers $\left(\Delta \overline{T}\right)$ of data set 7, the origin of the *x*, *y*, *z* axis (0,0,0) indicates the bottom-right front corner of the experimental trailer (viewed from the rear).

GROUP 2 – TWO FANS

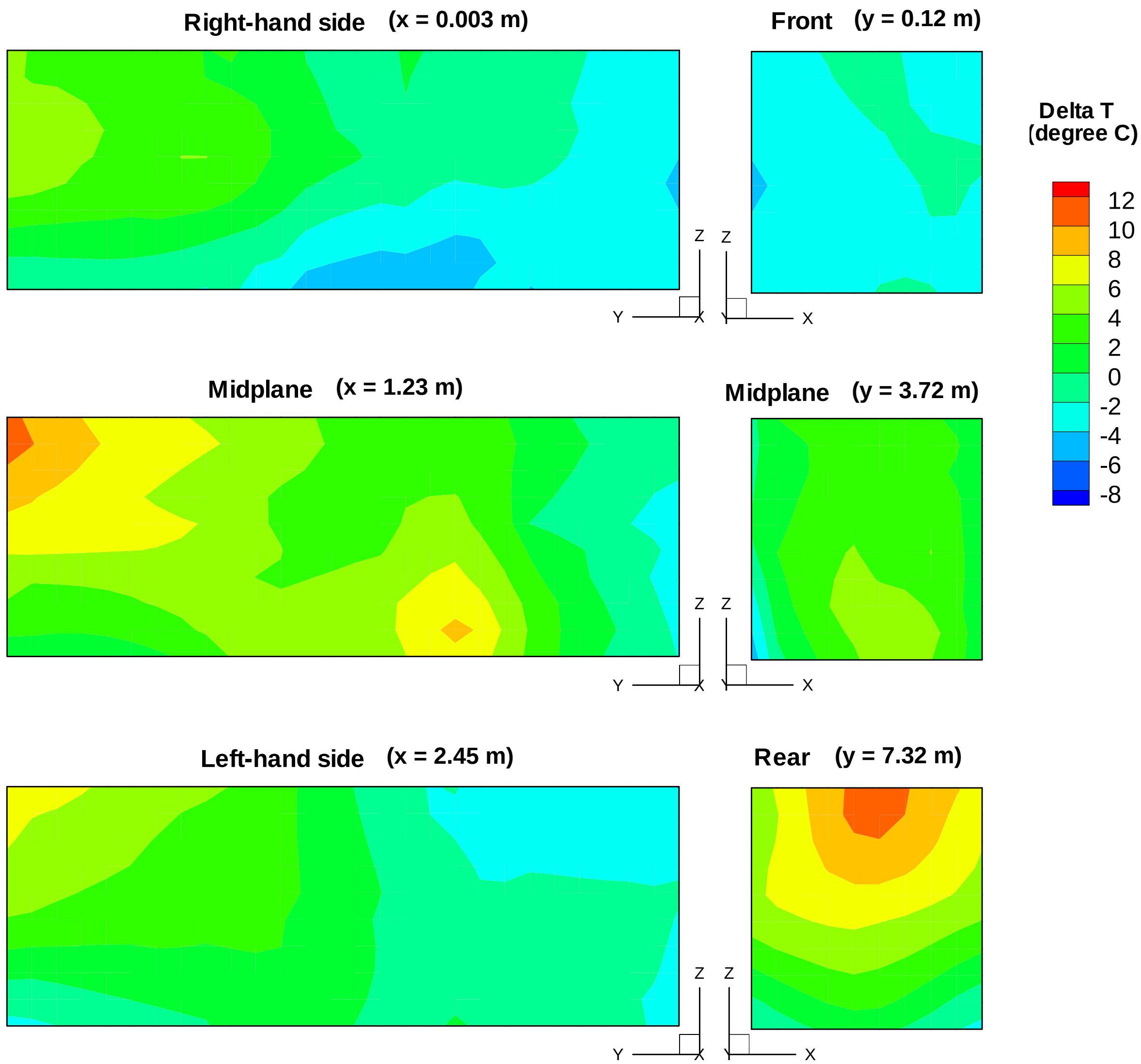

Data set #	1
Amb. T at Saskatoon airport, degree C	-15.43
Nb. fans used	2 (Btm & Mid)
Nb. heaters used	1 (Top)
Inlet opening, %	50%
Date	23-Feb-05a

Figure E.4. Profiles of temperature gain in inlet air for data loggers $\left(\Delta \overline{T}\right)$ of data set 1, the origin of the *x*, *y*, *z* axis (0,0,0) indicates the bottom-right front corner of the experimental trailer (viewed from the rear).

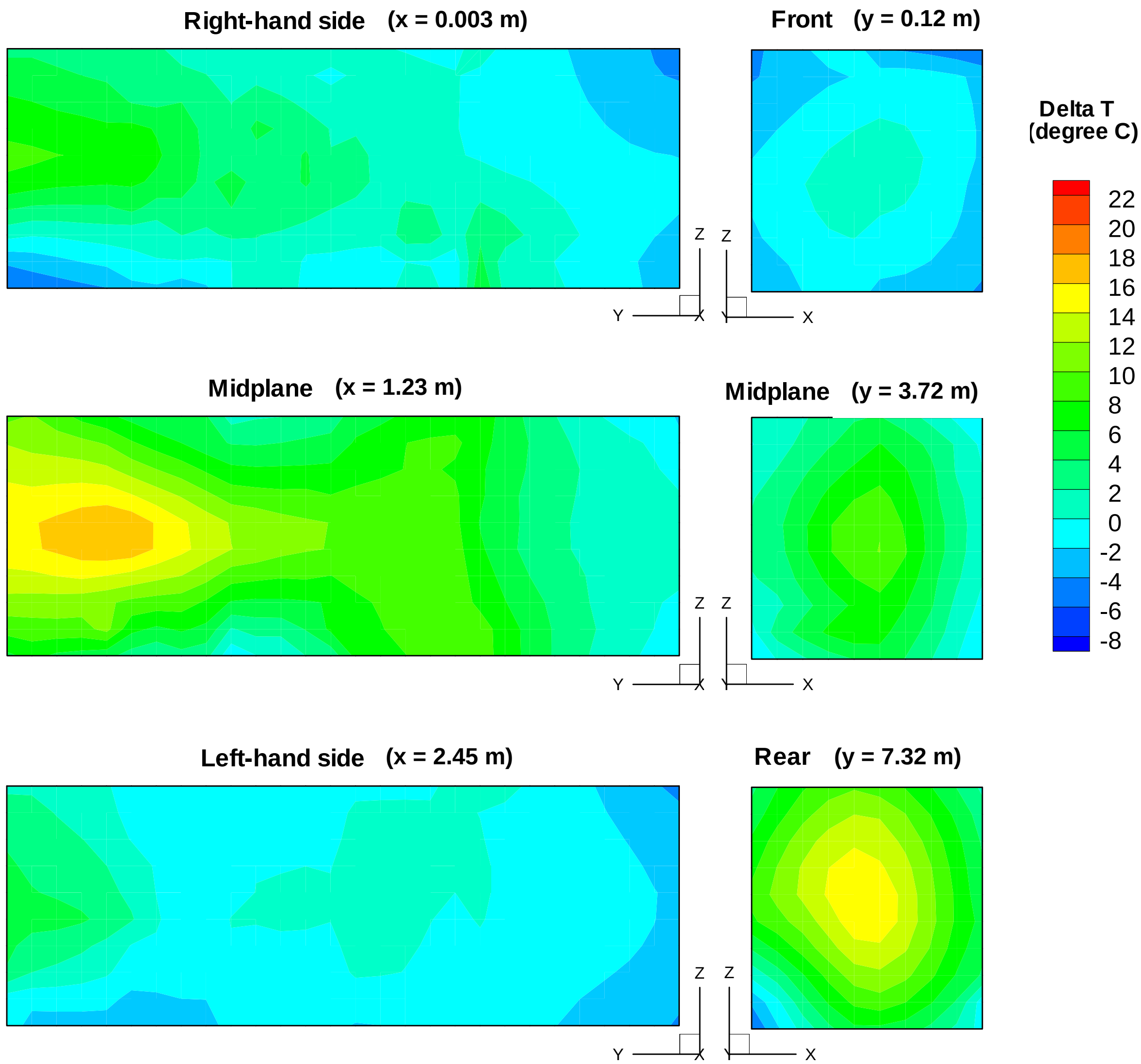

Data set #	9
Amb. T at Saskatoon airport, degree C	-16.47
Nb. fans used	2 (Btm & Mid)
Nb. heaters used	1 (Btm)
Inlet opening, %	50%
Date	24-March-05

Figure E.5. Profiles of temperature gain in inlet air for data loggers $\left(\Delta \overline{T}\right)$ of data set 9, the origin of the *x, y, z* axis (0,0,0) indicates the bottom-right front corner of the experimental trailer (viewed from the rear).

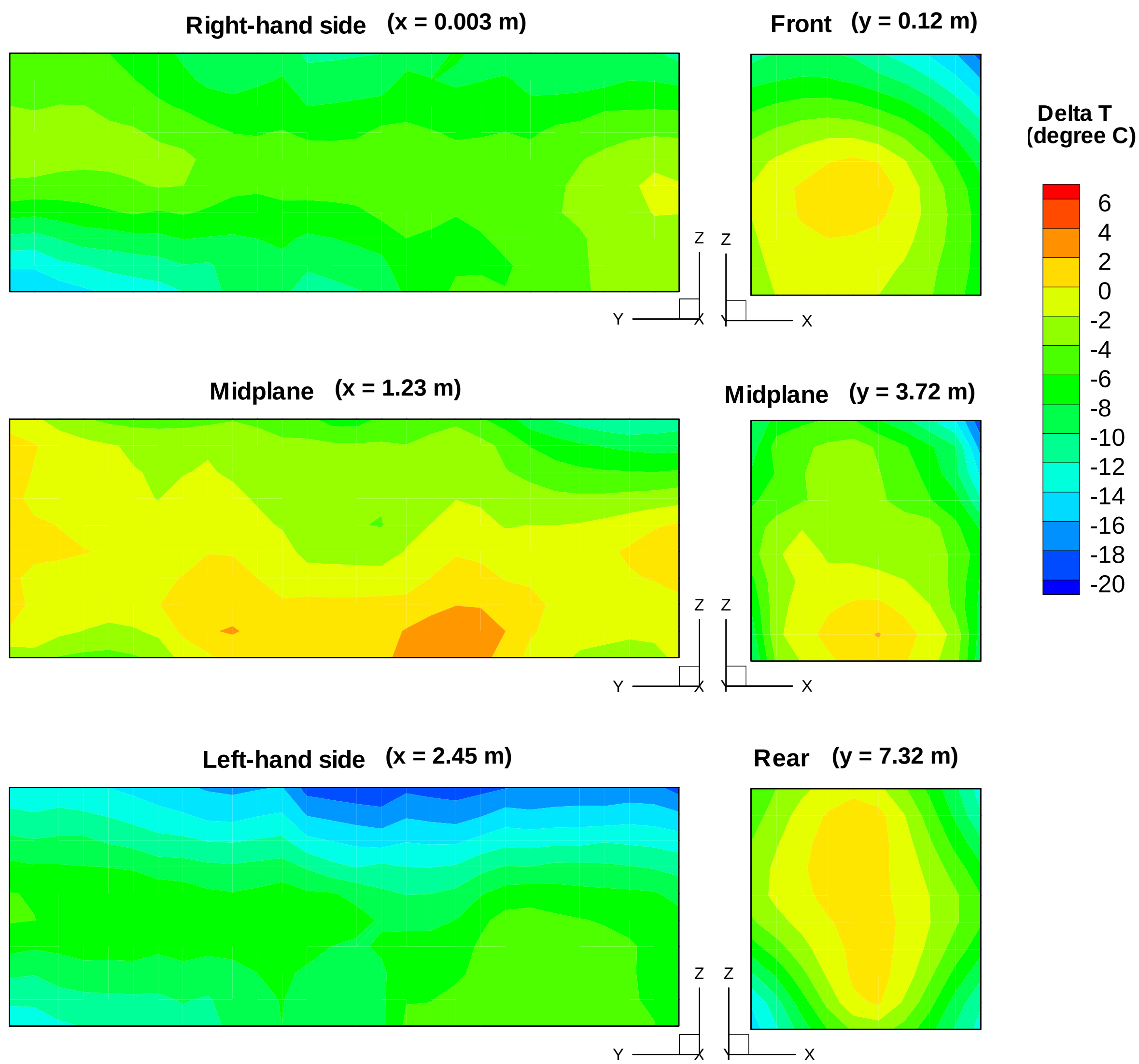

Data set #	4
Amb. T at Saskatoon airport, degree C	-15.45
Nb. fans used	2 (Btm & Mid)
Nb. heaters used	2 (Btm & Top)
Inlet opening, %	50%
Date	18-Feb-05

Figure E.6. Profiles of temperature gain in inlet air for data loggers $\left(\Delta\overline{T}\right)$ of data set 4, the origin of the *x, y, z* axis (0,0,0) indicates the bottom-right front corner of the experimental trailer (viewed from the rear).

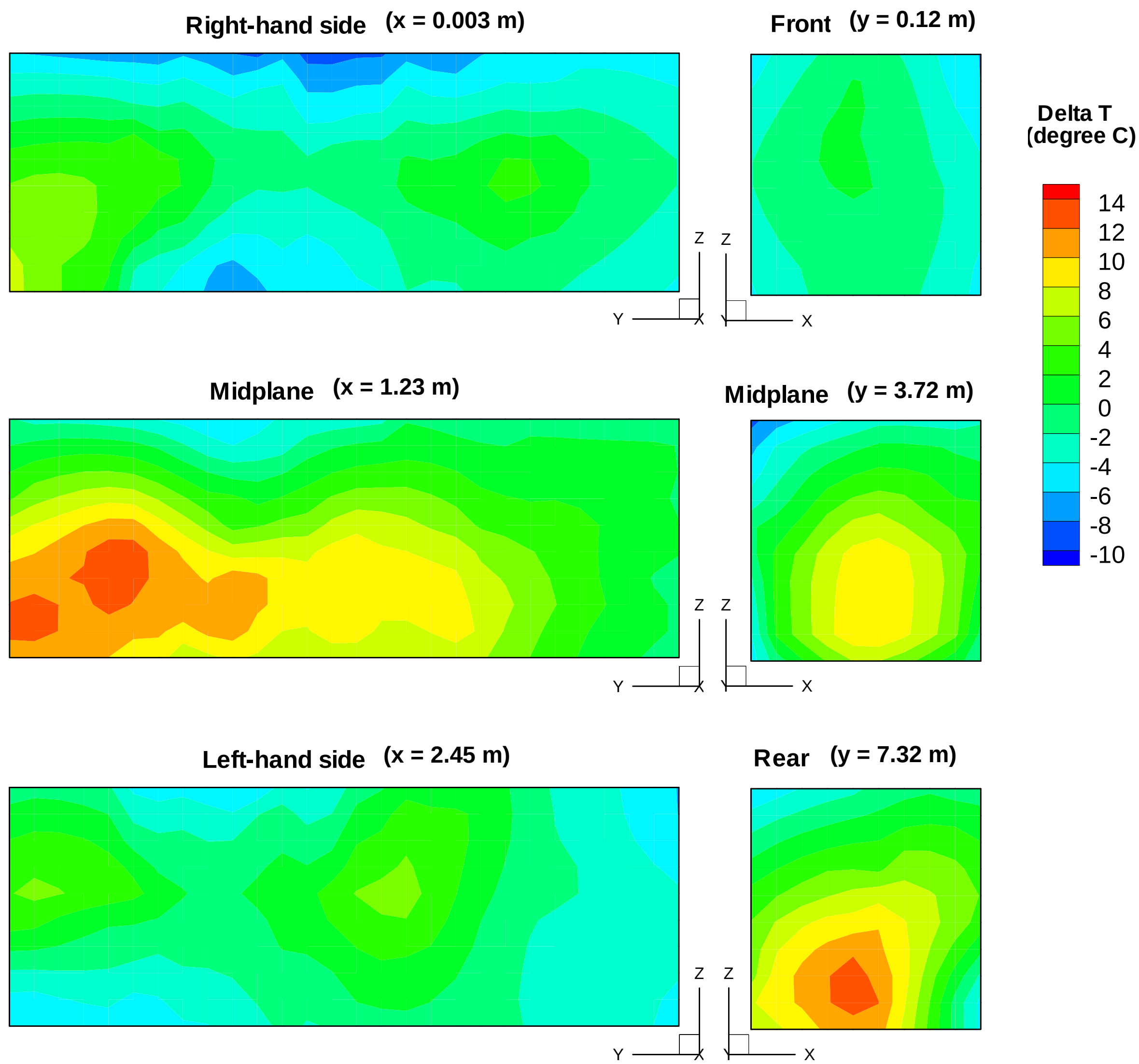

Data set #	**5**
Amb. T at Saskatoon airport, degree C	**-10.83**
Nb. fans used	**2 (Btm & Top)**
Nb. heaters used	**1 (Btm)**
Inlet opening, %	**50%**
Date	**17-Mar-05**

Figure E.7. Profiles of temperature gain in inlet air for data loggers $\left(\Delta\overline{T}\right)$ of data set 5, the origin of the *x*, *y*, *z* axis (0,0,0) indicates the bottom-right front corner of the experimental trailer (viewed from the rear).

GROUP 3 – THREE FANS

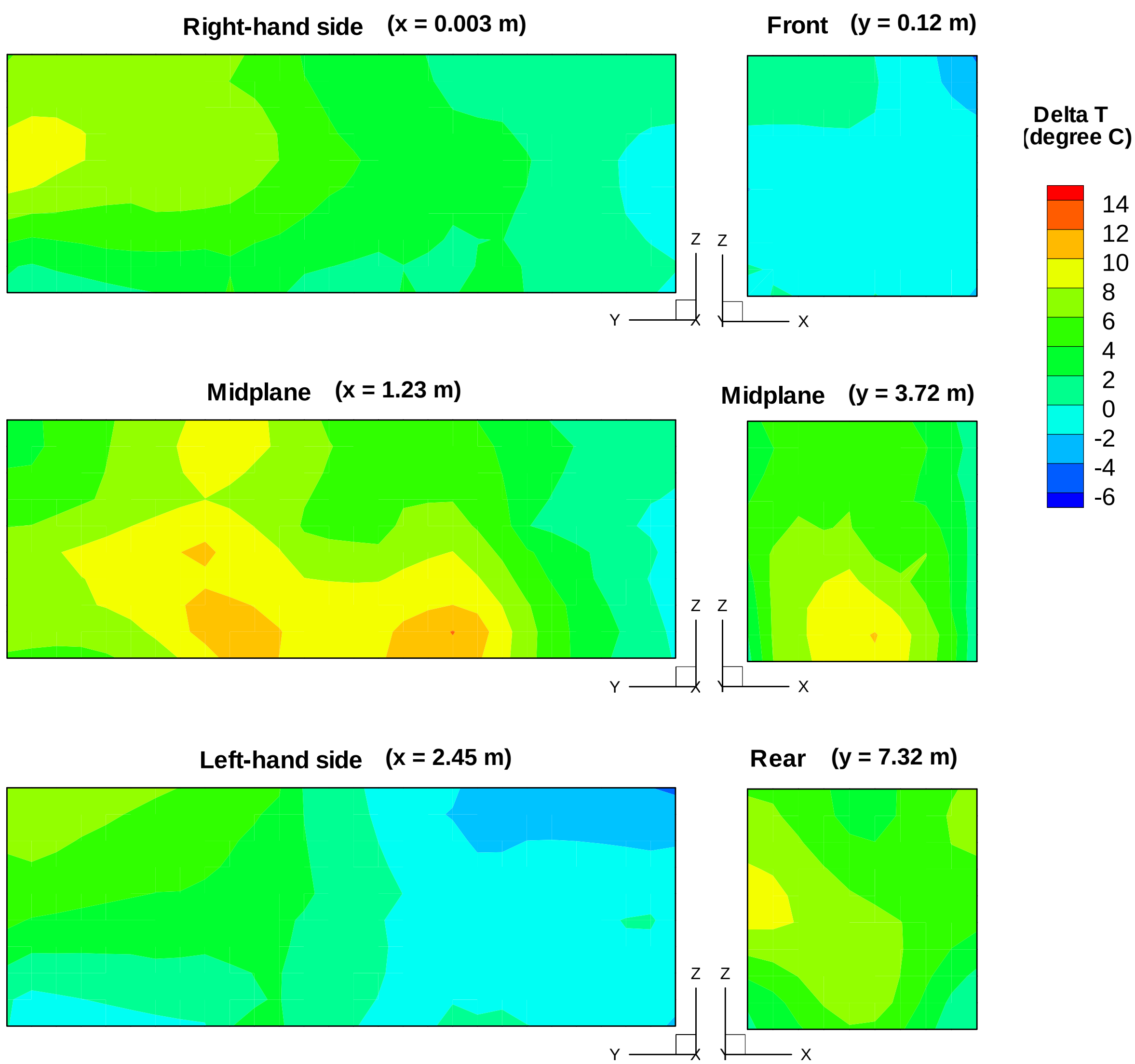

Data set #	2
Amb. T at Saskatoon airport, degree C	-13.15
Nb. fans used	3 (Btm, Mid & Top)
Nb. heaters used	1 (Btm)
Inlet opening, %	50%
Date	23-Feb-05b

Figure E.8. Profiles of temperature gain in inlet air for data loggers $(\Delta \overline{T})$ of data set 2, the origin of the *x, y, z* axis (0,0,0) indicates the bottom-right front corner of the experimental trailer (viewed from the rear).

APPENDIX F - *RH** HUMIDITY PROFILES FROM FIELD TESTS

GROUP 1 – ONE FAN

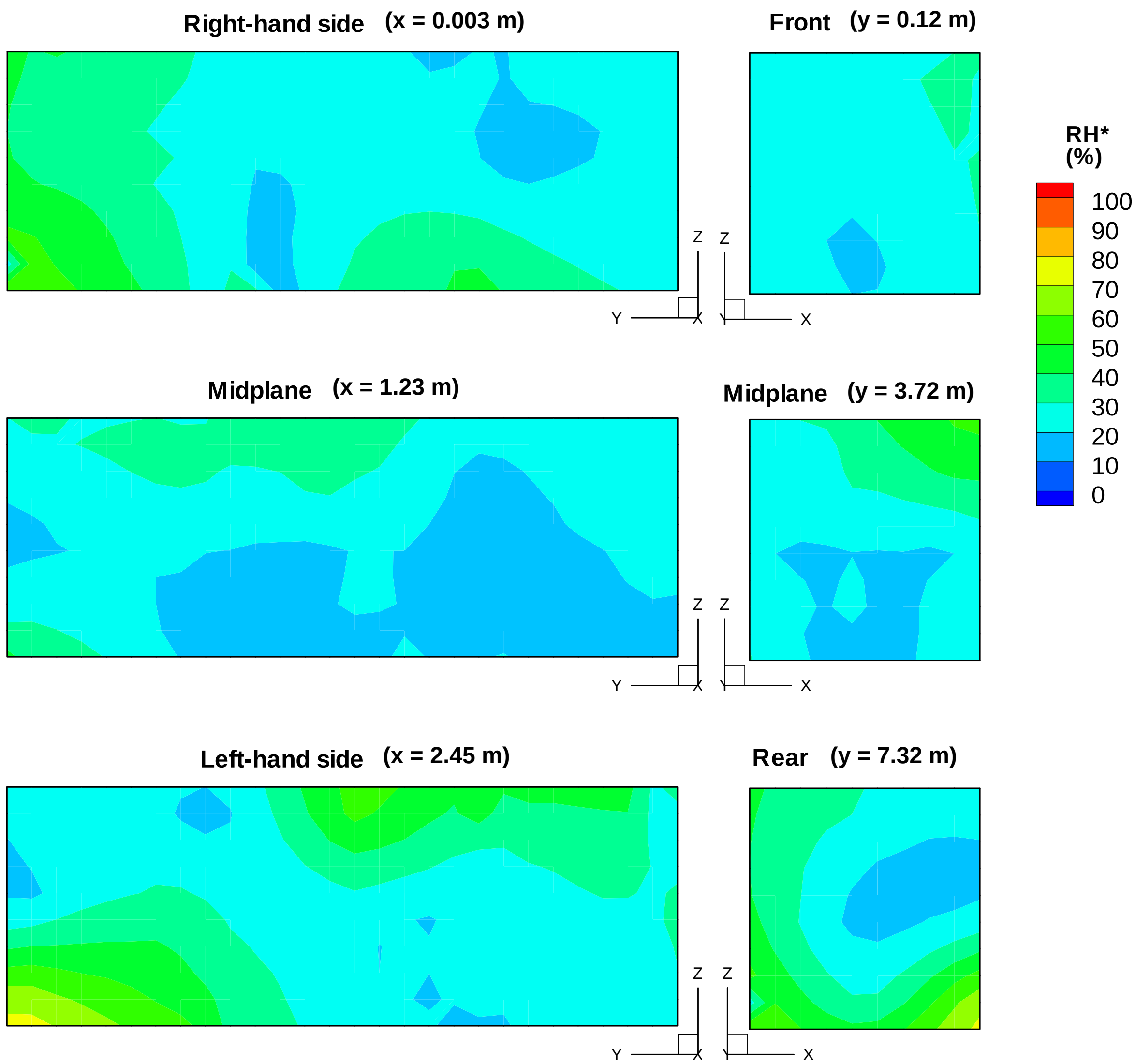

Data set #	8
Amb. T at Saskatoon airport, degree C	-11.90
Nb. fans used	1 (Btm)
Nb. heaters used	0
Inlet opening, %	60%
Date	4-Feb-05b

Figure F.1. Representative relative humidity *(RH*)* profiles for data set 8, the origin of the *x, y, z* axis (0,0,0) indicates the bottom-right front corner of the experimental trailer (viewed from the rear).

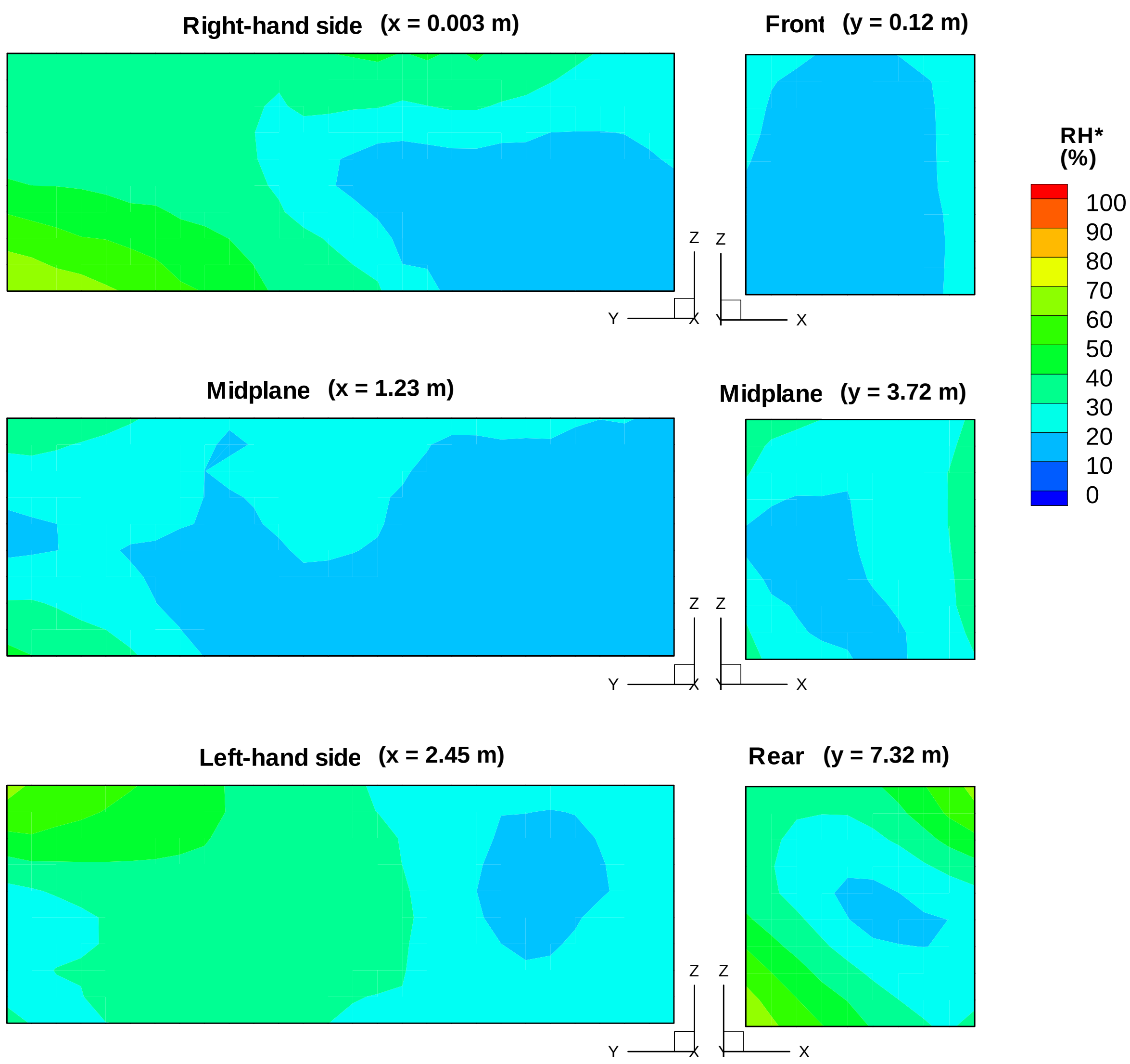

Data set #	3
Amb. T at Saskatoon airport, degree C	-17.10
Nb. fans used	1 (Btm)
Nb. heaters used	1 (Btm)
Inlet opening, %	50%
Date	15-Feb-05

Figure F.2. Representative relative humidity *(RH*)* profiles for data set 3, the origin of the *x, y, z* axis (0,0,0) indicates the bottom-right front corner of the experimental trailer (viewed from the rear).

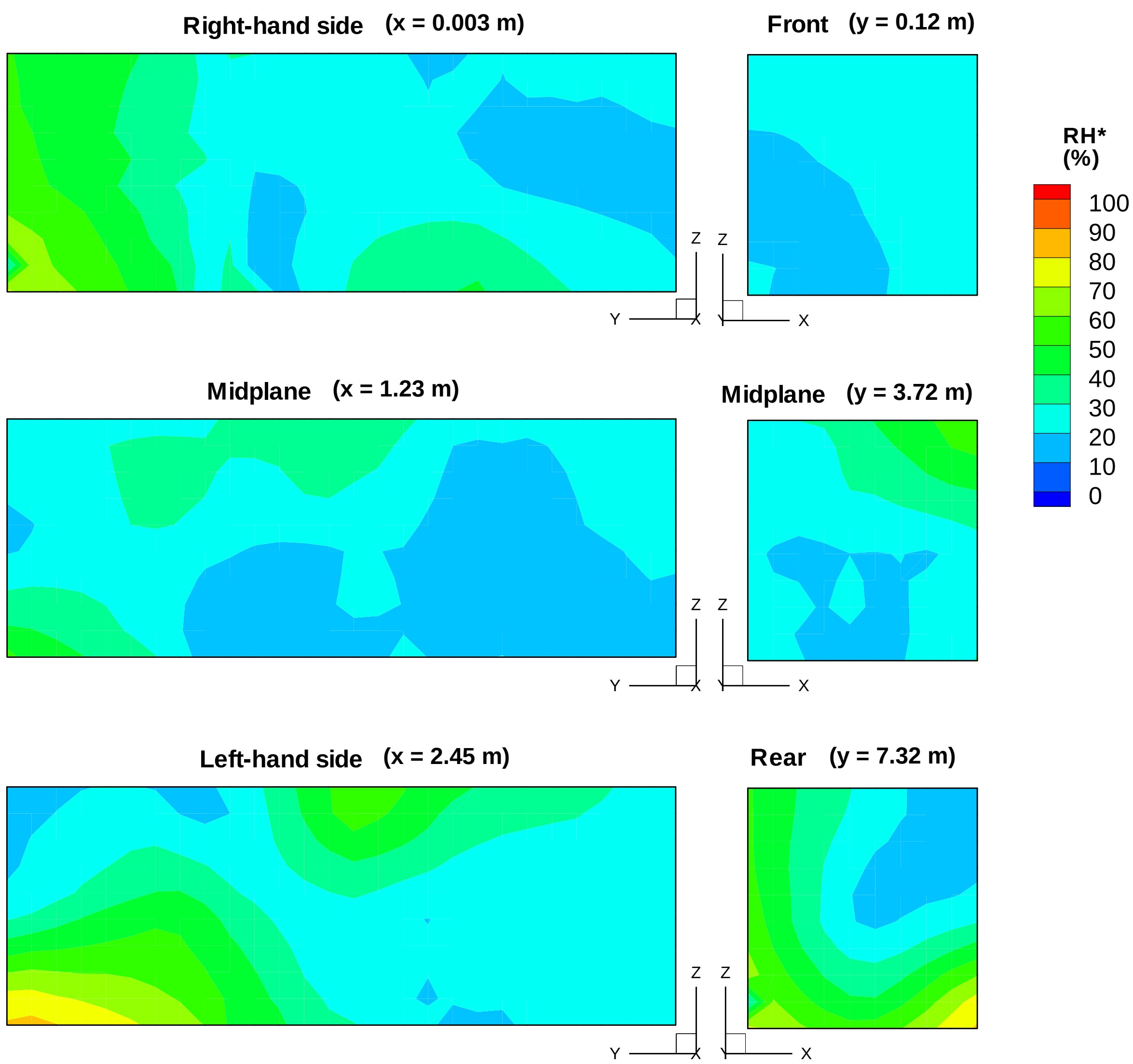

Data set #	7
Amb. T at Saskatoon airport, degree C	-9.80
Nb. fans used	1 (Btm)
Nb. heaters used	1 (Btm)
Inlet opening, %	60%
Date	4-Feb-05a

Figure F.3. Representative relative humidity *(RH*)* profiles for data set 7, the origin of the *x, y, z* axis (0,0,0) indicates the bottom-right front corner of the experimental trailer (viewed from the rear).

Group 2 – Two Fans

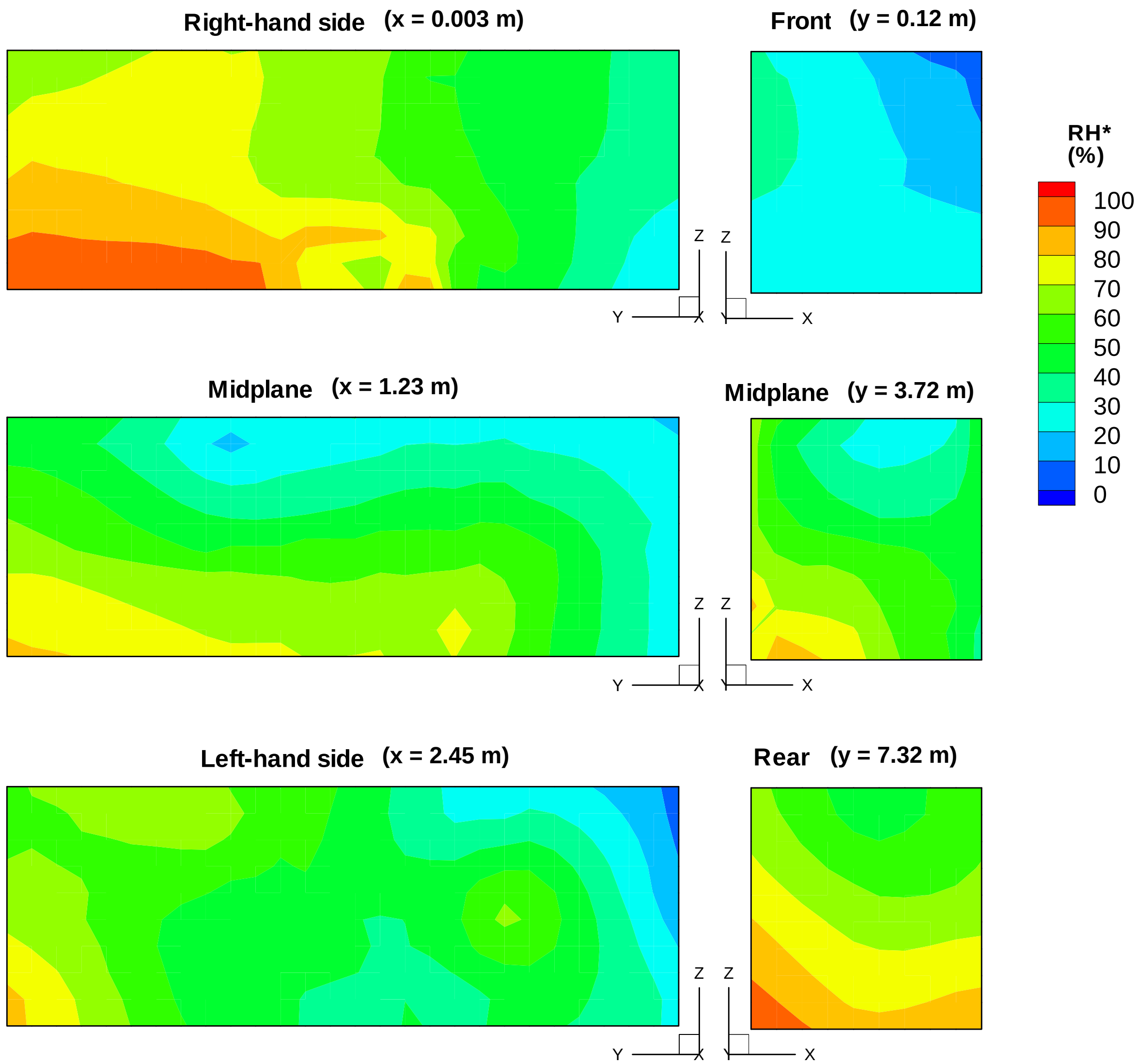

Data set #	1
Amb. T at Saskatoon airport, degree C	-15.43
Nb. fans used	2 (Btm & Mid)
Nb. heaters used	1 (Top)
Inlet opening, %	50%
Date	23-Feb-05a

Figure F.4. Representative relative humidity *(RH*)* profiles for data set 1, the origin of the *x, y, z* axis (0,0,0) indicates the bottom-right front corner of the experimental trailer (viewed from the rear).

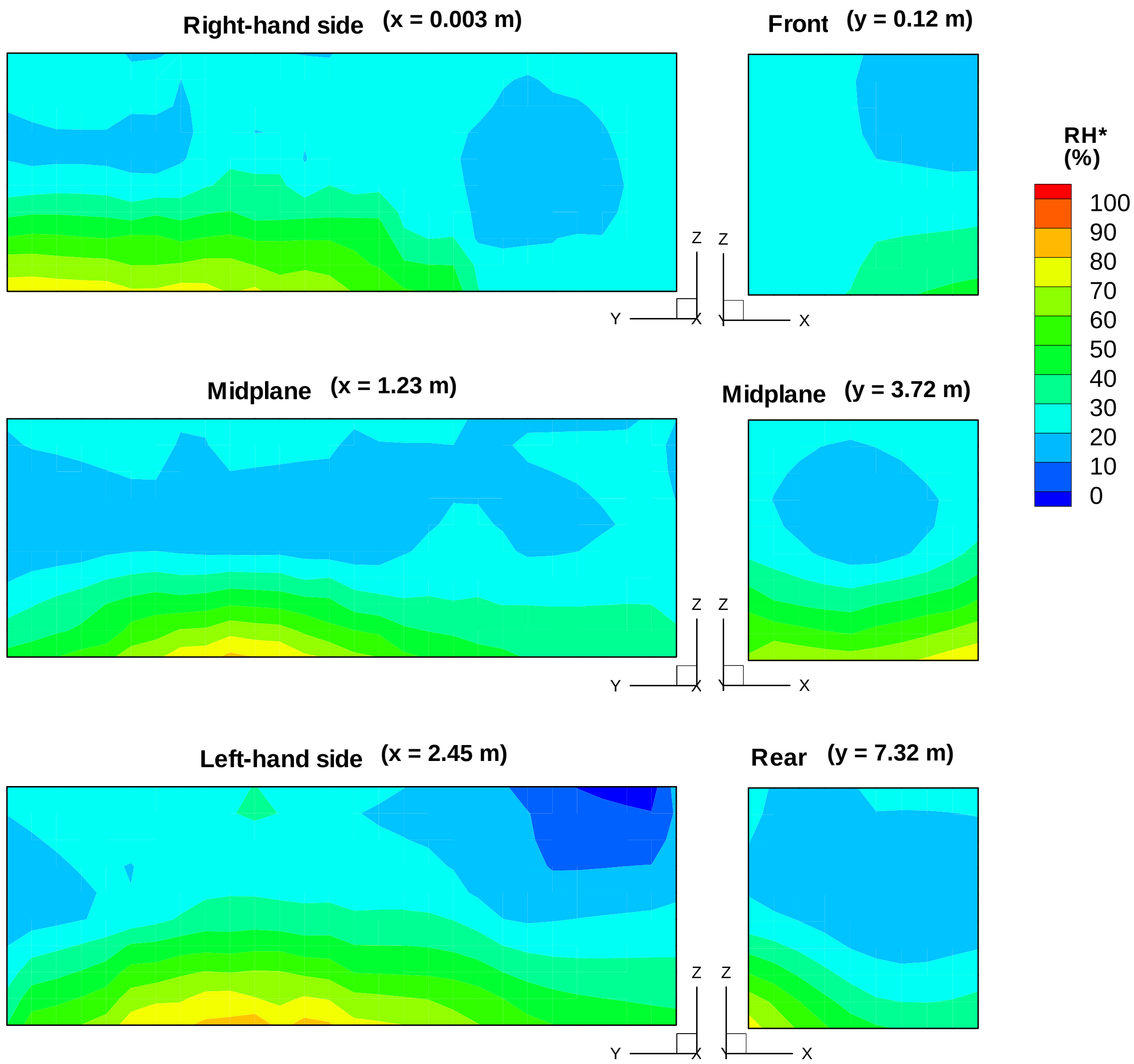

Data set #	**9**
Amb. T at Saskatoon airport, degree C	**-16.47**
Nb. fans used	**2 (Btm & Mid)**
Nb. heaters used	**1 (Btm)**
Inlet opening, %	**50%**
Date	**24-March-05**

Figure F.5. Representative relative humidity *(RH*)* profiles for data set 9, the origin of the *x, y, z* axis (0,0,0) indicates the bottom-right front corner of the experimental trailer (viewed from the rear).

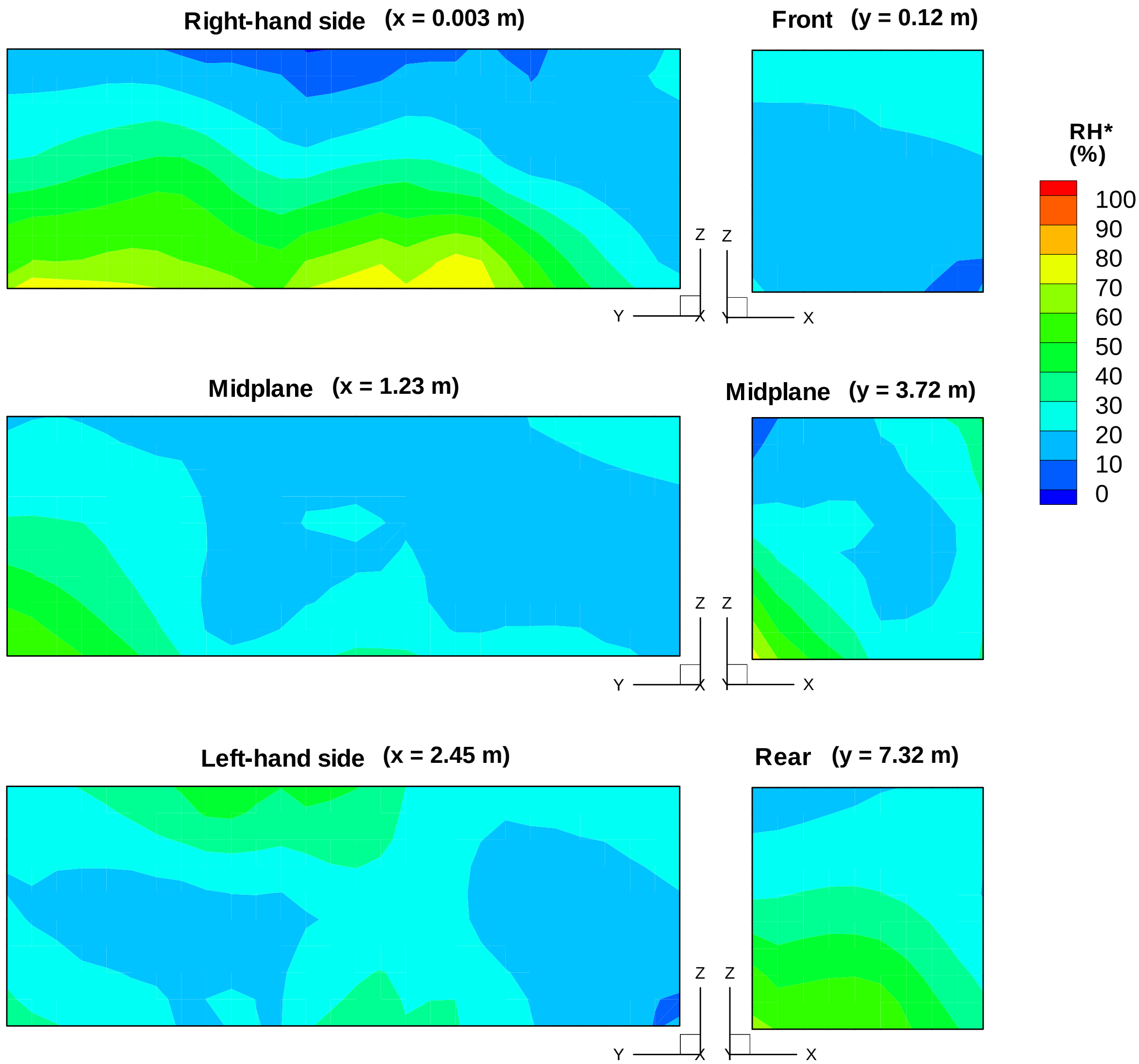

Data set #	**4**
Amb. T at Saskatoon airport, degree C	**-15.45**
Nb. fans used	**2 (Btm & Mid)**
Nb. heaters used	**2 (Btm & Top)**
Inlet opening, %	**50%**
Date	**18-Feb-05**

Figure F.6. Representative relative humidity *(RH*)* profiles for data set 4, the origin of the *x, y, z* axis (0,0,0) indicates the bottom-right front corner of the experimental trailer (viewed from the rear).

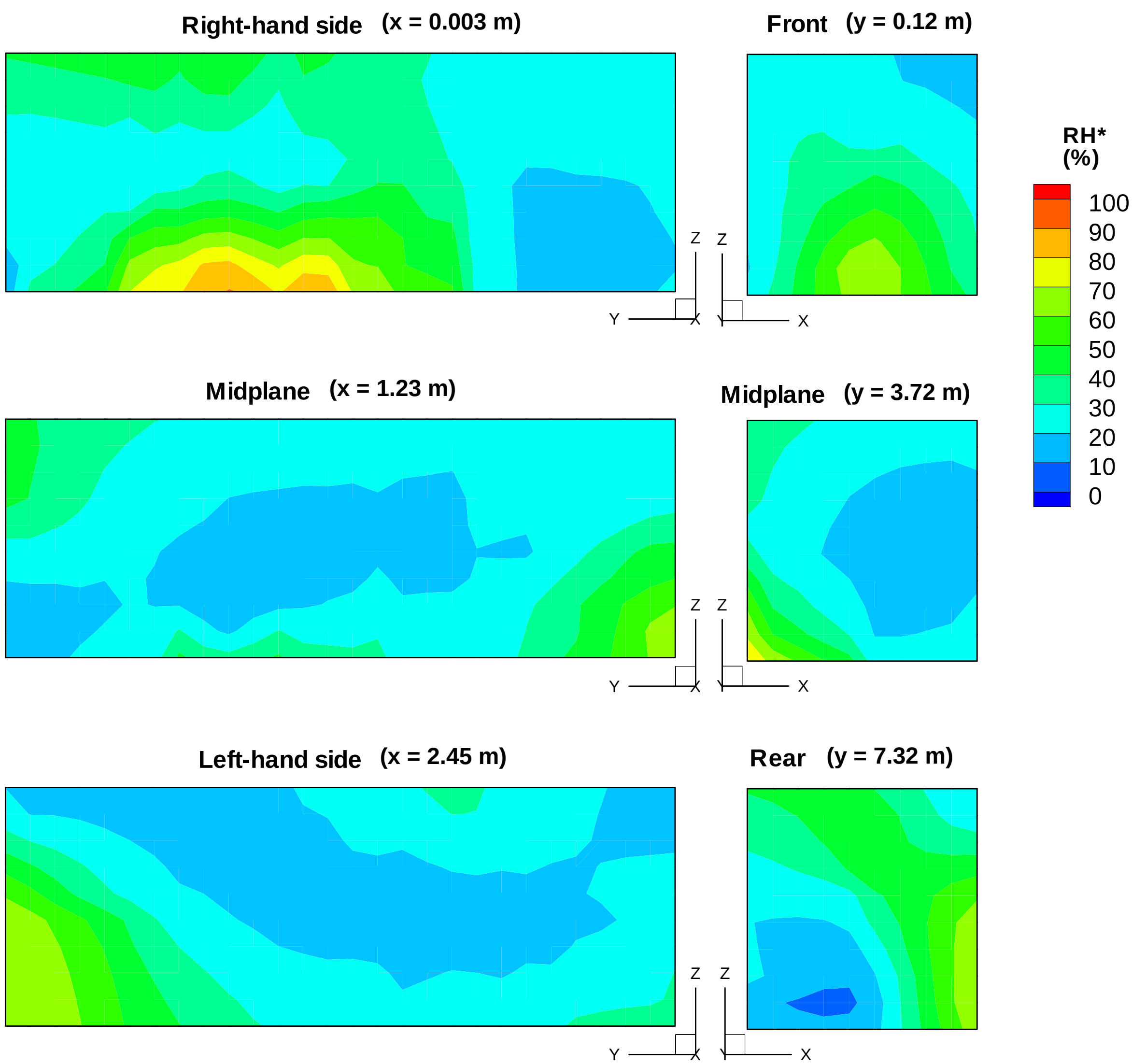

Data set #	5
Amb. T at Saskatoon airport, degree C	-10.83
Nb. fans used	2 (Btm & Top)
Nb. heaters used	1 (Btm)
Inlet opening, %	50%
Date	17-March-05

Figure F.7. Representative relative humidity *(RH*)* profiles for data set 5, the origin of the *x, y, z* axis (0,0,0) indicates the bottom-right front corner of the experimental trailer (viewed from the rear).

GROUP 3 – THREE FANS

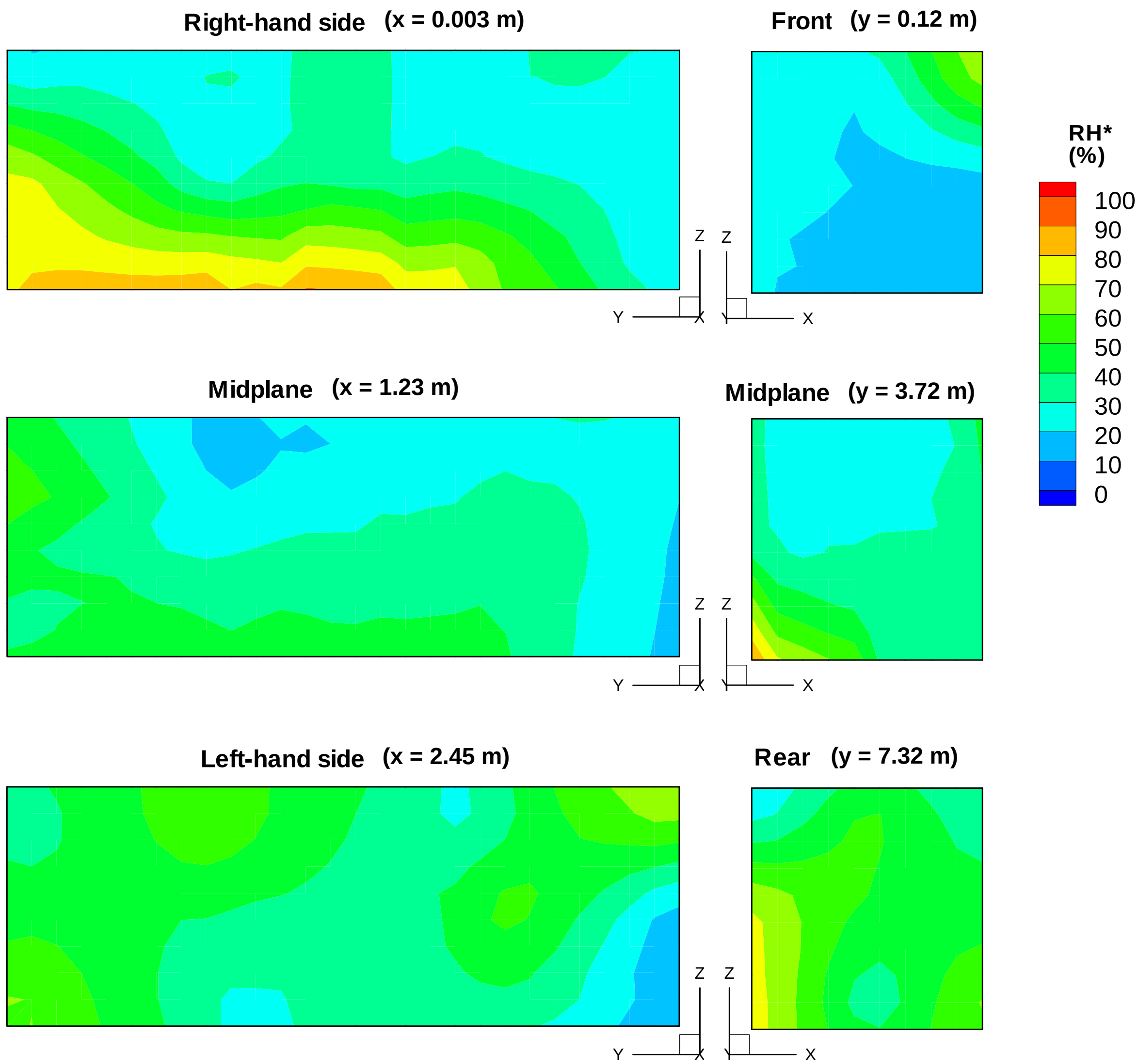

Data set #	2
Amb. T at Saskatoon airport, degree C	-13.15
Nb. fans used	3 (Btm, Mid & Top)
Nb. heaters used	1 (Btm)
Inlet opening, %	50%
Date	23-Feb-05b

Figure F.8. Representative relative humidity *(RH*)* profiles for data set 2, the origin of the *x, y, z* axis (0,0,0) indicates the bottom-right front corner of the experimental trailer (viewed from the rear).

Appendix G - Calculations of Mass Fraction

The follow equations show how to compute mass fraction. Saturation pressure of water vapour in the absence of air (for temperature of 0 to 200ºC) can be calculated using

$$\ln p_{ws} = C_8 / T + C_9 + C_{10}T + C_{11}T^2 + C_{12}T^3 + C_{13} \ln T \qquad \text{(G.1)}$$

where

C_8 = constant = -5.800 220 6 E+03,

C_9 = constant = 1.391 499 3 E+00,

C_{10} = constant = -4.864 023 9 E-02,

C_{11} = constant = 4.176 476 8 E-05,

C_{12} = constant = -1.445 209 3 E-0.8,

C_{13} = constant = 6.545 967 3 E+00,

p_{ws} = pressure of saturated pure water (Pa) ≈ p_s (vapour pressure of water in moist air at saturation) and

T = absolute temperature (K).

Partial pressure of water vapour is a function of

$$p_w = \phi\, p_{ws} \quad \text{at constant temperature \& pressure} \qquad \text{(G.2)}$$

where

p_w = partial pressure of water vapour in moist air (Pa),

ϕ = relative humidity (in decimal point) and

p_{ws} = pressure of saturated pure water (Pa).

Humidity ratio can be calculated using

$$W = 0.62198 \frac{p_w}{p - p_w} \tag{G.3}$$

where

W = humidity ratio,

p = total pressure of moist air assumed equal to atmospheric pressure (Pa) and

p_w = partial pressure of water vapour in moist air (Pa).

Finally, mass fraction can be calculated using

$$\gamma = W/(1 + W) \tag{G.4}$$

γ = specific humidity of moist air (decimal point) = mass fraction in this case (mass of water per unit mass of moist air).